SCRAPIE PATHOLOGY AND ITS RELATIONSHIP TO INFECTIVITY FOLLOWING INTRAOCULAR INFECTION.

BY

J. R. SCOTT

Submitted for the Degree of

Doctor of Philosophy

of the University of Edinburgh

1990

DECLARATION

I have composed this thesis myself, and the work described here is substantially my own in design and execution except where indicated in the text.

CONTENTS

ABSTRACT

Different strains of scrapie can be distinguished by the characteristic pattern of vacuolar degeneration which develops in the murine brain, and by the length of the incubation period. The causal agent has not been identified, and the presence of infection within tissues can only be demonstrated by bioassay. In this study, the intraocular route of infection was exploited to examine the development of the pathology produced by six different scrapie strains, and to compare the pattern of lesion targeting within this well-studied anatomical system with the spread of infectivity. Scrapie incubation period is controlled by the murine *Sinc* gene, which has two alleles; lesion development was recorded in both mouse genotypes following infection with several of the scrapie strains. The pattern of lesion development was found to correspond closely with the neuroanatomical pathways from retina via the optic nerve to the visual projection areas in the brain. The earliest lesions in all models appeared in the second half of the incubation period, and were confined to the visual projection areas on the contralateral side of the brain to the injected eye (there is almost complete decussation at the murine chiasma). The first lesions were seen either in the superior colliculus or the dorsal lateral geniculate nucleus, depending on the scrapie model; these are both major projections of the optic nerve. The pattern of subsequent lesions within the visual system also varied, gradually affecting both sides of the brain, until in the terminal mouse, the lesions were usually similar to those resulting from an intracerebral route of infection.

The spread of infectivity following intraocular infection

was studied by bioassay of tissues throughout the incubation period. The rise in infectivity levels of ME7 scrapie correlated closely with the sequence of lesion targeting, although infectivity was detected much earlier in the incubation period. Several questions relating to the sites of replication, and the spread of infectivity were investigated by bioassay of appropriate tissues. The lower levels of infectivity in retinas from mice with an inherited retinal defect, compared to normal mice, suggested that the photoreceptor cells support scrapie replication; these cells are destroyed following infection with 79A scrapie. The Sinc gene was shown to delay replication in the single neuronal relay to the superior colliculus by 50 - 60 days, suggesting that this gene acts on the transport and/or replication of infectivity. High levels of infectivity were found in the spleen following intraocular infection, indicating that inoculum escaping from the eye initiates replication in the lymphoreticular system. Similarly, disease could also be produced by conjunctival instillation of inoculum with no evidence of contralateral targeting of lesions.

The way in which infectivity spreads within neurons was studied using serial enucleation after infection, alteration of retinal ganglion cell number in mice, and attempted modification of initial infection. Following serial enucleation of the infected eye, the lesion pattern and incubation periods with ME7 scrapie indicated that infectivity spread at a similar rate to that of slow axoplasmic transport. Preliminary results with two other scrapie strains show similar timings, suggesting that spread within axons is a passive process associated with normal cellular metabolism. This means that Sinc gene control is exerted through its effect on replication rather than transport.

CHAPTER 1. INTRODUCTION

1.1 Natural scrapie and other unconventional viral infections.

Scrapie, a natural disease of sheep, is the best known of the unconventional subgroup of 'slow virus' infections, which were first defined by Sigurdsson in 1954. Similar infections have been recognised in man, mink, cattle, several types of deer, and most recently in cats. They all result in fatal neurodegenerative disease, and the agents are considered unconventional because of their resistance to procedures which would inactivate conventional viruses (Millson, 1976), and their failure to induce a host response to infection (Gardiner et al, 1965; Porter et al, 1971). The infectious agent has not been identified, and it is a matter of some controversy whether its genome contains a small nucleic acid, or is unlike that of any recognised organism (reviewed by Carp et al, 1989). Disease can only be confirmed at post-mortem by the presence of characteristic degenerative pathology in the CNS, or by the extraction of an aggregated altered protein in the form of fibrils, which have been shown to be specific to these infections (Merz et al, 1981).

Scrapie has been transmitted experimentally to laboratory rodents (1.2), and much of the present knowledge of unconventional viral infections derives from these models. Historically, scrapie has been a problem for British sheep farmers for hundreds of years (Vancouver, 1794), and is now known to have an almost world-wide distribution. The first successful experimental sheep-to-sheep

transmission was by Cuille and Chelle (1936) who not only recognised scrapie as an infectious disease, but realised that previous attempts at transmission had not anticipated its long incubation period. It is interesting that of nine ewes which they inoculated by various routes, only the two infected by the intraocular route with a suspension of spinal cord survived intercurrent death to succumb to scrapie with incubation periods of 16 and 23 months. Chelle (1942) also described natural scrapie in the goat, possibly occurring as a result of contact with infected sheep. The natural disease in sheep spreads mainly from ewe to lamb. However, placenta is known to contain high levels of infectivity (Pattison et al, 1964), which may lead to pasture contamination, and infection of unrelated members of the flock. Most cases occur between two and five years of age. Clinical signs of infection are variable, but usually include ataxia and the pruritis over the flanks and hindquarters which gave rise to the name scrapie. Death occurs within weeks to months of the first clinical signs. The only pathognomic changes are in the CNS, consisting of vacuolation seen predominantly in the medulla and mid-brain (Palmer, 1957; Zlotnik, 1958). Cerebrovascular amyloidosis has also been reported (Gilmour et al, 1986).

Breeding studies, set up to establish flocks either susceptible or resistant to experimental scrapie (Dickinson et al, 1968a; Davies and Kimberlin, 1985; Nussbaum et al 1975), revealed the presence of a gene, '<u>Sip</u>' (for scrapie incubation period), which has two alleles, sA and pA. Sheep homozygous for sA rapidly succumb to experimental subcutaneous infection with the 'A-group' of scrapie strains, whereas the pA homozygotes only develop clinical disease

when infected by the intracerebral route, after a prolonged incubation period (Dickinson and Outram, 1988). The Sip genotype of individual sheep can now be determined from a sample of DNA, using restriction fragment length polymorphism (RFLP) analysis (Hunter et al, 1989).

Much less is known about the other scrapie-like diseases. In man, two diseases have been recognised. Firstly, Creutzfeldt-Jakob disease (CJD) is a rapidly progressing dementia which occurs world-wide, but with a very low incidence (reviewed by Brown, 1980 and Brown et al, 1987). The epidemiology of CJD is not understood, but no association with scrapie in sheep has been shown. There is a familial variant of CJD, Gerstmann-Straussler-Scheinker disease (GSS); recent studies of families suffering from GSS suggests that its occurrence may depend on genetic susceptibility (Collinge et al, 1989); genetic control of incubation period length has been identified in both sheep and mice (1.2). The second disease affecting man is kuru, a dementing illness which was confined to the Fore tribe in Papua, New Guinea, and is thought to have been transmitted through ritual handling of the brains of deceased tribe members. This disease no longer occurs, since the cessation of these ritual practices (Gajdusek, 1977).

Transmissible mink encephalopathy (TME) occurs as a rare disease of farmed mink (Burger and Hartsough, 1965) and is thought to result from dietary exposure, either orally or through scratches acquired through fighting at feeding times (Marsh and Hanson, 1979). Since there is no evidence for natural mink-to-mink transmission, mink are regarded as a 'dead-end host' for the infection.

In 1986, the scrapie-like disease bovine spongiform

encephalopathy (BSE) was recognised in dairy cattle (Wells et al, 1987). The present incidence is around 600 cases per month, with no evidence of maternal or cow-to-cow transmission.This disease is thought to have resulted from dietary exposure, through inclusion of scrapie-infected carcasses in the preparation of meat and bone meal, which was fed as a protein supplement (Southwood, 1989; Tyrrell, 1989). The feeding of meat and bone meal to ruminants was banned in mid-1988; if cattle are also dead-end hosts, the disease should disappear over the next few years. If, however, BSE can be transmitted maternally or between cattle, it could either become endemic in the U.K., or be self-limiting by the end of the century, depending on the efficiency of transmission. The recent identification of spongiform encephalopathy in several domestic cats (first reported by Wyatt et al, 1990) is presumably due to a similar dietary exposure either to scrapie or BSE.

Scrapie-like diseases have also been reported in mule deer (chronic wasting disease) and elk in North America, and single cases in three species of antelope; nyala and gemsbok in a British wildlife park, and kudu in London zoo. It is highly likely that the aetiology of these diseases is the same as BSE, since all have been identified within the past 10 years, and many of the animals involved appear to have been fed similar protein supplements.

1.2 Rodent scrapie models.

Scrapie was first transmitted to laboratory mice by Chandler

(1961) and Zlotnik and Rennie (1962). Subsequent passages by Dickinson and co-workers isolated several scrapie strains in inbred mice on the basis of incubation period and pathological changes (Fraser and Dickinson, 1973; Dickinson, 1976). Between 15 and 20 strains of scrapie have now been isolated, six of which were used in the present investigation (see 2.2, Table 2). Incubation periods in mice range from about 150 days to beyond the murine lifespan (i.e. mice killed at over 1000 days can have infectivity present in the spleen and/or early lesions in the CNS). The shortest scrapie model is in hamsters infected intracerebrally with the 263K strain, which has an incubation period of about 70 days following high doses of infection (Kimberlin and Walker, 1977).

The strain-specific distribution and severity of vacuolar degeneration can be quantified using the lesion profile system devised by Fraser and Dickinson (1967). The range of lesions in experimental mice is much broader than that seen in sheep, and includes, in specific models, severe spongiosis of grey or white matter (Fraser, 1979), neuronal loss in the hippocampus (Scott and Fraser, 1984), amyloid plaques and congophilic angiopathy (Bruce et al, 1976) and photoreceptor degeneration in the retina (Hogan et al, 1981; Buyukmihci et al, 1982; Koslowski et al, 1982; Foster et al, 1986b).

Incubation period length is largely controlled by the gene '*Sinc*' (Dickinson et al, 1968b), which has a similar effect to *Sip* in sheep. *Sinc* has two alleles, s7 and p7; following intracerebral infection with a specific scrapie strain, the incubation period can differ by over 400 days in mice homozygous for the two *Sinc* genotypes. Hunter et al (1987) demonstrated that RFLP analysis could

be used to determine the Sinc genotype of individual mice.

In 1981, Merz and others discovered that extracts from infected brain tissue, viewed under the electron microscope, contained 'scrapie-associated fibrils' (SAF), which have since been shown to be diagnostic for the unconventional virus diseases. The major component of SAF is a post translationally modified form of a normal, highly conserved sialoglycoprotein, PrP, which is found in neurons and some other cells. Co-purification of SAF and infectivity led to the controversial ('prion') hypothesis that modified PrP was the infective agent (Prusiner et al, 1982; McKinley et al, 1983); however the 'prion' hypothesis is difficult to reconcile with the existence of strain diversity (Bruce and Dickinson, 1987; Kimberlin et al, 1989). Transgenic mice have recently been created which express the hamster PrP gene (Scott et al, 1989). There is no Sinc allelism in hamsters, but the dramatic shortening of the incubation period in these transgenic mice indicates that PrP is probably the product of the Sinc gene. The role of this protein in pathogenesis has yet to be revealed, although it may be a likely candidate for the host-coded protein coat for the scrapie genome postulated in the 'virino' hypothesis (Dickinson and Outram, 1973 and 1983; see 6.3). Immunostaining with antisera to PrP in tissue sections has recently revealed early changes in brain areas which subsequently become vacuolated, and strain-specific targeting of labelling both in the neuropil, and of amyloid plaques (Bruce et al, 1989).

Since there is no marker for the infectious organism, the progress of scrapie infection has to be established using bioassay in which the sequential levels of infectivity are compared in different tissues. This is done by infecting groups of mice

intracerebrally with a series of dilutions of tissue homogenate to be assayed; this gives a series of incubation periods from which an estimated number of i.c. ID_{50} infectious units can be calculated using the Karber method (see 2.7), and from which a dose-response curve can be drawn. The mean incubation period from a group of mice infected with a single dilution can also give an estimate of the level of infection from an existing dose-response curve (see 2.4). The first large-scale investigation of pathogenesis was that of Eklund et al (1967), who showed that following subcutaneous injection, infection became established in spleen and lymph nodes of the lymphoreticular system (LRS) before spreading to the spinal cord and eventually to the brain. This pattern was shown by subsequent studies to be common to peripheral routes of infection (Kimberlin and Walker 1988b). The cell types which support replication in the LRS are not known, but the absence of an effect on incubation period of whole-body irradiation suggests a post-mitotic population (Fraser and Farquhar, 1987). Kimberlin and Walker (1989a) showed that infection spreads from the spleen and visceral lymph nodes to mid-thoracic cord via sympathetic nerves. *Sinc* appears to have little, if any effect on pathogenesis in the LRS (Kimberlin and Walker, 1988a). Once neuroinvasion has been initiated, scrapie spreads in the CNS and PNS at a similar slow rate of about 1mm per day (Kimberlin and Walker, 1982; Kimberlin et al, 1983; Kimberlin et al, 1987b). Pathogenesis within the CNS, which comprises replication, transport within neurons, and cell-to-cell spread is controlled by the *Sinc* gene, although its mode of action is not known. In homozygous mice, incubation period length appears to be determined by the proximity (in terms of neuroanatomical relays) of infected

neurons to unidentified sites in the CNS which are vital for the maintenance of life (termed 'clinical target areas' by Kimberlin and Walker, 1983). This concept is substantiated by the differences in incubation period resulting from stereotaxic infection into different CNS sites (Kim et al, 1987). Evidence for transport of infectivity within axons comes from the targeting of vacuolation and infectivity to the contralateral retinal projections following intraocular (i.o.) infection (Fraser, 1982; Fraser and Dickinson, 1985). This thesis aims to extend these studies by relating the pathological changes resulting from i.o. infection in various scrapie models to the levels of infectivity in the retina and visual projection areas. It also provides an opportunity to examine the basis of the Sinc control of pathogenesis in a simple neuronal model.

1.3 The murine visual system and axoplasmic transport.

The visual system is one of the most studied and best understood neuroanatomical systems in the mammalian nervous system. However, the majority of investigators use the cat or monkey as a model for the human visual system. The retinal projections in these species differ from the mouse, about which less is known. More information is available on the rat visual system, which has been considered here to be largely similar to the mouse, and specific details of murine visual anatomy have been added where possible.

The retina from a normal C57BL mouse is shown in Fig. 1.

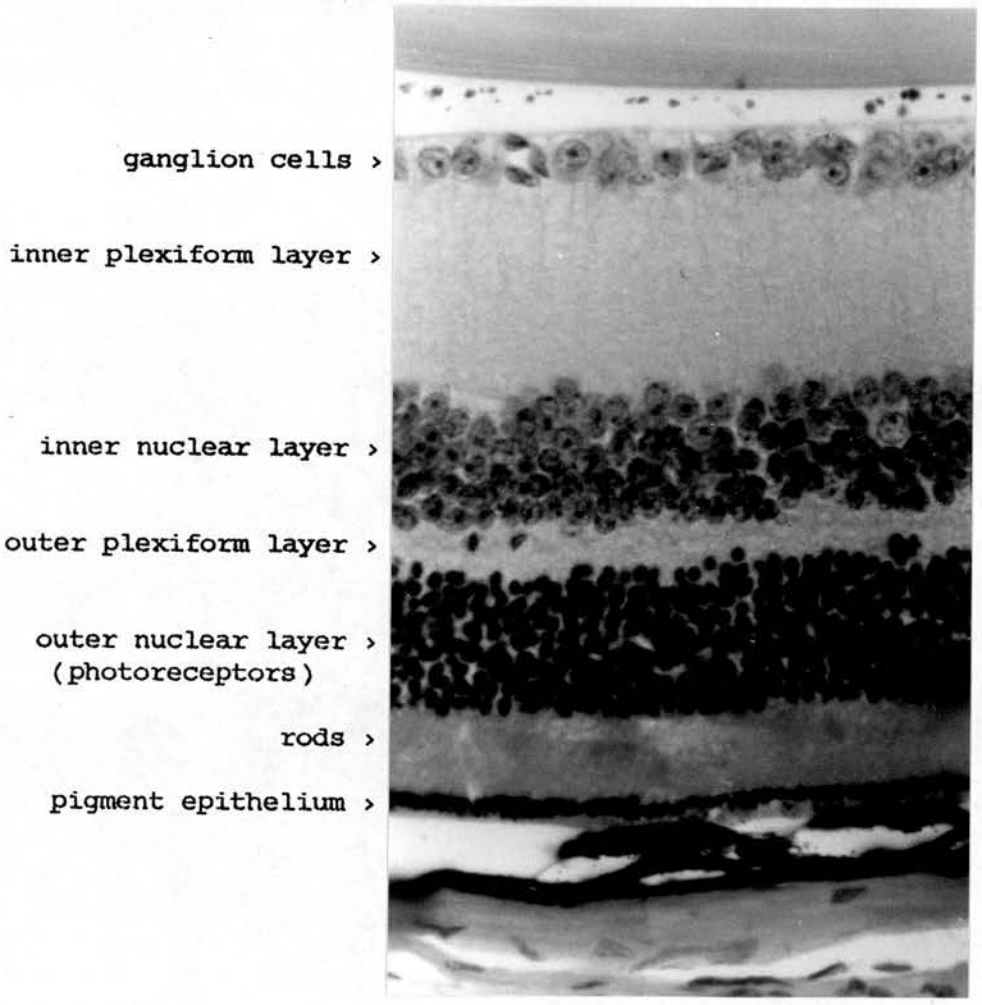

Figure 1. Normal mouse retina (from C57BL mouse) showing the major retinal cell populations. Section stained with haematoxylin and eosin, magnification X 500.

Like other rodents, the mouse has a rod-dominated retina (Dowling, 1987), which contains 48,000 to 65,000 retinal ganglion cells (RGCs)(Drager and Olsen, 1980), compared to around 110,000 in the rat (Sefton and Dreher, 1985). There are five classes of RGC in the rat, but no equivalent to the prominent class of X and X-like cells found in the cat and primates. Adult mice of strains which express the rd gene for 'rodless' retina (Noell, 1958; see 2.1) have only the inner nuclear layer, the inner plexiform layer and the RGC layer, none of which show any morphological defects. However, Grafstein et al (1972) showed that these mutants had 20% fewer RGCs, and that the rate of ^{3}H amino-acid incorporation was about 35% slower. The rate of slow axonal transport (see below) was reduced by one third, but fast transport was unaffected.

The major murine retinal projections are shown diagrammatically in Fig. 2 (simplified from Sefton and Dreher, 1985). Virtually all of the five classes of ganglion cell in the rat project to the contralateral superior colliculus (SC) or tectum in the midbrain, and many of these axons branch to supply both the SC and dorsal lateral geniculate nucleus (dLGN) in the thalamus (Sefton and Dreher, 1985). Linden and Perry (1983) demonstrated that all RGCs in the rat could be labelled after horseradish peroxidase (HRP) had been injected into the SC, and concluded that all other retino-central projections must be composed mainly of collaterals of retinotectal axons. The decussation at the murine chiasma varies from 95% in pigmented mice to 99% in albino strains (Drager, 1974). The superficial layers of the SC (superficial grey and upper optic layers, Paxinos and Watson, 1986) are innervated by retinal axons, and the cells in these layers project in turn to deeper layers

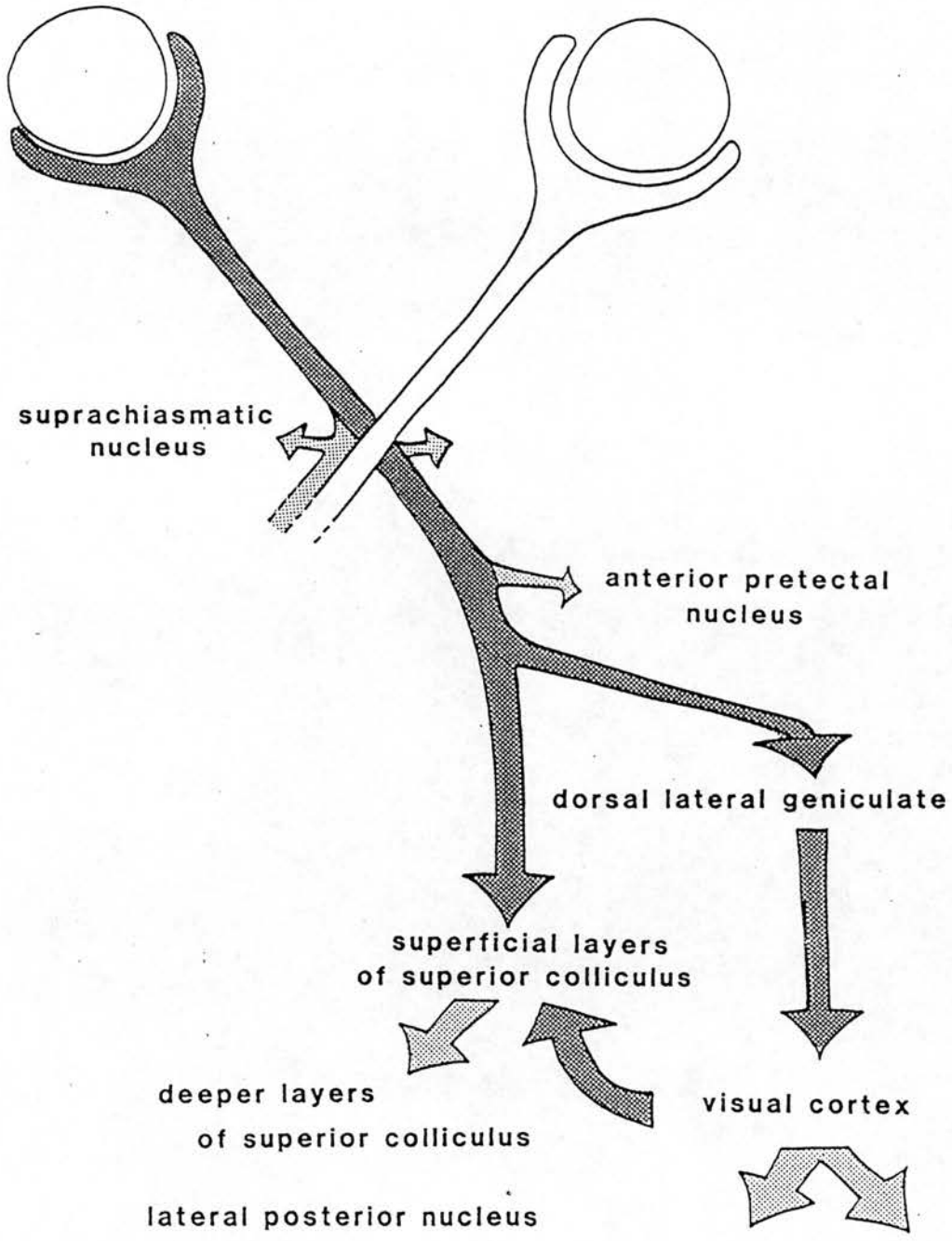

Figure 2. Diagram showing the principal projections of the rodent optic nerve (simplified fron Sefton and Dreher, 1985).

(intermediate grey and white, deep grey and white). On the basis of the distribution of radioactive material following i.o. injection, the dLGN receives the equivalent of one- quarter of the projection to the SC. There is no obvious lamination of the dLGN in rats comparable to that found in cats and primates, although different classes of RGC project to different areas of the dLGN, and there is a 'concealed' lamination from the ipsilateral projection (Sefton and Dreher, 1985).

Neurons in the SC also project to the motor nuclei of the IIIrd (oculomotor), IVth (trochlear) and VIth (abducent) cranial nerves, and via the tectospinal pathway to the cervical spinal cord. These projections are responsible for the reflex movements of the eyeballs and head in response to visual stimuli (Bowsher, 1979).

The major secondary visual projection is from the dLGN to the visual cortex. This area accounts for about 10% of the surface area of the neocortex in rats, and up to 40% in primates (Sefton and Dreher, 1985). As in other mammals, the rat visual cortex has 6 layers, of which layer 4 is the most prominent (Sefton and Dreher, 1985). The majority of the thalamic afferents (principally from the dLGN) terminate in layer 4 and lower layer 3, although some geniculocortical afferents reach layers 1 and 6. Neurons in layer 5 project back to the SC and ventral LGN. Grafstein and Laureno (1973) showed that ^{3}H proline injected i.o. in the mouse could be detected 5 hours later in the visual cortex. Since there was no difference between normal mice and rd mutants which have reduced electrical activity, they concluded that this was due to 'transcellular' transfer; however Drager (1974) also showed labelling of layer 4 of the visual cortex of C57BL mice by autoradiography following i.o.

injection of a mixture of ^{3}H fucose and proline, and concluded this was due to synaptic transfer. Fabian and Coulter (1985) showed a similar phenomenon using lectins, which confirmed the Grafstein and Laureno interpretation; they concluded that this transneuronal transport indicates a mechanism whereby large proteins may be exchanged between nerve cells. Several viruses are also thought to spread in this way (see 6.2).

Additional major visual projections include the parabigeminal nucleus in the midbrain, which is innervated by the ipsilateral SC, and in turn projects to the contralateral SC (Graybiel, 1978); the pretectum, which consists of four nuclei in the thalamus which together receive 13% of the retinofugal projection (Sefton and Dreher, 1985); and the suprachiasmatic nucleus which receives afferents from the retina, ventral LGN, midbrain raphe, septal nuclei and ventral subiculum (Berk and Finkelstein, 1981).

The optic nerve has been widely used to study the physiology of axoplasmic transport because of its accessibility and homogeneity. Virtually all axonal and dendritic constituents, and many exogenous materials, such as lectins, HRP and viruses are conveyed by axoplasmic transport (Weiss, 1982a). Despite the often considerable length of an axonal projection, axons contain no ribosomes, and are dependent on proteins synthesised in the cell body for the maintenance of axonal metabolism and synaptic function. Transport is in both directions (anterograde and retrograde), and various velocities specific to particular materials have been identified (Grafstein and Forman, 1980; Black and Lasek, 1980). In a

review of the general properties of axoplasmic transport, Weiss (1982a) tables four anterograde transport groups in optic nerve. The first has a velocity of 20 - 410 mm per day, and carries synaptic vesicles, membranous and soluble materials to the axon and axon terminal; the second transports mitochondria at between 20 and 70 mm per day; the third (slow component b or SCb (Tytell et al, 1981)) is the axoplasmic matrix which moves at between 2 and 20 mm per day, and involves transport of actin, clathrin and other proteins; and the fourth (SCa) transports cytoskeletal elements such as tubulin and the neurofilament proteins at between 0.5 and 2mm per day (Lasek et al, 1984). These velocities are common to all vertebrates, and the slow rates at least appear to be consistent in all optic nerves, although there is some evidence for variation in other nerve types (Weiss, 1982b).

Since the slowest rate of axoplasmic transport has been implicated in the spread of scrapie (see 5.1 and 6.3) the mechanism of the transport of cytoskeletal elements is of interest. This is a subject of some controversy; Lasek and others maintain that the cytosteleton is assembled in the cell body and transported unaltered (see Lasek, 1980), whereas Bamburg et al (1986) contend that studies of colchicine sensitivity in cultured cells indicate that the growth cone is a major site of microtubule polymerisation. Black et al (1986) used pulse-chase experiments to determine the interval between synthesis and assembly of tubulin and neurofilament proteins in synaptic neurons in culture. They concluded that the short times found (15 to 120 mins) indicated a small distance, and therefore that the cytoskeleton was assembled in the neuronal cell body. Matus (1987) reviews these differences, and suggests that they may reflect the changes in demand between the growing and mature neuron.

CHAPTER 2. MATERIALS AND METHODS

2.1 Experimental mice.

All experimental mice were from the Neuropathogenesis Unit's colony, which is maintained in the "barrier breeder" category designated by the Laboratory Animal Breeder Association Accreditation Scheme set up in 1983. The different inbred mouse strains used are listed in Table 1. These strains carry either the s^7 or p^7 allele of the gene Sinc, which controls the length of the incubation period. The effects of the Sinc gene are described in 3(g). BSC and C3H mice express the rd gene for rodless retina (Noell, 1958), described in 1.3. The effect of this gene on intraocular scrapie infection is tested in 3(a).

In theory, all experiments which did not require a specific mouse strain could have been done using the same strain in order to limit biological variation. In practice, due to limitations on their availability, especially during the first two years of this work, several different mouse strains were used. However the close similarity between these mouse strains both in breeding source, Sinc genotype and the well-studied effect of scrapie infection means that experiments using similar strains of mice often remain comparable.

A major decision was taken in the course of these experiments to change the strain of mouse in which tissues were assayed for infectivity (see 2.4) from C57BL to C3H. This was because of breeding problems with C57BL mice, and the greater fecundity of the C3H strain, which meant that many more mice were

TABLE 1. Inbred mouse strains.

strain designation	abbreviation	Sinc genotype
BSC/Dk*	BSC	s^7
C57BL/FaBtDk	C57BL	s^7
C3H/LaDk*	C3H	s^7
IM/Dk	IM	p^7
LM/Dk	LM	s^7
MB/Dk	MB	p^7
MM/Dk	MM	s^7
RIII/FaDk	RIII	s^7
SM/RrChBtDk	SM	s^7
VM/Dk-Sinc^{s7}(congenic)	SV	s^7
VL/Dk	VL	s^7
VM/Dk	VM	p^7

* these strains carry the rd (retinal dystrophy) gene.

available. The difference between these strains in terms of response to scrapie infection is known to be minimal (Outram, 1980 and unpublished data); the C3H rd gene had no effect since all assays are by the i.c. route.

Several experiments used the F_1 cross between C57BL and VM.

2.2 Strains of scrapie and experimental models.

The majority of the experiments used the ME7 strain of scrapie, since this is widely studied, and produces precise incubation periods in all mouse strains. Five other scrapie strains (22A, 22C, 22L, 79A, and 87V) were also used. The source and passage history of these strains is summarised in Table 2. All except 22L have been purified by 'cloning' i.e. at least two consecutive passages through mice infected with inoculum of high dilution (Dickinson and Outram 1983, Kimberlin and Walker 1978).

The experimental model is defined by the scrapie strain and the mouse genotype used: the same strain of scrapie can have very different effects in mice of each *Sinc* genotype (see 3(g)). Different strains of mice with the same *Sinc* genotype, infected with the same strain of scrapie, can produce a variety of pathological changes and incubation periods (see Chapter 3.)

2.3 Preparation of inocula.

Standard inocula

Standard inocula were prepared from stocks of brains from

TABLE 2. Scrapie strains.

ME7	This strain was originally isolated from a Suffolk sheep with naturally acquired scrapie in 1962, by intragastric infection of Moredun random bred mice. Subsequent i.c. passage was once in Moredun random bred, and 9 times through C57BL mice.
22A	Isolated from a sheep experimentally infected with SSBP/1 scrapie in 1962 by i.c. infection of MM strain mice. Seven subsequent i.c. passages in VM mice.
22C	This strain comes from the same source as 22A, but after the initial pass in MM mice, i.c. passage was in C57BL mice. Inocula were obtained from the 8th subsequent passage.
*22L	Isolated in 1967 from a Cheviot ewe experimentally infected with SSBP/1, but which had an unexpectedly long incubation period, by combined i.c. and i.p. infection of C57BL mice, followed by 9 i.c. passages.
79A	Isolated in 1966 from an experimental passage line derived from SSBP/1 in goats by i.c. infection of C57BL mice, followed by 8 similar subsequent passages.
87V	Isolated from the formalised brain of a natural case of scrapie in a North Country Cheviot X Border Leicester sheep in 1967, by i.c. and i.p. infection of VM mice. Inocula were prepared from the 8th and 9th subsequent i.c. passage in VM mice.

* this strain has not been 'cloned' through high dilution passage.

terminally infected mice. These are removed using aseptic techniques, kept in carefully labelled individual glass bijoux with sealed lids at -30°C, and indexed in the freezer records. Pieces of thawed, macerated brain tissue were weighed and transferred to a glass tube fitted with a Teflon plunger, and homogenised in physiological saline at a dilution of 1% or 10% wet weight for approximately 60 seconds (until all visible fragments of tissue had disappeared). The homogenate was either used unspun, or transferred to a small glass centrifuge tube, and spun at 500g for 10 mins. The supernatant was used as inoculum. The results of the first experiments showed that spinning could reduce the infectivity titre by as much as 10-fold, so some subsequent experiments used a standard unspun 10% dilution. Occasionally inocula were prepared as pools, and frozen as aliquots (e.g. for experiments involving sequential infection). These aliquots were reground in Teflon tubes before use.

All inocula were prepared under stringent conditions, designed to avoid contamination with other strains of scrapie, and maintain asepsis. Sterile disposable equipment was used whenever possible; equipment which had to be reused was first autoclaved, then washed and packed, and finally reautoclaved. Each autoclave cycle was at a temperature of 134-138°C and pressure of 29.5 - 34.5 psig. for 18 minutes in a large porous load autoclave, and 2 hours in a gravity displacement benchtop model.

Titrations

Tissue samples to be titrated were prepared in the same way

as standard inocula, except that centrifugation was at 2000g for 15 minutes. This is to attempt to remove 'aggregates' of infectious material which may increase the range of incubation periods for any given dilution. Titrations required dilutions of inoculum ranging between 10^{-1} to 10^{-8}. These were made by preparing a labelled series of small glass tubes containing 9 parts saline, adding one part of inoculum to the first, mixing and continuing the series. Each transfer was made with either a new disposable syringe, or a sterile Gilson pipette tip.

Purified inocula

These inocula were prepared as SAF (scrapie-associated fibril) preparations from 2-3 fresh brains from terminally infected mice. This involved high speed centrifugation on sucrose density gradients (Hope et al, 1986). These procedures were carried out by Laura Reekie and James Hope. Samples both with and without proteinase K treatment were used. The standard control inoculum for comparison in these experiments was taken after the first preparative stage of homogenisation (made in distilled water not saline); dilutions were less than 10% wet weight of brain, and are noted where appropriate. Purified inoculum for titration (and standard control) were stored at $-20^{o}C$ until the results of the PAGE were available (about 48 hours) and showed that the protein was present. For titration, protein samples (with and without proteinase K treatment) were dried in Eppendorf tubes and resuspended with 0.5ml saline, as nominal 1% dilutions. Further serial dilutions were made as described above. Since the exact dilution of the purified

inoculum was not known, infectivity levels in the purified and control samples could only be compared by relating the eventual estimate of infectivity (Karber calculation of ID_{50}) to the original brain equivalent amount (4(h)).

2.4 Preparation of tissues for bio-assay

Tissues for assay were taken serially, over as long as 350 days after injection, and stored as a pool from 3-6 mice at $-30^{o}C$, until groups of recipient mice became available. Some tissues provided sufficient material to treat as standard inocula (spleen, trigeminal ganglion, hypoglossal nucleus, cerebellum), but since most visual system areas yielded only small amounts of tissue, inoculum was prepared from pools of tissues taken from 4 or 6 mice depending on the experiment. It was not possible to thaw and weigh such tissue pools when the inoculum was prepared (optic nerve pools dried out as they were taken, and some freeze-drying took place in all tissues, depending on the length of time in storage) and so a standard weight for each tissue was derived from a series of 10 fresh samples. The mean weights and inoculum dilutions are given in Table 3. When tissues were taken for assay, great care was taken to sample a similar amount of tissue on each occasion. The details of removal of each tissue are described in Table 4. Pools were stored in small plastic tubes with sealing lids. Each tube was removed from the freezer individually, and the frozen mass of tissue placed on the plunger of the homogeniser with the tip of a heat-sealed Pasteur pipette. This method proved successful in handling small amounts of

TABLE 3. Standard weights and dilutions for assayed tissues.

tissue	mean weight of 10 samples (mg)	dilution
retina	6.31 ±0.16	10%
optic nerves	0.72 ±0.044	1%
superior colliculus	5.62 ±0.33	10%
dorsal lateral geniculate	22.45 ±1.40	10%
visual cortex	37.04 ±1.64	10%
cerebellum	41.13 ±1.83	10%

TABLE 4. Removal of tissue samples for assay.

tissue	method of removal
optic nerves*	before removal of the eyes, the roof of the cranium was removed and the forebrain eased up until the optic chiasma was visible. The optic nerves were cut close to the chiasma, and the brain replaced. When the globes were removed with curved forceps, the optic nerve remained attached. The nerves were cut just behind the hilus, and gently pulled from the surrounding sheath of muscle and connective tissue.
retina*	globes were bisected at the scleral margin, then retina eased out with watchmaker's forceps. Optic nerve cut behind the optic disc.
superior colliculus visual cortex	the brain was dissected as shown in Fig. 3, and the area approximately 0.5mm above the aqueduct, between coronal levels 343 to 407 (Sidman et al, 1971) removed. This included two large areas of occipital cortex, within which lies the visual cortex. The cortices could easily be lifted free from the superior colliculus, which could then be bisected if required.
dorsal lateral geniculate nuclei	a second slice of brain was taken approximately between coronal levels 200 to 334. The areas containing the two dLGN were each dissected out with three cuts, as shown in Fig. 3. Each cut was made with a clean razor blade.
cerebellum	the cerebellum was dissected from the remaining hindbrain section and bisected sagittaly. The left side was frozen for assay.

* these operations were made with the aid of a dissecting microscope.

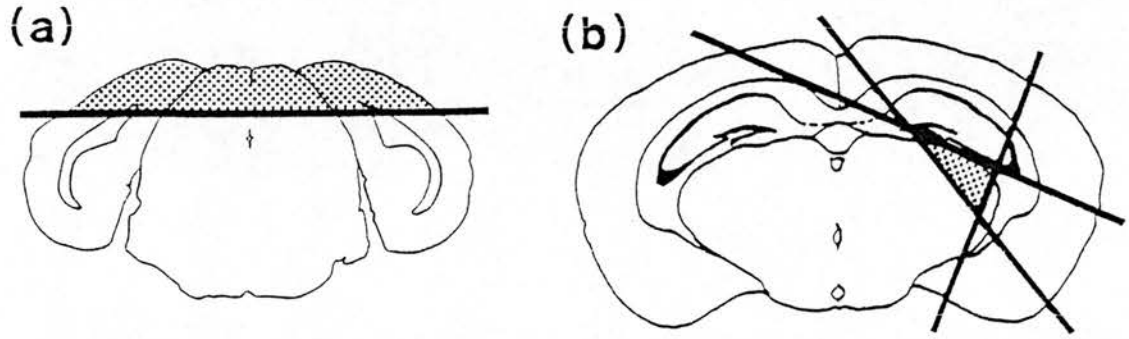

Figure 3. Diagram showing dissection of (a) superior colliculus and visual cortex, and (b) dorsal lateral geniculate nucleus from murine brain.

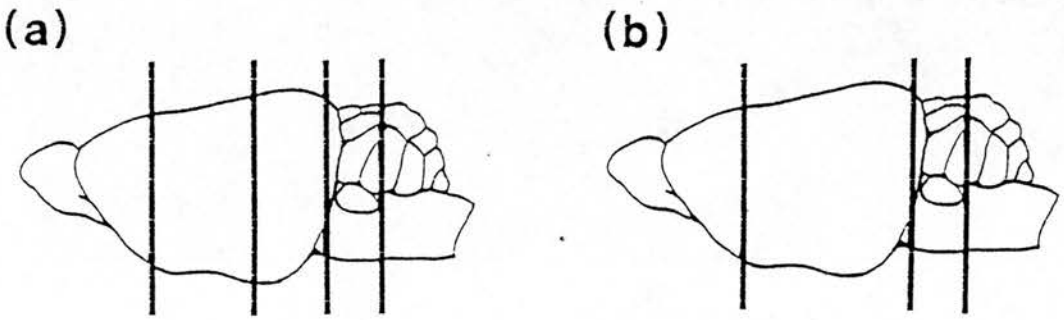

Figure 4. Diagram showing trimming for (a) standard levels (for lesion profiles) and (b) special levels (for visual projections).

tissue, even the retina samples, which became liquid and sticky when thawed. The minimum amount of saline was added to provide enough inoculum to infect 9-12 recipient mice (0.02ml i.c. per mouse). This resulted in a 10% dilution for most samples except optic nerves, which were assayed at 1%. Since dilutions of less than 10% have been known to kill mice when injected i.c., 10% was the minimum dilution made, even where greater amounts of tissue were available. The purpose of an assay is to detect infectivity, and so none of the samples were spun during preparation: although centrifugation may remove aggregates from the sample, it also reduces the titre, as previously noted.

Some tissue pools taken for assay were titrated as described above. In these cases, the dilution of injected inoculum ranged from 10^{-1} or $^{-2}$ to 10^{-6} or $^{-7}$.

No allowance was made for any changes in weight, during the incubation period, of tissues which were prepared to a standard dilution. Differences in tissue weights occurred only in (a) those retinas taken from VL mice treated with MSG (in 4(b) and 5(b)), which had lost ganglion cells, and appeared thinner and more fragile than those from untreated controls; and (b) retinas from BSC mice with the rd gene which had no photoreceptors (in 4(b). The volume of saline used was the same as if there had been no change in weight, since the purpose of the assay was to provide a comparison in infectivity levels in the retina as a whole.

2.5 Injection procedures

The procedures used for different injection sites are described below:

Intracerebral

Until April 1987, mice were injected with a 25g 0.5 inch needle to the right side of midline of the cranium, above the parietal cortex, penetrating the brain tissue between coronal levels 220-300 (Sidman et al, 1971). The needle passed through the cortex and hippocampus, and extended into the thalamus and hypothalamus. After April 1987, as a result of the introduction of the Animal (Scientific Procedures) Act 1986, the standard i.c. injection was modified by the addition of a 'needle guard' which limited the depth of the needle's penetration of the brain to 2mm, effectively confining the injection site to the cortex. No change in incubation periods were identified following this change in practice. Injection volumes were between 1 and 20ul. Intracerebral injections were performed for me by Hugh Fraser and David Davies (I am left-handed, and find the standard i.c. injection site difficult to acheive).

Intraocular

Under pentobarbitone anaesthesia, the right eye was slightly everted by pressing above and below the orbit. The injection site was at the scleral margin of the right eye using a 27g needle, inserted so that the tip of the needle could be seen in the centre of the vitreous chamber, behind the lens. Injections were completed in about 5 seconds; pilot experiments using longer times (up to 4

minutes) had shown no obvious advantages. In some experiments, the injection site was the outer canthus of the globe and the injections were made by Hugh Fraser; because of my left-handedness, I made all other injections into the inner (nasal) canthus. Care was taken to avoid damaging the retina; any slight damage was noted on the identity card, and the occasional mouse given a poor injection was replaced. On recovery from anaesthetic, mice looked quite normal, and ocular pressure appeared to be restored within 24 hours. For some assay experiments, both eyes were injected in order to generate more tissue. Injection volume was 1ul, except for one experiment where it ranged from 0.05 to 1ul. Intraocular injections of ^{3}H proline were made to determine how much of the inoculum remained in the eye (see 2.10).

Intravenous

Mice were restrained in a 50ml syringe barrel, and injected into the tail vein with a 27g needle, after warming the tail with a pad soaked with warm water. Poor injections were either replaced or noted as such on the individual identity card. Injection volume was 1ul or 20ul. Intravenous injections were performed by myself or Hugh Fraser.

Intraperitoneal

Mice were injected into the mid-abdominal region using a 25g needle, carefully inserted to avoid major organs. Injection volume was 1ul or 20ul. Injections were performed by myself or Hugh Fraser.

Conjunctival instillation

The right eye was slightly everted under anaesthesia, as for i.o. injection, but inoculum (or other solution) was merely dropped behind the globe, using a 27g needle blunted to avoid damage to the tissues. Injection volume was 1ul.

Intraorbital

As above, except that 1ul of inoculum was injected into the tissues behind the globe with a standard 27g needle.

Tongue

Under anaesthesia, the tongue was gently extended with forceps: a 27g needle was inserted to the right side of the mid-line, about 1.5mm from the tip, and extended subcutaneously for 3 - 4mm befoe the injection was made, to limit escape of inoculum. Some initial swelling of the tongue occurred, but on recovery from the anaesthetic, the mice showed no signs of distress and rapidly resumed normal feeding. Injection volume was 1ul. Tongue injections were performed by Hugh Fraser.

Vibrissae

Under anaesthesia, a 27g needle was inserted at the caudal margin of the right vibrissal pad, and extended 3 - 4mm subcutaneously, while lifting the tip of the needle slightly in order to maximise the spread of inoculum in the vibrissal area. Injection volume was 1ul. Vibrissal injections were performed by Hugh Fraser.

2.6 Surgical techniques and drug treatments.

Two surgical procedures were used - enucleation and splenectomy, which are described below. Mice were also treated with monosodium glutamate (MSG) in order to deplete the retinal ganglion cell population.

Anaesthesia

Sodium pentobarbitone (Sagatal, May and Baker) was given i.p., at a dilution of between 7 and 10-fold of the commercial, 60mg/ml solution, administered at 1ml per 100g body weight. This was supplemented with ether as required. Mice were kept warm until recovery from the anaesthetic was complete. Since ether appeared to increase the likelihood of bleeding occurring after enucleation, the dose of Sagatal was slightly increased for this operation. Post-operative (and post-injection) problems were rare. The most common problem, which occasionally resulted in death, was the reaction to the anaesthetic. Different anaesthetic doses were required by different mouse strains, and a table of dilutions was drawn up based on experience.

Enucleation

The right eye was everted until the globe was visible. Small ('butterfly') curved artery forceps were clamped just behind the globe, and left in place for 1 - 2 minutes, before the globe was removed with a pair of fine forceps. The artery forceps were left in

place for a further 3 - 5 minutes to minimise bleeding, then carefully removed.

Splenectomy

Under anaesthesia, the fur was clipped from the left flank, and the area swabbed with alcohol. An incision of up to 10mm was made through the skin and peritoneal wall. The spleen was drawn to the exterior, and carefully separated from connective tissue and fat. The incision was closed with 2 - 3 stitches or a Michel clip.

MSG treatment.

Neonatal mice were treated with MSG as described by Potts et al (1960), slightly modified by shortening the duration of treatment to 10 days. Mice were given an i.p. injection of 2.2mg MSG per g body weight on the second post-natal day; the dose was steadily increased until by the eleventh and last day of treatment they received 4.4 mg per g. MSG treatment was by Jim Foster and is fully described in Foster et al (in press).

2.7 Experimental design and incubation period assessment

The experiments described in this thesis were set up as part of the ongoing programme of work of the AFRC and MRC Neuropathogenesis Unit. The standard experimental procedures of the Unit were followed. Once an experimental protocol had been accepted, and the mice were produced (for large experiments this could involve expanding the breeding colony), the experiment was set up, and monitored on a day-to-day basis by a member of the animal house staff. This person was also responsible for clinical scoring of mice, collating experimental data and drawing up lesion profiles (see 2.9) on completion of the experiment.

Mouse husbandry

Mice were ear-punched at weaning, so that each mouse in a cage of six could be identified. Each mouse was allocated a card showing breeding details which was attached to a second card carrying an individual experimental number and clipped to the front of the cage. Copies of the second card, showing which treatment each mouse had received, were held until the completion of the experiment, and then attached to the other cards and filed. Mice were examined twice weekly at cleaning, then also scored weekly for clinical signs of disease (see below) from 30 to 50 days before the predicted end-point. All minor clinical observations not relating to scrapie (e.g. inflamed eye, skin abrasions) were entered on the breeding card, and also any signs that mice may have cannibalised a dead cage mate. Eventually, histological findings were also

attached, and the final analysis of experiments was based on these cards. The coding of individual mice within experiments was designed to reduce observer bias when scoring for clinical signs of scrapie; for example, end-point groups given different treatments were mixed within cages.

Mice were maintained in artificial light with a 12 hour on/off cycle. The light intensity within the animal room varied from 50 to 200 lux (Foster et al, 1986a), and the humidity was between 35 and 55%. The temperature was maintained between 20 and 22^{o}C. Mice were fed *ad libitum* on Laboratory Animal Diet 1 (Biosure, Manea).

Incubation period assessment

The 'incubation period' referred to in this thesis is measured from the day of infection until the clinical end-point of the disease (Dickinson et al 1968b). At clinical assessment, each mouse (identified by ear-punch and experimental number) is scored as 'unaffected', 'possibly affected' or 'definitely affected'. The end-point is defined according to the following criteria: (a) the day on which the mouse receives a third consecutive 'definite' score, (b) the day on which the fourth definite score is given within 5 weeks, (c) the day on which it is killed *in extremis*, or is found dead, having received a definite score in the preceding week. In many of the results in Chapters 3, 4 and 5 the incubation period refers to the mean incubation period of a group of mice, $\pm$ the standard error of the mean (SE).

Experimental design

In sequential experiments, where groups of mice were killed at various times during the incubation period to provide tissues for bioassay or histology, mice were allocated to specific dates from the outset. When the first mouse in any treatment group was killed with clinical signs of scrapie, the remaining sequential groups were allowed to survive until terminal, or else the group results were disregarded (since they were a sample from an already affected population). Brains were taken from sick and dying mice without clinical scrapie scores (unless autolysis rendered this impossible). All clinical assessments were substantiated by histological findings. Where brain tissues were removed for bioassay, identical groups of mice infected mice were killed to monitor the pathological changes.

Mice used for infectivity assays which had good clinical signs of scrapie, and with incubation periods of less than between 300 - 400 days were not sent for histological assessment. All brains from mice with longer incubation periods, or with equivocal clinical signs were taken for histological diagnosis. Each cage in a titration experiment contained mice injected with a least two adjacent dilutions to prevent subjective clinical assessment of the cage as a whole. Where mice had been given low levels of infectivity, or a negative result was expected, a compromise was needed between maintaining them until senility, risking the loss of tissues through unexpected deaths, and killing them while still incubating the disease. Generally experiments were terminated about 700 days post-infection, or at least 200 days after the last

positive case. Mice killed at this time, which had no pathological signs of disease, were considered to be survivors. The infectivity titre was calculated using the method of Karber (1931) to give number of infectious units in a given volume of tissue. The results are expressed as ID_{50} units (rather than LD_{50}) since the mice are not left until death, but are killed when clinical signs of infection are manifest.

Dose-response curves

Dose-respose curves were drawn up from titration results. A 'best fit' curve was fitted using Graphwriter II software on an Elonex PC (examples in Appendix B). These graphs were used to calculate the amount of infectivity in a given tissue from the mean incubation period of the recipient mice. Dose-response curves were not available for each individual tissue assayed (and it would have been impracticable to set them up). Therefore, the values for retinal infectivity, for example, were read from a dose-respose curve for brain tissue. It is unlikely that any difference in dose-response curve exists between these tissues; any small difference would be unlikely to affect the result, given the limitations on sensitivity of this method of estimating titre.

2.8 Histological preparation

Brains were removed within 2 minutes after mice were killed by cervical dislocation. When mice were found dead, brains were

taken unless autolysis made this impossible. All tissues except eyes were fixed in 10% formol saline at room temperature for 1 - 3 days. Eyes were fixed in Davidson's solution, which gave better preservation of the retina. Brains taken for lesion profile scoring (see 2.9) were sectioned coronally to give five standard levels (Fig. 4a, page 26). For visual system scoring, the block from inferior colliculus to paraterminal body (Fig 4b) was embedded separately. Sections were cut at 6um, and stained with haematoxylin and eosin (H&E); two consecutive sections from standard blocks, and semi-serial sections through the visual system (1 section in every 20). Sections were examined using either a Reichert Biovar or an Olympus BH-2 microscope; the latter was also used for photomicrography.

2.9 Scoring systems for observed lesions

Lesion profiles

The distribution and intensity of vacuolar degeneration in the brain was estimated by scoring 9 standard grey matter areas of brain on a scale from 0 - 5 to give a 'lesion profile'(Fraser and Dickinson 1968). A score of 1 has been described as 'few vacuoles, widely and unevenly scattered' and 5 as 'dense vacuolation with most of the field confluent'. The nine areas are: 1 medulla, 2 cerebellum, 3 superior colliculus, 4 hypothalamus, 5 thalamus, 6 hippocampus, 7 paraterminal body, 8 cerebral cortex (posterior midline) and 9 cerebral cortex (anterior midline). These areas are

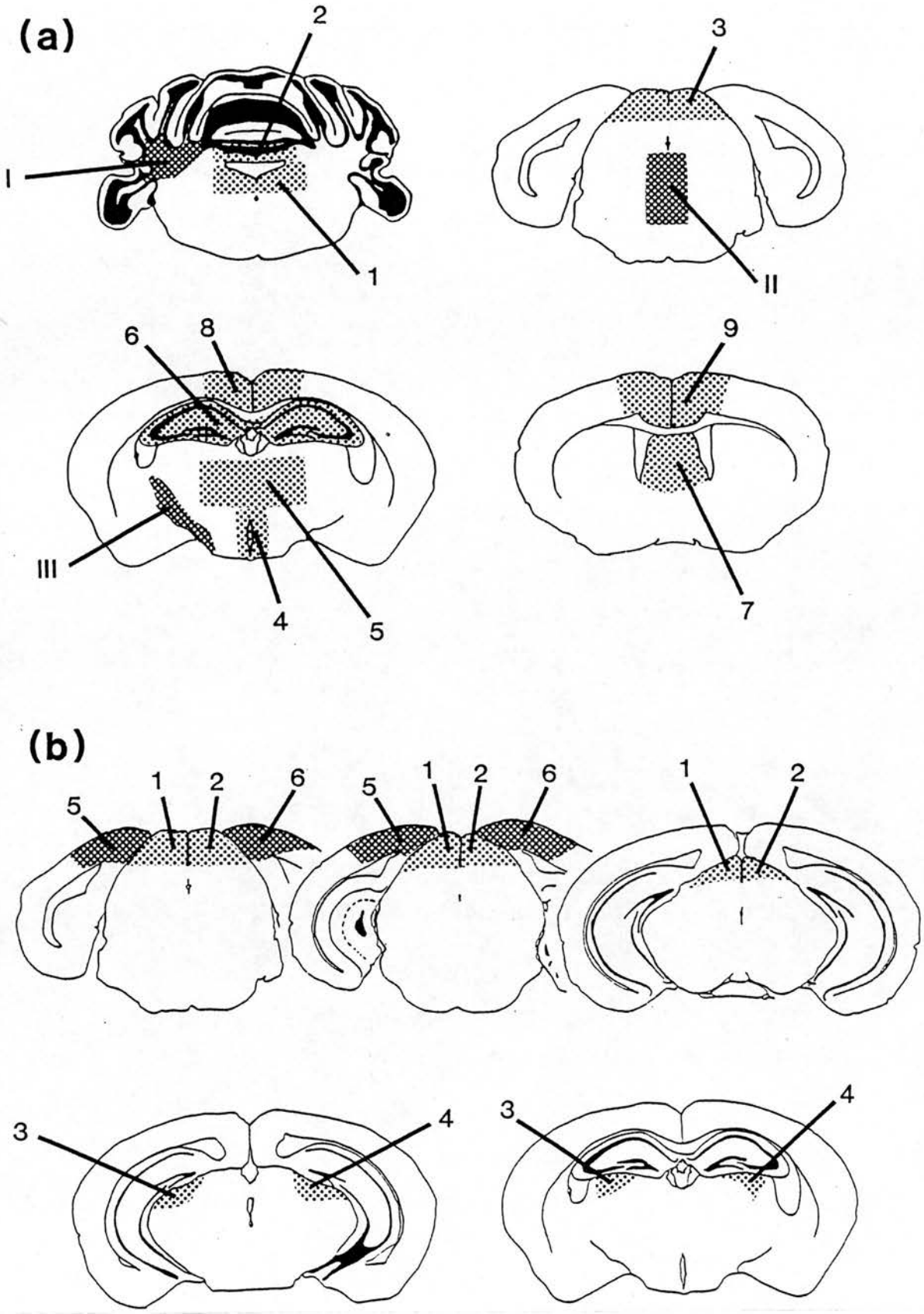

Figure 5. (a) The nine grey matter areas and three white matter areas (I, II and III) which are scored to give lesion profiles, and (b) the six scoring areas for visual system profiles.

shown in Fig. 5a. Three white matter scoring areas (scored on a similar scale but from 0 - 3) are also shown. This assessment of the pathological changes in the mouse brain has been widely used in scrapie studies, especially in distinguishing different scrapie strains (Fraser and Dickinson, 1973; Kimberlin et al, 1987a; Bruce and Dickinson, 1987).

Standard lesion profile scoring of the experiments in this thesis was done by Hugh Fraser and Moira Bruce as part of a routine pathological examination of experimental tissues. This also involves noting any other abnormalities seen, which are recorded and can be referred to if necessary.

Visual projection scoring

Lesion profiles scores amalgamate both sides of the brain, since scrapie vacuolation is almost invariably symmetrical (if any difference is discernable, e.g. as a result of uneven trimmimg, the score is taken from the most severely affected side). However, the intraocular route of infection produces asymmetrical targeting of lesions within the visual projections. For the purpose of this thesis, these lesions were scored in 6 areas from the semi-serial sections taken between inferior colliculus and paraterminal body: left and right superior colliculus, left and right dorsal lateral geniculate nucleus and left and right visual cortex (Fig. 5b, 1 - 6). Other minor visual projections were examined (e.g. parabigeminal nucleus, suprachiasmatic nucleus) and any changes noted.

Retinopathy scoring

The severity of retinopathy was estimated adjacent to the optic disc, where the greatest loss of outer nuclear layer neurons was seen. The normal retina has 10 -12 cells in the ONL (Fig. 1); severe retinopathy can reduce this to a single scattered layer. The scores are defined in Table 5, which is taken from Foster et al, (1986b).

2.10 Tracers, scintillation counting and autoradiography

Tracers

Trypan blue was used to demonstrate the extent of the subarachnoid space which surrounds the optic nerve. Under anaesthesia, up to 0.1ml of a 5% solution in saline was infused i.c. The mouse was maintained under anaesthesia for 1 hour, then killed with an overdose of pentobarbitone, and the optic nerve dissected out. The extent of the staining is shown in Fig. 6a.

A solution of carbon particles (Pelikan Ink, Gunther Wagner) was injected intraorbitally in an attempt to demonstrate lymphoid drainage from the orbit. When the mouse was killed 24 hours later, black labelling of the cervical lymph nodes could be seen (Fig. 6b).

Horseradish peroxidase (HRP) was used to demonstrate both retrograde and anterograde neuronal transport. The methods used are

TABLE 5. The criteria for retinopathy scoring, from Foster et al (1986b).

lesion intensity	minimum depth of cells in central area of retina adjacent to optic nerve	retinopathy score
severe	0 - 2	4
moderate	3 - 4	3
low	5 - 7	2
marginal	8 - 9	1
control retina	10 - 12	0

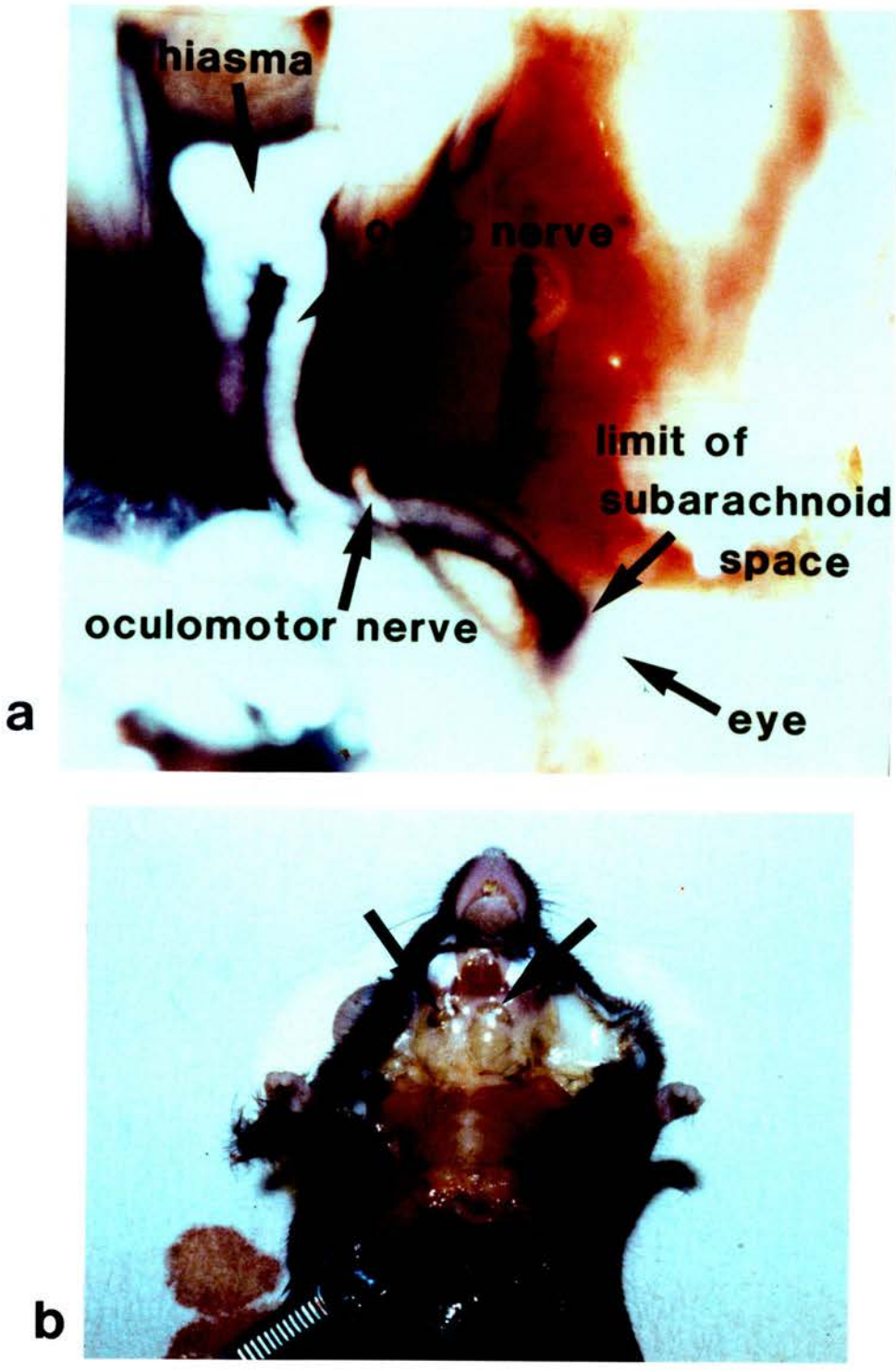

Figure 6. (a) The extent of the sub-arachnoid space shown by i.c. infusion of trypan blue, and (b) carbon particles in the cervical lymph nodes 24 hours after intraorbital injection.

described in Mesulam (1982). Retrograde transport of HRP was demonstrated in the facial (Fig. 7a) and trigeminal (Fig 7b) nuclei following injection into the vibrissal area, and in the hypoglossal nucleus (Fig. 7c) after HRP was injected into the tongue. Demonstration of anterograde transport of HRP from the retina to the visual projection areas requires a more sensitive technique; this was moderately successful, but was not pursued since autoradiography (see below) produced suitable mapping of retinal projections.

Scintillation counting

This method was used to assess rates of transport of labelled tracers (^{3}H proline and ^{35}S methionine) to retinal projections following intraocular injection. Various tissue preparative methods were tested including those of Grafstein et al (1972), Grafstein and Laureno (1973), Sprecht and Grafstein (1973 and 1977) and LaVail et al (1978). A standard procedure was evolved, shown below:

1. mouse injected i.o. as described in 2.5 with 200KBq ^{3}H proline or 400KBq ^{35}S methionine.
2. mouse killed 24 hrs. post-labelling to assay fast transport, 10 days post-labelling for slow transport.
3. brain removed and fixed in formol saline, or Bouin's fixative.
3. Formol/ Bouin's washed out overnight with saline.
4. tissue trimmed, e.g. whole globe, left and right superior colliculus, dorsal lateral geniculate and visual cortex. Samples placed in 0.5ml Optisolve or Lumasolve (tissue solvent) in small

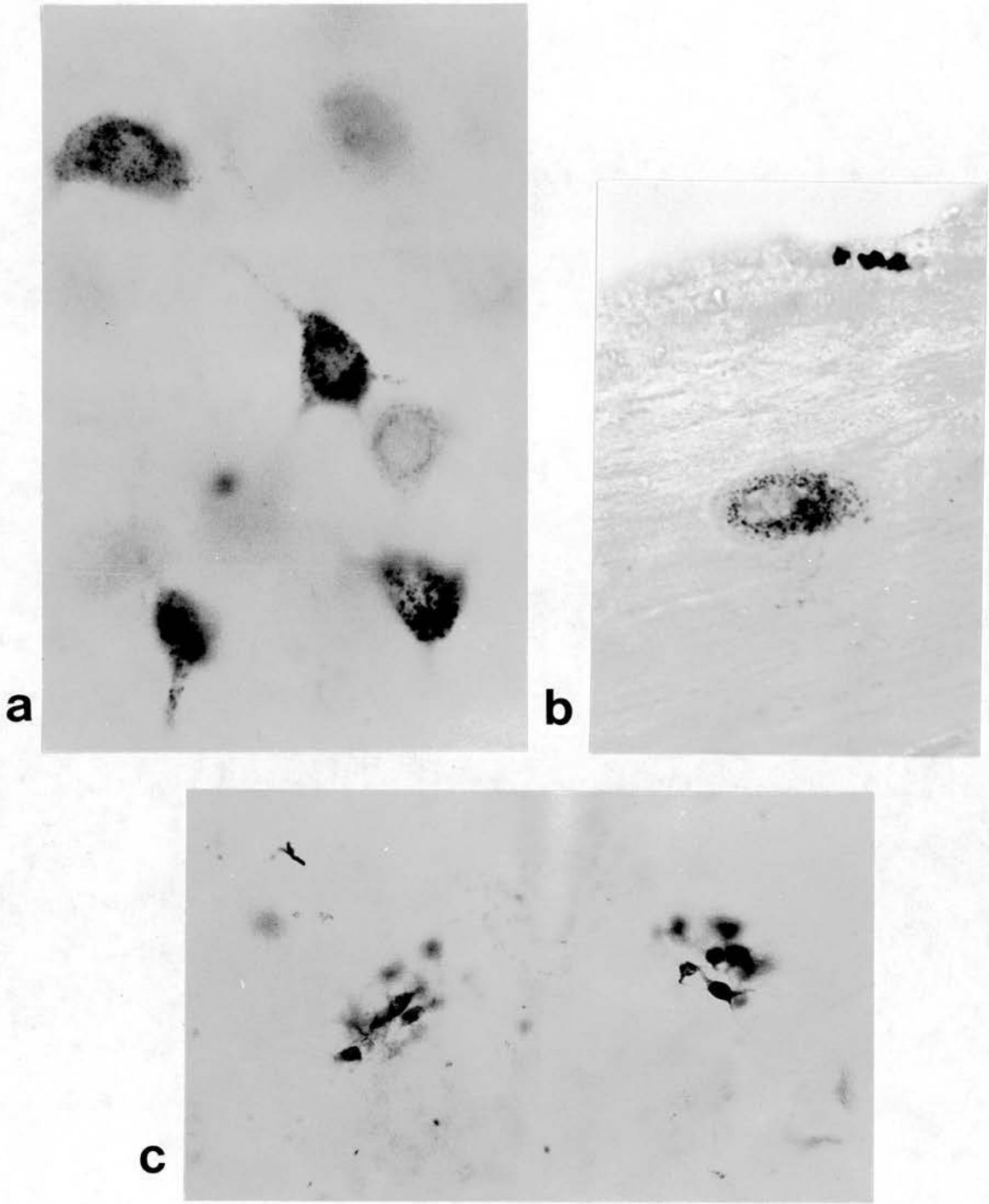

Figure 7. Labelling in (a) the facial nucleus and (b) the trigeminal nucleus following injection of HRP into the trigeminal nucleus; labelling in (c) the hypoglossal nucleus following injection into the tongue.

glass tubes for 2 - 5 days.

5. Sonication for about 20 secs at maximum power on Kontes sonicator, probe tip cleaned in distilled water between each sample.
6. 10ul of each sample put into 5ml scintillant (Optiphase M P) in insert tubes, and 50ul 2N hydrochloric acid added to prevent chemoluminescence. Tubes well shaken.
7. DPM counts made on Rackbeta Spectral scintillation counter.

Protein determination were performed on selected samples by James Hope following tricarboxylic acid extraction (TCA), using the method of Lowry et al (1951).

Scintillation counting was also used to assess the leakage of injected fluid after i.o. injection. The eyes of six mice were wiped with a small pledget of filter paper after bilateral injection of 1ul ^{35}S methionine (0.5MBq), which was dropped directly into scintillant and counted. 1ul of ^{35}S methionine was dropped directly on to a pledget of filter paper as a control. The results are shown in Table 6.

Autoradiography

Eleven SV mice were killed 24 hours after right i.o. injection of 1ul (200kBq) of ^{3}H proline. Right eyes were taken for scintillation counting to assess the effeciency of injection, and brains were fixed in formol saline. Semi-serial sections were prepared as described in 2.8. Autoradiographs were made using Ilford K2 liquid emulsion as described in Rogers (1979). Exposure was at $4^{o}C$ for 28 days.

TABLE 6. Counts (dpm x 10^4)) from eyes injected with 1ul ^{35}S methionine, wiped immediately with a pledget of filter paper, and globe and superior colliculus counted after 24 hours.

mouse no.	tissue	filter paper pledget	total globe	superior colliculus
1.	left eye	9.4	13.5	0.12
	right eye	4.9	18.0	0.13
2.	left eye	2.4	16.0	0.08
	right eye	38.7	6.1	0.05
3.	left eye	52.6	12.3	0.02
	right eye	10.5	0.7	0.07
4.	left eye	37.5	1.5	0.05
	right eye	68.5	4.3	0.03
5.	left eye	6.4	7.5	0.03
	right eye	13.3	3.1	0.07
6.	left eye	22.7	12.5	0.05
	right eye	22.6	7.9	0.08
1ul ^{35}S methionine		68.1		

CHAPTER 3. Targeting of pathological lesions within the visual system

Intraocular infection with various strains of scrapie is known to produce progressive lesions in the contralateral visual projections in the CNS (Fraser and Dickinson, 1985). In this chapter, these observations are extended to six scrapie strains and twelve inbred mouse strains, giving a diverse range of scrapie models, and including all three *Sinc* genotypes. In these models, the appearance and progression of vacuolation following intraocular infection is recorded and analysed, both to highlight the strain-dependent differences in targeting, and to relate the pattern of lesion spread to that of infectivity, which is investigated in Chapter 4. The vacuolar lesion is described below, and in the seven subsequent sections, experiments involving each of the six strains of scrapie have been grouped together in the first six sections, while the seventh examines the effects of the *Sinc* gene.

The nature of the lesions

Vacuolar degeneration of the brain is recognised as the hallmark of scrapie pathology. In mice, unlike sheep, this lesion is seen predominantly in the neuropil, and vacuolated cell bodies are rare. Some scrapie strains (e.g. 79A) produce vacuolation in the white matter. Although the pattern and severity of the grey matter vacuolation varies with each strain of scrapie, the type of lesion remains the same. The range and quality of the lesions seen following i.o. infection were the same as with any other route of

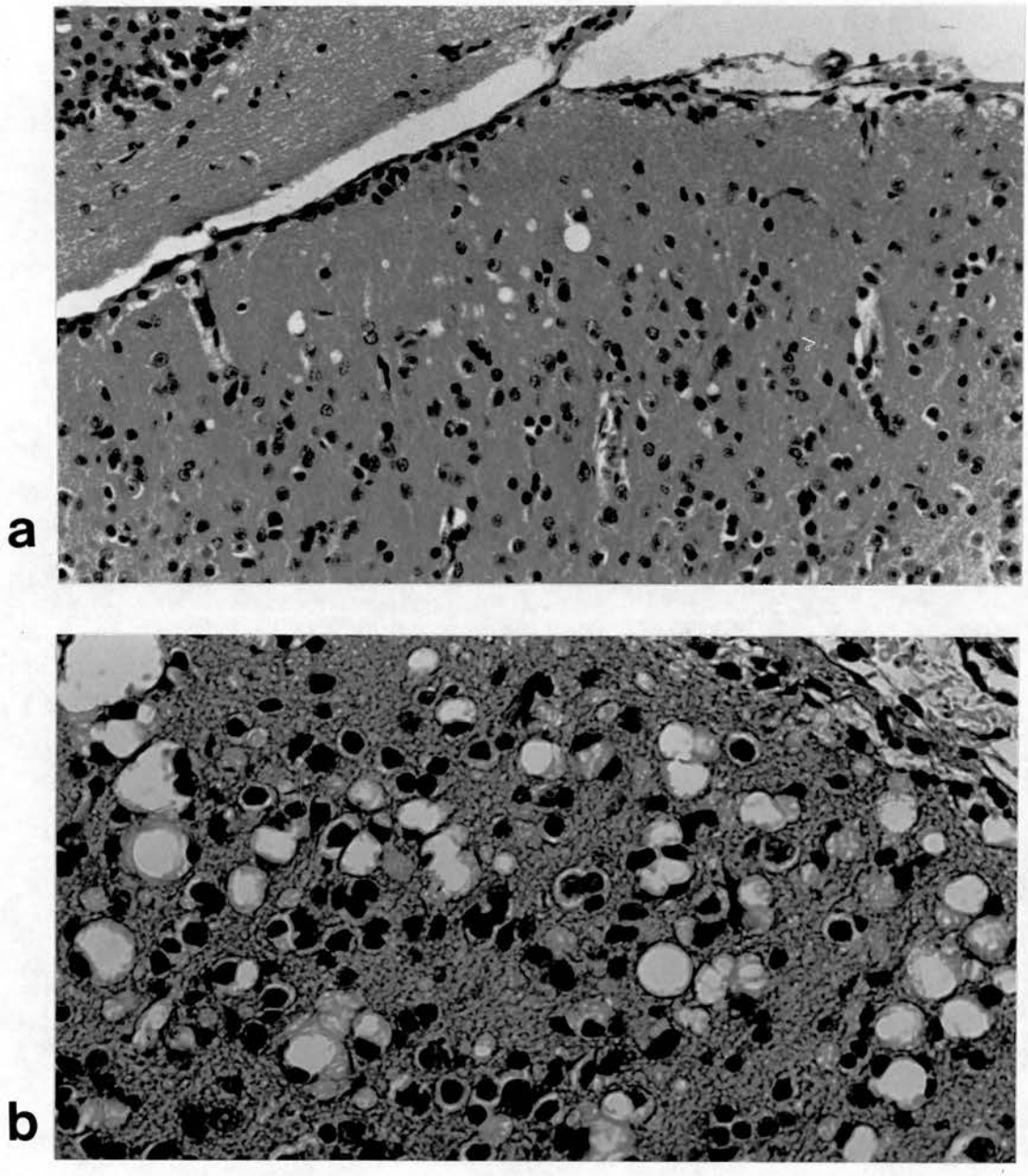

Figure 8. Examples of (a) early, subtle vacuolation and (b) severe vacuolation in the SC.

infection; the only difference being the precise targeting of lesions to visual system projections. The severity of the vacuolar degeneration ranged from a small number of vacuoles seen in otherwise normal tissue (Fig. 8a), to a status spongiosis where the neuropil was reduced to a meshwork of confluent vacuoles and glial scarring (Fig. 8b). Astrocytic hypertrophy was obviously associated with moderate to severe lesions, and could be seen in sites of mild vacuolation with the appropriate staining technique (Hadlow 1961). Astrocytic mitosis and hyperplasia is associated with a more destructive pathology (Scott and Fraser, 1984).

Fraser and McBride (1985) pointed out the problem of distinguishing the spongiosis seen in normal aged mice from scrapie vacuolation. Although ageing lesions could be seen in many of the mice over 600 days old in the experiments described here, both the quality of these lesions (vacuoles with definite boundaries) and their site (usually in the white matter tracts), together with the absence of glial changes, distinguished them from those of scrapie. In a very few cases, however, ageing changes may have masked mild scrapie vacuolation, and made an unequivocal assessment impossible.

Another lesion which superficially resembles that of scrapie vacuolation was produced as a result of enucleation, which leads to a Wallerian degeneration of the optic nerve and tract, and possibly also the geniculo-cortical tract. This is discussed in 5.1(a).

Since many of the experiments described in this thesis demanded early detection of scrapie lesions in specific areas, it was important to identify the minimum criteria necessary for a positive diagnosis. Early, subtle vacuolation in the SC is shown in Fig. 8(a). Several vacuoles show the indistinct boundary typical of

the scrapie lesion. Recognition of such mild lesions was made against a background of experience of the range of 'normal' changes which produce holes in the neuropil (e.g. an artefact of poor fixation). Since all scoring was on coded sections, any inappropriate scores would have become obvious on decoding.

One problem in tabulating the lesion progression arose where mice with lesions only in one area occurred in the same sampling group as mice with more advanced lesions. The tables showing lesion timings also give an incidence figure for primary and secondary lesions; these scores do not include mice with primary lesions in groups with secondary lesions. (Primary and secondary are used here in a temporal, and not pathological sense.) Although mice with primary and secondary lesions occurred in the same sampling group, secondary lesions were never seen in the absence of primary lesions.

Amyloid plaques were produced by the 87V strain of scrapie which is described in 3(b).

3(a) the ME7 strain

The majority of the experiments in this thesis were made with the ME7 strain of scrapie. The three experiments selected below (together with the two experiments in 3(g) on Sinc differences) demonstrate well the targeting of pathological changes after i.o. infection with this strain of scrapie. Before describing the sequence of lesions seen in these models, the parameters of each experiment must be defined.

The i.o. and i.c. incubation periods from experiments 1, 2

and 3 are shown in Table 7. Each experiment continued until the mice developed terminal signs of disease. Other groups in experiment 3 provided the tissues for the sequential assay described in 4(a). All experiments included a group of i.c. infected mice, which meant that the titre of the infecting inoculum (in terms of i.c. ID_{50} infectious units) could be calculated from the mean incubation period by reference to a standard dose-response curve (Appendix B). The differences in the dose of infection given depended on the preparative technique described in 2.3; details for each experiment are given in Table 7.

The differences in i.o. incubation periods were reflected in the progression of the lesions detected; the sampling times and the sites of lesions are shown in Table 8. The pattern of development was the same for all models in experiments 1 and 2; left SC, then left dLGN and in some cases right SC, followed by left VC and right dLGN. Examples of these lesions are shown in Fig. 9, where they are compared with the same areas radiolabelled with ^{3}H proline. The sites of vacuolation at 141, 162 and 190 days in three individual brains are shown diagrammatically in Fig. 10. These are taken from the SM mice in experiment 2, but are representative of the progression of lesions seen in experiments 1 and 2. When the intensity of vacuolation in the 6 visual scoring areas was assessed, the sequence of development was again similar in all models, but differed from those infected with other scrapie strains. This pattern can clearly be seen in SM mice in Fig. 11a, which shows the average lesion severity for each group as the infection progresses. Vacuolation in the VC was never seen in the absence of lesions in the dLGN.

TABLE 7. Experiments with the ME7 strain of scrapie.

experiment no.	mouse strain	i.o. incubation period (n mice)	i.c. incubation period (n mice)	number of i.c. infectious units injected
1.[a]	C3H	298 ±4 (12)	198 ±7 (4)	$10^{2.1}$
2.[b]	SM	237 ±3 (16)	170 ±3 (5)	$10^{4.5}$
	C3H	244 ±9 (6)	177 ±1 (6)	$10^{3.3}$
	VM	539 ±15 (7)	344 ±0 (6)	$10^{4.7}$
3.[c]	C57BL	234 ±3 (29)[d]	166 ±1 (10)	$10^{4.4}$
	C57BL	241 ±4 (4)		

a infected with a 1% suspension spun at 500g for 10 mins.
b infected with a 10% unspun suspension
c infected with a 10% suspension spun at 500g for 10 mins.
d bilateral i.o. infection

TABLE 8. Sites of initial lesions in ME7 experiments.

experiment no.	mouse strain	primary lesions			secondary lesions		
		time	incidence	site	time	incidence	site
1.	C3H[a]	160	1/5	left SC	183	1/8	left dLGN
2.	SM[b]	141	1/5	left SC	162	3/5	left dLGN, VC
	C3H[b]	176	1/5	left SC	176	3/5	left dLGN
	VM[c]	284	1/4	left SC	284	3/4	left dLGN
3.	C57BL[d]	140	1/3	left/right SC	140	1/3	left/right dLGN

a sampling times: 100, 127, 140, 150, 160, 170, 183, 190, 195, 200, 204, 210, 215, 220, 225, 230, 240, 250 and 255 dpi: n = 4–8.
b sampling times: 120, 141, 162, 176, 190, 204, 218 and 232 dpi: n = 4–5.
c sampling times: 200, 221, 242, 263, 284, 298, 312 and 326 dpi: n = 3–4.
d sampling times: 56, 77, 98, 120, 140, 161, 182, 203, 225 and 245 dpi: n = 3.

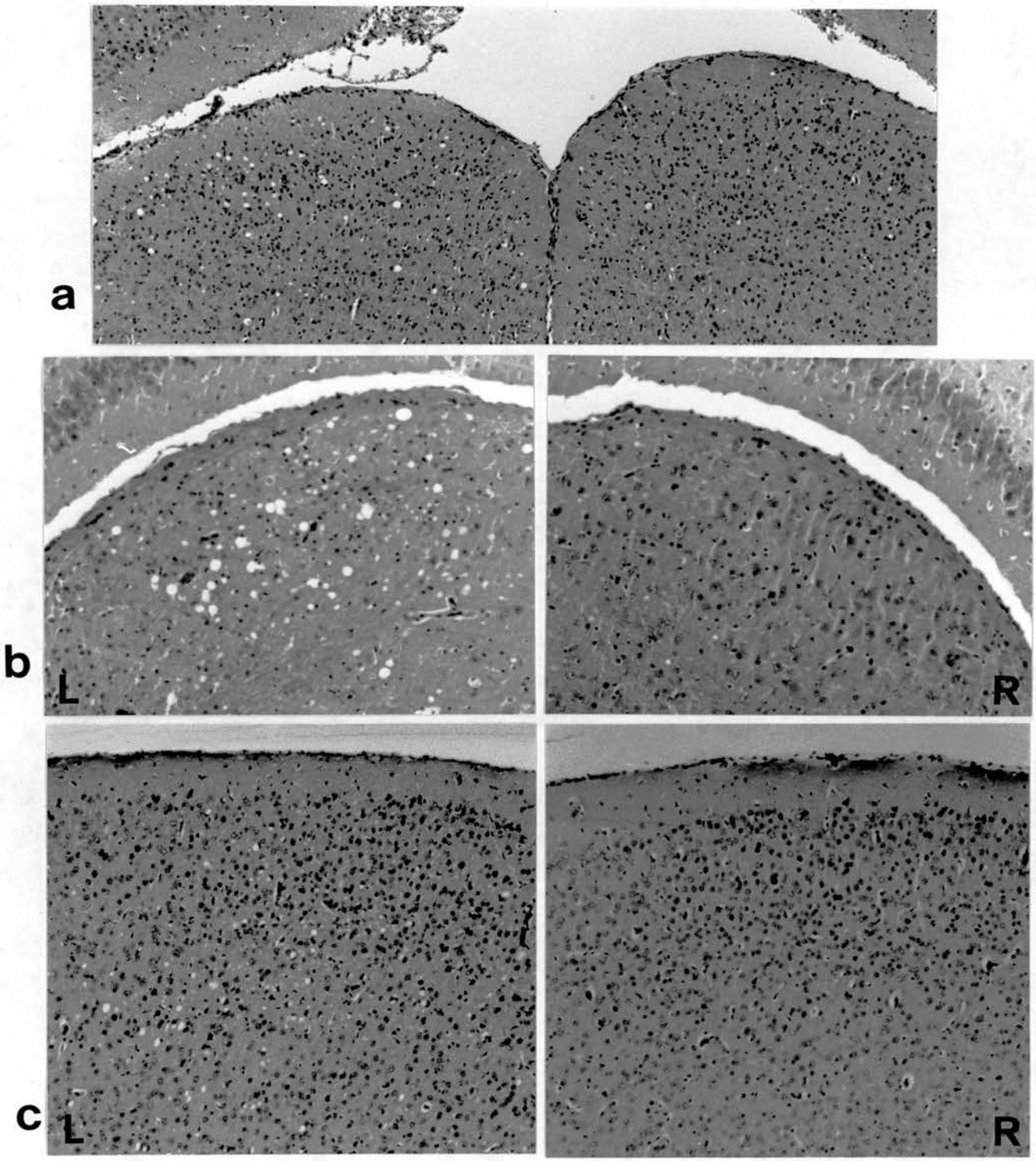

Figure 9. Examples of early lesions targeted to the contralateral CNS in C57BL mice i.o. infected with ME7 scrapie (a) SC, (b) dLGN (c) visual cortex and (d) suprachiasmatic nucleus. Compare these lesions with the labelling in (e) SC, (f) dLGN and (g) suprachiasmatic nucleus produced by i.o. injection of ^{3}H proline.

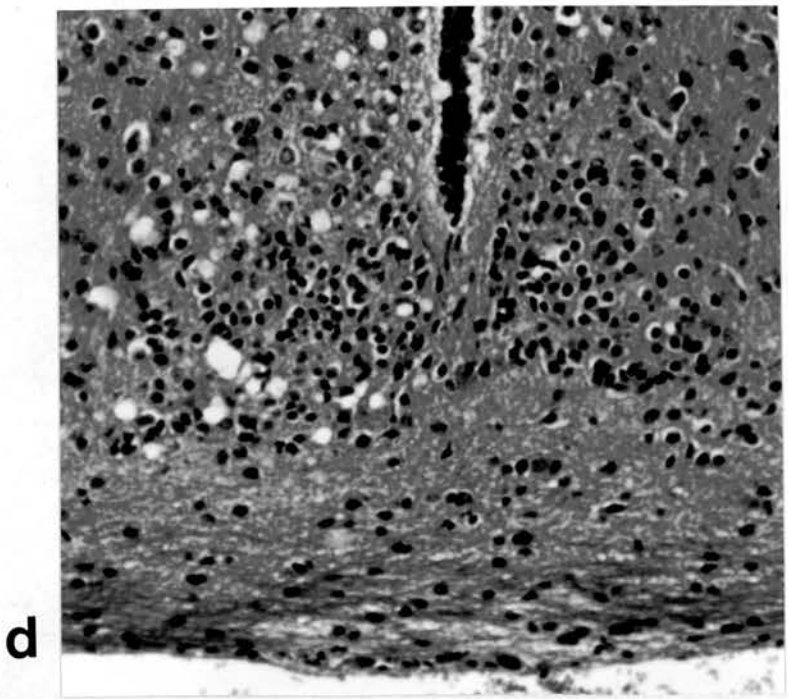

d

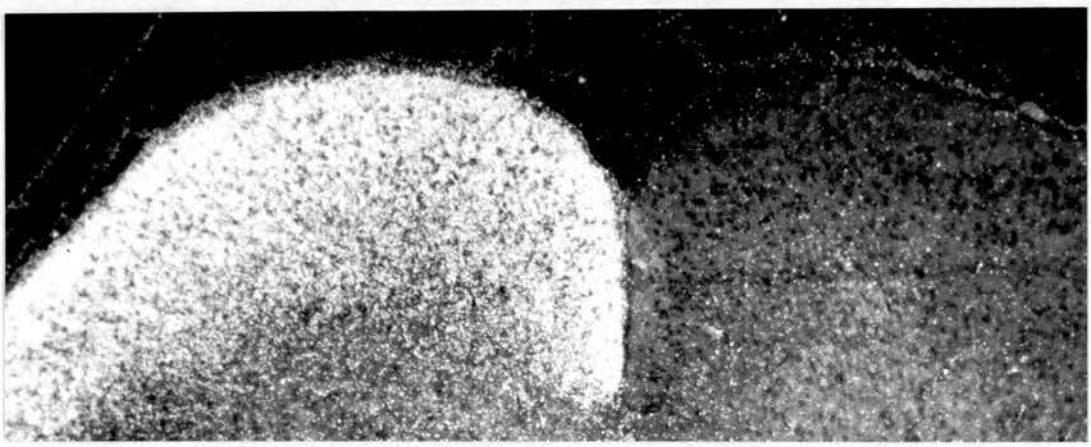

e

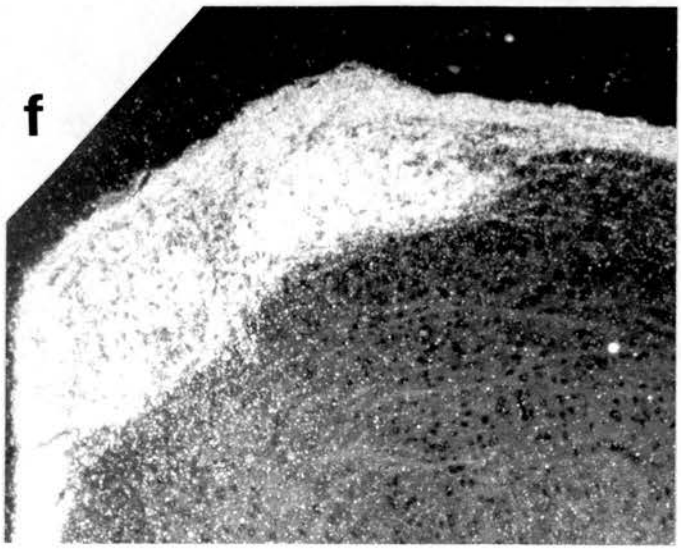

f

g

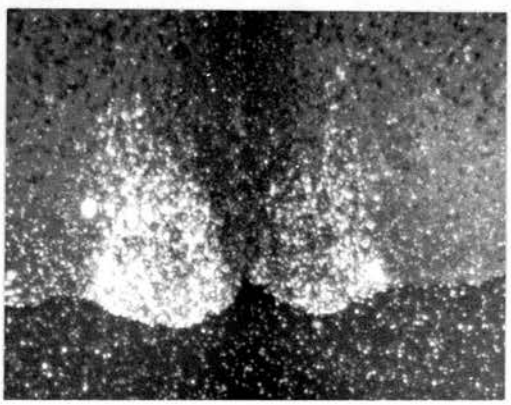

Grey matter vacuolation shown in red, white matter vacuolation in blue.

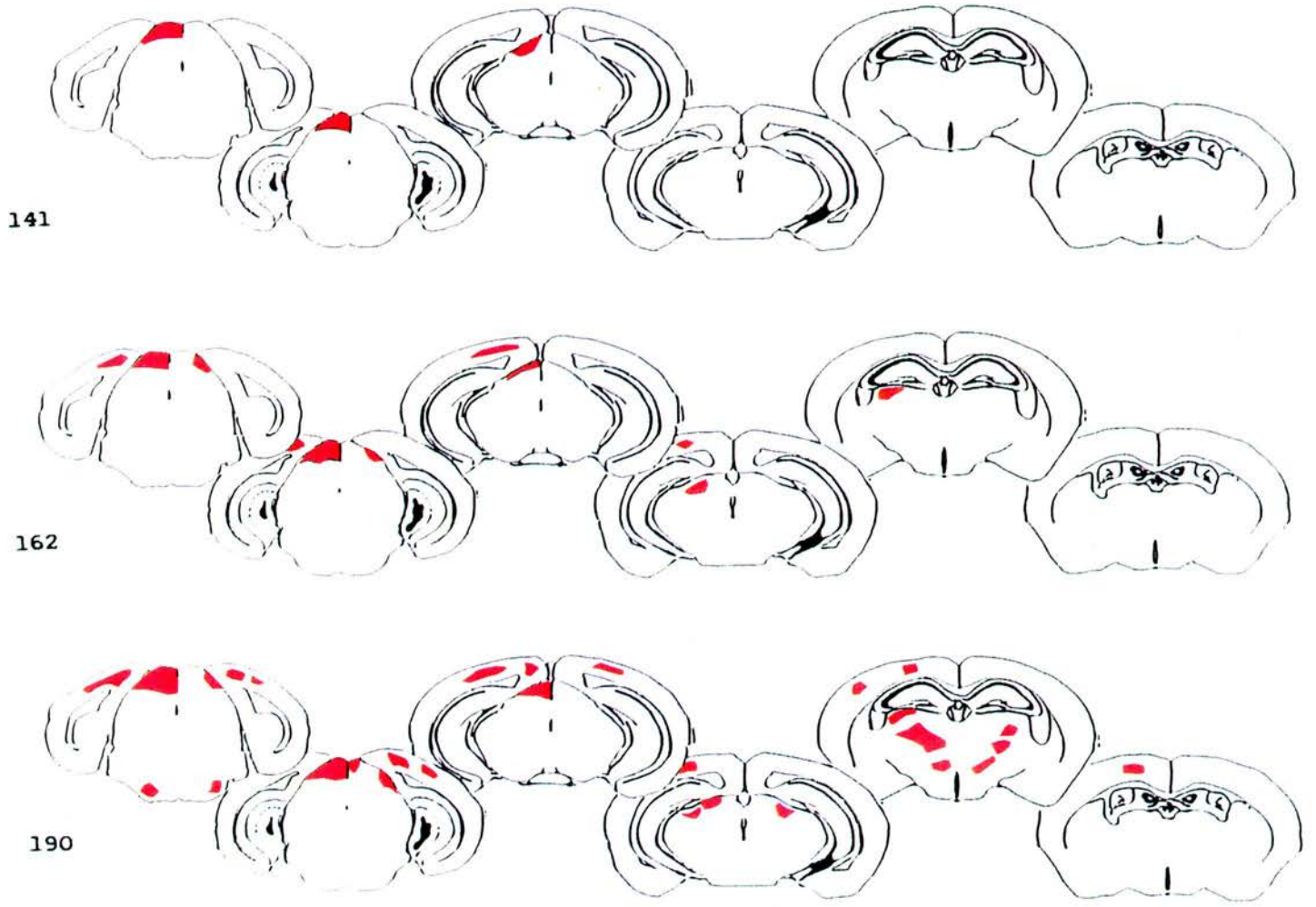

Figure 10. Sites of vacuolation in individual SM mice at 141, 162 and 190 days post-injection, from experiment 2.

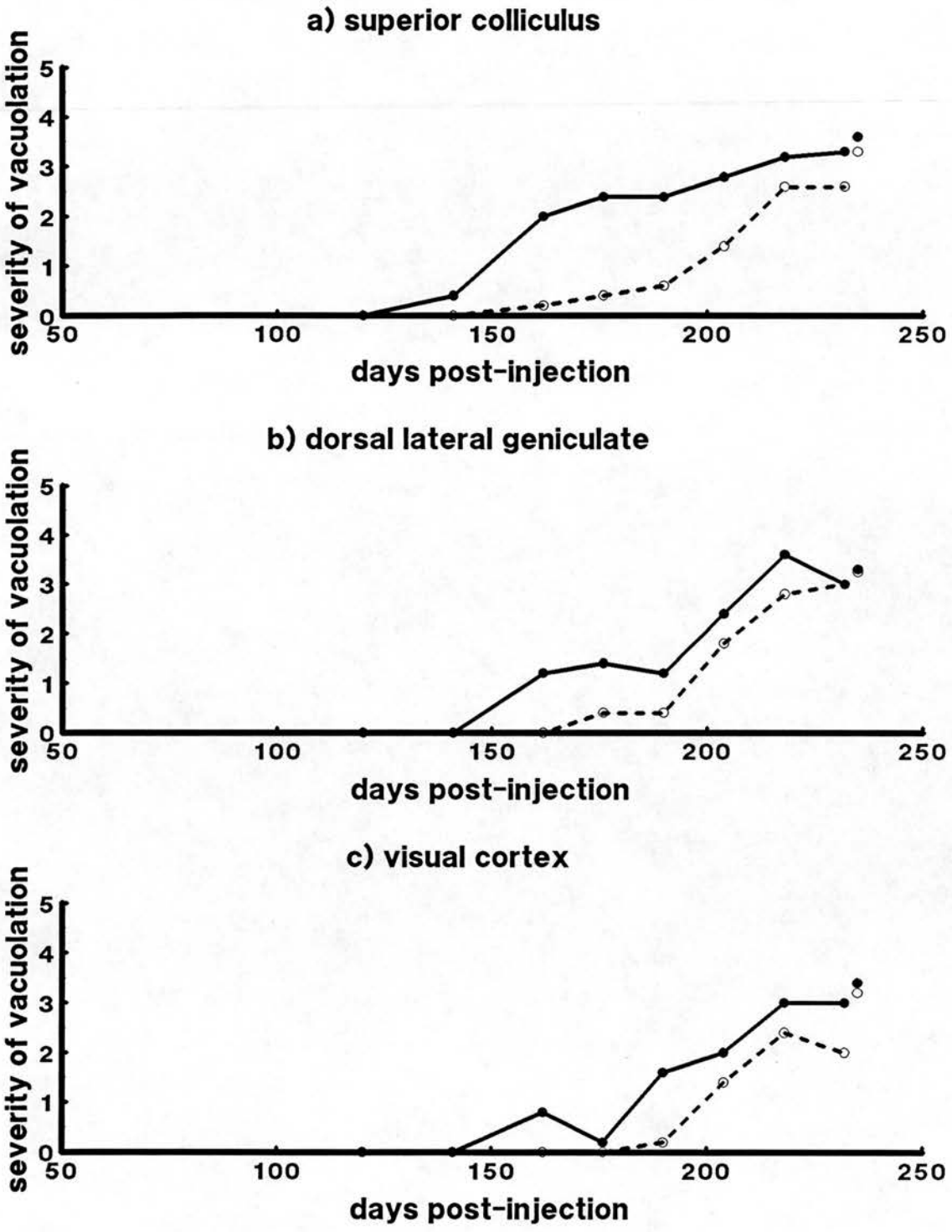

Figure 11(a).
Sequential mean severity of vacuolation in visual scoring areas in SM mice infected with ME7 scrapie from experiment 2. Left side = solid line, right side = broken line. Each group = 5 to 15 mice. The single circles show the mean vacuolation severity in terminal mice; left = solid, right = open.

In experiment 3, which was injected bilaterally, initial lesions occurred on either side, although one side was usually predominant (in the same way that lesions in unilaterally injected mice developed at different rates). By 182 dpi, all mice showed lesions of both colliculi and dLGN.

The only other discrete lesions seen subsequently were in the suprachiasmatic nucleus in VM mice (Fig. 9). It can be seen from Fig. 11b that vacuolation rapidly developed in other areas throughout the brain in these models, obscuring the early asymmetrical lesions. The pattern of vacuolation produced by ME7 scrapie in the terminal i.o. infected mouse, shown by the lesion profile (see 2.9) is very similar to that seen after an i.c. route of infection (Fig. 12b). The i.o. profile in SM mice was slightly lower than that of C3H mice (Fig. 12a).

The timing of the first lesions as a proportion of the incubation period was remarkably consistent in all except the C3H mice, given the limitations imposed by the varying intervals between sampling times. The first lesions occurred at between 50% and 60% of the incubation period in all models, except the C3H mice in experiment 2, in which the first lesions were not seen until 72% of the incubation period had passed. Variations in the timing of the first lesions (Table 8) in comparable models, e.g. 160 and 176 days in C3H mice from experiments 1 and 2 may be exaggerated by the length of time between sampling groups. However, the rate of appearance of detected lesions (shown graphically in Fig. 13) varied with different mouse strains. For example, in experiment 2, groups of SM mice killed up to and on 120 days post-injection were all negative; by 176 days, all in the group were positive. In contrast,

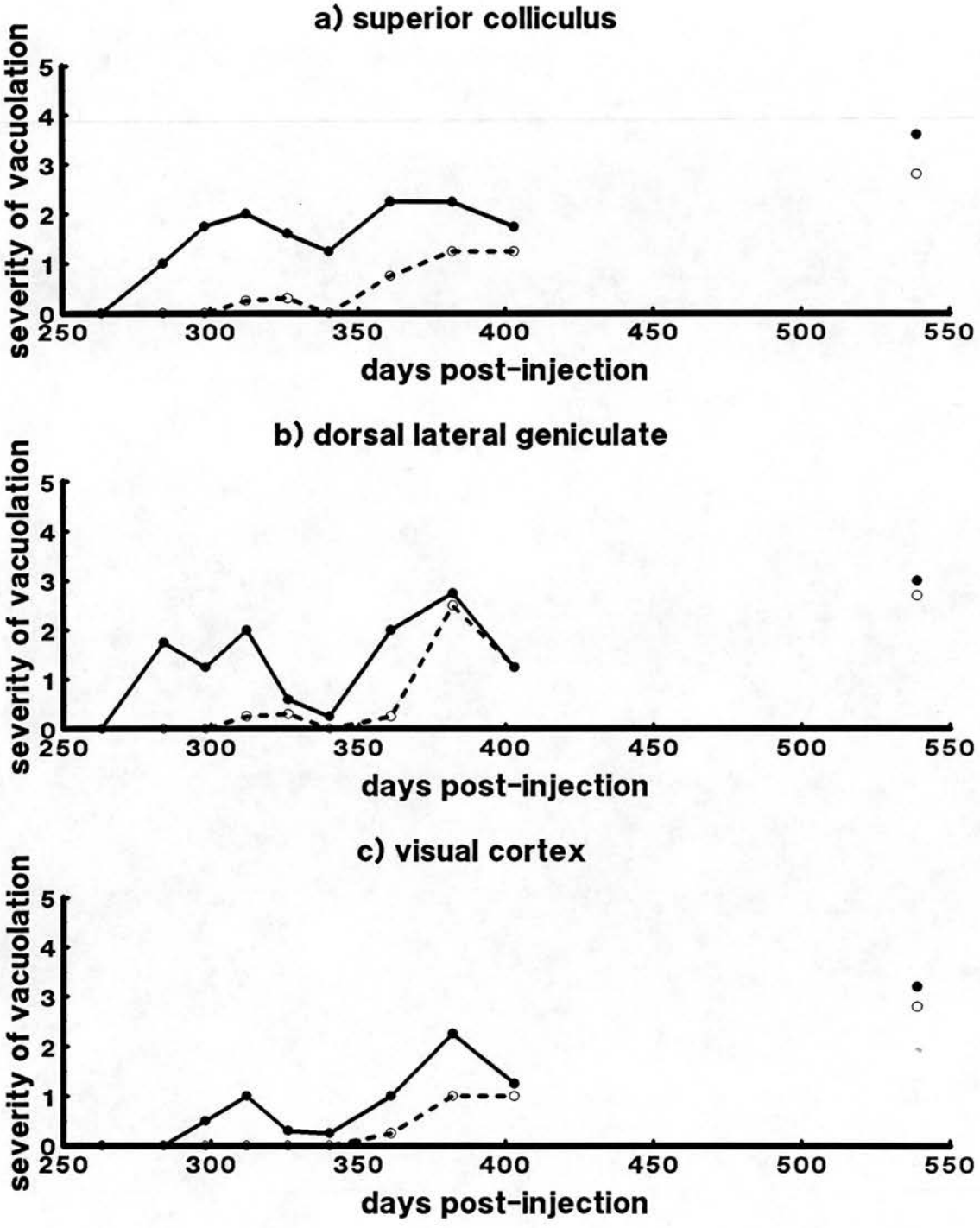

Figure 11(b)
Sequential mean severity of vacuolation in visual scoring areas in VM mice infected with ME7 scrapie from experiment 2. Left side = solid line, right side = broken line. Each group = 4 to 5 mice. The single circles show the mean vacuolation severity in terminal mice; left = solid, right = open.

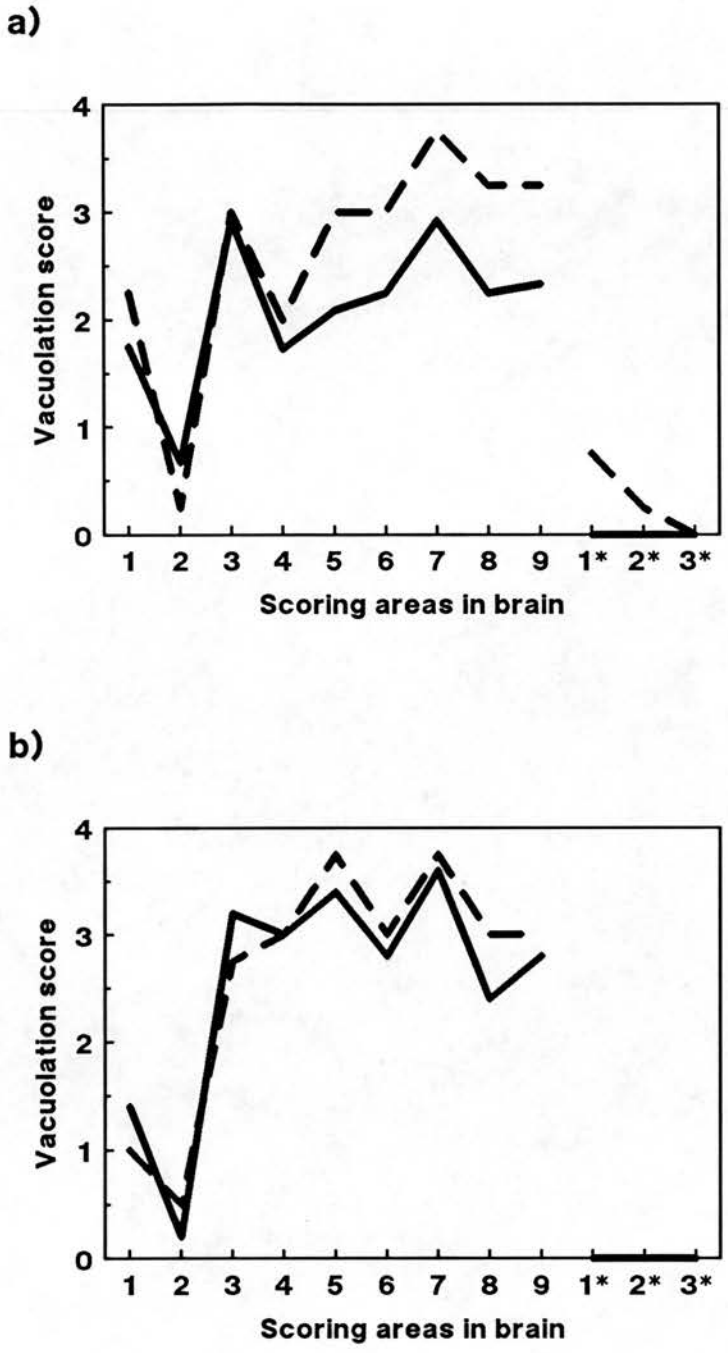

Figure 12.

Lesion profiles from experiment 2. (a) SM (solid line, n = 12) and C3H mice (broken line, n = 4) after i.o. infection; (b) VM mice after i.o. (solid line, n = 5) and i.c. (broken line, n = 4) infection.

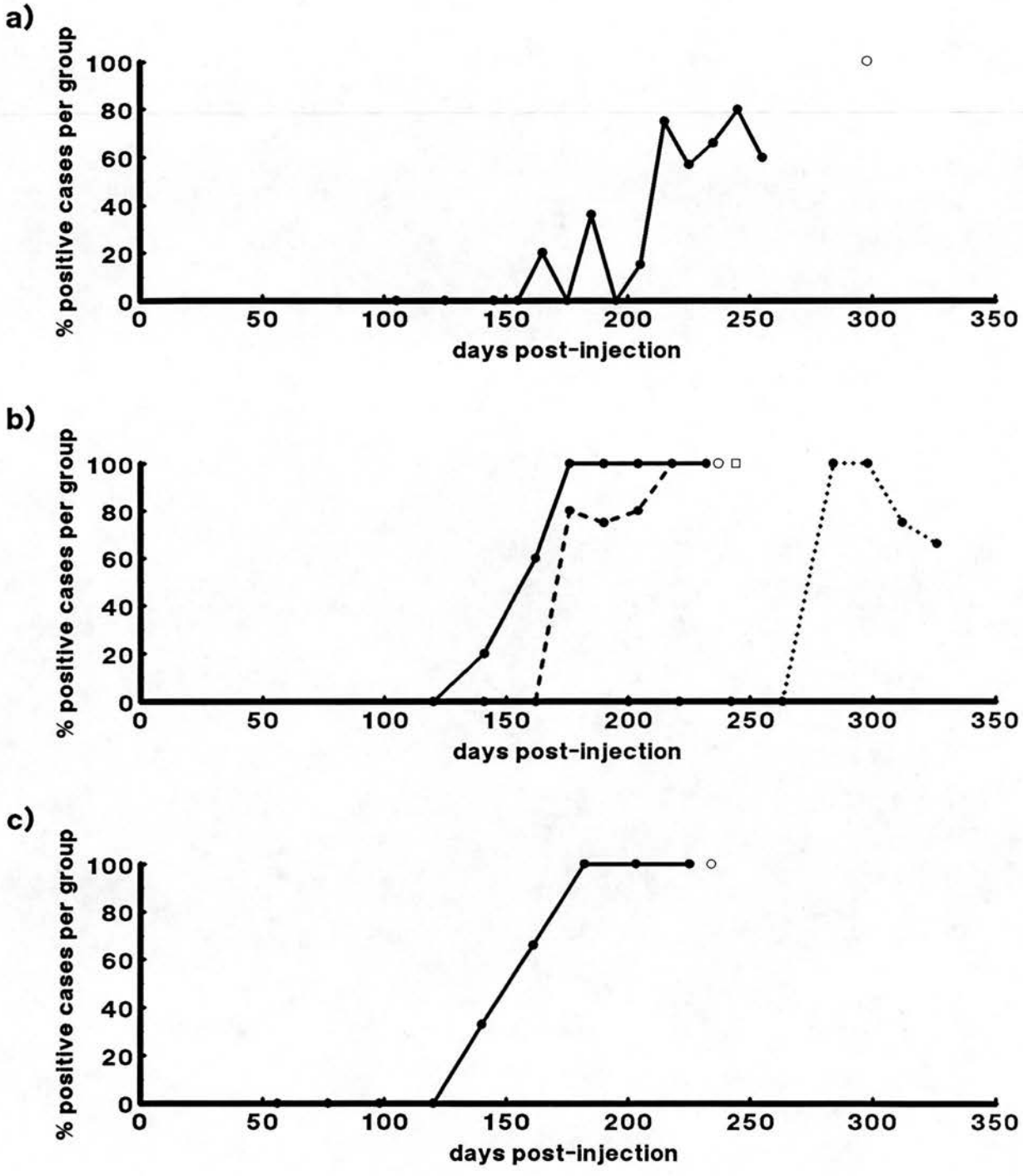

Figure 13.
Sequential percentage of positive cases per group, from (a) experiment 1, (b) experiment 2 (solid line = SM mice, broken line = C3H mice, dotted line = VM mice; and (c) experiment 3. Single circles show incubation periods (except C3H mice in (b), shown by square, and VM incubation period in the same experiment, which was 539 days - not shown).

all C3H mice in the same experiment were negative at 162 days; and not all mice were positive until 218 days. These differences between the C3H mice and other Sinc s7 strains could be associated with the rd gene in the C3H mice (see Discussion).

3(b) the 87V strain

This strain of scrapie is known to produce large numbers of amyloid plaques in VM and especially MB mice, which are both Sinc p7 (Bruce and Dickinson, 1985). The development of PrP labelling using immunocytochemistry is presently being investigated in the Unit, and is not a part of this thesis; analysis of the vacuolar lesion is the principal objective here.

The i.o. route of infection with this strain of scrapie was studied in Sinc p7 mice, since the incubation period in both Sinc s7 mice and the heterozygote is over 700 days. Three experiments were carried out; the incubation periods, and infectivity titres of the infecting doses are shown in Table 9. The shortest i.c. incubation period, and hence the highest titre, was produced by the 10% unspun dilution in the second experiment.

The incubation periods from experiment 4 (Table 9) are only estimates, since there were survivors in both the i.o. and i.c. groups. This is difficult to explain, since the incubation periods of the mice which developed the disease are not long enough to suggest that a limiting dilution was being approached. This anomalous result may have been due to the aggregation of infectious units in the inoculum (discussed by Somerville and Carp, 1983), or

TABLE 9. Experiments with the 87V strain of scrapie.

experiment no.	mouse strain	i.o. incubation period (n mice)	i.c. incubation period (n mice)	number of i.c. infectious units injected
4.[a]	VM	>438 ±16[b]	>296 ±5[b]	$<10^{3.2}$
5.[c]	MB	452 ±4	270 ±2[d]	$10^{4.4}$
6.[e]	VM	466 ±62[f]	298 ±7	$10^{3.4}$

a infected with a 1% unspun suspension
b there were survivors in these groups
c infected with a 10% unspun suspension
d the i.c. incubation period was determined in VM mice
e infected with a 10% suspension spun at 2000g for 10 mins.
f – one mouse in this group died 641 dpi with clinical signs of scrapie (hence large SE); no pathological examination possible.

the effect of injecting small (1ul) volumes of inoculum. Experiment 6 included a full titration of the inoculum to give a dose-response curve, and a precise estimate of the infectious dose, in an attempt to clarify this problem; the results of the titration are not yet available. However, the lack of incubation period data has not affected the sequential lesion targeting results.

The time and site of the appearance of vacuolation after infection with the 87V strain is shown in Table 10. Unlike ME7, the initial lesions all occur in the left dLGN. The sequence of development was similar in all three experiments; left dLGN, then left SC, right dLGN and possibly oculomotor nucleus (OCM), the ventral thalamic nuclei and the dorsal raphe in the midbrain. Examples of early lesions are shown in Fig. 14, including the normal SC in a mouse with obvious left dLGN lesions. Three examples of the areas affected at 280, 320 and 340 days are shown diagrammatically in Fig. 15, taken from individual VM mice in experiment 6. The lesions of the OCM were most apparent in experiment 5 in MB mice, and developed earlier in the sequence than in VM mice; they were always symmetrical. The earliest case to show lesions in experiment 5 was in the first group to be killed; it is possible that an even earlier case may have occurred had there been an earlier group.

Although lesions in the dLGN became severe, and occurred earlier than in any other area, associated lesions in geniculocortical projection areas were absent in the majority of cases in this model. This is best illustrated in Fig. 16, which shows the progression of lesions scored in the 6 visual areas. In general, vacuolar lesions in the cortex are not seen with this

TABLE 10. Sites of initial lesions in 87V experiments.

experiment no.	mouse strain	primary lesions			secondary lesions		
		time	incidence	site	time	incidence	site
4.	VM[a]	255	1/3	left dLGN	317	2/2	left SC
5.	MB[b]	209	1/2	left dLGN	267	2/3	left SC
6.	VM[c]	280	2/4	left dLGN	320	3/4	left SC, thalamus[d]

a sampling times: 226, 240, 255, 275, 289, 303, 317, 331, 336, 345, 359, 373, 387, 401 and 415 dpi: n = 2-3.
b sampling times: 209, 238, 267, 295, 322, 352, 380, 408 and 435 dpi: n = 2-8.
c sampling times: 240, 260, 280, 300, 320, 340 and 360 dpi: n = 2-4.
d ventral thalamic nucleus

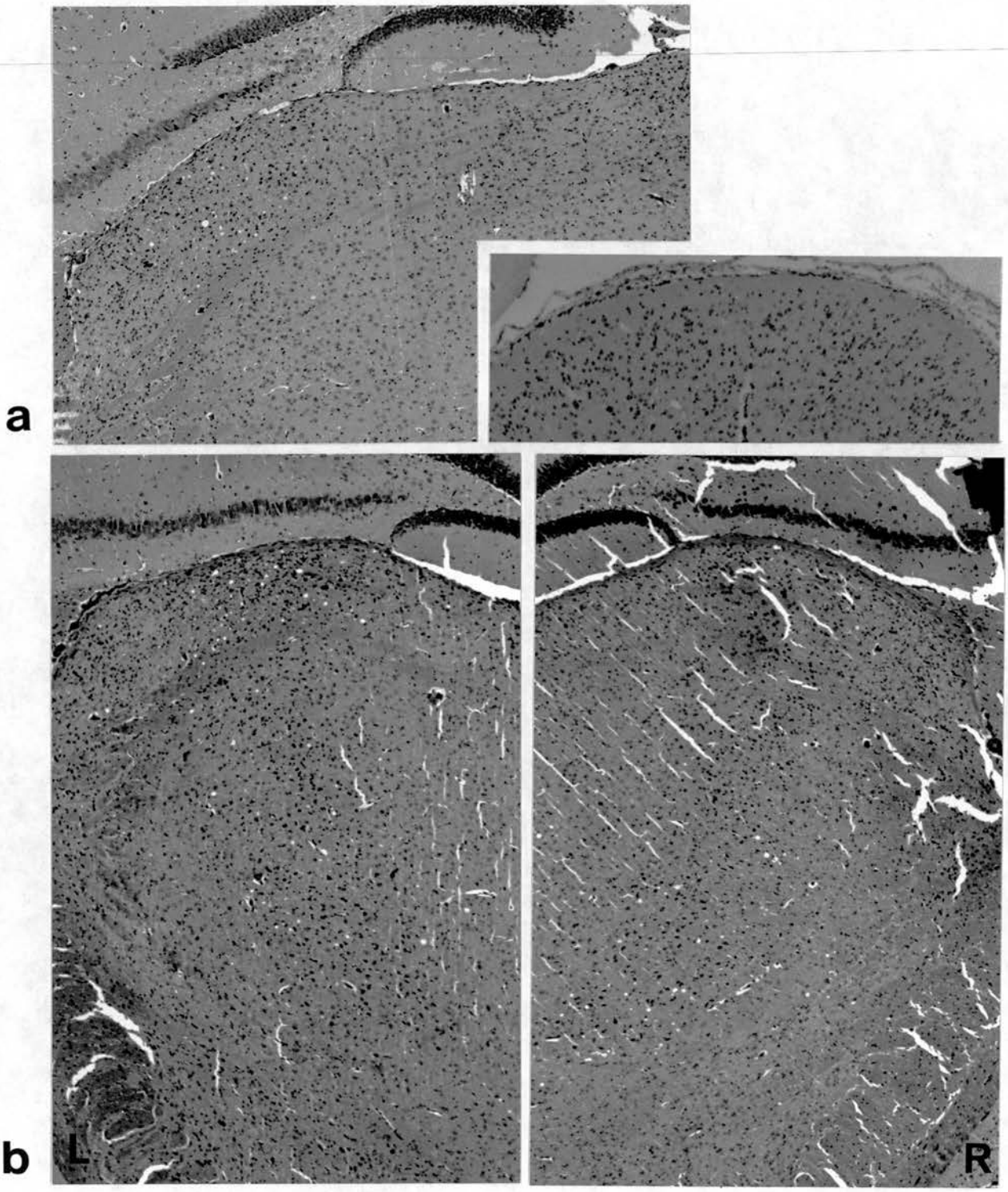

Figure 14. Examples of early lesions in the CNS with 87V scrapie (a) left dLGN (inset shows SC with no lesions), (b) left and right ventral thalamic nuclei.

Grey matter vacuolation shown in red, white matter vacuolation in blue.

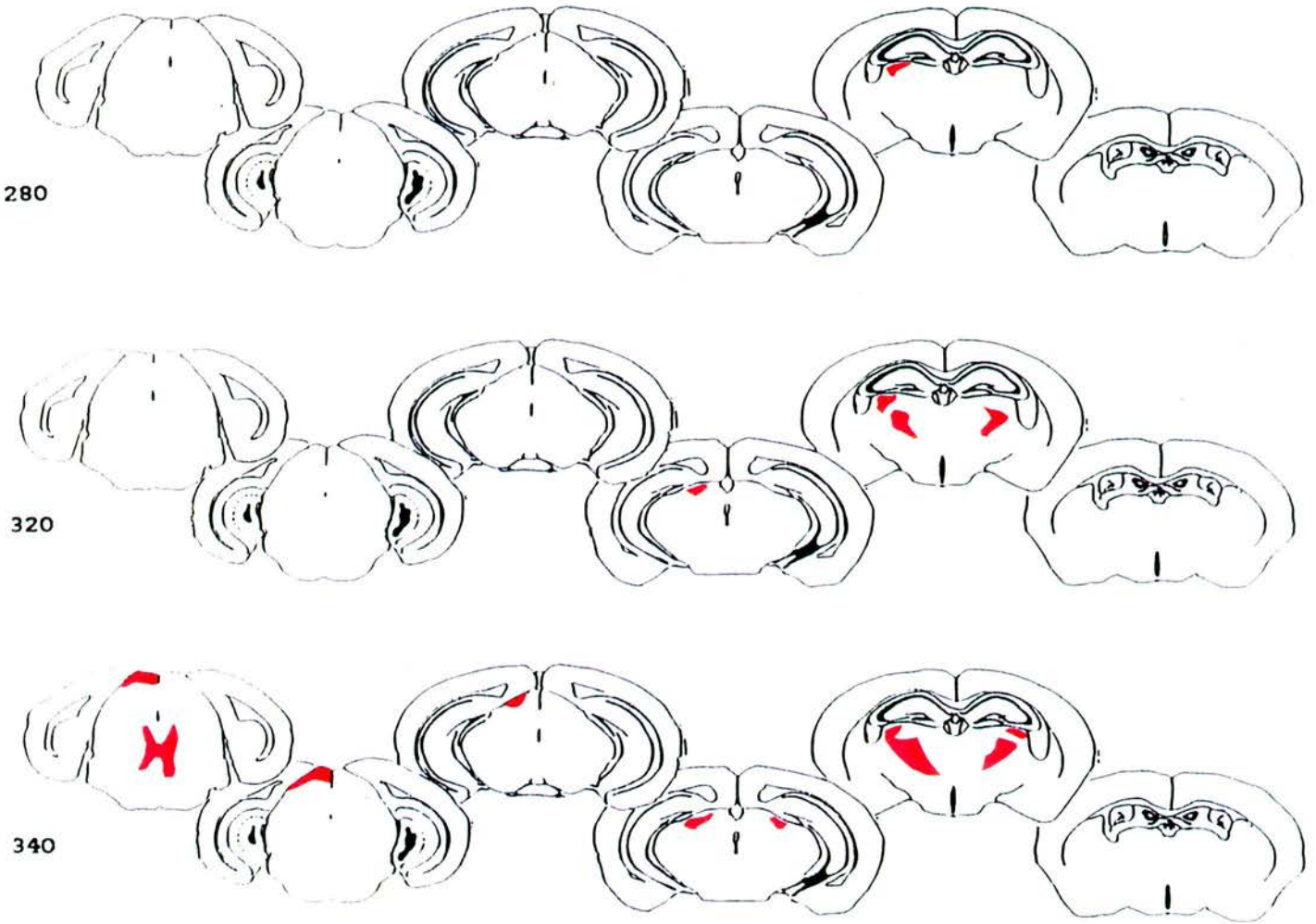

Figure 15. Sites of vacuolation in individual VM mice at 280, 320 and 340 days post-injection from experiment 6.

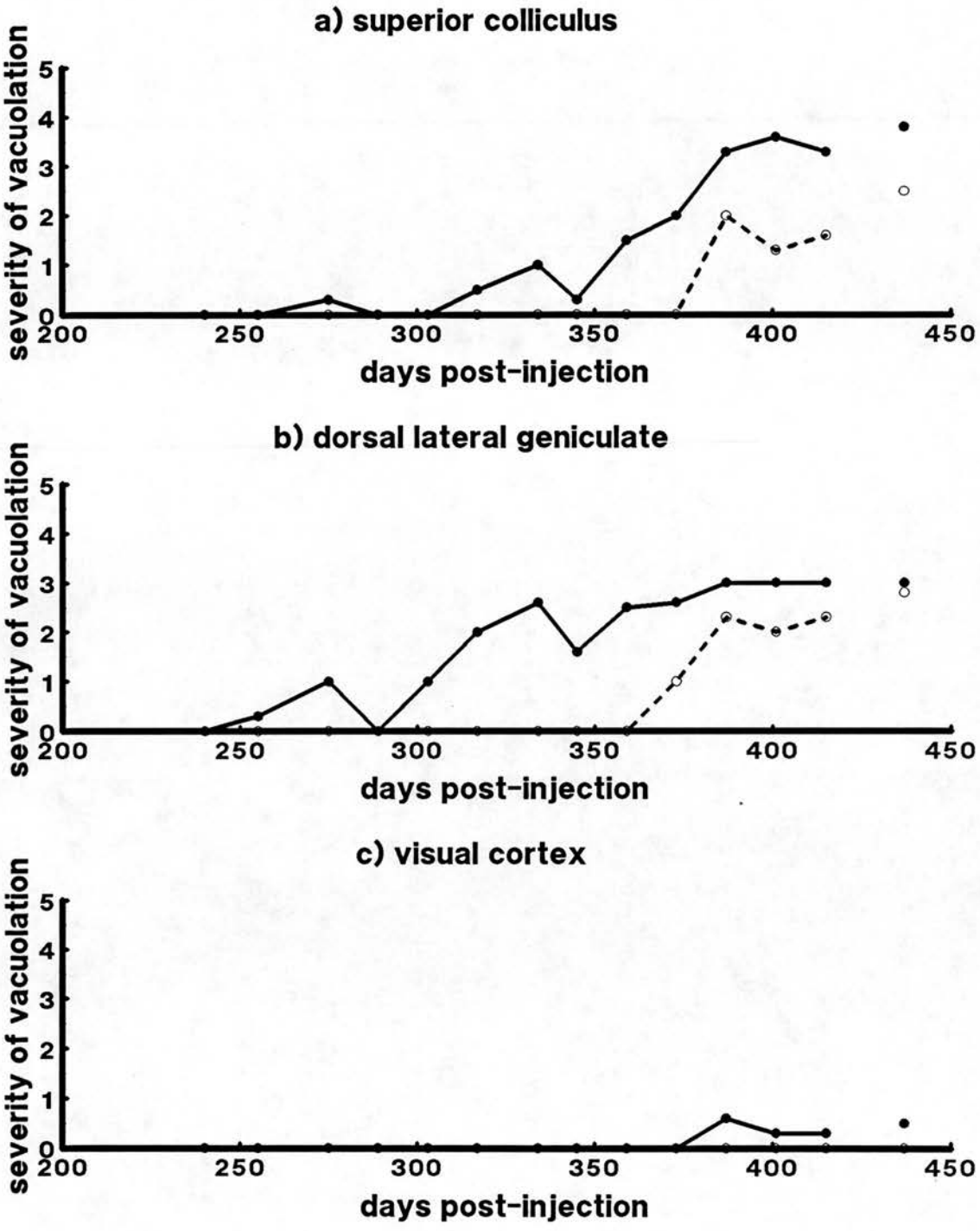

Figure 16.
Sequential mean severity of vacuolation in visual scoring areas in VM mice infected with 87V scrapie from experiment 4. Left side = solid line, right side = broken line. Each group = 2 to 4 mice. The single circles show the mean vacuolation severity in terminal mice; left = solid, right = open.

strain of scrapie, even after i.c. infection, although high numbers of plaques develop there (Bruce et al, 1981). The i.o and i.c. lesion profiles are compared in Fig. 17; although similar, the vacuolation score for the SC (area 3) is much higher in the i.o. profile. There is also a lesser increase in lesion severity in the hypothalamus (4).

The number of mice with positive vacuolar lesions in each group is shown in Fig. 18. Although there was a survivor in the i.o. incubation group in experiment 4 , there are no equivalent negative mice in the groups killed between 317 and 415 days. Experiment 5, in contrast, produced a compact incubation period (452 ±4), but there were negative individuals in some of the later groups (352, 380 and 408 days). In experiment 6, the incidence of lesions increased from zero to 100% between 260 and 320 days, and remained at 100% in the later groups. These results, together with those of experiment 30, emphasise the need to use the highest possible dose of infection when using 87V scrapie by the i.o. route.

3 (c) the 79A strain

This strain of scrapie is characterised by its relatively short incubation period following i.c. infection, and the vacuolar degeneration of the white matter produced in addition to grey matter lesions. It also produces a primary lesion in the retina - a widespread loss of photoreceptor cells (see 1.3). Lesion targeting after i.o. infection was investigated in one major experiment (no. 7) in three strains of mice, and was also checked in a limited

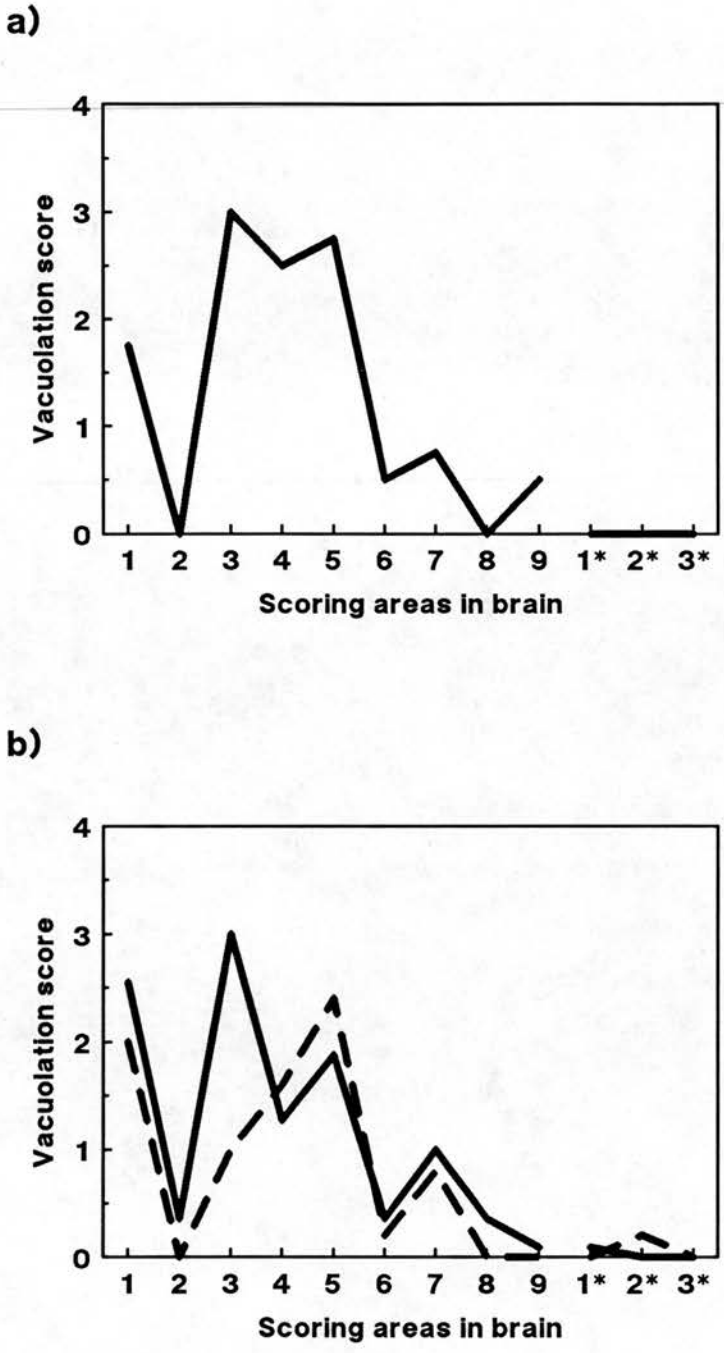

Figure 17.
Lesion profiles from (a) experiment 4; VM mice (n = 4) after i.o. infection; and (b) experiment 6; MB mice (solid line, n = 11) after i.o. infection (broken line, n = 5) after i.c. infection.
1 - 9 are grey matter areas, 1 - 3 are white matter areas.

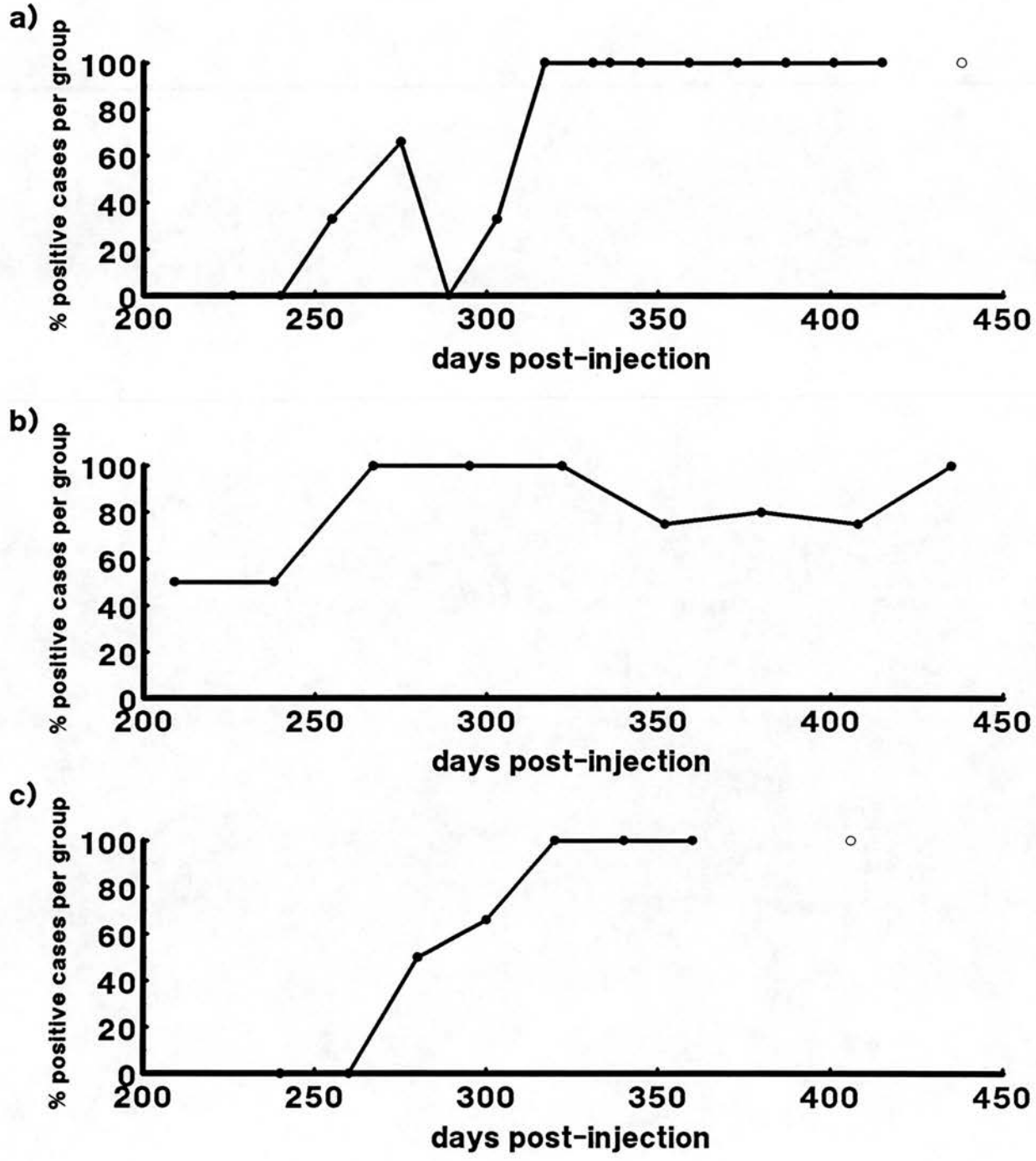

Figure 18.

Sequential percentage of positive cases per group, from (a) experiment 4, (b) experiment 5 and (c) experiment 6. Single circles show incubation periods.

number of groups in a second experiment (no. 8) which provided the source material for an assay of infectivity titres in visual projection areas (see 4(a).

Experiment 7 was set up as a series of injections, to provide mice at different stages of the incubation period (for electroretinography, outside the field of this thesis; see Curtis et al, 1989). The i.o. incubation periods for the three strains in experiment 7, and the i.o. and i.c. incubation periods from experiment 8 are shown in Table 11. For each i.o. injection group in experiment 7, a group of SV mice were also injected by the i.c. route. The dates of injection and i.c. incubation periods for these SV mice are shown in Appendix C, with the estimated number of infectious units per dose. Unfortunately, there was a considerable range of infectious doses, so that the the sampling times do not represent a chronological progression. In order to be able to standardise the i.o. sampling times, the i.c. incubation periods have been expressed as a percentage of the incubation period of the shortest group, so that the dates of killing can be reestimated by subtracting the original sampling day from the same percentage difference as between the i.c. incubation period for the group and the shortest incubation period (calculations given in Appendix C). The estimated sampling intervals are shown as a footnote to Table 12.

In experiment 8, three mice were killed at 100 and three at 140 days. None had vacuolar lesions. Lesion profiles from the end-point groups in this experiment are shown in Fig. 19; note the relatively low grey matter, and higher white matter scores typical of 79A as compared to ME7 and 87V.

TABLE 11. Experiments with the 79A strain of scrapie.

experiment no.	mouse strain	i.o. incubation period (n mice)	i.c. incubation period (n mice)
7.[a]	SV	253 (2)	-
	C3H	244 ±27 (3)	-
	MM	289 ±12 (5)	-
8.[b]	C57BL	205 ±6 (6)	155 ±8 (6)

a infected with aliquots from a 1% unspun suspension, and reground before use.

b infected with a 5% suspension diluted from a 10% pool, reground and spun at 500g for 10mins.

TABLE 12. Sites of initial lesions in 79A experiments.

experiment no.	mouse strain	primary lesions			secondary lesions		
		time	incidence	site	time	incidence	site
7.	SV[a]	153	1/12	left dLGN	153	3/12	left VC
	C3H[b]	169	1/6	left dLGN	178	2/6	right dLGN
	MM[c]	169	1/4	left dLGN,SC	178	2/6	right dLGN, left/right VC
8.	C57BL[d]	all mice in both sampling groups were negative					

a sampling times: 113, 127, 138, 153, 158, 164, 166, 176, 180 and 183 dpi: n = 5-12.
b sampling times: 92, 113, 127, 138, 153, 158, 167, 169, 178, 183 and 188 dpi: n = 3-6.
c sampling times: 113, 127, 138, 153, 158, 169, 178, 180, 183 and 221 dpi: n = 3-6.
d sampling times: 100 and 140 dpi: n = 3.

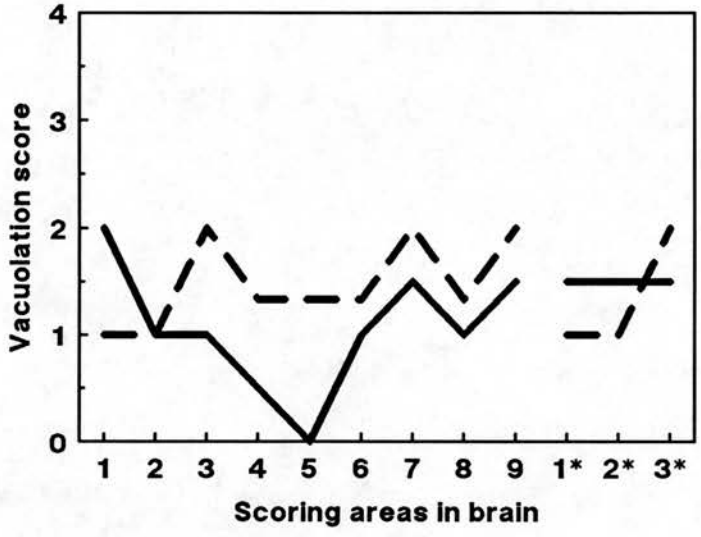

Figure 19.

Lesion profiles from experiment 8. C57BL mice after i.o. (solid line) and i.c. (broken line) infection with 79A scrapie.

Despite the relatively long i.o. incubation periods in experiment 7 compared to experiment 8 (and experiment 29, also 79A), when the date of each killing group was recalculated to correct for the difference in dose, a clear system of lesion development emerged, which is similar in each strain of mouse (Table 12). The earliest lesions just involve the left dLGN, but within 8 days, the left visual cortex and SC are affected (Fig. 20). White matter vacuolation, especially in the ventral mid-brain tracts, did occur with early grey matter lesions, but was always symmetrical. At later sampling times, lesions were seen in both SC and the visual cortices, both dLGN, and extending into the thalamus. Eyes were examined from the MM mice. Some inconsistent early photoreceptor loss in the right eye was probably due to injection damage, but consistent loss of the outer nuclear layer in the left eye was seen in mice killed from 169 days (estimated date) onwards.

The estimated dates of killing were used to construct Fig. 21, which shows the progression in the percentage of positive cases in the three mouse strains. The earliest lesions occur in the SV mice, although the C3H mice had the shortest incubation period. The first lesions developed at 60%, 69% and 58% of the incubation period in the SV, C3H and MM mice respectively, again suggesting that the rd gene in C3H mice is delaying the development of lesions.

3(d) the 22A strain

This strain of scrapie, in contrast to ME7, has a 'short' incubation period in mice which are homozygous for the p7 allele of

Grey matter vacuolation shown in red, white matter vacuolation in blue.

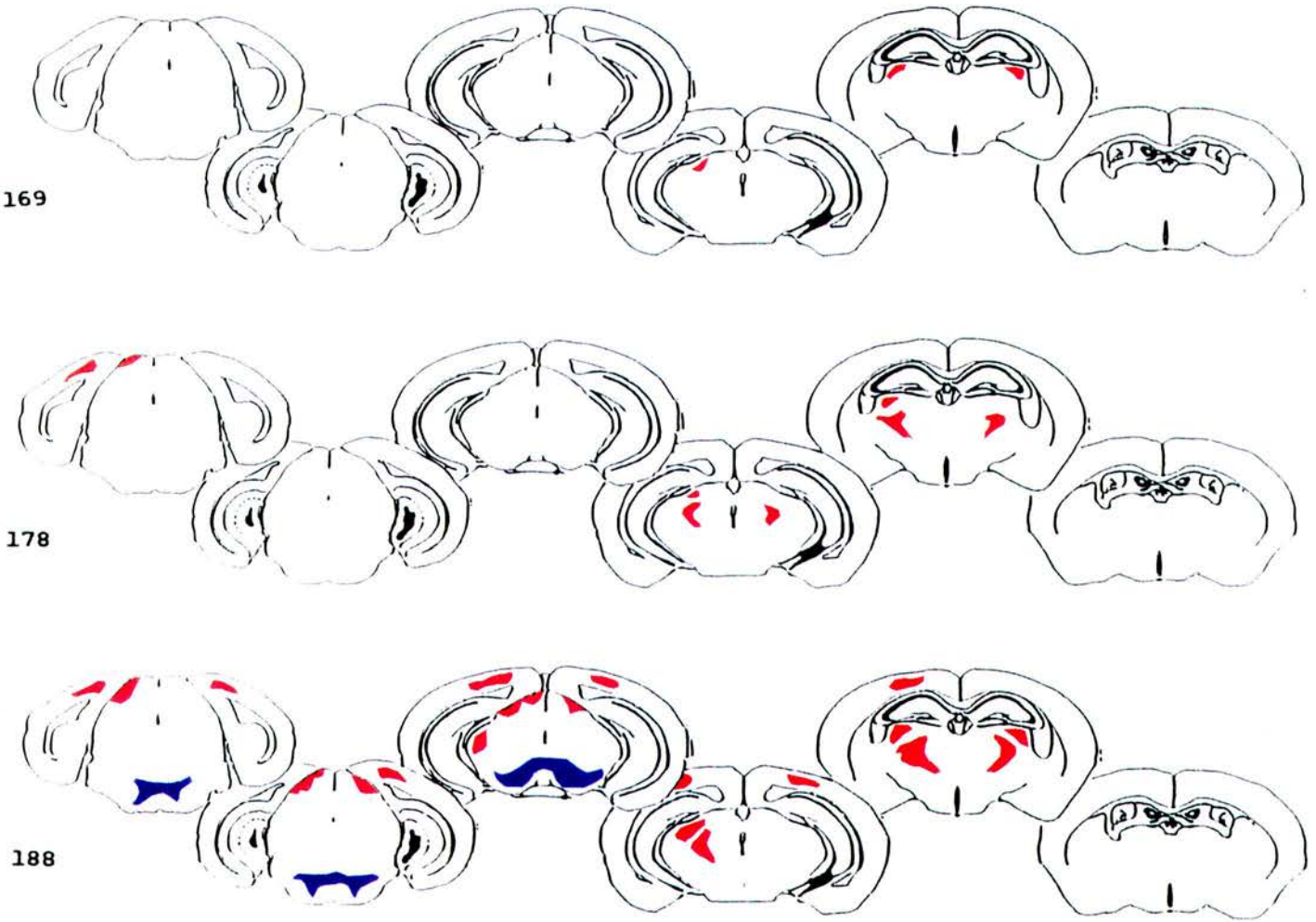

Figure 20. Sites of vacuolation in individual C3H mice at 169, 178 and 188 days post-injection from experiment 7.

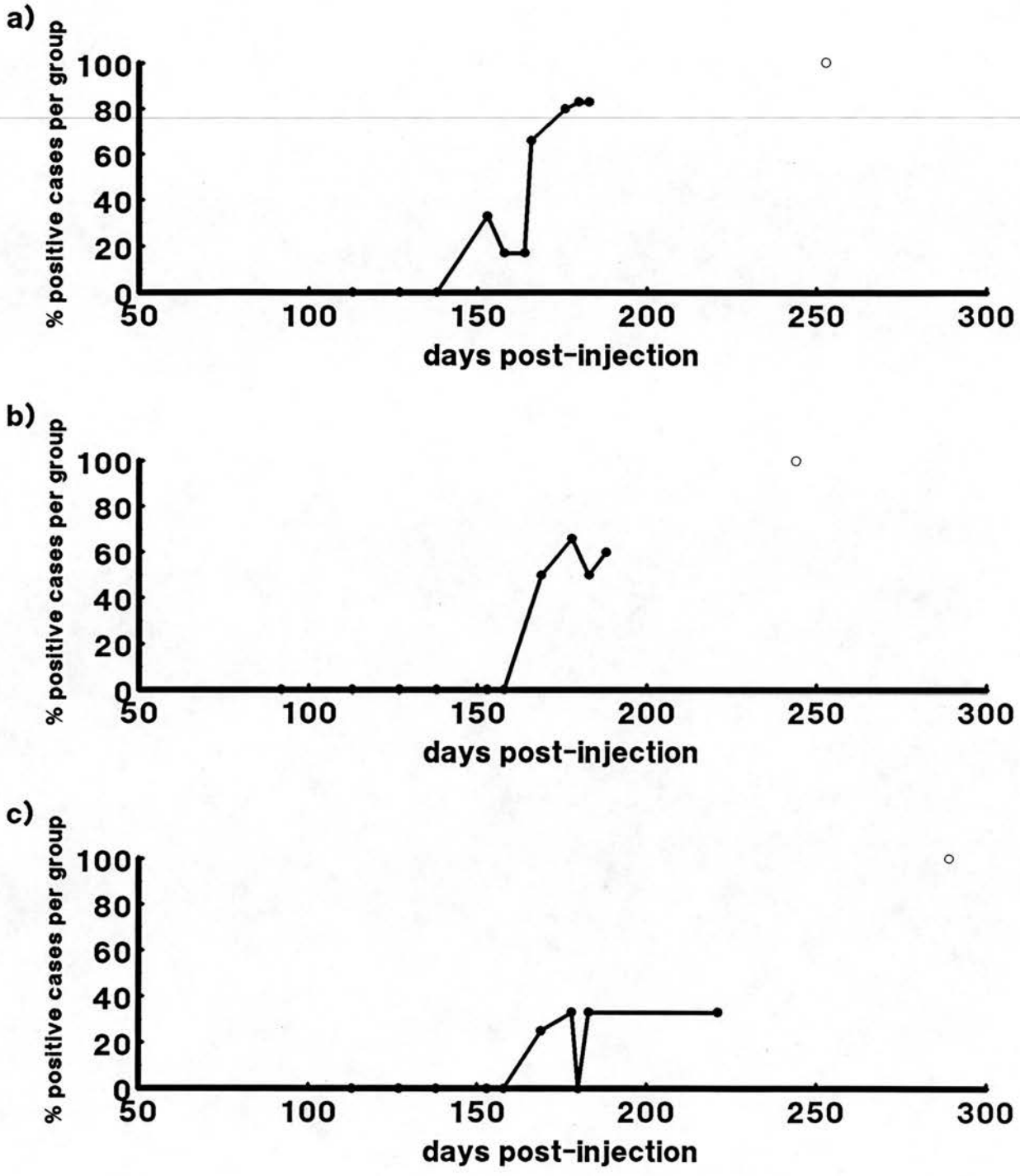

Figure 21.

Sequential percentage of positive cases per group, from experiment 7; (a) SV mice (n = 5 - 12), (b) C3H mice (n = 3 - 6), and (c) MM mice (n = 3 - 6). Single circles show incubation periods.

the Sinc gene, and a 'long' incubation period in Sinc s7 homozygotes. Both genotypes were examined following i.o. infection in a series of three experiments. The third experiment was set up in LM mice as a result of the observation that they developed severe SC lesions following i.c. infection with the 22A strain. This strain of scrapie was also used in a large sequential experiment which was set up to study overdominance in relation to the Sinc gene (see 3(g)).

The i.o. and i.c. incubation periods for experiments 9, 10 and 11, and the estimated number of infectious units injected, are shown in Table 13. All three experiments showed evidence of a low infectious dose; either survivors, or else mice killed at the end of the experiment with scrapie-positive pathology, or mice killed around the expected incubation period but for other reasons which showed no scrapie pathology.

The development of initial lesions in the three mouse strains was largely consistent, despite the great differences in timing which correlated with the incubation periods (Table 14). In the VM and SV mice, lesions first developed in the left SC and dLGN simultaneously, but slightly earlier in the left dLGN than SC in the LM mice (Fig. 22). In the VMs, lesions in the left and subsequently right VC were seen in some of the earliest cases simultaneously with lesions in the SC and dLGN. However, cortical lesions did not develop in the SV or LM mice until very late in the incubation period. In all strains, lesions involved the ventral thalamic nuclei before becoming widespread. Lesion profiles from experiments 9 and 10 are shown in Fig. 23. It can be seen that the terminal lesion pattern with this strain of scrapie changes with the i.o. route of infection. In both experiments, although the i.c. profiles are quite

TABLE 13. Experiments with the 22A strain of scrapie.

experiment no.	mouse strain	Sinc genotype	i.o. incubation period (n mice)	i.c. incubation period (n mice)	number of i.c. infectious units injected
9.[a]	VM	p7	419 ±37 (5)[b]	266 ±6 (8)	$<10^{1}$
10.[a]	SV	s7	599 ±17 (13)[c]	>492 ±12 (8)[d]	$<10^{1.8}$
11.[e]	LM	s7	623 ±14 (6)[f]	570 ±2 (6)	$<10^{1}$

a infected with a 1% suspension spun at 500g for 10 mins.
b one mouse killed at 554 days with clinical signs had no scrapie pathology
c there were three survivors in this group
d the one remaining mouse in this group was positive when the experiment was terminated at 668 days.
e infected with a 10% suspension spun at 500g for 10mins
f – one mouse killed at 603 days with epidermal erosion had no scrapie pathology

TABLE 14. Sites of initial lesions in 22A experiments.

experiment no.	mouse strain	primary lesions			secondary lesions		
		time	incidence	site	time	incidence	site
9.	VM[a]	210	1/6	left SC/ left dLGN	231	2/5	left VC
10.	SV[b]	400	2/5	left SC/ left dLGN	415	1/1[c]	right dLGN
11.	LM[d]	280	1/4	left dLGN	338	2/4	left SC

a sampling times: 168, 184, 196, 210, 218, 224, 231, 245, 259, 273, 287, 301, 315 and 338 dpi: n = 2-6.
b sampling times: 200, 250, 300, 350, 400, 464, 512, 560 and 600 dpi: n = 3-8.
c mouse killed with jaw abscess
d sampling times: 210, 252, 280, 308, 338, 364, 393, 421, 477, 505 and 533 dpi : n = 3-8.

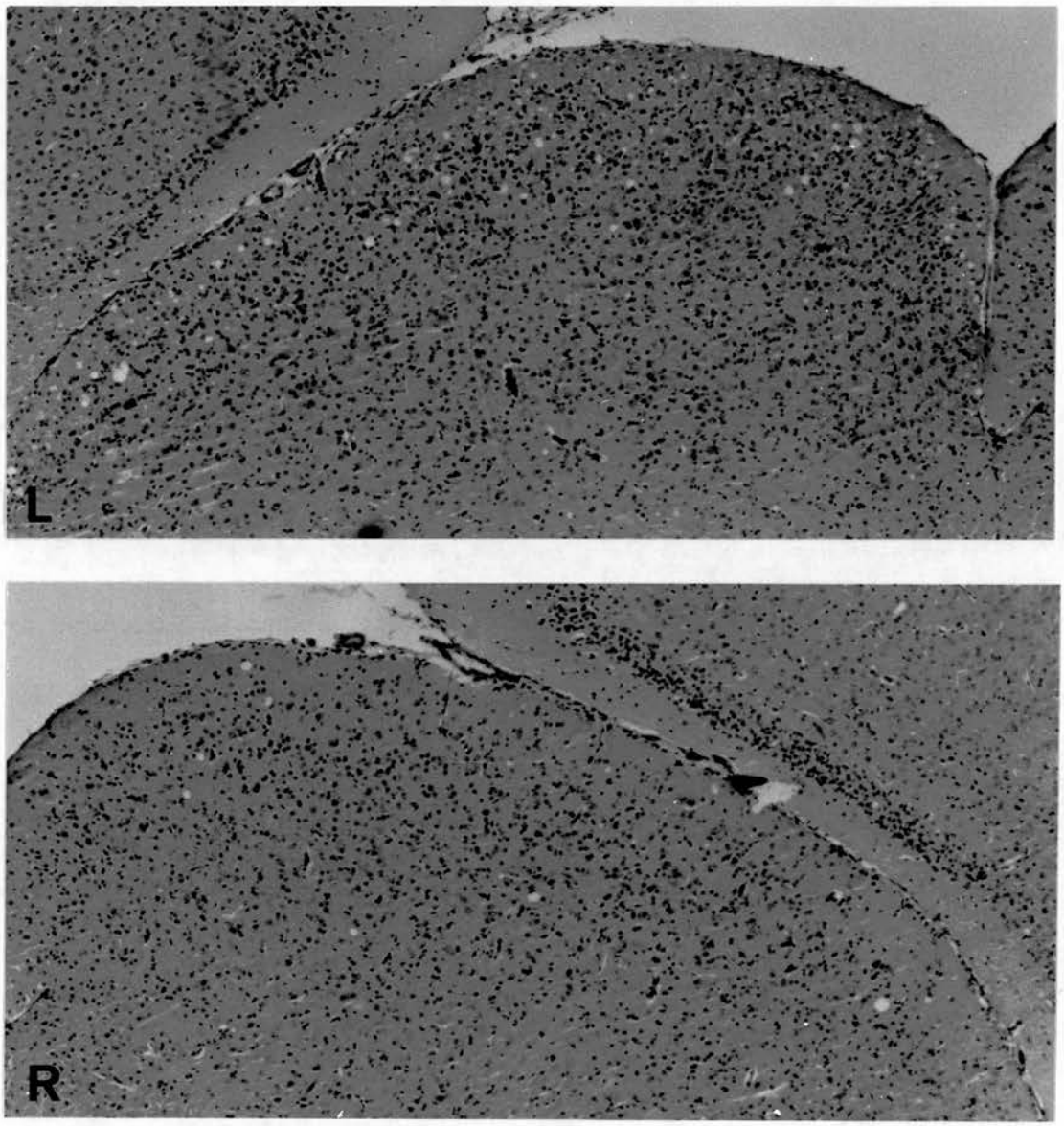

Figure 22. Severe lesions in the left SC in LM mice infected with 22A scrapie.

a)

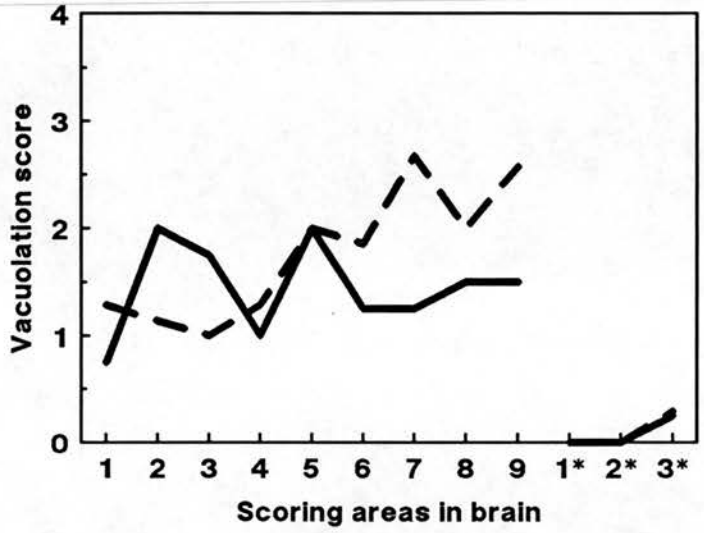

b)

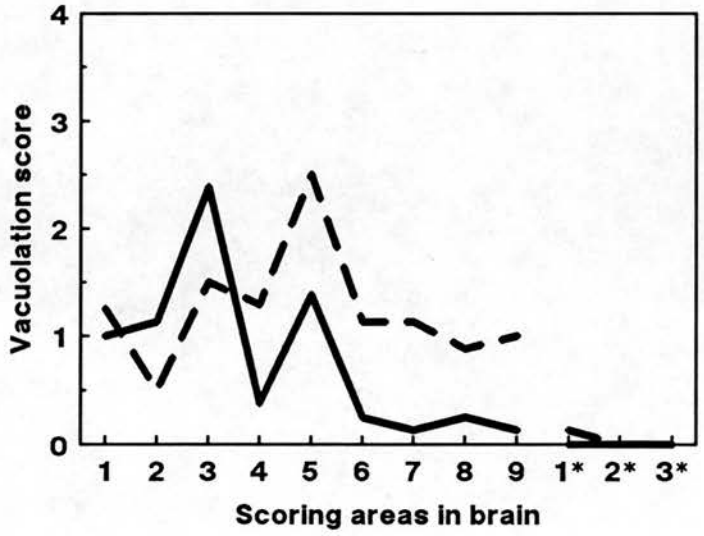

Figure 23.
Lesion profiles from (a) experiment 9; VM mice after i.o. (n = 4) solid line) and i.c. (n = 7, broken line) infection, and (b) experiment 10; SV mice after i.o. (n = 8, solid line) and i.c. (n = 8, broken line) infection. 1 - 9 are grey matter areas, 1* - 3* are white matter areas.

different in the two mouse strains, the i.o. route of infection has had the effect of increasing the severity of terminal lesions in the medulla and SC, and decreasing their severity in the forebrain, especially in the cerebral cortex.

The diagrams in Fig. 24, illustrating the lesion distribution, are taken from experiment 11 and show the targeting in the LM mice. The progression of lesion development shown by the percentage of positive cases per group is given in Fig. 25. The zero percent at 338 days in experiment 9 looks surprising, but it represents a group of only two mice which had no scrapie lesions. Since the infectious dose was low in all three experiments, each group killed during the incubation period probably contained a percentage of uninfected mice.

3(e) the 22C strain

This strain of scrapie, like ME7, is characterised by severe grey matter vacuolation seen in terminal mice infected by an i.c. route, and the absence of white matter lesions. Only one experiment (no. 12) was carried out with the 22C strain, in SM mice, which have the $\underline{Sinc}^{s7}$ genotype. The i.o and i.c. incubation periods, and the estimated infecting dose are shown in Table 15.

The lesion targeting in this experiment was precise and showed great consistency within groups (Table 16). The first lesions were seen at 129 days in the left dLGN of one mouse, and by 142 days all mice in the group had positive lesions, although a progression could be seen in the relative severity of the lesions within each

Grey matter vacuolation shown in red, white matter vacuolation in blue.

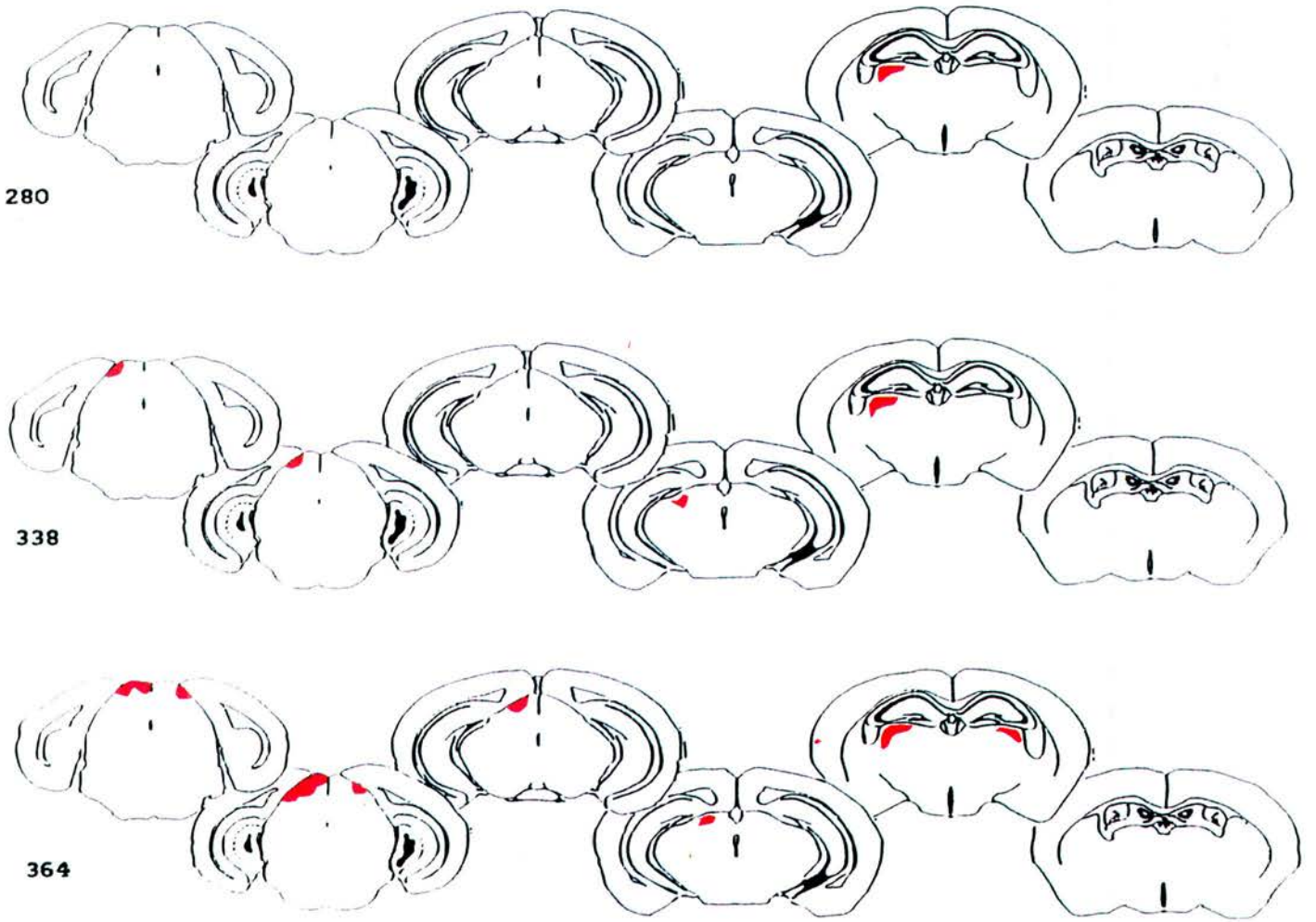

Figure 24. Sites of vacuolation in individual LM mice at 280, 338 and 364 days post-injection from experiment 11.

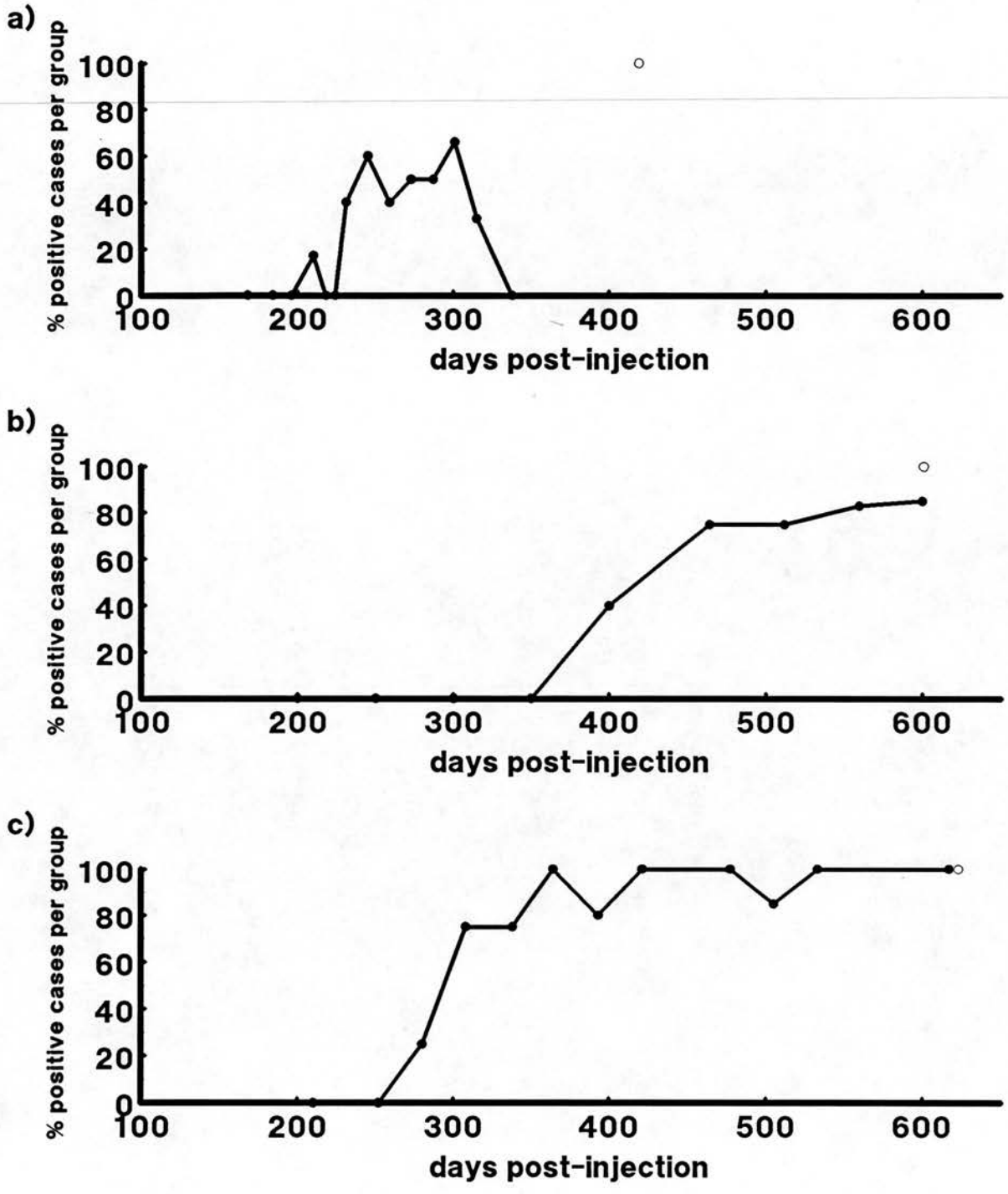

Figure 25.
Sequential percentage of positive cases per group, from (a) experiment 9; VM mice, n = 2 - 6. (b) experiment 10; SV mice, n = 3 - 8. (c) experiment 11; LM mice, n = 3 - 8. Single circles show incubation periods.

TABLE 15. Experiment with the 22C strain of scrapie.

experiment no.	mouse strain	i.o. incubation period (n mice)	i.c. incubation period (n mice)	number of i.c. infectious units injected
12.[a]	SM	233 ±2 (11)	173 ±1 (4)	$10^{4.5}$

a infected with a 10% suspension spun at 500g for 10 mins.

Table 16. Sites of initial lesions in 22C experiment.

experiment no.	mouse strain	primary lesions			secondary lesions		
		time	incidence	site	time	incidence	site
12.	SM[a]	129	1/5	left dLGN	142	3/6	left SC, right dLGN

a sampling times: 114, 129, 142, 156, 163, 177, 191, 205, 219 and 240 dpi: n = 3-7.

TABLE 17. Experiments with the 22L strain of scrapie.

exp. no.	mouse strain	i.o. incubation period (n mice)	i.c. incubation period (n mice)	i.p. incubation period (n mice)	i.o. + i.p. incubation period (n mice)	number of i.c. infectious units injected by each route
13.[a]	RIII	215 ±7 (15)	158 ±3 (4)	-	-	$10^{3.4}$
14.[b]	SM	193 ±2 (26)	157 ±1 (9)	217 ±5 (11)	201 ±2 (9)	$10^{3.4}$
	RIII	180 ±6 (11)	140 ±1 (9)	-	-	$10^{4.0}$

a infected with a 1% unspun suspension
b infected with a 10% suspension spun at 500g for 10 mins.

group. These included vacuolation in the left SC, both dLGN, and the suprachiasmatic nucleus (Fig. 26a). Individuals in later groups had discrete lesions in the parabigeminal nucleus (Fig. 26b) and some evidence of neuron loss in the oculomotor and trochlear nuclei (Fig. 26c). Diagrams of the lesion distribution in individual mice from the 129, 142 and 163 day groups are shown in Fig. 27. Lesions in the visual cortex occurred from 191 days, and became severe in later groups. The i.o. and i.c. lesion profiles (Fig. 28a) are similar in shape, but the i.o. profile was generally lower, especially in the hippocampus.

The graph of the percentage of positive cases per group (Fig. 28b) illustrates the precision of lesion timing in this experiment.

3(f) the 22L strain

This strain is known to have one of the shortest incubation periods in Sinc^{s7} mice following i.c. infection; it also produces severe vacuolation of the cerebellar grey matter, particularly in RIII mice. Two i.o. experiments (nos. 13 and 14) were carried out with the 22L strain. In experiment 14, an i.p. injected group, and an i.p. plus i.o. group (injected simultaneously) were included, to give comparative incubation periods for these routes, and incubation period groups of RIII mice were also included to compare with the RIIIs in experiment 13. The incubation periods and infective doses are shown in Table 17. The i.o. and i.p. incubation periods are very similar; the combined route slightly shortens the incubation period,

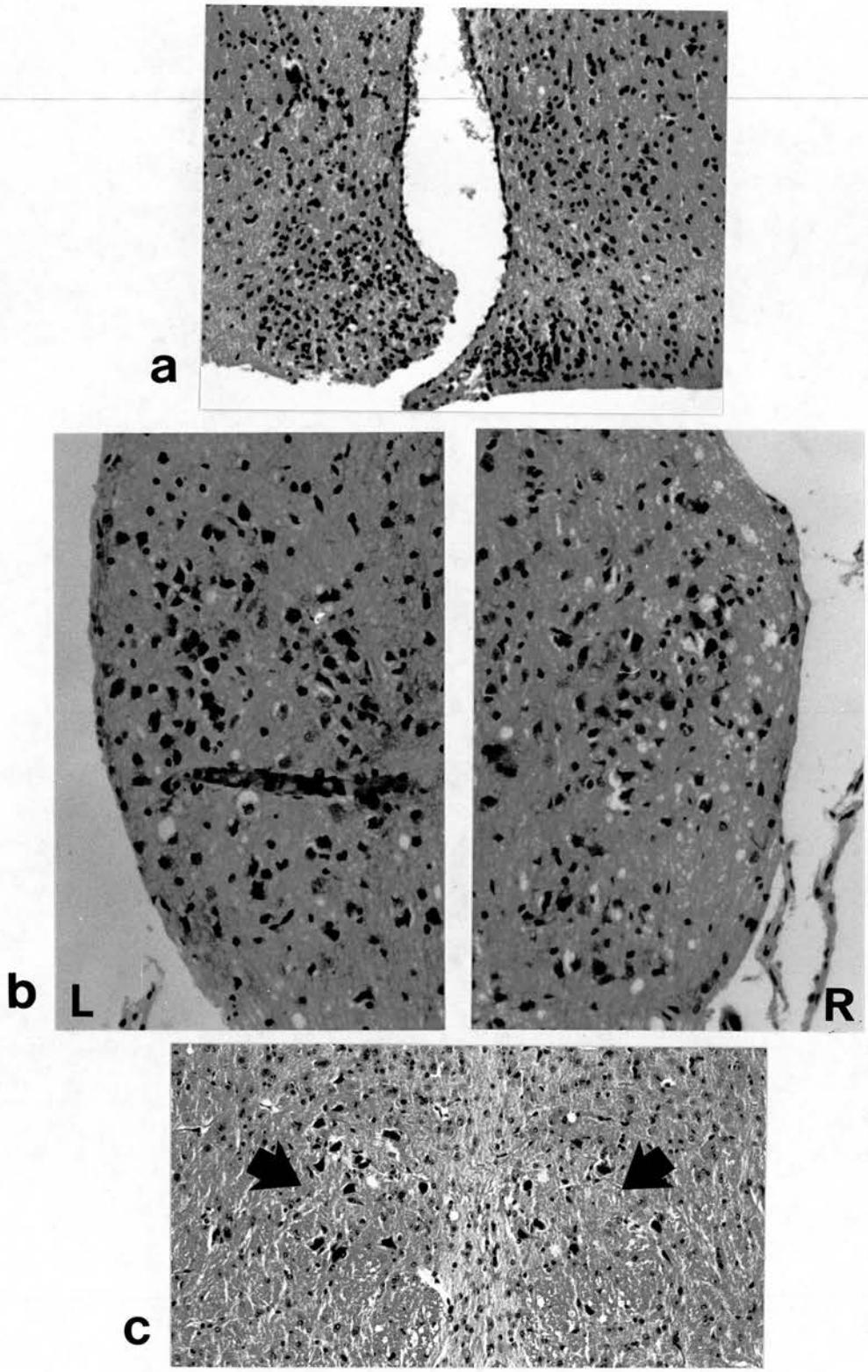

Figure 26. Vacuolation in (a) the suprachiasmatic nucleus, (b) the parabigeminal nucleus and (c) neuronal loss in the oculomotor and trochlear nuclei.

Grey matter vacuolation shown in red, white matter vacuolation in blue.

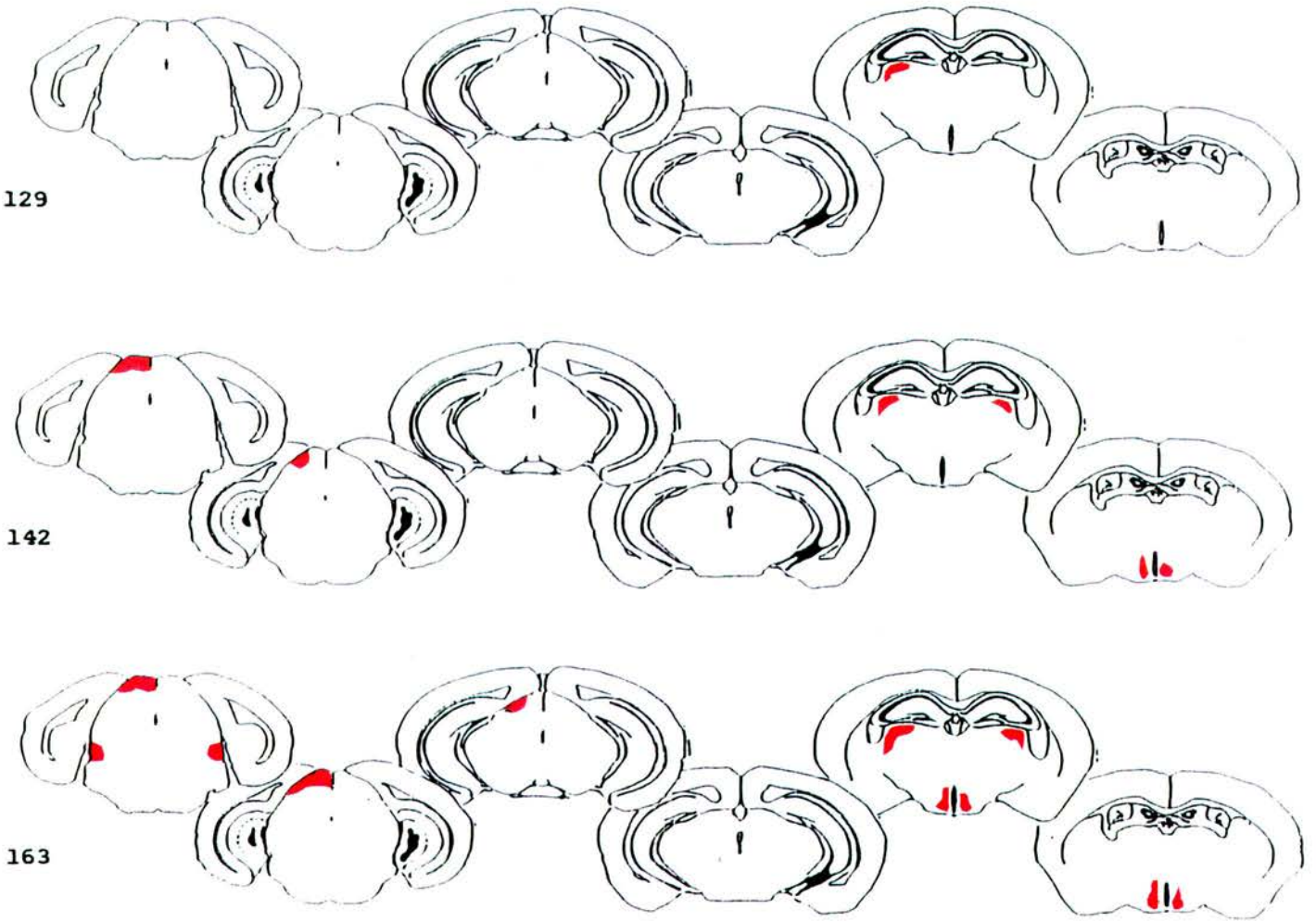

Figure 27. Sites of vacuolation in individual SM mice at 129, 142 and 163 days post-injection from experiment 12.

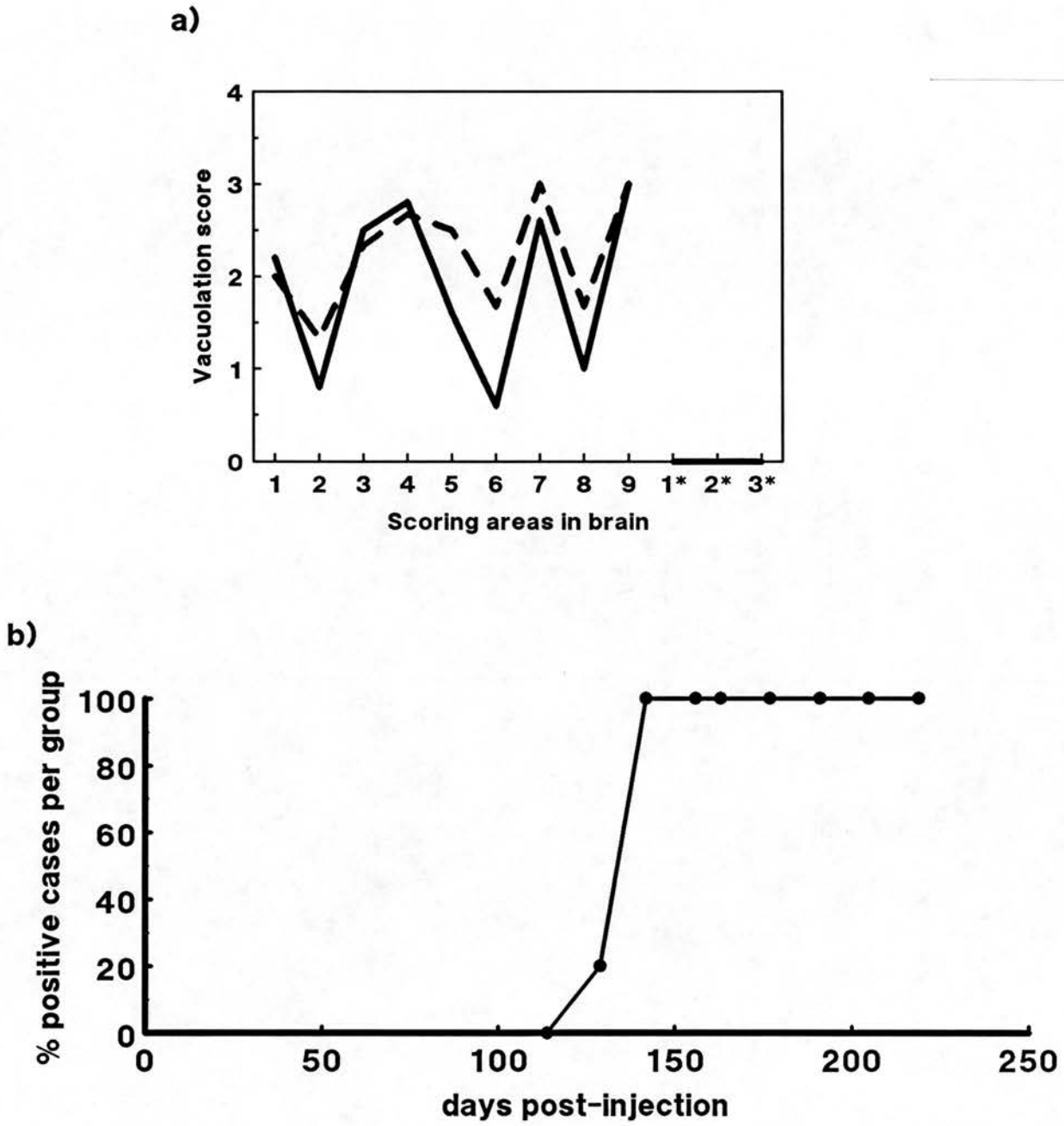

Figure 28.

(a) lesion profiles from experiment 12; SM mice after i.o. (solid line, n = 5) and i.c. (broken line, n = 3) infection. 1 - 9 are grey matter areas, and 1* - 3* are white matter areas.

(b) sequential percentage of positive cases per group, from experiment 12 (n = 3 - 7). Single circle shows incubation period.

TABLE 17. Experiments with the 22L strain of scrapie.

exp. no.	mouse strain	i.o. incubation period (n mice)	i.c. incubation period (n mice)	i.p. incubation period (n mice)	i.o. + i.p. incubation period (n mice)	number of i.c. infectious units injected by each route
13.[a]	RIII	215 ±7 (15)	158 ±3 (4)	-	-	$10^{3.4}$
14.[b]	SM	193 ±2 (26)	157 ±1 (9)	217 ±5 (11)	201 ±2 (9)	$10^{3.4}$
	RIII	180 ±6 (11)	140 ±1 (9)	-	-	$10^{4.0}$

a infected with a 1% unspun suspension
b infected with a 10% suspension spun at 500g for 10 mins.

but of course the total dose of i.c. ID_{50} units was doubled.

The initial lesions occurred in the left SC in both mouse strains (Table 18), and at the same percentage of the duration of the incubation period (65% - 66%). However, the sites where the next lesions developed were the left dLGN and VC in RIII mice, and the left dLGN and dorsal medulla (scoring area 1 on the lesion profile) in the SM mice. The diagrams showing early lesion distribution (Fig. 29) are taken from SM mice at 126, 140 and 154 days. In SM mice killed on or after 182 days, severe vacuolation of the cochlear nucleus (Fig. 30a) was seen. Cerebellar grey matter vacuolation occurred in RIII mice (Fig. 30b), but again not until late in the incubation period (at least 199 days). The shape of the lesion profiles is similar for both mouse strains (Fig. 31); the i.o. profile is slightly lower than the i.c. in experiment 13, and considerably lower in experiment 14, as are the i.p. and combined i.o. and i.p. profiles. It is interesting that all profiles show very little vacuolation in position 6 (hippocampus); this is more marked here than in profiles from previous 22L experiments.

The graphs of the percentage positive cases per group (Fig. 32) show that in both strains, all mice in the group developed lesions within a relatively short time (60 and 27 days in RIII and SM mice respectively).

3(g) the effect of the Sinc gene

Two experiments were designed to investigate the action of the Sinc gene following i.o. infection, and whether Sinc controls

TABLE 18. Sites of initial lesions in 22L experiments.

experiment no.	mouse strain	primary lesions			secondary lesions		
		time	incidence	site	time	incidence	site
13.	RIII[a]	142	2/3	left SC	164	1/3	left dLGN and VC
14.	SM[b]	126	2/4	left SC	126	1/4	left dLGN medulla

a sampling times: 124, 143, 164, 171, 184, 191 and 208 dpi: n = 2-3.
b sampling times: 98, 126, 140, 154, 168 and 182 dpi: n = 4-5.

Grey matter vacuolation shown in red, white matter vacuolation in blue.

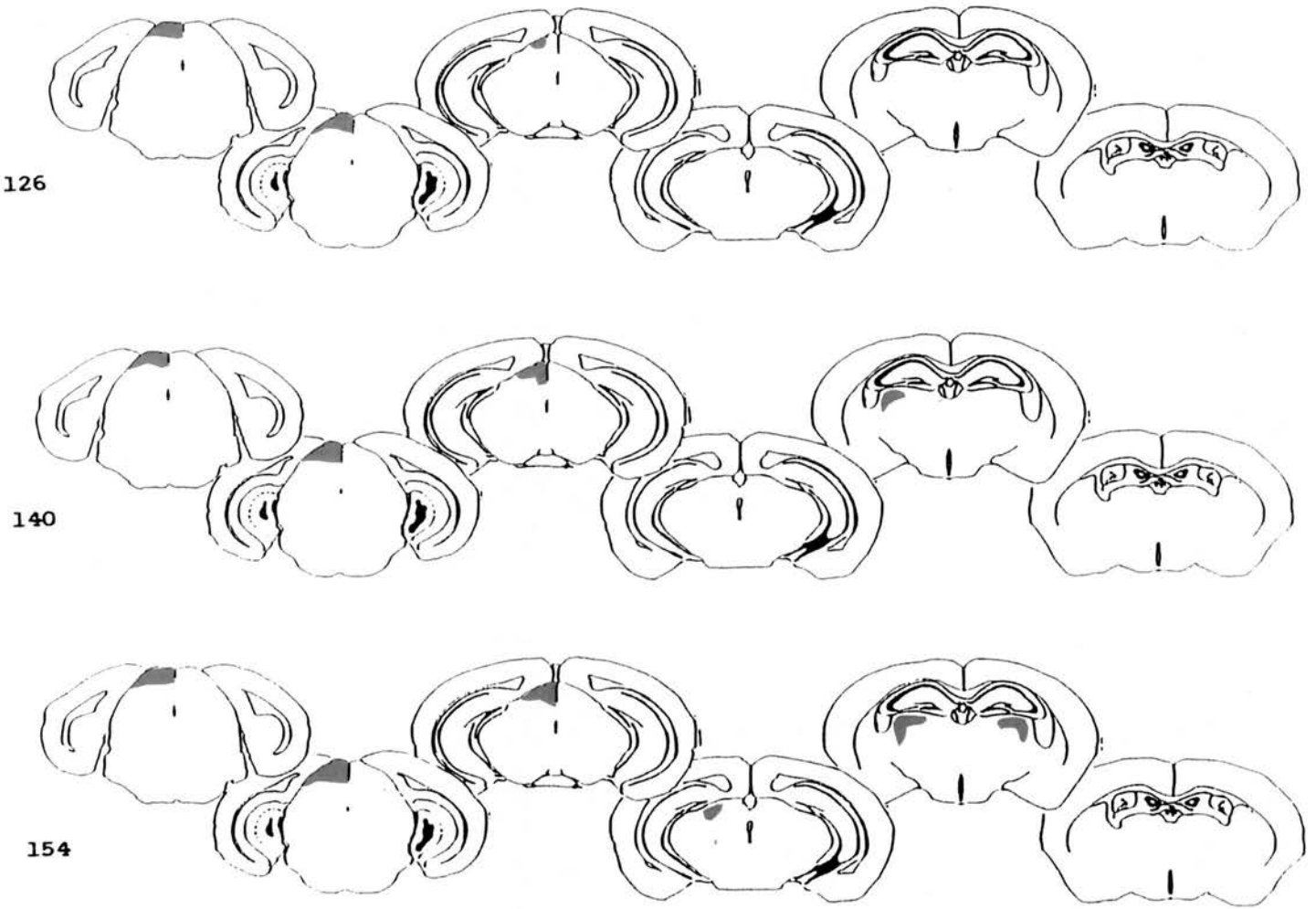

Figure 29. Sites of vacuolation in individual SM mice at 126, 140 and 154 days from experiment 14.

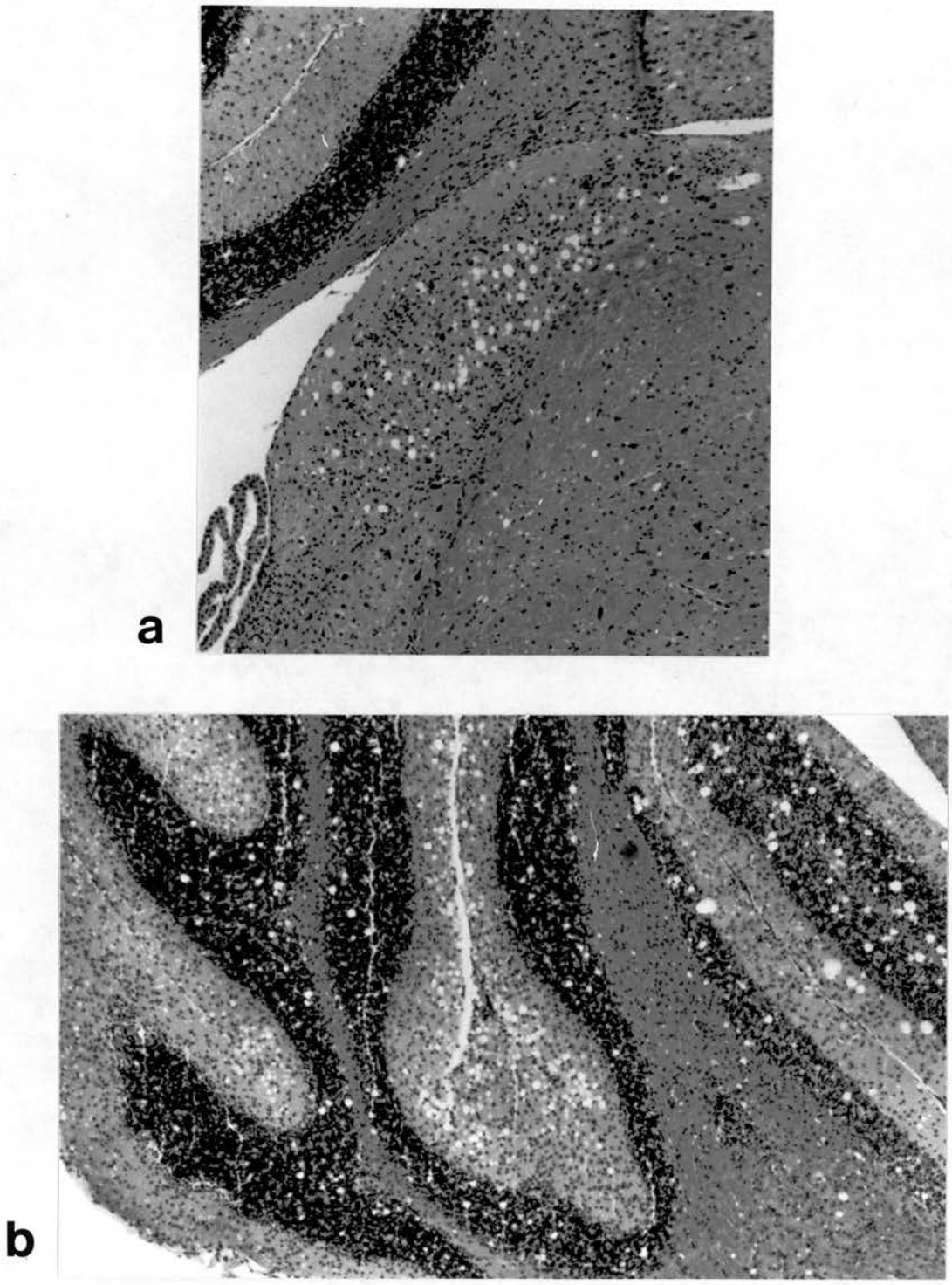

Figure 30. (a) Severe vacuolation of the cochlear nucleus, and (b) vacuolation of the cerebellar grey matter in RIII mice infected with 22L scrapie.

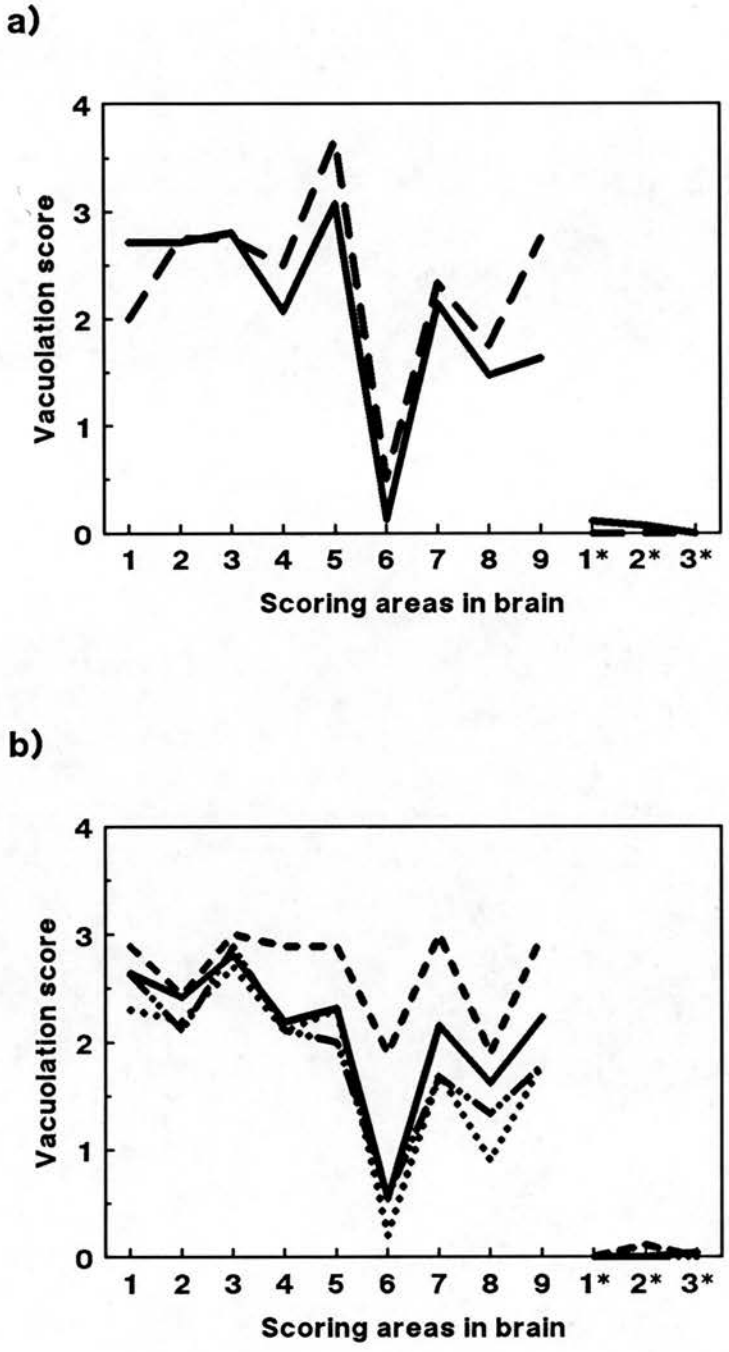

Figure 31.
Lesion profiles from experiment 13 (a) RIII mice after i.o (solid line, n = 15) and i.c. infection (broken line, n = 4). and (b) SM mice after i.o. (solid line, n = 26), i.c. (dashed line, n = 9), i.p. (dotted line, n = 10) and i.o. + i.p. infection (chain, n = 9). 1 - 9 are grey matter areas, 1* - 3* are white matter areas.

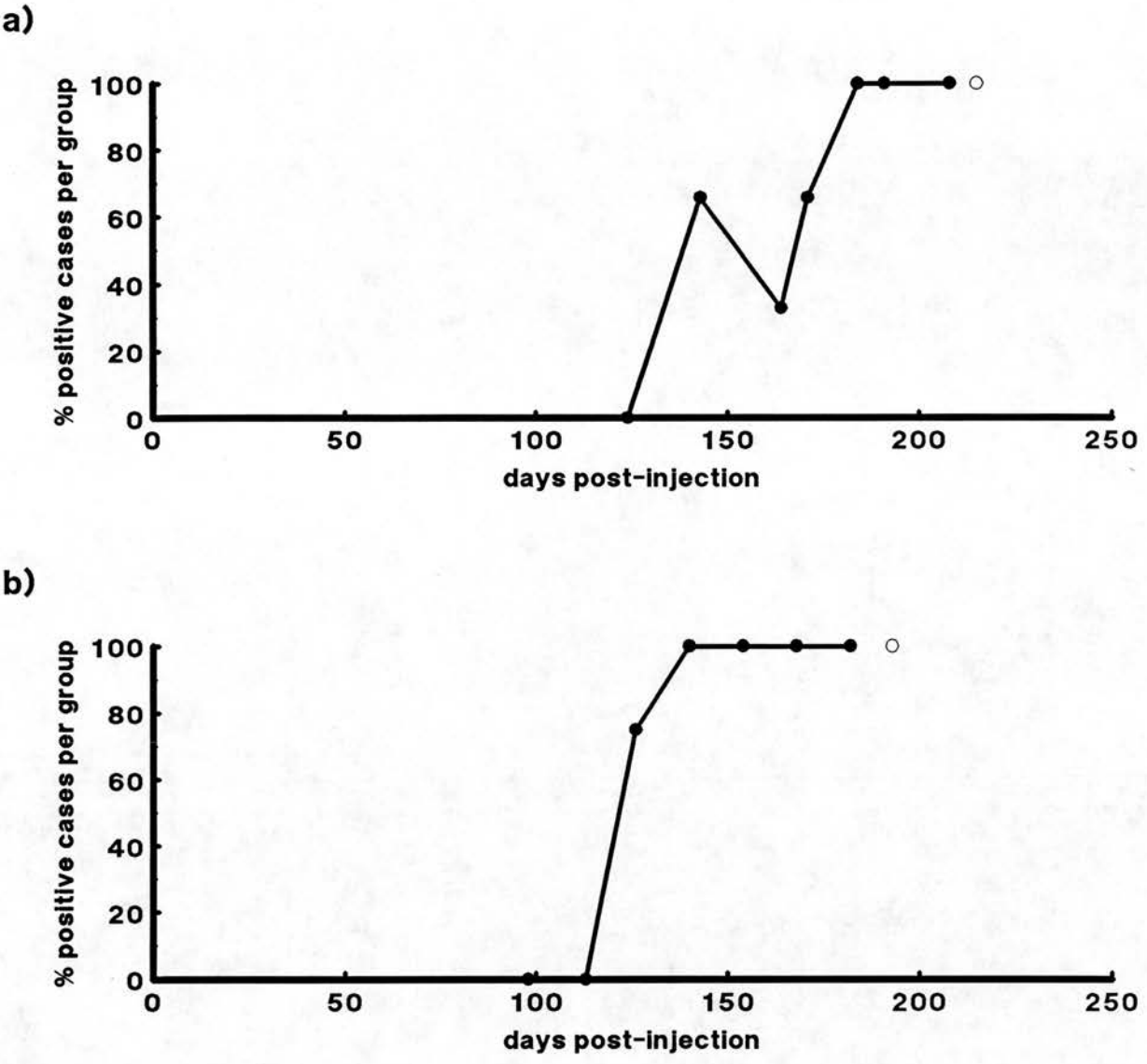

Figure 32.
Sequential percentage of positive cases per group, from (a) experiment 13 in RIII mice (n = 2 to 3) and (b) experiment 14 in SM mice (n = 4 to 5). Single circles show incubation periods.

the timing of lesions in the single neuronal relay from RGC to SC. In the experiment 15, ME7 scrapie was injected bilaterally into mice homozygous for the s7 (SV) or p7 (VM) alleles of Sinc. Groups killed from 48 days post-injection provided tissues for the sequential assay experiment described in Chapter 4 and brains were taken for histological examination from 188 days for SV mice, and 244 days for VM mice.

Experiment 16 was set up to see if the apparent overdominance (Dickinson and Meikle, 1971) seen when the 22A strain is used to infect all three Sinc genotypes (s7, p7 and the heterozygote) can also be detected in the timing of the lesions in the retinal projections. VM mice (p7) and C57BL mice (s7) and their F_1 cross were infected by the i.o. route with 22A scrapie. Groups of mice were killed from 176, 232 and 190 days respectively. Since it was difficult to anticipate the timing of lesions in the F_1 mice, groups were killed up to 596 days (sampling times given in footnote to Table 20). The incubation periods for both experiments are shown in Table 19. The incubation period sequence (p7, s7, F_1) using 22A with the i.o. route is the same as with the i.c. route. However, in experiment 15, the i.o. incubation periods with ME7 are 45% longer in both mouse strains than those for the i.c. route, whereas the VM, C57BL and F_1 mice in experiment 16 are 38%, 26% and 15% longer respectively.

In experiment 15, lesions in the SC (left/right) were present in both SV mice killed at 188 days in experiment 15, and mice in all subsequent groups were positive (Table 20). Of the VM mice, however, one mouse from each of the sampling times had lesions in the SC, and the others were negative. Clearly, earlier dates were

TABLE 19. Experiments examining the effect of the *Sinc* gene.

experiment no.	scrapie strain	mouse strain	i.o. incubation period (n mice)	i.c. incubation period (n mice)	number of i.c. infectious units injected
15.[a]	ME7	SV	254 ±5 (18)	175 ±1 (8)	$10^{4.0}$
		VM	474 ±8 (6)	326 ±3 (7)	$10^{5.1}$
16.[b]	22A	VM	273 ±4 (19)	198 ±2 (16)	$10^{4.1}$
		C57BL	>615 ±18 (9)[c]	490 ±6 (8)	-[d]
		F_1	700 ±6 (27)	609 ±10 (4)	-[d]

a infected bilaterally with a 10% suspension spun at 500g for 10 mins.
b infected with a 10% suspension spun at 500g for 10 mins.
c survivors in this group.
d no adequate dose-response curves available.

TABLE 20. Sites of initial lesions caused by two strains of scrapie in mice of the three *Sinc* genotypes.

experiment no.	mouse strain	primary lesions			secondary lesions		
		time	incidence	site	time	incidence	site
15.	SV[a]	188	2/2	left/right SC	188	1/2	left/right dLGN
	VM[b]	244	1/3	left/right SC	–	–	–
16.	VM[c]	176	1/5	left dLGN	197	3/5	left SC, right dLGN
	C57BL[d]	315	1/5	left SC	315	2/5	left dLGN
	F_1[e]	330	1/6	left dLGN	358	1/5	left SC

a sampling times: 188, 216 and 244 dpi: n = 2–3.
b sampling times: 244, 272 and 300 dpi: n = 2–3.
c sampling times: 176, 190, 197, 204, 211, 218, 232 and 252 dpi: n = 4–6.
d sampling times: 232, 252, 281, 315, 330, 344, 358, 372, 386, 400, 415, 428 and 442 dpi: n = 4–5.
e sampling times: 190, 204, 232, 252, 281, 315, 330, 344, 358, 372, 386, 400, 415, 428, 442, 456, 470, 484, 498, 514, 526, 540, 554, 570, 582 and 596 dpi: n = 3–6.

needed for the SV mice, and later dates for the VM groups. But the limited number of brains for histology in this experiment were designed to confirm the timing of pathological changes already known from previous experiments, and permit correlation with the infectivity studies. The lesion profiles (Fig. 33) reveal a similarity between both routes of injection and mouse strains. The lesions in SC (position 3) are more severe in the i.o. than i.c. infected SV mice, which reflects a residual asymmetry of lesions (the lesion profile is scored on the most severely affected side).

In experiment 16 the first lesions occurred in the left dLGN in the VM and F_1 mice at 176 and 330 days respectively, and in the left SC in the C57BL mice at 315 days. Comparison of these times with corresponding incubation periods shows that Sinc can affect the timing of the initial pathology. The lesion profiles (not shown) are similar to those in Fig. 33.

Conclusions

These experiments have revealed a progression of lesion targeting following i.o. infection. The lesions vary in site and severity depending on the strain of scrapie, the genotype of the mouse and the stage of the incubation period, and their timing is controlled by the Sinc gene. All lesions are consistent with the known neuroanatomical pathways from the retina. These results reinforce the existing evidence for neural spread of scrapie, especially within the CNS. In some models, the infective dose was near the limiting dilution, and i.o. incubation periods were not clear-cut. This did not affect the detection of the pathological

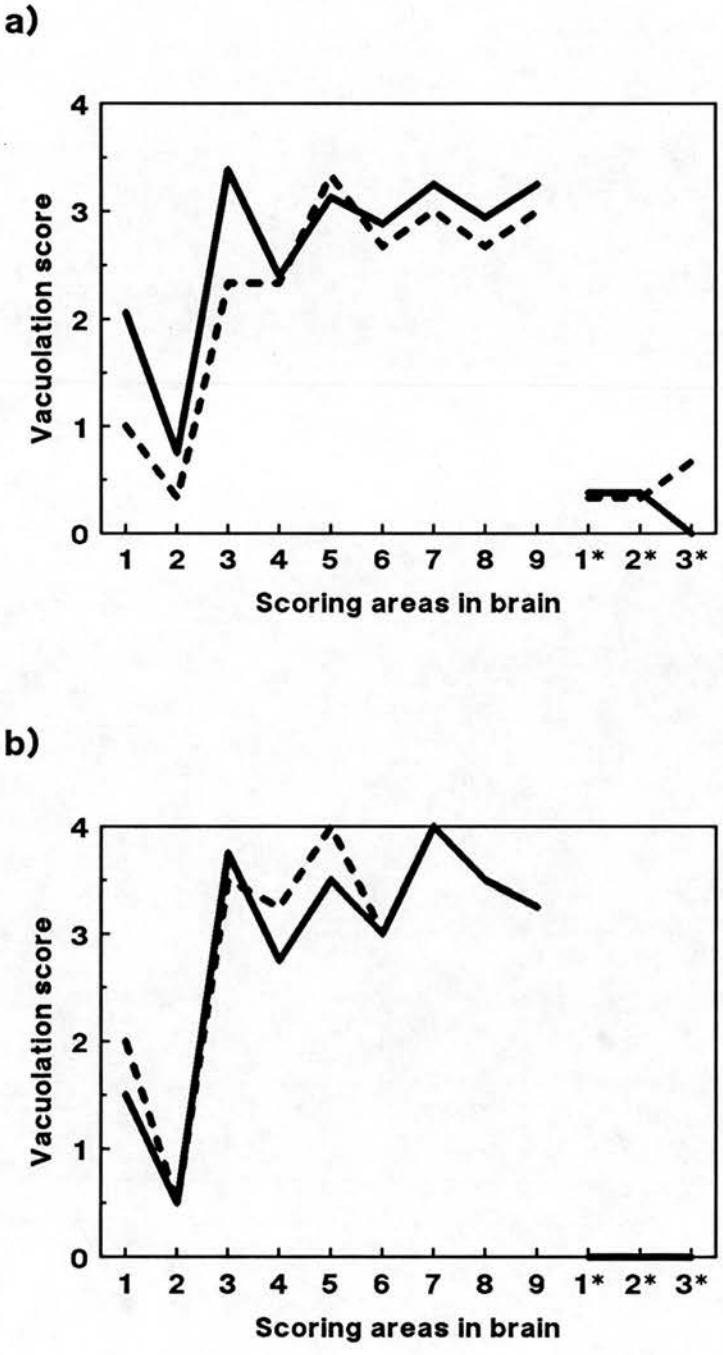

Figure 33.
Lesion profiles from experiment 15; (a) SV mice after i.o. (solid line, n = 16) and i.c. infection (broken line, n = 4):
(b) VM mice after i.o. (n = 4) and i.c. infection (n = 4),
key as above. 1 -9 are grey matter areas, 1* - 3* are white matter areas.

changes, although future experiments should ensure that the highest possible dose of infection is given by this route of infection.

The basis for the differences in targeting between models is not known. One of the most obvious examples is that ME7 and 87V strains both produce lesions in the dLGN, yet lesions in the geniculo-cortical projection only develop following ME7 infection. Possible reasons for these differences are discussed in Chapter 6.

Chapter 4. The development of infectivity after intraocular infection.

The relationship between the spread of infectivity, and the development of the pathology described in the previous section was studied in 6 experiments, using sequential assays of visual projection areas in selected models to answer specific questions. Studies were limited by the prolonged time course of experiments involving infectivity assays, and the large number of mice required. The relationship between dose of infection and incubation period was also investigated in 2 experiments. In addition, partial purification of the inoculum was achieved by using SAF preparations (see 2.3), which were then compared with a standard brain homogenate in 2 experiments using ME7 and 87V strains of scrapie.

The six experiments (17 to 22) relating to infectivity spread are described below; three have been completed, but some results from one, and the assays from two others are still in progress.

4(a) What is the sequence of infectivity spread in the visual system?

This key experiment (17) used a standard *Sinc*^{s7} mouse strain (C57BL) to investigate the development of infectivity in retina, optic nerve, SC, dLGN and visual cortex and permit comparison with the pathological lesions identified in experiments 1, 2, 3 and 15.

Cerebellum was also assayed to identify infectivity levels in an area unconnected with the visual system. Groups of mice from this experiment provided the sequential pathology for experiment 3. As described in 3(a), mice were bilaterally infected with 1ul of inoculum containing in total $10^{4.4}$ i.c. ID_{50} units of ME7. The incubation period was 234 ±3.3 days. Tissues were removed for assay (see 2.4) at 13 intervals between 7 and 224 dpi. Tissue pools were prepared as described in 2.4, and injected i.c. into 12 C57BL recipient mice. Retina, SC, optic nerve and dLGN pools from all 13 intervals were assayed using the i.c. route; visual cortex assays were from 8 representative dates and cerebellum assays from 6 dates. The mean incubation period of each assay group was compared with an i.c. dose-response curve derived from a titration of unspun ME7 already used as a standard in this laboratory (shown in Appendix B).

Retina

The sequential rise in the level of infectivity in retina is shown in Fig. 34. The higher initial level at 7 dpi must be due to the presence of residual inoculum within the retina. This has dropped by 14 days, is unaltered at 21, and is rising by 35 days, which must be due to replication initiated within the retina from between 14 and 21 days. Since there is little or no retinal pathology even in terminal C57BL mice infected with ME7 (retinopathy score of 0.3 in 2 out of 13 mice examined by Foster et al, 1986b), the rapid subsequent rise in titre was unexpected. Identification of the retinal cell type(s) which support scrapie replication was further investigated in experiment 18.

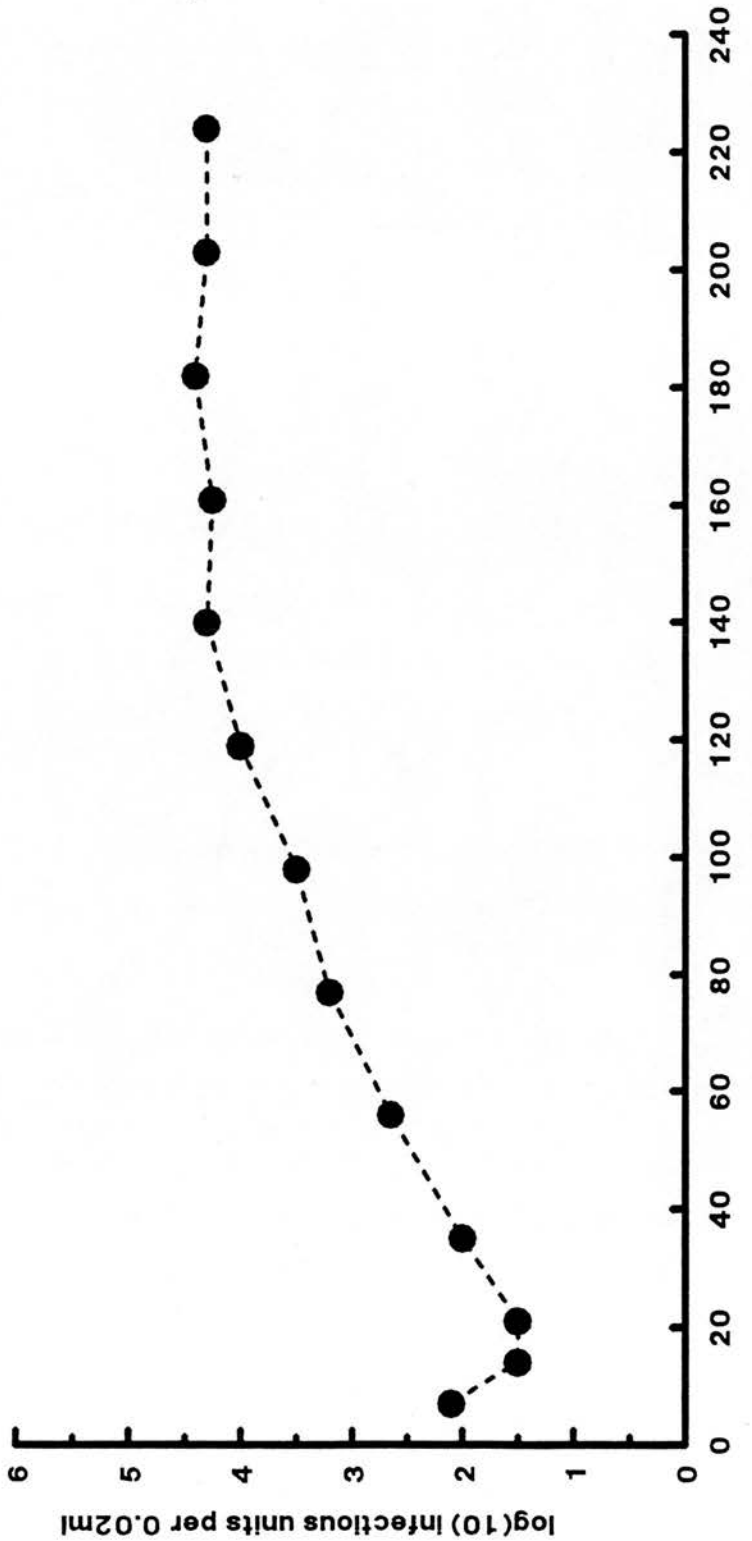

Figure 34.

Infectivity titres in sequential retinal pools from experiment 17.

From Fig. 34, infectivity reached an apparent plateau at about $10^{4.3}$ from 140 dpi until the end of the incubation period, 100 days later. It is impossible to tell whether this is a real plateau, since the incubation periods of the assay mice were all around 160 days, which is the minimum i.c. incubation period for ME7 in this model. It is possible then, that a higher titre occurring later in the incubation period was not detected by using an assay of a single dilution. In subsequent experiments, some of the later assays were extended to full titrations, so that where apparent plateaux occurred, titres calculated by the Karber method could be compared.

Superior colliculus

Fig. 35 shows sequential infectivity levels in SC compared with retina. Infectivity is first detected in SC at 56 dpi, although one mouse (out of 12) in the 35 day group was positive, with a scrapie incubation period of 300 days. The level rises rapidly to $10^{3.4}$ at 98 days, and remains similar to the retinal titres thereafter, although a gradual rise of about 1 log was detectable between 119 and 224 days.

Optic nerve

The infectivity levels detected in optic nerve are shown in Fig. 36 again in comparison with retina and SC. Because of the small amount of tissue involved (approximately 0.07mg per nerve; see Table 3) optic nerves were assayed at a dilution of 10^{-2} (all other tissues are at 10^{-1}). The values in Fig. 36 were therefore increased

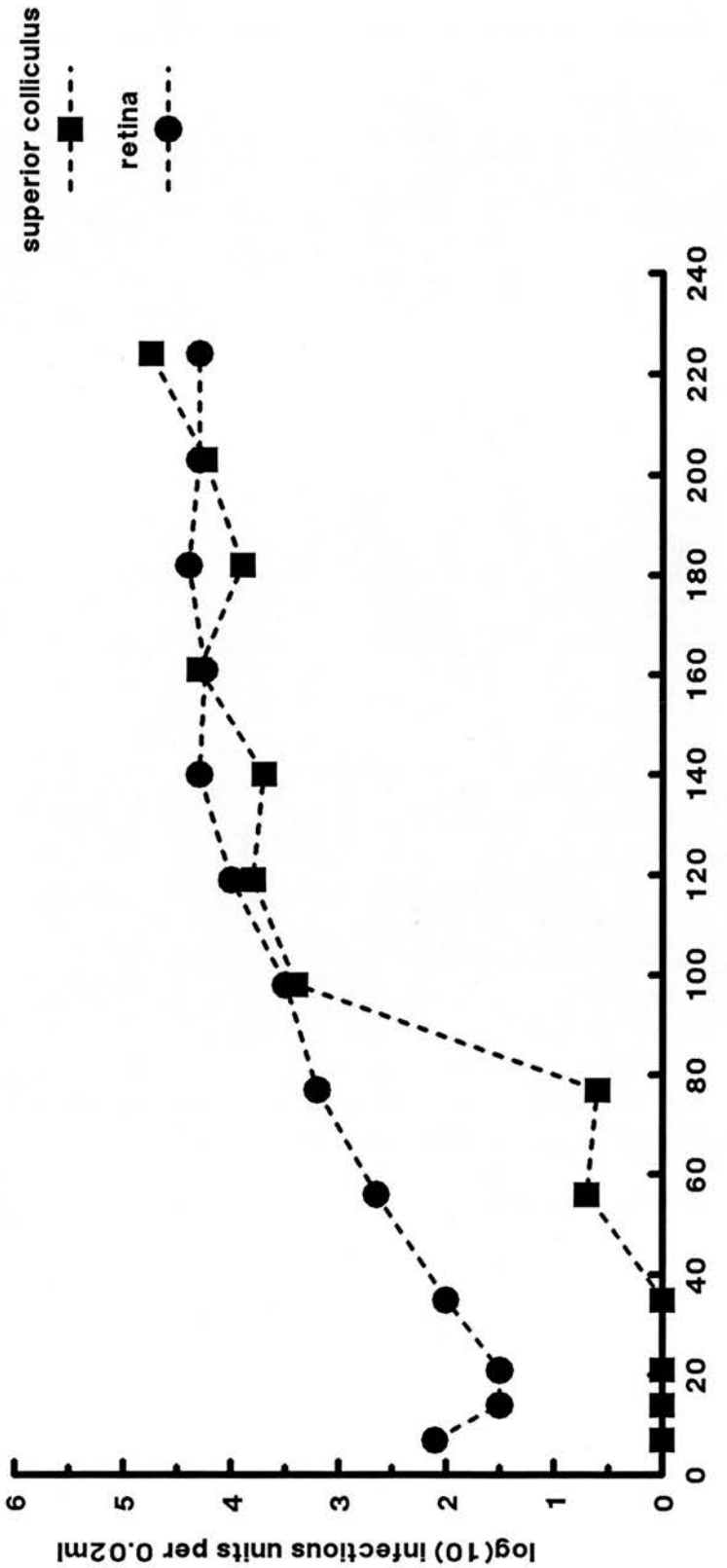

Figure 35. Infectivity titres in sequential superior colliculus and retina pools from experiment 17.

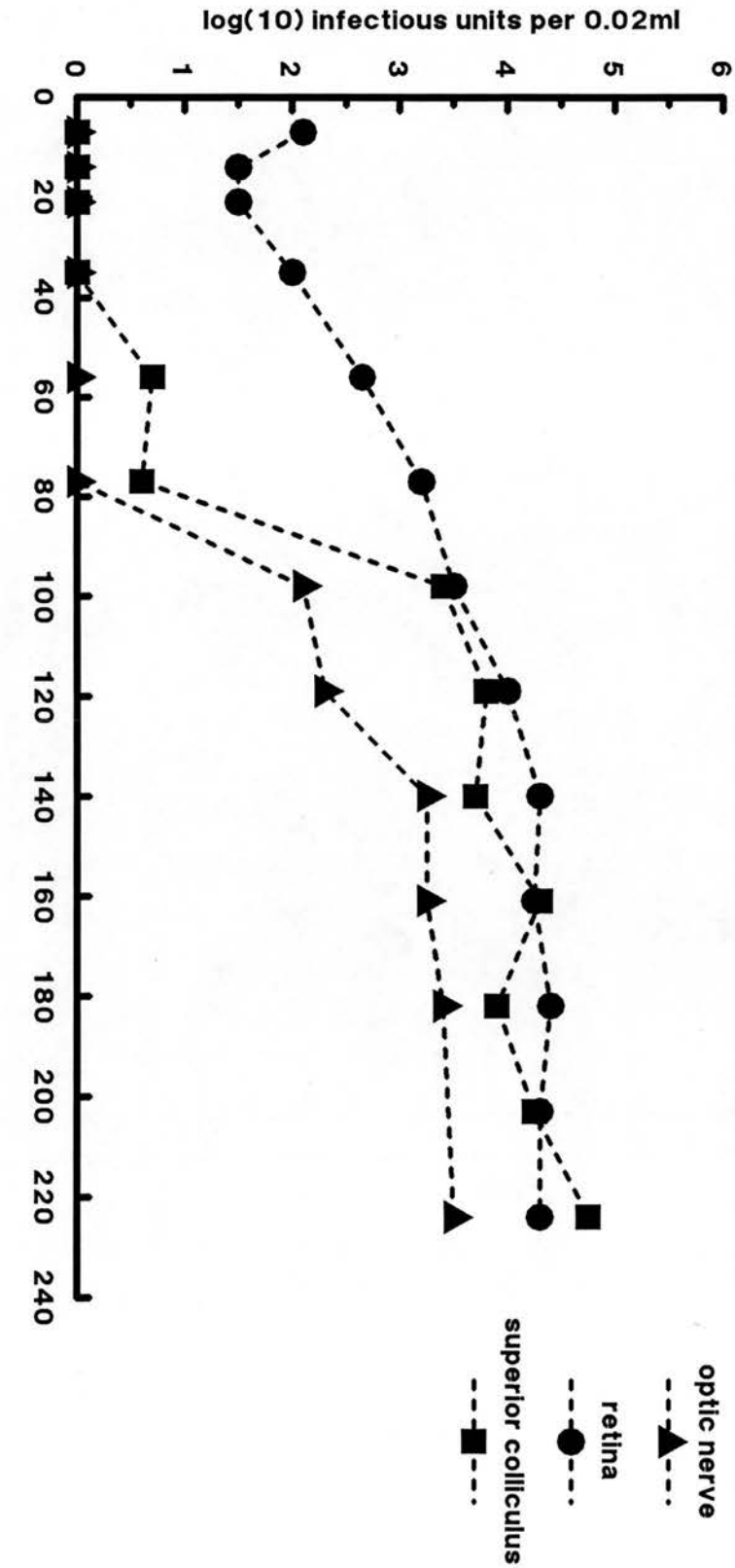

Figure 36. Infectivity titres in sequential optic nerve, retina and superior colliculus pools from experiment 17.

by a factor of 10 to make them comparable to the other tissue pools. The earliest group in which all 12 of the recipient mice developed scrapie and thus gave a mean incubation period to compare with the dose-response curve was at 98 dpi; however, between 1 and 5 of the mice in earlier groups (21, 35, 56 and 77 dpi) died with scrapie. This means that these early groups received less than one ID_{50} infectious unit of inoculum. Although the optic nerve titres were corrected for dilution, the plateau from 140 days is lower than that of retina and SC.

Dorsal lateral geniculate nucleus

The levels of infectivity in the dLGN are shown in Fig. 37, with the SC for comparison. These two tissues have very similar replication curves throughout the incubation period, although infectivity was first detected in dLGN at 77dpi, one sampling time (21 days) later than in SC. One mouse in the 56 dpi group was killed with scrapie at 230 days. Titres in the dLGN rise steadily from 98 to 224 dpi, and do not show the plateaux seen in the retina and optic nerve. This may reflect the crude dissection technique, which removed a quantity of tissue including the dLGN. This means that although a maximum level of infectivity may have been reached in the dLGN by about 100 days, background levels in the surrounding tissue in the sample would still be rising.

Visual cortex

In the visual cortex (Fig. 38) infectivity was first

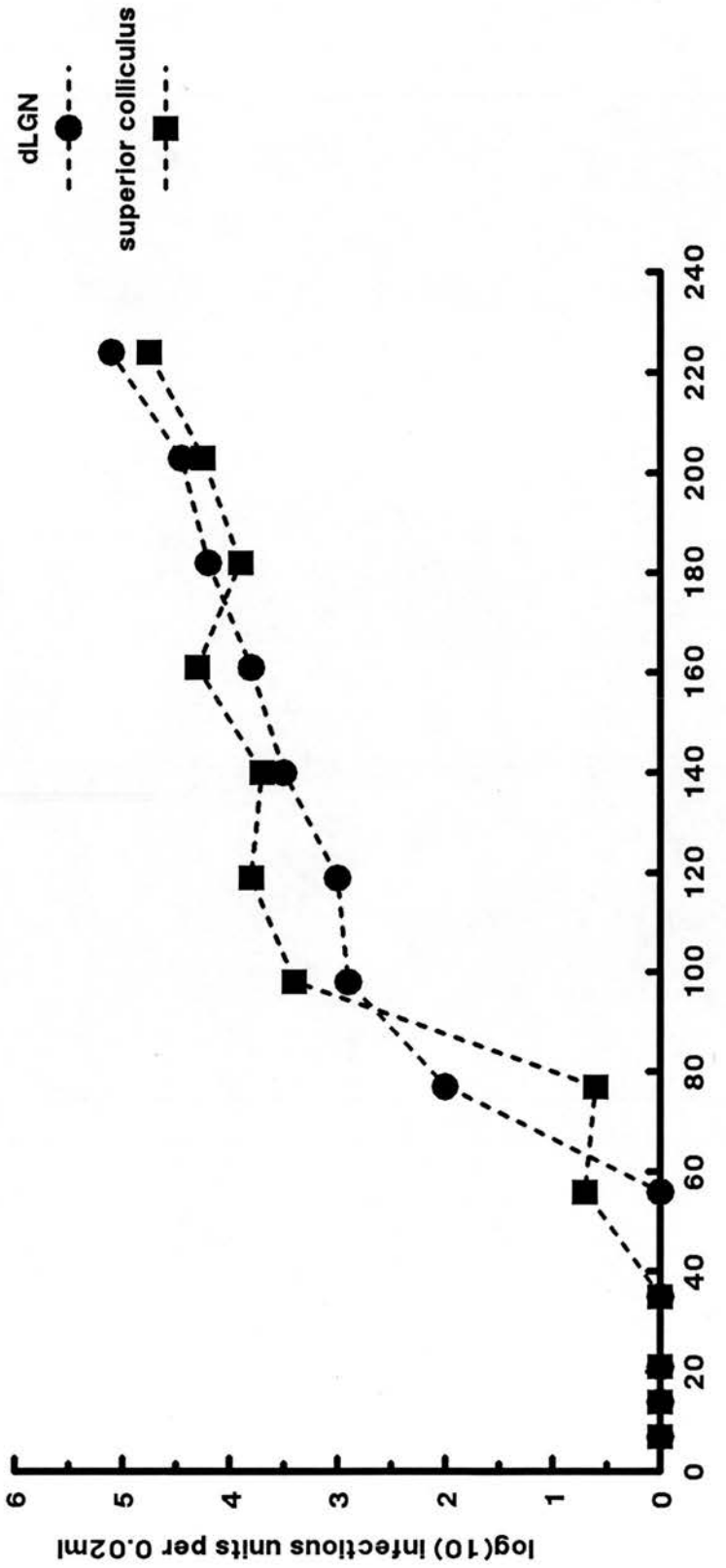

Figure 37. Infectivity titres in sequential dLGN and superior colliculus pools from experiment 17.

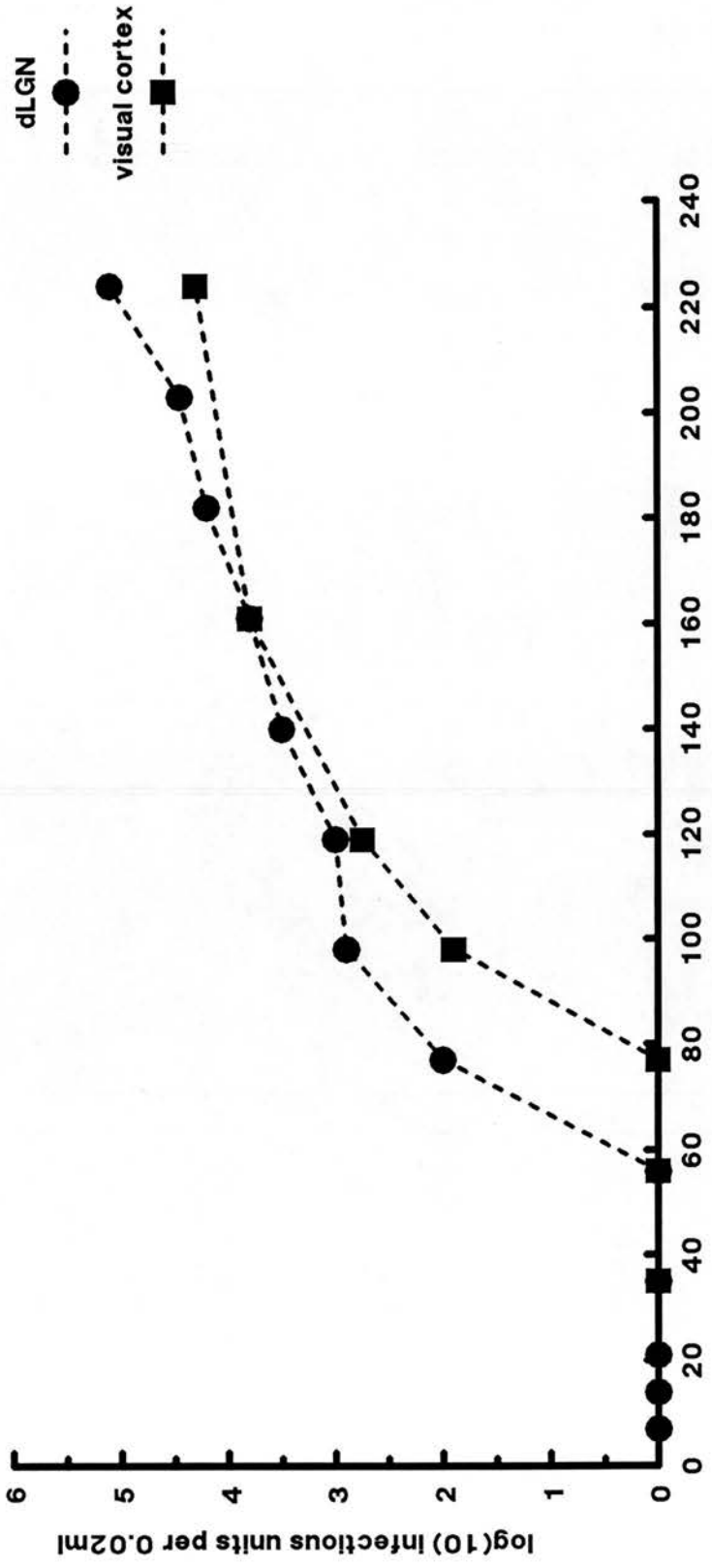

Figure 38. Infectivity titres in sequential dLGN and visual cortex pools from experiment 17.

detected at 98 dpi, and rose to levels comparable to those in the dLGN from 120 dpi, with no clear evidence of a plateau. However, titres in visual cortex began to rise 21 days after those in dLGN, as would be predicted from the neuroanatomy and the timing of vacuolar pathology. It is interesting that titres in the visual cortex were similar to the cerebellar titres (see below); this suggests that the visual cortex results are only reflecting the levels of infectivity in the brain as a whole, because the dissection was too crude to provide information on this brain area alone.

Cerebellum

This tissue was assayed to monitor background levels of infectivity in the brain since it receives no known direct projections from the retina. The titres, shown in Fig. 39, are compared with retina and visual cortex. The similarity with visual cortex suggests that by 98 dpi, infectivity has become widespread in the brain.

Summary

This experiment was designed to identify the sequence of onset of replication of scrapie in the major visual projections, in comparison with the timing of pathological lesions. A clear progression is apparent, starting with retina at 14 to 21 days, SC at 56 days, dLGN at 77 days, and optic nerves, visual cortex and cerebellum at 98 days.

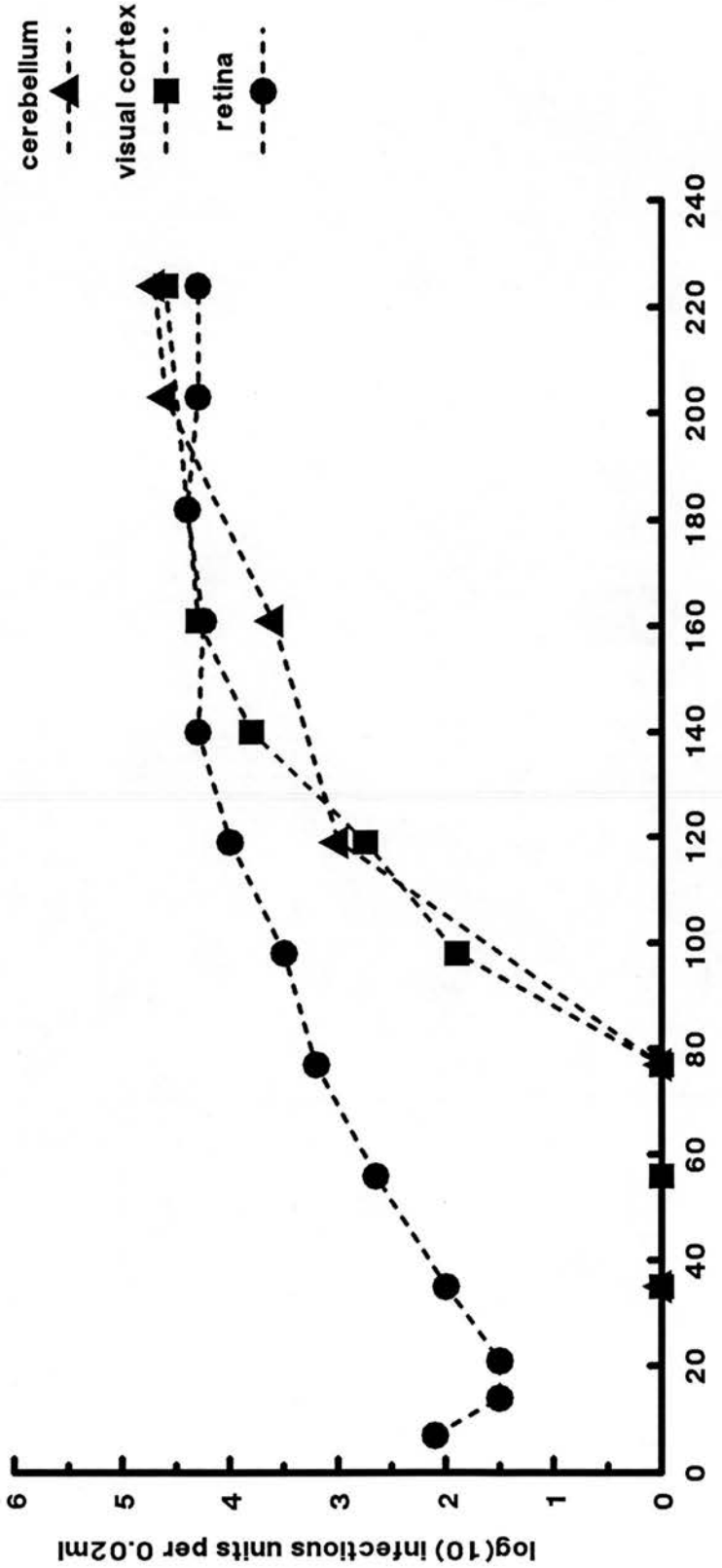

Figure 39. Infectivity titres in sequential cerebellum, visual cortex and retina pools from experiment 17.

4(b) Which retinal cell types support replication?

The previous experiment revealed high levels of infectivity in the retina from early in the incubation period. Since it was impossible to assay the different cell types in the retina, experiment 18 was devised to compare levels of infection when retinal cells were depleted either genetically or chemically before infection. Comparisons were made between (i) C57BL mice and BSC mice (which express the rd gene for rodless retina as described in 1.4); and (ii) VL mice which were either normal, or had been treated with MSG as neonates to partially or completely destroy the retinal ganglion cell population (see 2.6). The results from the first comparison are described below; the assays from the second part of the experiment are still in progress.

(i) C57BL and BSC comparison

C57BL and BSC mice were infected by the bilateral i.o. route, with 1ul per eye of a 10% suspension of ME7 infected brain, which had been spun at 500g. Groups of three mice of each strain were killed at 24 hours and 20, 60, 100 and 140 days to provide pools of retina and SC tissue for assay. Unfortunately, only small numbers of mice survived in each terminal group to develop clinical scrapie: the incubation periods were: C57BL, 256 ±2.7 (n = 3) and BSC, 204 ±5.5 (n = 2). Three C57BL mice did not develop clinical signs of disease, and showed no scrapie pathology when killed at 356

dpi. This difference in incubation periods between mouse strains was unexpected, and was not revealed until after the tissue assays had been set up. Groups of 12 C3H mice were also injected i.c. with a 5% inoculum prepared from each pool. The 140 day group from C57BL mice was also assayed by titration with dilutions from 10^{-2} to 10^{-6}. Numbers of infectious units were calculated from the incubation periods of the single dilution assays using the same C57BL dose-response curve as in experiment 17.

Retina

The sequential infectivity levels in C57BL and BSC retina are shown in Fig. 40. The 24 hour and 20 day levels must reflect decreasing amounts of residual inoculum, but by 60 days the infectivity level in the C57BL retina is 2.5 units, compared to 1.25 in the BSC retina; this difference is confirmed by the SC result. At 100 and 140 days, levels are similar.

Superior colliculus

Fig. 41 shows that infectivity is initially detected in C57BL SC at 60 dpi, which is exactly the timing already shown for this model in experiment 17 (Fig. 35). At this time, no infectivity is found in BSC SC, in fact all 12 recipient mice in the 60 day BSC assay were killed at 503 days, with no scrapie pathology. Although the level in BSC SC is higher than in C57BL at 100 days, by 140 days, the levels are the same. The titration of the 140 day C57BL group produced a Karber estimate of $10^{-5.75}$ i.c infectious units,

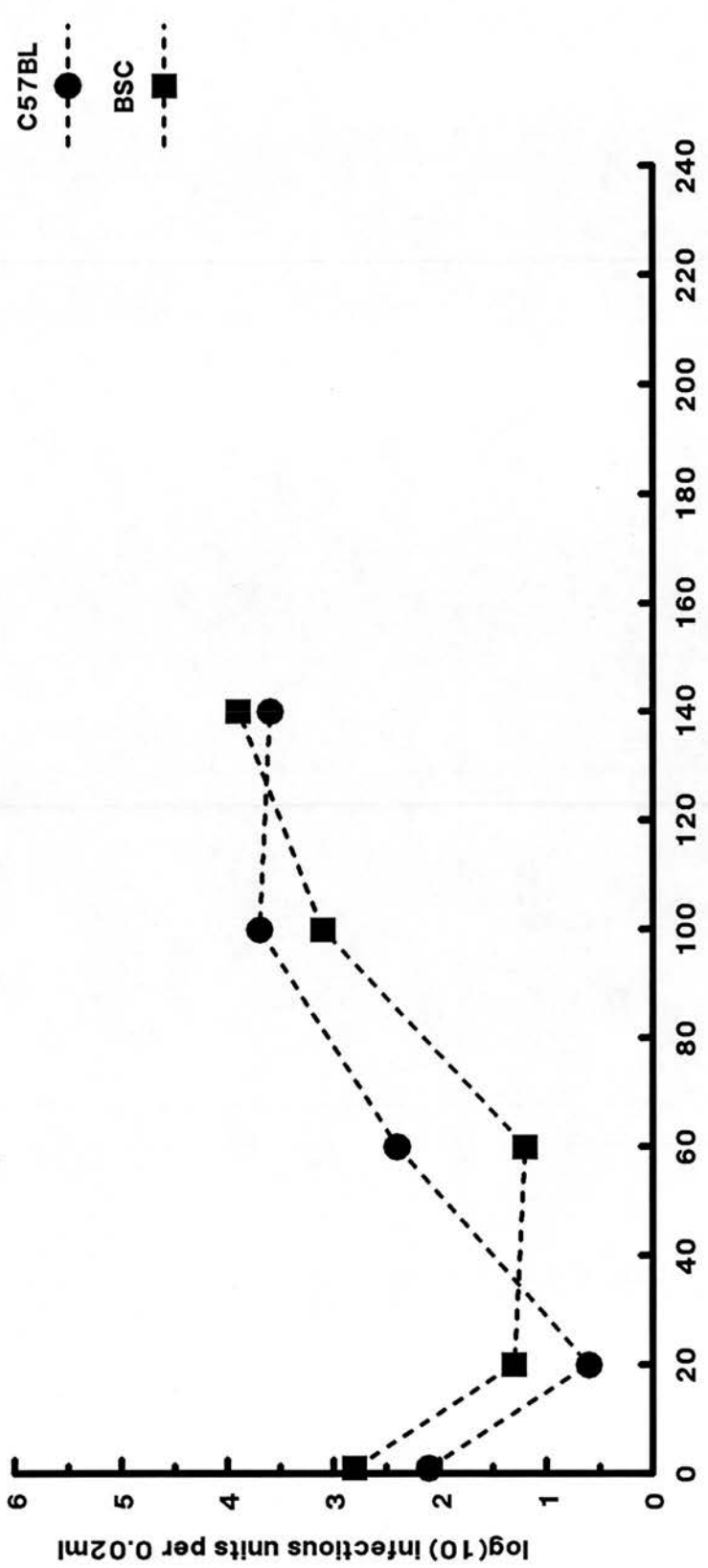

Figure 40. Infectivity titres in sequential retina pools from C57BL and BSC mice in experiment 18.

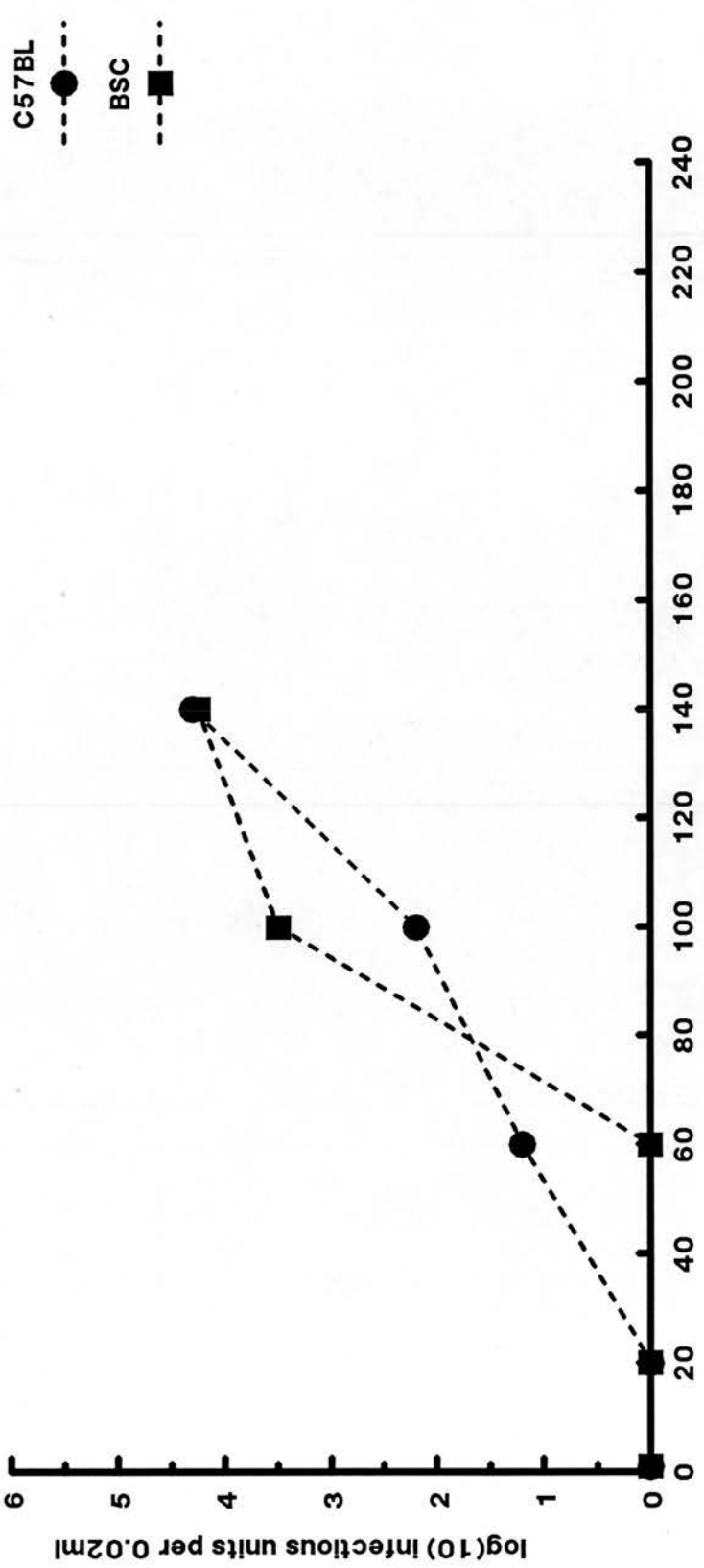

Figure 41. Infectivity titres in sequential superior colliculus pools from C57BL and BSC mice in experiment 18.

which at a dilution of 5% is equivalent to $10^{4.25}$ infectious units per 0.02 ml, exactly the same as the estimate from the incubation period.

Summary

The results show that the BSC mice have markedly lower retinal titres at 60 dpi, when replication is increasing rapidly in the C57BL retina. The sequential levels in SC confirm this result. Although it is impossible to conclude that replication does not take place in the BSC retina, the loss of the photoreceptor cell layer is obviously associated with a significant reduction in the amount of infectivity. The unexpectedly lower incubation periods in the BSC mice suggests that they received a higher operational titre of inoculum than the C57BL mice; if so, then the differences between mouse strains in the replication curves would be underestimated. However, the similarity between the two 140 day SC titres in Fig. 41, and the Karber titre for the C57BL SC indicate that the infectious doses were not different as the incubation periods suggest.

Retinal titres were compared on a 'per retina' basis, and the retina pools from both strains of mouse were prepared in the same volume of saline; no allowance was made for a possible weight difference due to the lack of photoreceptors in the BSC retina (the dilutions were based on a standard weight of normal C57BL retina (see 2.4)). Again, this could only lead to an overestimate of the difference in concentration of infectivity in BSC retina compared to

C57BL.

The similarity in replication curves obtained for retina and SC in C57BL mice in experiments 17 and 18, with tissue pools from quite different sources, testifies to the reproducibility of the incubation period assay.

(ii) Normal and MSG-treated VL mouse comparison

Groups of normal and MSG-treated VL mice were infected i.o. bilaterally with the same inoculum as used in (i). Three mice from each group were killed at 24 hours, and 20, 40, 60 and 100 days, and pools of retina and SC tissue taken. Tissue pools were also taken from three terminal mice in each group. The incubation periods of the donor groups were: control VL, 227 ±3.9 (n = 10); MSG-treated VL, 246 ±5.6 (n = 7), which was a significant prolongation ($p < 1\%$). This means that comparison of the assay results should be able to show if replication in ganglion cells is important in pathogenesis.

4(c) Is retinopathy associated with high levels of infectivity?

Experiment 18 indicates that replication in the retina is associated with the photoreceptor cell layer. These cells are destroyed as a primary result of scrapie infection in several models (Foster et al, 1986b). Experiment 19 was set up to compare infectivity levels in the retina (and other tissues) after i.o. and i.c. infection of C57BL mice with (i) ME7 scrapie, in which there is little or no retinopathy in terminal i.c. infected mice, and (ii)

79A scrapie, which produces a severe retinopathy in terminal i.c. infected mice (mean retinopathy score of 3.8 in 16/16 C57BL mice examined by Foster et al, 1986b; see 2.9, and also retinopathy results from experiment 8).

(i) The sequential infectivity levels in retina and SC following i.o. infection of C57BL mice with ME7 scrapie are presented in experiment 18. These, and additional groups infected with the same inoculum, either by the bilateral i.o. route or i.c. (with an equivalent 2ul dose) provided tissue pools for assays of retina, SC and spleen after both i.o. and i.c. infection. As with the i.o. infected mice, groups of three i.c. infected mice were killed at 24 hours and 20, 60, 100 and 140 days after i.c. infection. The 140 day i.c. SC pool was also titrated (with dilutions from 10^{-2} to 10^{-6}). The i.c. incubation period of the donor mice was 167 ±1.5 (n = 9), indicating an infectivity dose of $10^{4.0}$ i.c. ID_{50} units. All infectivity titres were calculated using the same C57BL dose-response curve as in experiments 17 and 18.

(ii) Groups of C57BL mice were infected by i.o. (bilateral) or i.c. routes with a 10% dilution of 79A scrapie, prepared in the same way as for ME7. Donor groups of 3 mice, infected by each route, were killed at the same intervals as the ME7-infected mice, and included groups of 3 terminal mice. These animals provided tissue for bioassay. Further groups were killed to provide tissues for pathological examination, described in experiment 8. The 140 day and terminal i.c. SC pools were titrated (from 10^{-2} to 10^{-7}). The incubation periods for the donor mice were: i.c. 155 ±7.9 (n = 3),

giving an i.c. ID_{50} of $10^{3.1}$; i.o. 205 ±6.0 (n = 3). Infectivity titres were calculated from an existing dose-response curve from a titration of unspun 79A scrapie in C57BL mice (Appendix B).

Retina

Infectivity levels in retina pools from C57BL mice after i.o. infection with ME7 and 79A scrapie are compared in Fig. 42. Infection with 79A scrapie produces a similar progression to ME7 (from experiment 18), but with higher titres. Both groups show evidence of residual inoculum at 24 hours, which has declined by 20 days, but by 60 days the level in the 79A infected retina is over a log higher than the ME7 infected retina. Although the initial level of 79A is higher, in fact nearly 10-fold fewer i.c. ID_{50} units were injected. The cell loss in the retina with 79A means that this is at least a 10-fold higher titre than with ME7; this may be the basis of the subsequent degenerative pathology produced by the 79A strain.

The results after i.c. infection of the donor mice are shown in Fig. 43. Infectivity was first detected in retina pools from both strains of mice at 60 days. Again, 79A infected mice had higher retinal infectivity levels, which increased steadily to $10^{5.8}$ in terminal mice, with no plateau. The titres in the ME7 infected retina pools were similar to those of the i.o. infected mice, and appeared to plateau between $10^{3.5}$ and $10^{4.0}$ at 100 and 140 days. The differences in titre following i.c. infection substantiates the similar results following i.o. infection.

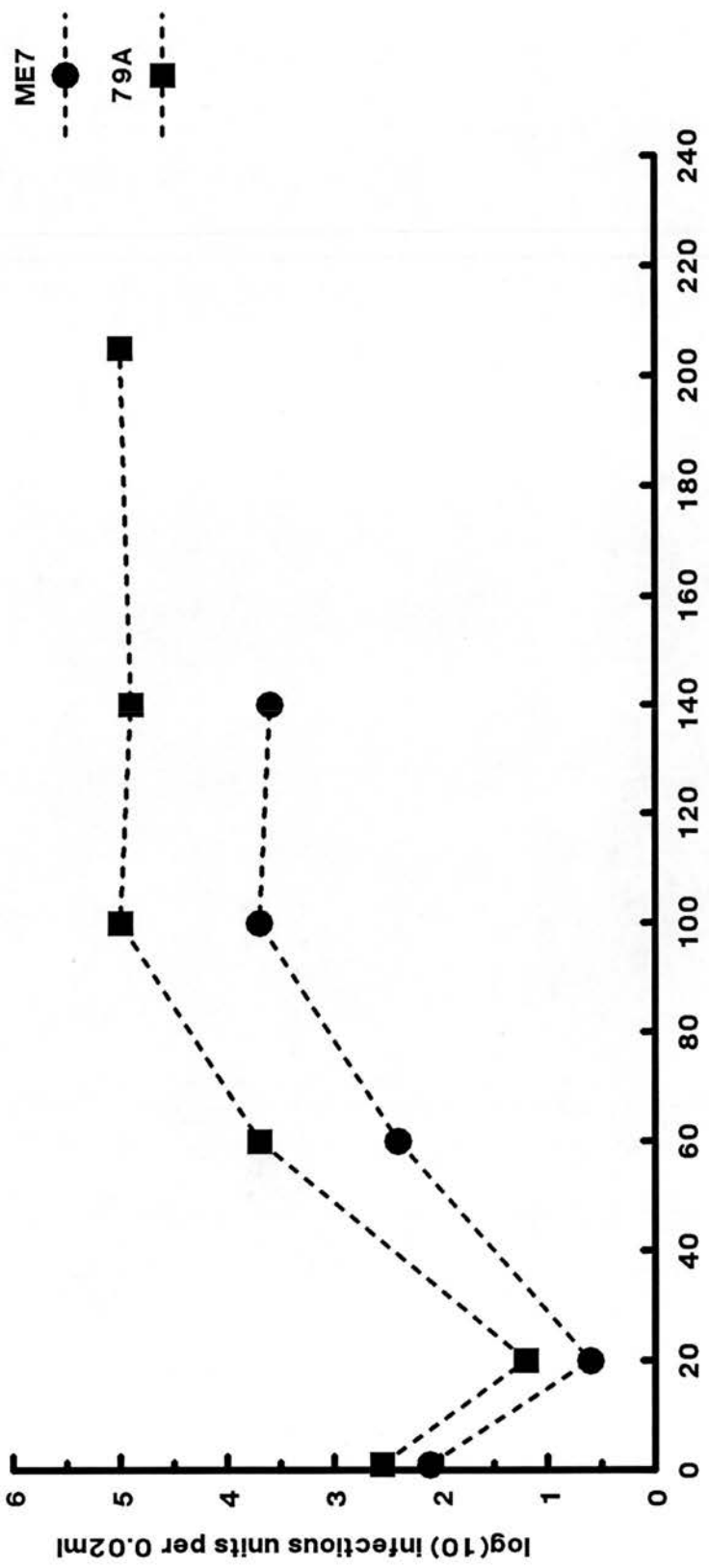

Figure 42. Infectivity titres in sequential retina pools from C57BL mice infected i.o. with ME7 or 79A scrapie, from experiment 19.

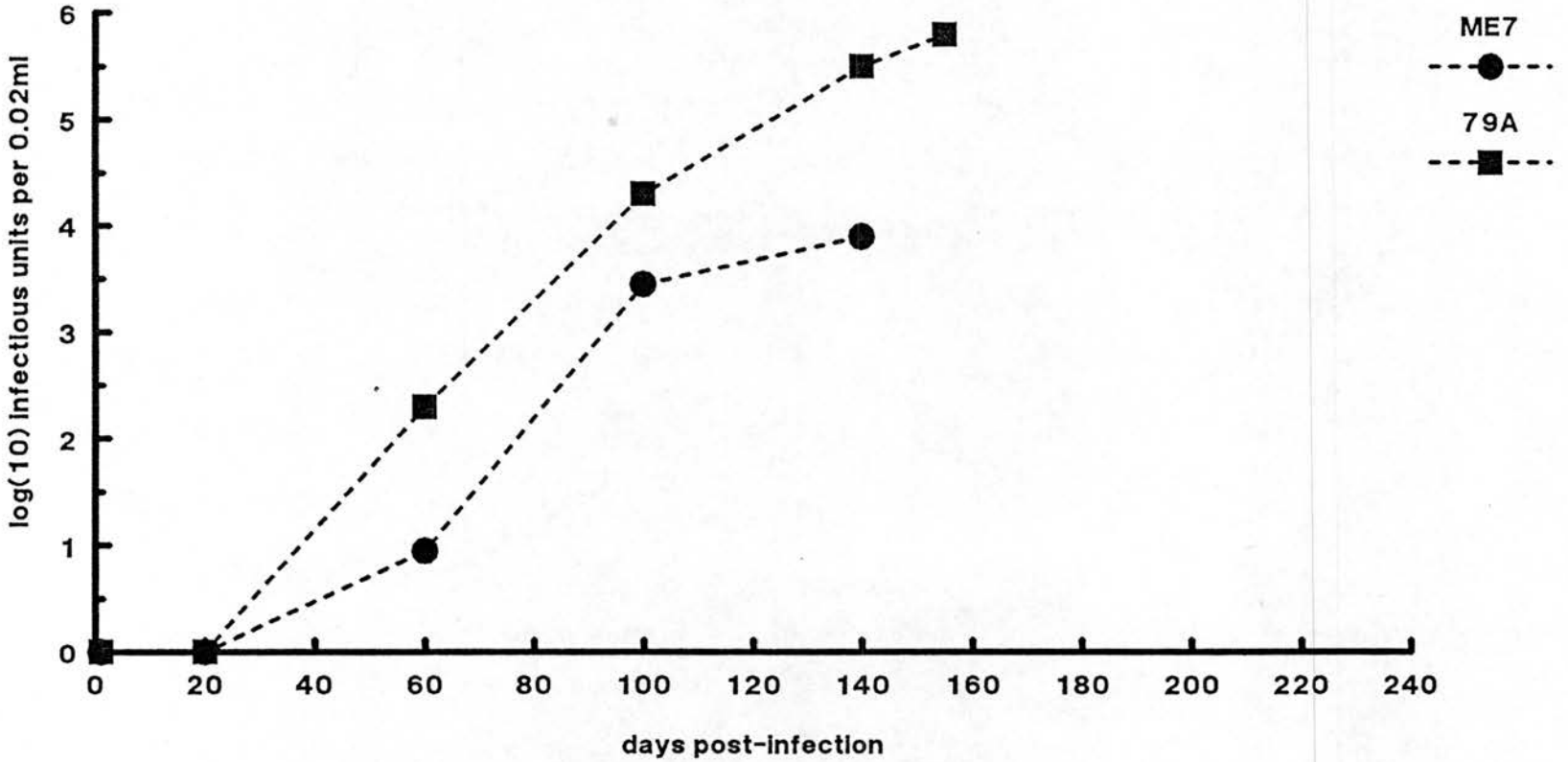

Figure 43. Infectivity titres in sequential retina pools from C57BL mice infected i.c. with ME7 or 79A scrapie, from experiment 19.

Superior colliculus

The sequential levels of infection in SC after i.o. infection with ME7 or 79A scrapie are shown in Fig. 44. As previously noted, the ME7 levels are very similar to those found in experiment 17, and from Fig. 44 it can be seen that both strains of scrapie reach a similar level by 60 days. Thereafter, 79A again produces consistently higher levels than ME7, reaching $10^{4.9}$ at 140 days, and $10^{5.8}$ in terminal mice. The titrations of the 140 day and terminal pools gave Karber estimates of titre of $10^{4.7}$ and $10^{5.5}$ respectively. The 140 day ME7 pool had a titre of $10^{4.3}$ by the incubation period assay, and was slightly higher ($10^{4.7}$) by the Karber estimate from the titration. The similarity in these estimates confirms the accuracy of the incubation period assay based on an appropriate dose-response curve.

Sequential titres in SC following i.c. infection with ME7 are shown in Fig. 45, which includes retina data for comparison. The assays of SC after i.c. infection with 79A are still in progress. Fig. 45 shows residual inoculum from the i.c. injection in SC at 24 hours and 20 days, but as with retina, the infectivity has increased markedly by 60 days, and reached a titre of $10^{5.5}$ by 140 days. The Karber titre estimate from the titration of the 140 day SC pool was $10^{5.5}$ or greater; all the mice in the 10^{-6} dilution group developed the disease, making a more precise estimate impossible. This result shows that the retinocollicular relay also transports infectivity in a retrograde direction (c.f. Fig. 35).

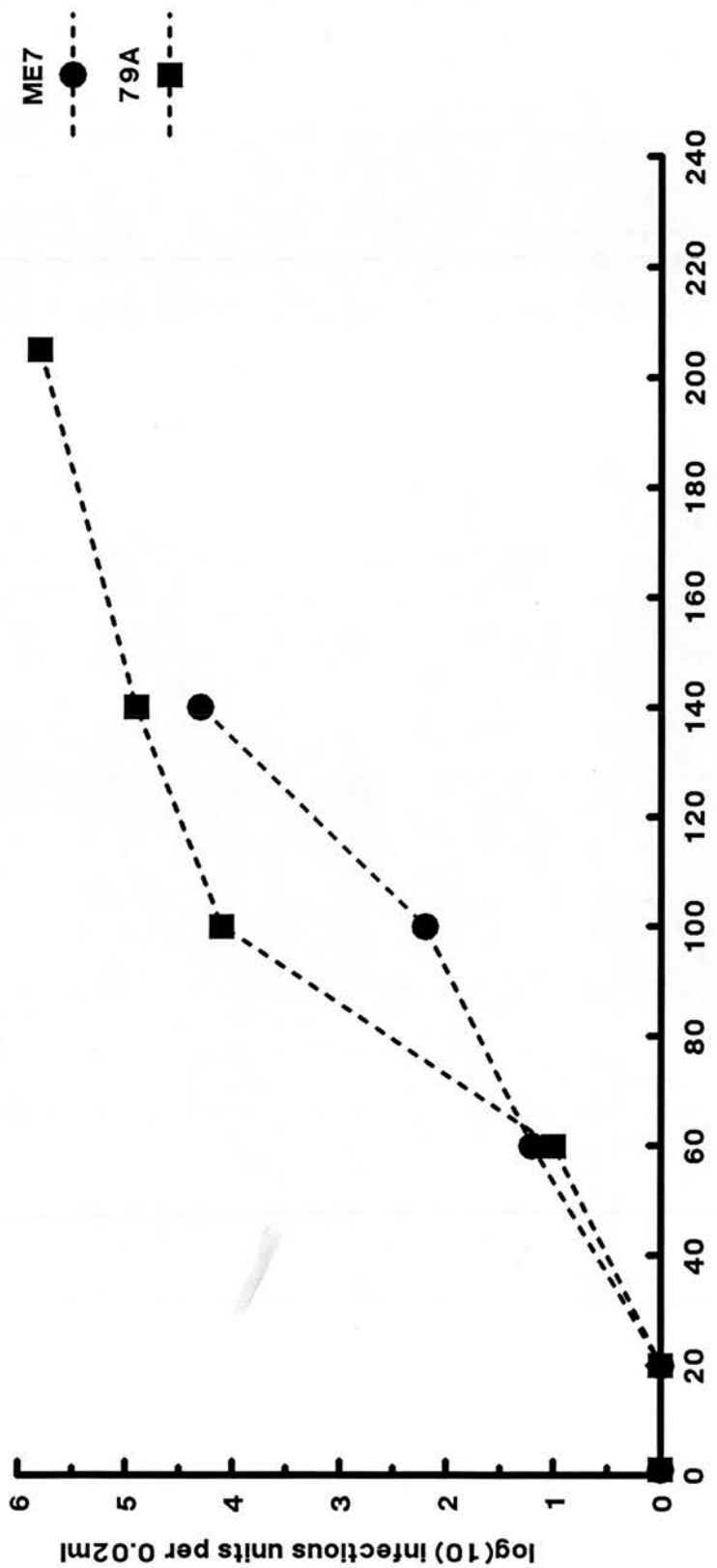

Figure 44. Infectivity titres in sequential SC pools from C57BL mice infected i.o. with ME7 or 79A scrapie, from experiment 19.

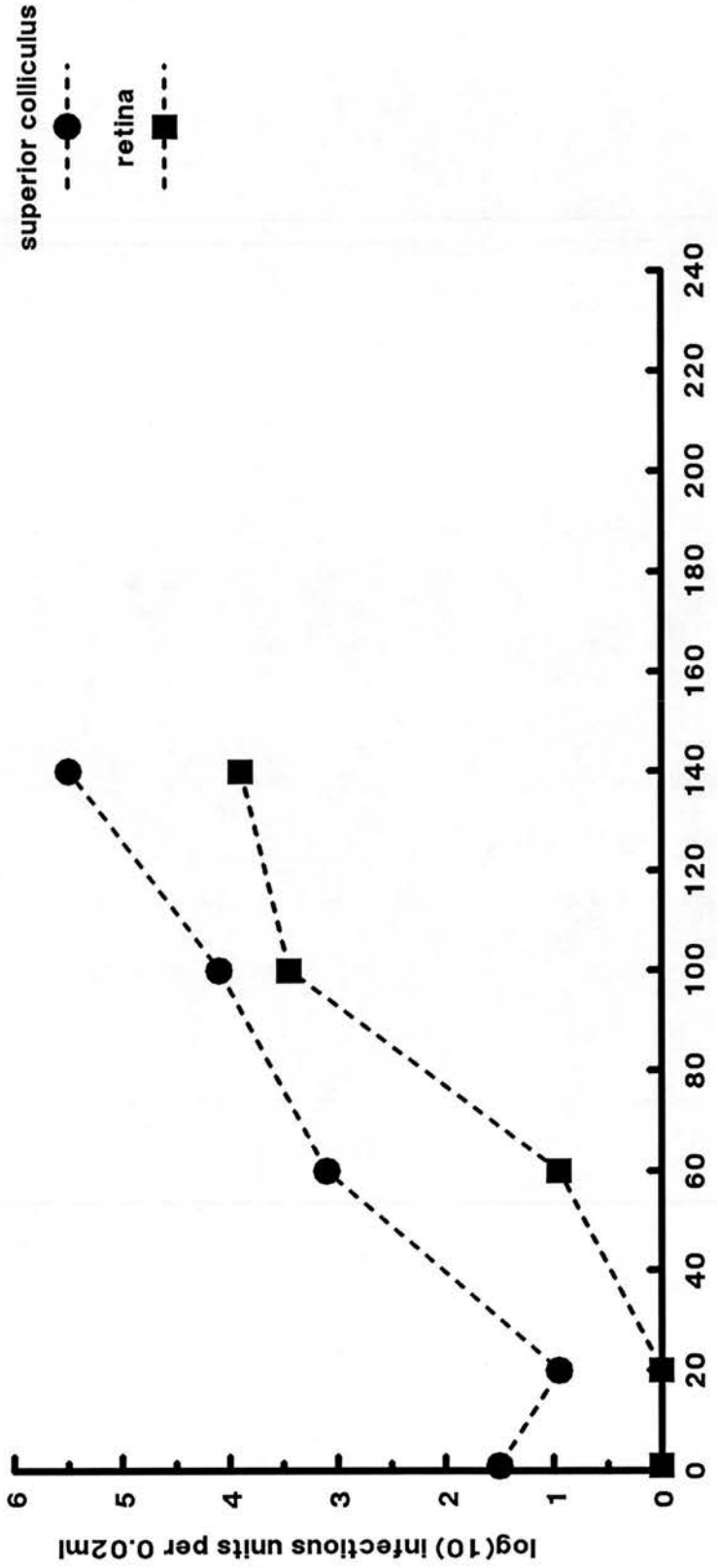

Figure 45. Infectivity titres in sequential SC and retina pools from C57BL mice infected i.c. with ME7 scrapie, from experiment 19.

Spleen

Sequential spleen assay following i.o. and i.c. infection with ME7 and 79A scrapie were included to investigate the extent of early extraneural replication resulting from i.o infection compared with i.c. (see 5.1 and 5.2). A low level of ME7 was detected in spleen at 24 hours, and although no titre estimate was possible, 2 mice out of 12 in the 79A 24 hour assay group developed the disease, demonstrating that low levels of infectivity were present in spleen at 24 hours following i.o. infection with either strain of scrapie. Fig. 46 shows that very high levels of 79A are found in spleen from 20 days after i.o. infection, and lower levels of ME7 at 24 hours, 20 and 60 days, which plateaus at around 10^4 infectious units from 100 days. After i.c. infection (with an identical 2ul dose: see above) the sequential titres for both strains are almost identical to those following i.o. infection (Fig. 47). The similarity in spleen titres after i.o. and i.c. infection was an unexpected and interesting result, which is important for the interpretation of the enucleation experiments described in Chapter 5.

4(d) How does the Sinc gene affect infectivity levels?

This experiment (20) was set up to study sequential infectivity levels in two congenic mouse strains which differ at the Sinc gene locus, in order to relate infectivity to the pathology described in experiment 8 (see 3(g)). SV ($Sinc^{s7}$) or VM ($Sinc^{p7}$) mice were bilaterally i.o. infected with a 10% spun dilution of ME7

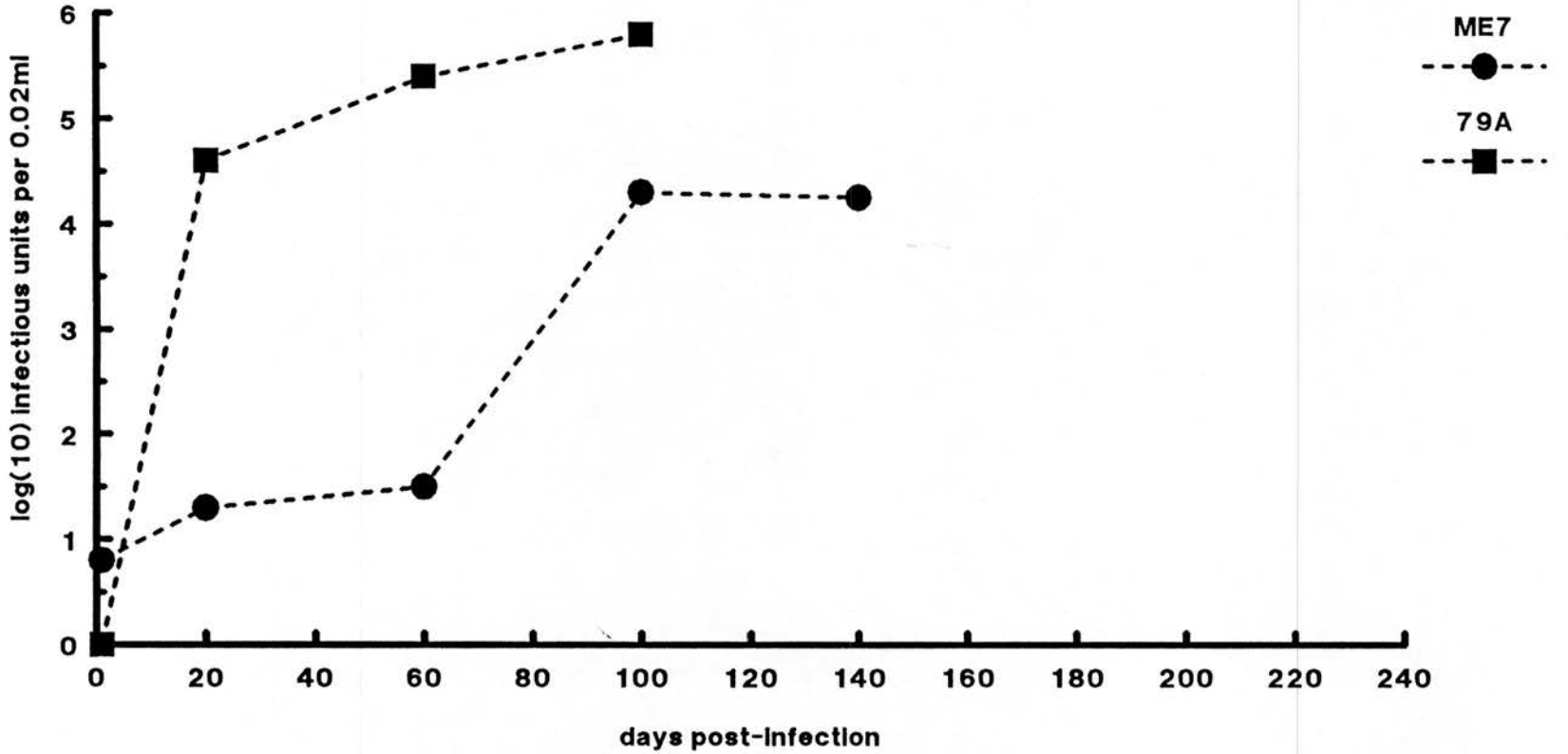

Figure 46. Infectivity titres in sequential spleen pools from C57BL mice infected i.o. with ME7 or 79A scrapie, from experiment 19.

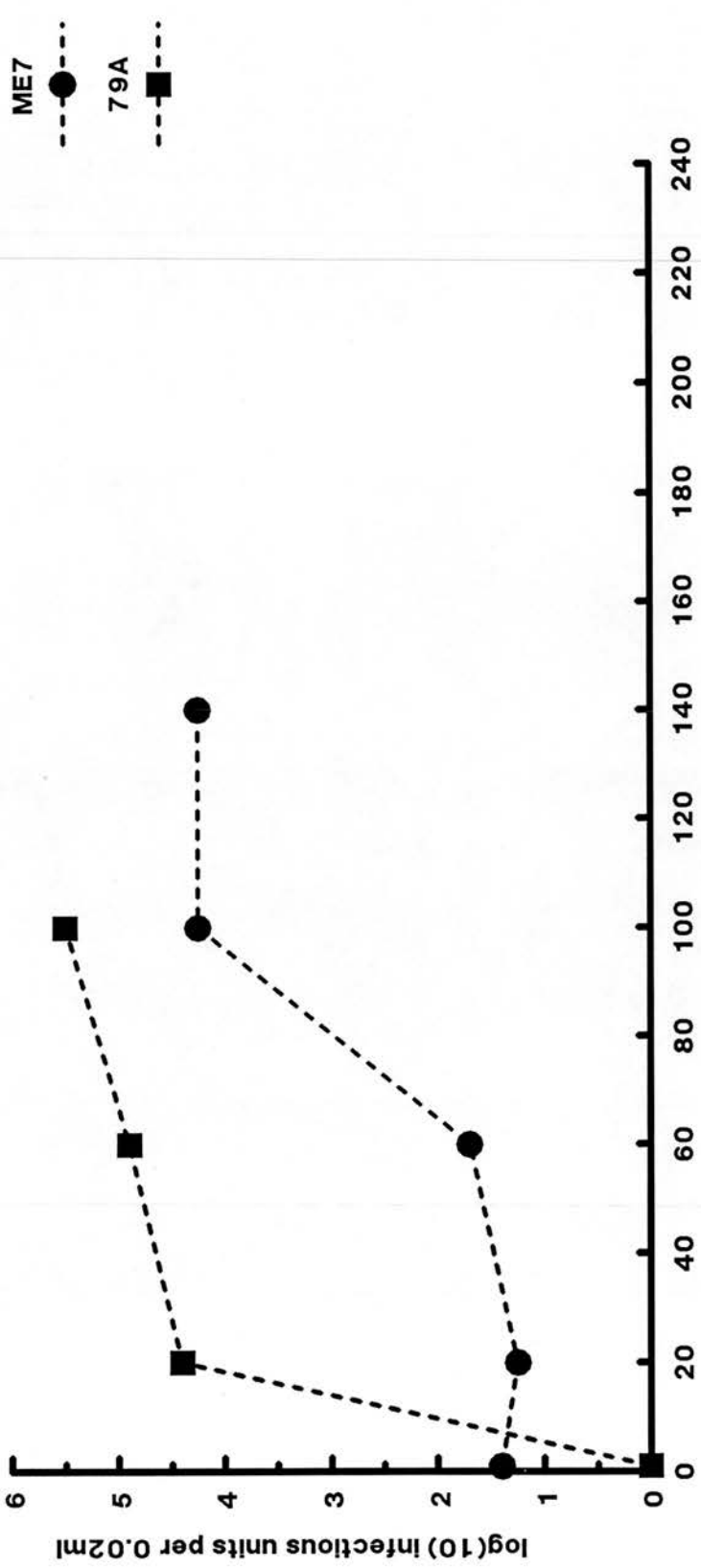

Figure 47. Infectivity titres in sequential spleen pools from C57BL mice infected i.c. with ME7 or 79A scrapie, from experiment 19.

scrapie. Pools of 6 retina and SC tissues were removed at 48, 76, 104, 132, 160, 188 and 216 days from SV mice, and additionally at 244, 272 and 300 days from VM mice. The incubation periods (from Table 19) were SV: 254 ±4.9 and VM: 474 ±8.3. Retina and SC pools from each mouse genotype were assayed in 12 SV mice (it would have been impracticable to assay the VM tissue pools in VM mice because of the length of the incubation period). Of the retina pools, the only results completed so far are for the 48 and 76 day groups. The results for SC are complete. The 160 and 216 day assays from SV mice were titrated from 10^{-1} to 10^{-7}, as were the 160 and 244 day assays of VM tissue. Since there is no dose-response curve available in SV mice, the infectivity levels were calculated from the C57BL dose-response curve used in experiments 17, 18 and 19.

Retina

The early results of the retina assays are shown in Fig. 48. The relative incubation periods are shown as an open circle (SV), and an open square (VM), and are <u>not</u> an indication of titre. It is impossible to judge at this stage whether or not the infectivity detected in VM mice is due to residual inoculum, but in the SV retinas, the steep rise in titre indicates that replication has been initiated. The results so far for SV retina are similar, although the titres are slightly lower, to those found for C57BL retina with ME7 infection in experiments 17 (Fig. 34) and 19 (Fig. 42).

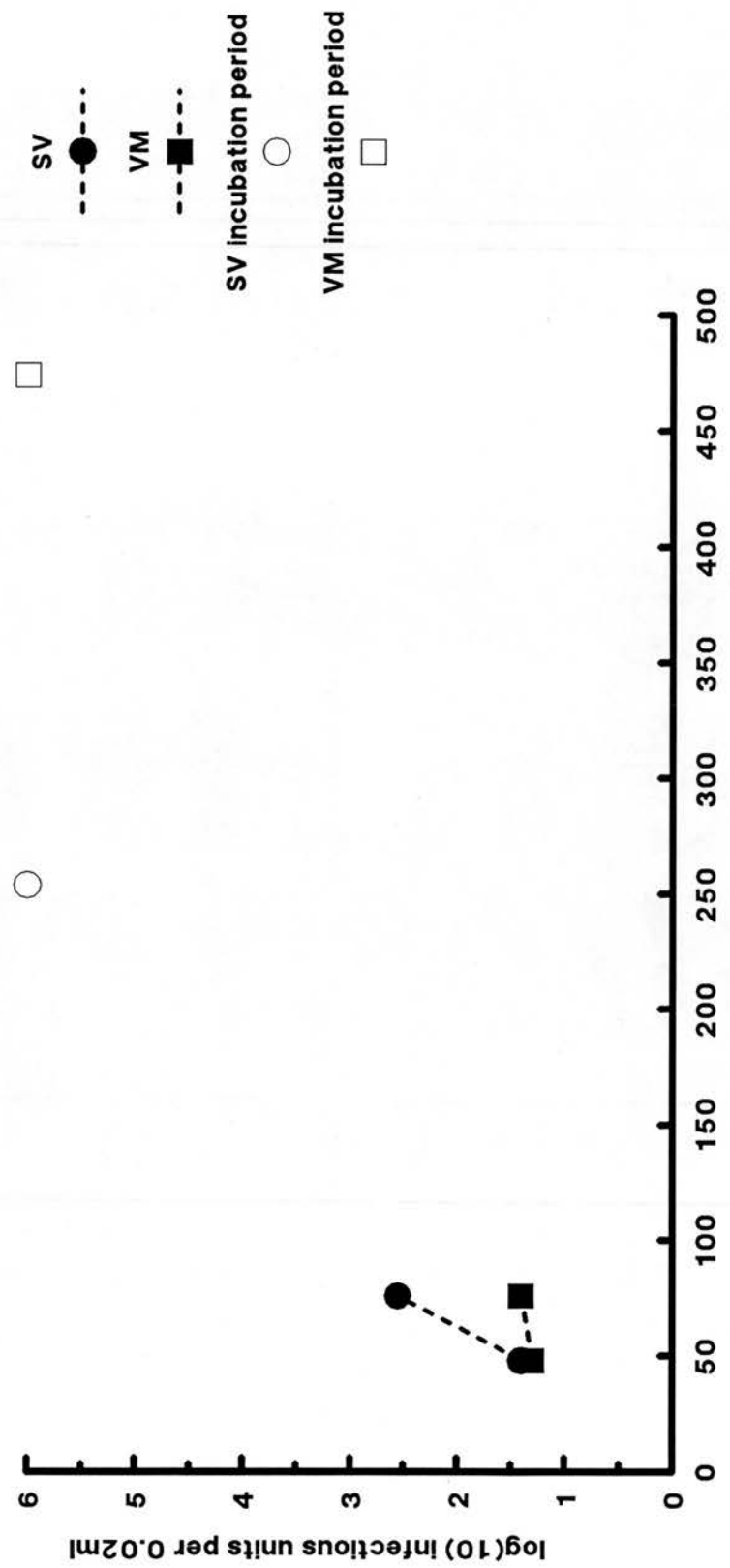

Figure 48. Infectivity titres in sequential retina pools from SV and VM mice infected i.o. with ME7 scrapie, from experiment 20.

Superior colliculus

Although two of the mice (out of 12) in the 48 day SV group developed scrapie, infectivity was first detected at 76 days, compared to 132 days in the VM SC (Fig. 49). The SV results are again similar to those shown in C57BL SC (Fig. 35), but in the VM SC, infectivity levels remained very low for another 50 to 60 days. By 300 days, the VM titre is similar to that of SV mice at 176 days. The titrations at 160 and 216 days in the SV mice gave Karber estimates of $>10^{4.3}$ and $>10^{4.72}$ respectively, which are identical to the incubation period estimates of $10^{4.4}$ and $10^{4.65}$ at a 1% dilution. The VM titrations at 160 and 244 days gave Karber estimates of $10^{2.3}$ and $10^{4.4}$ compared with the estimates of $10^{2.65}$ and $10^{2.5}$ from the dose-response curves, suggesting that the VM SC titre at 244 days are higher than indicated in Fig. 49.

This is an important result, since it reveals the action of the Sinc gene in a single neuronal relay (see 6.1).

4(e) Non-neural spread following i.o. infection.

The high levels of infection found in spleen soon after i.o. infection in experiment 19, and the development of disease, albeit after a prolonged incubation period, in mice enucleated as early as 24 hours after i.o. infection (5(a)), both signal the occurrence of a non-neural spread of infection following i.o. injection. Experiment 21 was designed to identify the levels of infection in lymphoreticular tissues and other possible non-neural replication sites to which inoculum can gain access after i.o. infection.

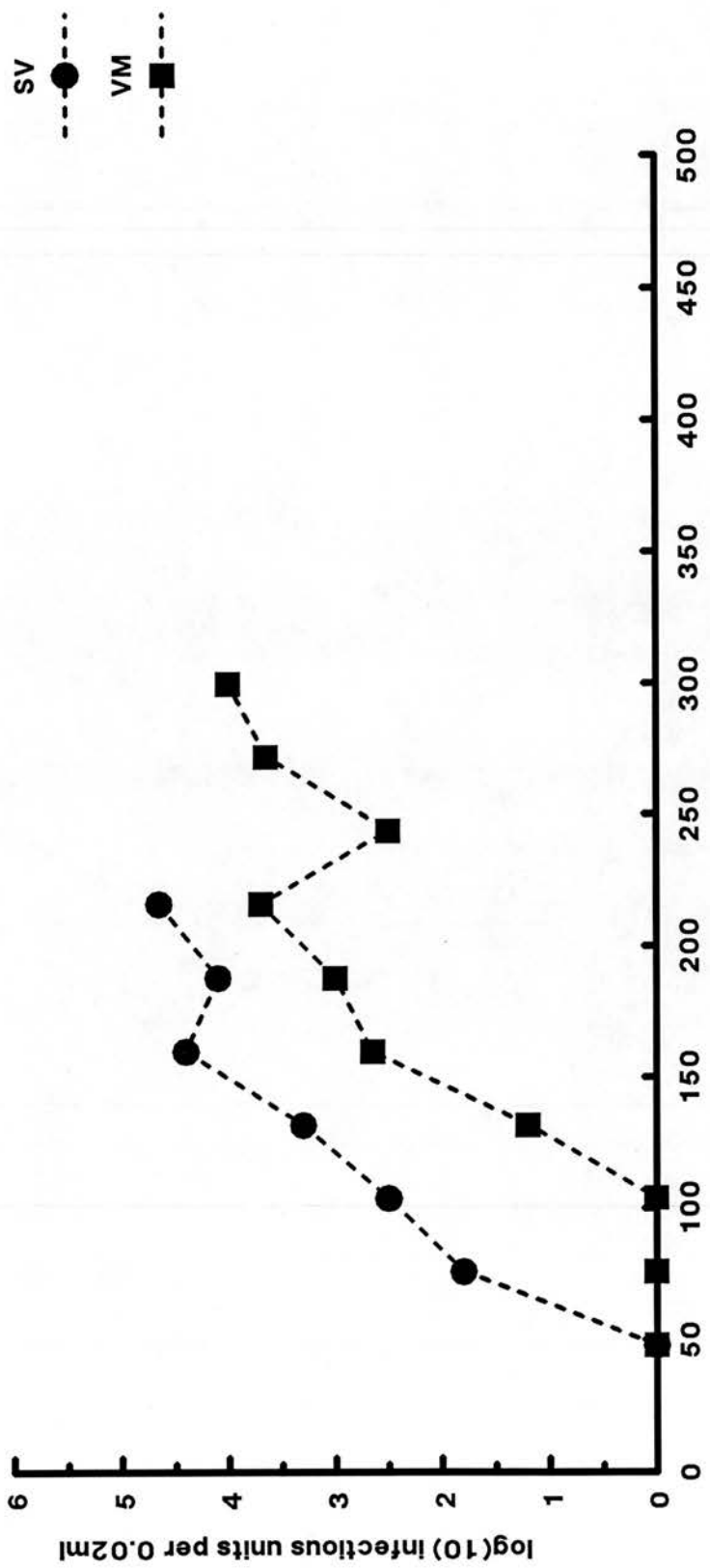

Figure 49. Infectivity titres in sequential SC pools from SV and VM mice infected i.o. with ME7 scrapie, from experiment 20.

Injection of carbon particles into the orbital tissues (2.10) resulted in black labelling of cervical lymph nodes 24 hours later (Fig. 4b). VL mice were bilaterally i.o. infected with a 10% dilution of spun ME7 scrapie. These mice also provided the control groups for experiment 18(b), for which retina and SC pools were taken. The additional non-neural tissues sampled were lacrimal gland, cervical lymph nodes, popliteal lymph nodes and Peyer's patches. Pools were made from each tissue at 24 hours, at 20 day intervals from 20 to 160 days, and also from a terminal group. The assays from these tissue pools have been set up, but the results will not be completed for at least another year.

4(f) Other neural routes of infection.

The spread of infectivity from the eye is apparently restricted to the anterograde pathway via the optic nerve (there was no evidence from the pathology of retrograde transport through the Gasserian or ciliary ganglia, for example; see 6.2). This raises the question of direction of transport of infectivity in central and peripheral nerves. Previous experiments in which infection was introduced into the tongue showed no targeting of lesions to the hypoglossal nucleus in the medulla, although HRP could easily be demonstrated in this nucleus from 24 hours after tongue injection (2.10, Fig. 5c). HRP was also demonstrated in the facial and trigeminal nuclei following injection into the vibrissal area (2.10, Figs. 5a and b). Experiment 22 employed tongue and vibrissal infection of SM mice with ME7 scrapie to study the incubation periods and to compare the levels of infectivity in target nuclei

with any pathological changes. Groups of mice were killed at 150, 200, 250, 275 dpi and at terminal stages after vibrissal infection to provide brains for pathological examination and trigeminal nucleus for assay. Hypoglossal nucleus was also removed to be assayed as a control. The tongue-injected mice developed clinical scrapie from as early as 180 days post-injection, so only the 150 and 200 day groups were available for assay of the hypoglossal nucleus, with trigeminal nucleus as a control. The incubation periods for these routes were: tongue 208 ±3.5, vibrissae 288 ±1.95, i.c. 160 ±1.1. As with the previous experiment, the assays from experiment 21 have been injected, but the results will not be complete for at least a year.

4(g) Does the dose of infection affect the i.o. incubation period?

Two experiments were designed to investigate this question. In the first (23), incubation periods were compared following infection with different volumes of inoculum in a titration, to see if the volume of the i.o. injection affected the efficiency of uptake and the subsequent pathogenesis. In the second, (24) the pathology and levels of infectivity in the SC during the incubation period were compared within a titration. This was intended to show whether there was a correlation between infectivity and the timing of pathology at different doses.

(i) In experiment 23, groups of C57BL mice were infected with one of 4 volumes (1ul, 0.5ul, 0.1ul or 0.05ul) of ME7 scrapie at dilutions

from 10^{-1} to 10^{-6}. The incubation period of the i.c. control group (which also received 1ul of a 10% suspension of inoculum) was 170 ±3, which is equivalent to a titre of $10^{3.7}$ i.c. ID_{50} units on the standard C57BL dose-response curve. The results are shown in Table 21(a). Unfortunately, the incubation periods of 2 cages of mice (from several groups) had to be disregarded, since they had been noted as possible cannibals (see 2.7), and some produced anomalous incubation periods. This means that there are too few mice in some groups to allow comparison of incubation periods. The Karber titres show a one log difference between 1ul and 0.05ul, which is what would be expected from the 20-fold difference in dose. This suggests that the volume of inoculum does not affect the efficiency of infection.

(ii) In experiment 24, C57BL mice were again i.o. infected with 1ul of dilutions from 10^{-1} to 10^{-6} of ME7 scrapie (from a different source brain). For each dilution, groups of 4 - 9 mice were killed at 140 and 160 dpi to provide brain tissue for histology. The incubation periods of the terminal groups are shown in Table 21(b). The Karber estimate of titre was $10^{-3.91}$. None of the mice killed at 140 dpi showed pathological signs of scrapie infection; at 160 dpi the positive cases were: 3/4 in the 10^{-1} group, 2/4 in the 10^{-2} group, 1/4 in the 10^{-3} group, and the remainder negative.

The results indicate that the development of the pathology in the SC is delayed in proportion to the incubation period of each dilution. Although there were survivors in the higher dilution groups, all of the mice in the groups with positive pathology would have been expected to develop the disease.

TABLE 21(a) Experiment 23 and (b) experiment 24: incubation periods and Karber estimates of titre from groups of C57BL mice after i.o. ME7 infection with various volumes of inoculum.

	(a) VOLUME				(b)
	1ul	0.5ul	0.1ul	0.05ul	1ul
DILUTION					
10^{-1}	263 ±6 (6)	-	290 ±12 (7)	393 ±14 (6)	250 ±4 (4)
10^{-2}	-	321 ±3 (3)	307 ±9 (5)	342 ±29 (3)	279 ±10 (5)
10^{-3}	317 ±8 (4)	334 ±3 (3)	404 (1)[a]	317 ±4 (3)	322 ±19 (3)
10^{-4}	302 (1)[a]	0	589 (1)[a]	0	502 ±49 (5)
10^{-5}	0	0	0	0	530[a]
10^{-6}	0	0	0	0	0
Karber	$10^{-3.75}$	$10^{-3.25}$	$10^{-2.88}$	$10^{-2.70}$	$10^{-3.91}$

a - only one positive case

4(h) Can purification of the brain homogenate shorten the incubation period?

The incubation period following i.o. infection is always longer than an i.c. infection with a similar dose of any strain of scrapie. If the i.o. route of infection is merely less efficient than i.c., then the incubation period might be shortened by increasing the dose of infection. However, there is a technical limitation on the amount of infectivity that can be introduced into the eye; 1ul is the maximum volume that can be injected, and a 5% brain homogenate is the minimum dilution possible. Since scrapie infectivity partially copurifies with scrapie-associated fibrils (Diringer et al, 1983, McKinley et al, 1983), two experiments were designed in which i.o. infection was with either a 5% homogenate or an SAF preparation of either ME7 or 87V scrapie. The SAF fractions were prepared with the minimum possible dilution, in an attempt to maximise the infectious dose. A full titration of standard brain homogenate, and both proteinase-K (pK) treated and untreated preparations of SAF was carried out in experiment 27.

(i) A 5% brain homogenate, and an SAF preparation were made from a pool of three terminal ME7 brains as described in 2.3. One half of the SAF fraction was treated with pK, and the other left untreated. One ul of the 5% homogenate was equivalent to a wet weight of brain of 0.05mg, whereas 1ul of either SAF fraction was equivalent to 3mg, giving a potential 60-fold difference in the amount of infectivity present (although the preparative technique would not be expected to give a 100% yield of infectivity in the SAF fractions (Somerville et

al, 1986). SV mice were bilaterally i.o. infected with either the 5% homogenate or the untreated SAF fraction, and groups of 4 to 12 mice were killed at 150, 175 and 200 dpi, and also in the terminal stages of the disease. Additional groups were i.c. infected with the 5% homogenate, the pK-treated fraction or the untreated fraction. One half of each brain was frozen in liquid nitrogen and stored at $-80^{\circ}C$ to provide pools from each group for PAGE identification of PrP, the major protein component of SAF. The other half was prepared for histology. The incubation period results are shown in Table 22. There was no significant difference between the incubation periods of mice infected with the 5% homogenate and the untreated SAF fractions with either route. However, the i.c. incubation period for mice infected with the pK-treated fraction was significantly longer than both other groups ($p > 0.01$) using Student's t-test.

SAF fractions were prepared from the half-brain pools from the mice infected with the 5% homogenate, and the PrP bands identified (see 1.3). The results are compared with the pathological findings in Table 23. Both PrP and vacuolation are first identified at 175 dpi; although all mice killed on or later than 199 dpi show lesions, the only group in which PrP is identified in all mice is the terminal group. Although this suggests that disease-induced PrP cannot be detected until vacuolation occurs, earlier detection may have been possible had the fractions been prepared from SC pools, and not half brains. Immunocytochemistry has shown that abnormal PrP can be seen in discrete brain areas several weeks before vacuolar degeneration with 87V scrapie (Bruce et al, 1989).

(ii) The above experiment was repeated using the 87V strain of

TABLE 22(a) Experiment 25: mean incubation periods following i.o. infection with 5% brain homogenate or SAF fractions of ME7 scrapie, and (b) experiment 27: Karber titre estimates from i.c. titration with similar inocula.

(a)	INOCULUM		
	5% homogenate	SAF untreated	SAF +pK
ROUTE OF INFECTION			
i.o.	240 ±3.5	238 ±4.7	-
i.c.	167 ±3.6	172 ±3.0	187 ±3.3
(b)	Karber estimates of titre		
i.c.	$10^{5.8}$	$10^{6.8}$	$10^{6.9}$

TABLE 23. Experiment 25: comparison of PAGE detection of the protein PrP, and the incidence of vacuolar degeneration in the SC of mice following bilateral i.o. infection with a 5% brain homogenate of scrapie.

	PrP protein			Vacuolar lesions
	+	+/-	-	
Days post-injection				
153	0	0	4	0/4
175	1	0	4	3/5
199	2	1	2	5/5
terminal (240 ±3.5)	6	0	0	6/6

scrapie in experiment 26. The 5% homogenate and two SAF fractions were prepared from 2 terminal IM mice. As smaller volumes were used in this case, 1ul of the 5% homogenate was equivalent to 0.05mg wet weight of brain, whereas the SAF fractions were equivalent to 3.8mg, a 76-fold difference. The incubation period results are shown in Table 24. Only the +pK SAF fraction produced a significantly shorter i.c. incubation period than the 5% homogenate, and the i.o. incubation periods were not significantly different. The incidence of vacuolar lesions in the dLGN following i.o. infection with 5% homogenate and untreated SAF inocula were compared at 250, 300 and 350 dpi. The incidence with the 5% homogenate was: 250 days - 1/5, 300 days - 3/4 and 350 days - 5/6, compared with the SAF inoculum: 250 days - 2/5, 300 days - 1/6, and 350 days - 3/6.

(iii) The similarity in the incubation periods and the timing of the first lesions in the previous experiments suggests that although the dose of infectivity was probably increased in the SAF preparations, this was not obvious since the incubation periods were all at the minimum for each model. This result could be substantiated by showing that the SAF fractions did contain significantly more infectivity than the standard 5% homogenate. This was attempted in experiment 27, by comparing the Karber estimates of titre from full titrations of each inoculum.

As in the previous experiments, a standard homogenate, a pK-treated and an untreated fraction were prepared as above and diluted as described in 2.3. Between 12 and 20 RIII mice were i.c. infected with each dilution of the three inocula. The Karber estimates (for the same doses as given in experiments 24 and 25) are shown in Table

TABLE 24. Experiment 26: incubation periods following i.o. infection with 5% brain homogenate or SAF fractions of 87V scrapie.

	INOCULUM		
	5% homogenate	SAF untreated	SAF +pK
ROUTE OF INFECTION			
i.o.	488 ±9	478 ±17	-
i.c.	302 ±0	294 ±7	287 ±2

22(b). Both SAF fractions produced cases in the 10^{-8} dilution. The significance of this one log difference in the titre of the injected dose would be increased if the same result could be shown in a replicate experiment; however, the result indicates that the dose of infection in experiments 25 and 26 was probably greater in the SAF fractions than in the homogenate, and that the incubation period minimum of about 240 days in SV mice is not a function of infectious dose.

Chapter 5.1 Evidence for axonal transport of scrapie.

There is overwhelming evidence from the infectivity and pathology studies that scrapie infectivity is carried by the optic nerve and tract to the retinal projections contralateral to the injected eye. Since the optic nerve is a branch of the CNS comprising the axons of the retinal ganglion cells, it provides an opportunity to examine the transport of infectivity in more detail than has been previously possible using mixed peripheral nerves (see 2.1).

Three approaches were made in the investigation of axonal transport. In the first, i.o. infected mice were serially enucleated between 12 hours and 35 days post-injection, in order to establish the length of time necessary for infection to become established in the SC, and hence the minimum time for infection to spread from the retina. This was carried out using ME7, 79A and 87V scrapie (experiments 28, 29 and 30). Much of this work has already been published (Scott and Fraser, 1989: Appendix C).

In the second approach, retinal ganglion cells were partially or completely destroyed by neonatal MSG treatment (see 2.6 and 4(b), experiment 18(b)), prior to i.o. infection, to see if any prolongation of incubation period, or delay in the appearance of vacuolation in the SC could be detected. These experiments (31(a), (b) and (c)) were with ME7 scrapie in VL and BSC mice. Some of this work has been accepted for publication (Foster et al, in press).

Thirdly, pilot experiments were devised in an attempt to disrupt the uptake and transport of infectivity by chemical

treatment of either the mice or inoculum. IDPN (iminodipropionitrile) intoxication has been shown to impair neurofilament transport in rats and guinea pigs (Parhad et al, 1986). Mice infected by i.o. and i.c. routes were maintained on IDPN throughout the incubation period, and examined for changes in the incidence of SC lesions and incubation period length (experiment 32). In another experiment (33) vinblastine, which blocks anterograde fast transport in rabbit optic nerve (Chihara et al, 1982) was mixed with the inoculum, and the incubation period compared with a control group. In a third experiment (34), inocula were treated with either poly-l-ornithine, a polycation additive, or DMSO (dimethyl sulphoxide) a penetrant. Both are known to enhance the uptake of HRP, probably by disrupting membrane integrity (Mesulam, 1982). The resulting incubation periods were compared with control groups.

5.1(a) Can serial enucleation identify the rate of spread of infection in the optic nerve?

In experiment 28(a), SV mice were infected by an i.c., i.o. or i.v. route with a spun 10% dilution of ME7 scrapie. The infected (right) eye was removed from groups of 14 i.o. infected mice at 12 and 24 hours, and 7, 14, 21 and 28 days post-infection. Four of the 8 i.v. infected mice were enucleated at 18 hours post-infection. One half of the i.o. infected groups were killed at 185 dpi for histology, and the other half retained until they were terminal. Vacuolation was scored in all brains from semi-serial sections to give a visual projection score (2.9) for left and right sides

independently.

The incidence and severity of lesions seen in the groups killed at 185 days is shown in Table 25. Eighty-eight per cent of the unenucleated control group had lesions in the left SC, and many of them had more widespread lesions. There were no lesions seen in the brains of mice enucleated on or before 7 dpi. Of the 14 day group, only one mouse out of 5 had lesions in the contralateral SC. This rose to 80% in mice enucleated at 28 days, almost as high as the control group. The visual projection scores (Table 25) show that lesions in the contralateral SC were inevitably more severe than those on the ipsilateral side.

The incubation periods and scores of terminal mice are shown in Table 26. Mice enucleated on or before 7 dpi had significantly longer incubation periods (see footnote), reflecting the lesion incidence at 185 dpi. Mice in groups with longer incubation periods also had less severe terminal lesions (Fig. 50), particularly in the SC, with no evidence of asymmetry. The lesion profiles of unenucleated mice, and mice enucleated on or after 14 dpi were indistinguishable, and resembled the profiles of mice infected by the i.c. route (Fig. 50). The possibility that enucleation *per se* induced the development of asymmetrical pathology in the SC, perhaps by triggering the release of circulating infectivity, was tested by the enucleation at 18 hours of the i.v. infected group. No difference was found in either the incubation period (Table 26) or the lesion profile.

Some evidence of Wallerian degeneration was seen in uninfected control mice killed between 30 and 86 days post-enucleation. However, infected mice were not examined until at least

Table 25. Experiment 28(a): effect of enucleation on the occurrence of lesions in the superior colliculus (SC) 185 days after i.o. infection of the right eye with ME7 scrapie.

time of enucleation	mice with lesions in left SC at 185 days	mean SC lesion score at 185 days	
		LEFT	RIGHT
12 hrs	0/7	-	-
24 hrs	0/9	-	-
7 days	0/8	-	-
14 days	1/5	3.0	1.0
21 days	5/9	2.4	1.2
28 days	4/5	2.5	0.3
unenucleated	7/8	2.1	0.4

Table 26. Experiment 28(a): differences in incubation period and terminal lesion severity in the superior colliculus (SC) in mice enucleated up to 28 days after intraocular infection or intravenous infection with ME7 scrapie.

time of enucleation	incubation period of (n) mice	mean terminal SC lesion score LEFT	RIGHT
Intraocular infection			
12 hrs	302 ± 12* (7)	1.8	1.8
24 hrs	313 ± 7*** (7)	1.9	1.7
7 days	304 ± 12** (6)	1.6	1.6
14 days	285 ± 14 (6)	2.2	1.8
21 days	283 ± 16 (6)	2.6	2.5
28 days	267 ± 11 (6)	3.0	2.5
Unenucleated	260 ± 4 (14)	3.2	3.2
Intravenous infection			
18 hrs	278 ± 7 (3)	3.0	3.0
Unenucleated	283 ± 9 (4)	2.5	2.5

Statistical analysis by Student's t-test; compared to unenucleated controls,
*** $p < 0.001$; ** $p < 0.01$; * $p < 0.02$.

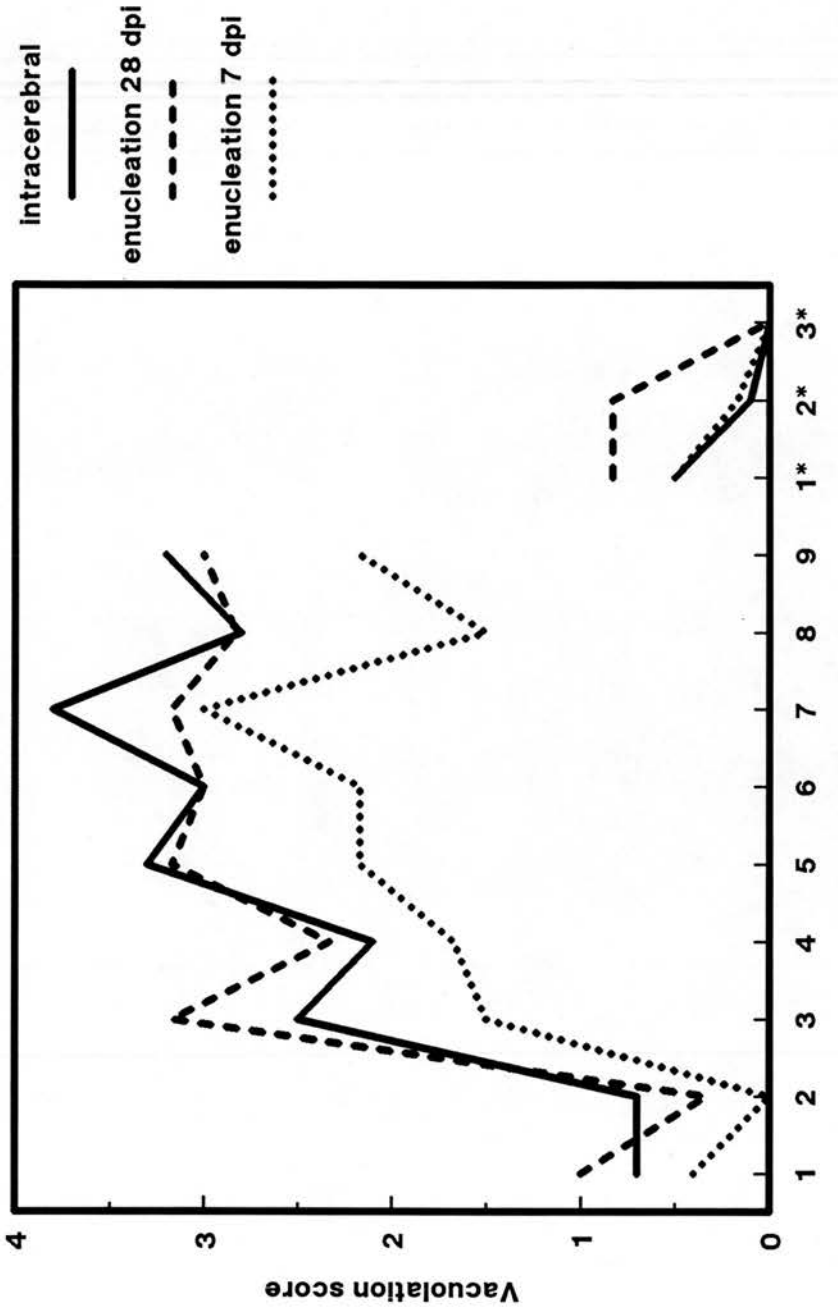

Figure 50. Lesion profiles from experiment 28(a)

157 days post-enucleation (185 dpi less a maximum of 28 days post-enucleation). By this time the degeneration had resolved to a withering and gliosis of the optic tract, and a condensation of the neuronal perikarya in the SC.

The results show that enucleation on or before 7 dpi prevented the early development of lesions in the contralateral SC and prolonged the incubation period. Enucleation at 14 days or later had no significant effect on incubation period, although the percentage of mice showing left SC lesions at 185 days only approached that of controls in mice enucleated at 28 dpi. The earliest enucleation time which still permits infection via the optic nerve in individual animals is 14 dpi. The pathogenesis of the infection which killed the mice infected on or before 7 dpi is investigated in Chapter 5.

This experiment was repeated (28b) using more closely spaced enucleation times between 6 and 14 days post-infection. The incidence of lesions in the SC at 185 dpi is shown in Table 27. No lesions were found in the mice enucleated at 6 dpi, but 2 to 3 out of 6 mice had lesions in each of the 8, 10, 12 and 14 day groups. Four out of 6 mice in the 28 day group had SC lesions (as in the previous experiment), and in this case all the unenucleated control mice had lesions. Table 27 shows that all affected mice, except those in the 6 day enucleation group, had asymmetrical lesions similar in severity to those in experiment 28(a) and shown in Table 25. Lesions in the two positive cases in the 6 day group were mild and affected both left and right SC, similar to those seen in terminal mice in early enucleation groups in the previous experiment. The incubation periods and terminal lesion scores also

Table 27. Experiment 28(b): effect of enucleation on the occurrence of lesions in the superior colliculus (SC) 185 days after i.o. infection of the right eye with ME7 scrapie.

time of enucleation (days)	mice with lesions in left SC at 185 dpi	mean SC lesion score at 185 dpi LEFT	RIGHT
6	0/6	0	0
8	2/6	1.0	1.0
10	3/6	2.7	1.7
12	2/6	1.5	1.0
14	3/6	3.0	2.0
28	4/6	2.0	0.8
unenucleated	6/6	2.7	1.3

confirmed the previous findings, with the 6 and 8 day groups showing a significant prolongation compared to the unenucleated controls (Table 28). This result more closely defines the period required for infection to become established in the SC at between 8 and 12 days.

Similar enucleation experiments were carried out using 79A and 87V scrapie. Firstly, 79A was used for experiment 29, a replicate of experiment 28(a). However, since the i.o. incubation period with 79A is considerably shorter than with ME7, some mice became clinically affected before 185 dpi. All mice were therefore retained until terminal. The resulting incubation periods are shown in Table 29. The 12 and 24 hour groups are significantly prolonged, and although the 7 day group incubation period is longer than the unenucleated control, it is not statistically significant. Since there is very little pathology in the SC of 79A infected mice, the mean terminal SC lesion scores have not been included.

An enucleation experiment (30) using 87V scrapie was designed to see if the timings suggested by the ME7 results were similar in a model which had a much longer incubation period. Since it was difficult to estimate when the initial SC lesions would occur, the same enucleation groups as experiment 28 were used, but separate groups of mice were killed at 280, 300, 320 and 340 days post-injection. The incidence of vacuolar lesions in these groups is shown in Table 30. No lesions were seen in any of the mice enucleated at 14 dpi or earlier. Between zero and 3 mice per group had positive lesions in the 21, 28 and 35 day enucleation groups. In no group did all the mice have lesions, but only 7 out of 15 mice in the unenucleated group were positive. These results are identical to those found with ME7 (c.f. Table 25), except that one mouse in the

TABLE 28. Experiment 28(b): differences in incubation period and terminal lesion severity in the superior colliculus (SC) in mice enucleated up to 35 days after intraocular infection with ME7 scrapie.

time of enucleation (days)	incubation period of (n) mice	mean terminal SC lesion score LEFT	RIGHT
6	263 ±11 (7)*	2.4	2.3
8	269 ±8 (7)**	2.0	1.9
10	252 ±8 (8)	2.1	2.0
12	238 ±9 (9)	3.2	2.3
14	256 ±12 (7)	2.3	2.0
28	240 ±8 (9)	3.3	2.5
35	232 ±8 (7)	2.6	2.1
unenucleated	235 ±6 (12)	3.1	2.7

Statistical analysis by Student's t-test; compared to unenucleated controls, * $p < 0.02$, ** $p < 0.01$.

Table 29. Experiment 29: incubation periods in mice enucleated up to 28 days after intraocular infection with 79A scrapie.

time of enucleation	incubation period mean ± SE of (n) mice
12 hrs	223 ±4* (6)
24 hrs	225 ±6* (6)
7 days	218 ±5 (6)
14 days	205 ±9 (8)
21 days	207 ±6 (8)
28 days	200 ±10 (5)
unenucleated	201 ±6 (14)

Statistical analysis by Student's t-test; compared to unenucleated controls,
* $p < 0.02$.

Table 30. Experiment 30: effect of enucleation on the occurrence of lesions in the superior colliculus (SC) at four intervals after i.o. infection of the right eye with 87V scrapie.

time of enucleation	mice with lesions in left SC at n dpi				
	280	300	320	340	total
24 hours	0/3	0/4	0/4	0/3	0/14
7 days	0/4	0/4	0/3	0/4	0/15
14 days	0/4	0/2	0/3	0/4	0/13
21 days	1/4	2/4	1/2	0/2	4/12
28 days	1/3	0/4	2/3	1/3	4/13
35 days	0/2	3/4	2/2	2/3	7/11
unenucleated	1/3	3/4	0/4	3/4	7/15

14 day enucleation group had SC lesions with ME7.

The incubation periods are shown in Table 31. Although a 10% unspun inoculum was used, the source brain may have been of low titre, since there were many survivors (which explains the 50% incidence of lesions in the unenucleated group in Table 30). However, the available incubation periods are consistent with the results from the other enucleation experiments; no mice were killed with scrapie in the 24 hour, 7 or 14 day groups, and the incubation periods in the other groups lie within the range of the unenucleated controls. This experiment is being repeated with a tested source of inoculum.

5.1(b) Does ganglion cell ablation with MSG affect i.o. pathogenesis?

In experiment 31(a), groups of MSG-treated and normal BSC mice were i.o. infected with a 10% unspun homogenate of ME7 scrapie. In 31(b), similar groups of VL mice were infected by i.o. and i.c. routes, and in 31(c) further groups of VL mice were infected by i.o., i.c. and i.p. routes. The incubation periods are shown in Table 32. There is a significant prolongation of the mean incubation period of all MSG-treated i.o. groups. This must be due to the effect of MSG on the retinal ganglion cells, since no equivalent prolongation occurs with either the i.c. or i.p. routes of infection. These experiments are of necessity designed around the small numbers of MSG-treated mice available at any one time; some mice in both MSG-treated and control groups in experiments 31(a) and

TABLE 31. Experiment 30: incubation periods from VM mice enucleated up to 35 days after intraocular infection with 87V scrapie.

time of enucleation	incubation period mean ±SE of (n) mice
24 hours	-*
7 days	-*
14 days	-*
21 days	453 (1)
28 days	487 (1)
35 days	>466 ±11.3 (5)
unenucleated	483 ±7.8 (4)

* the 12 mice in each group either died with intercurrent illness or were survivors.

Table 32. Incubation periods of mice treated with MSG, and untreated control groups, following i.o, i.c. or i.p. infection with ME7 scrapie.

			incubation periods (n)	
			MSG-treated	untreated
experiment	route of infection	mouse strain		
31(a)	i.o.	BSC	301 ±5 (5)	272 ±7 (6)
31(b)	i.o.	VL	277 ±6 (8)	258 ±7 (7)
31(b)	i.c.	VL	188 ±5 (9)	192 ±5 (9)
31(c)	i.o.	VL	296 ±4 (12)	276 ±11 (9)
31(c)	i.c.	VL	180 ±6 (6)	185 ±2 (6)
31(c)	i.p.	VL	305 ±5 (10)	310 ±8 (12)

(c) were killed serially between 140 and 217 dpi, but were too few to show any consistent result.

5.1(c) Can chemical treatment of mice or inoculum affect i.o. pathogenesis?

In experiment 32, mice were intoxicated with IDPN from the time of infection for the duration of the incubation period. The F_1 cross between C57BL and VM mice was used. IDPN-treated mice were given an i.p. dose of 0.3g/kg at infection, and maintained on 0.02% IDPN in drinking water as described by Parhad et al, 1986. Mice were infected by i.o., i.c. and i.p. routes. Groups of 4 treated and untreated mice were killed at 7 intervals between 220 and 346 dpi and their brains examined for pathological changes. The mean incubation periods of the treated and untreated groups are shown in Table 33. IDPN treatment had no significant effect on incubation period. Pathological examination also revealed no obvious difference between the groups. One mouse killed 203 dpi with paralysis and clinical signs consistent with lathyrism was found to have multiple small abscesses in the muscles of the spinal column; however this proved to be the sole example of this type of pathology. The results are inconclusive, since the IDPN regime may have been insufficient in mice to produce the interference with slow axonal transport produced in guinea-pigs.

In a companion experiment (33), an attempt was made to block fast axonal transport by mixing vinblastine with the inoculum. Chihara et al (1982) have shown that anterograde fast transport can be blocked by i.o. injection of 10 to 100ug of vinblastine in

TABLE 33. Experiment 32: comparison of the incubation periods of IDPN-treated mice and controls following i.o., i.c. or i.p. infection with ME7 scrapie.

	incubation periods (n)	
	IDPN-treated	untreated
route of infection		
i.o.	404 ±7 (22)	388 ±6 (16)
i.c.	265 ±3 (6)	257 ±2 (9)
i.p.	438 ±10 (8)	456 ±4 (8)

rabbits. The recovery of fast transport depends on the dose of vinblastine. Groups of LM mice were each given 100ug of vinblastine in 1ul of a 10% spun ME7 homogenate. Fast axonal transport was assessed by i.o. injection of ^{3}H proline one week later, and subsequent scintillation counting of right and left SC (see 2.10). The mean SC counts and incubation periods are given in Table 34. Although the counts suggest a slight depression of fast axonal transport, the incubation periods are almost identical. It is tempting to conclude that spread of infectivity is unaffected by blockade of fast axonal transport, but until the effect of vinblastine can be shown more convincingly in mice, it must be assumed that its effect is insignificant or transitory.

In the third pilot experiment (34), an attempt was made to enhance the uptake of infectivity from the inoculation site with either DMSO or poly-l-ornithine. SM mice were infected by an i.o. or i.c. route with a 5% homogenate of ME7 containing either 2% DMSO or 0.001% poly-l-ornithine (Itaya, 1980). Control groups were infected with ME7 alone. The results are shown in Table 35. DMSO had no effect, but poly-l-ornithine significantly prolonged both the i.o. and i.c. incubation periods. The i.o. lesion profile was also significantly depressed in the poly-l-ornithine group (Fig. 51), although the i.c. profile was unaffected. This apparent prolongation of incubation period remains to be confirmed by i.o. and i.c. titration of poly-l-ornithine-treated inoculum, in order to distinguish between a reduced efficiency of infection at the i.o. site, e.g. in the effective titre of the inoculum, and an effect on subsequent pathogenesis; the low lesion profile suggests the latter.

Table 34. Experiment 33: DPM counts from SC taken from LM mice one week post-infection with vinblastine and ME7 scrapie, and subsequent incubation periods.

	vinblastine + ME7		ME7 only	
	left SC	right SC	left SC	right SC
mean DPM count	175 ±60	73 ±7	244 ±45	92 ±20
incubation period (n)	276 ±6.2 (20)		274 ±6.0 (19)	

TABLE 35. Experiment 34: the effect of DMSO and poly-l-ornithine on the incubation periods of SM mice infected with ME7 scrapie by i.o. and i.c. routes.

	incubation periods (n)		
	DMSO-treated inoculum	PLO-treated inoculum	ME7 only
ROUTE			
i.c.	159 ±2 (6)	198 ±12** (8)	158 ±2 (7)
i.o.	266 ±10 (12)	301 ±16* (7)$	254 ±7 (9)

Statistical analysis by Student's t-test; compared to untreated controls, * $p < 0.02$, ** $p < 0.01$.

$ there were 3 survivors in this group

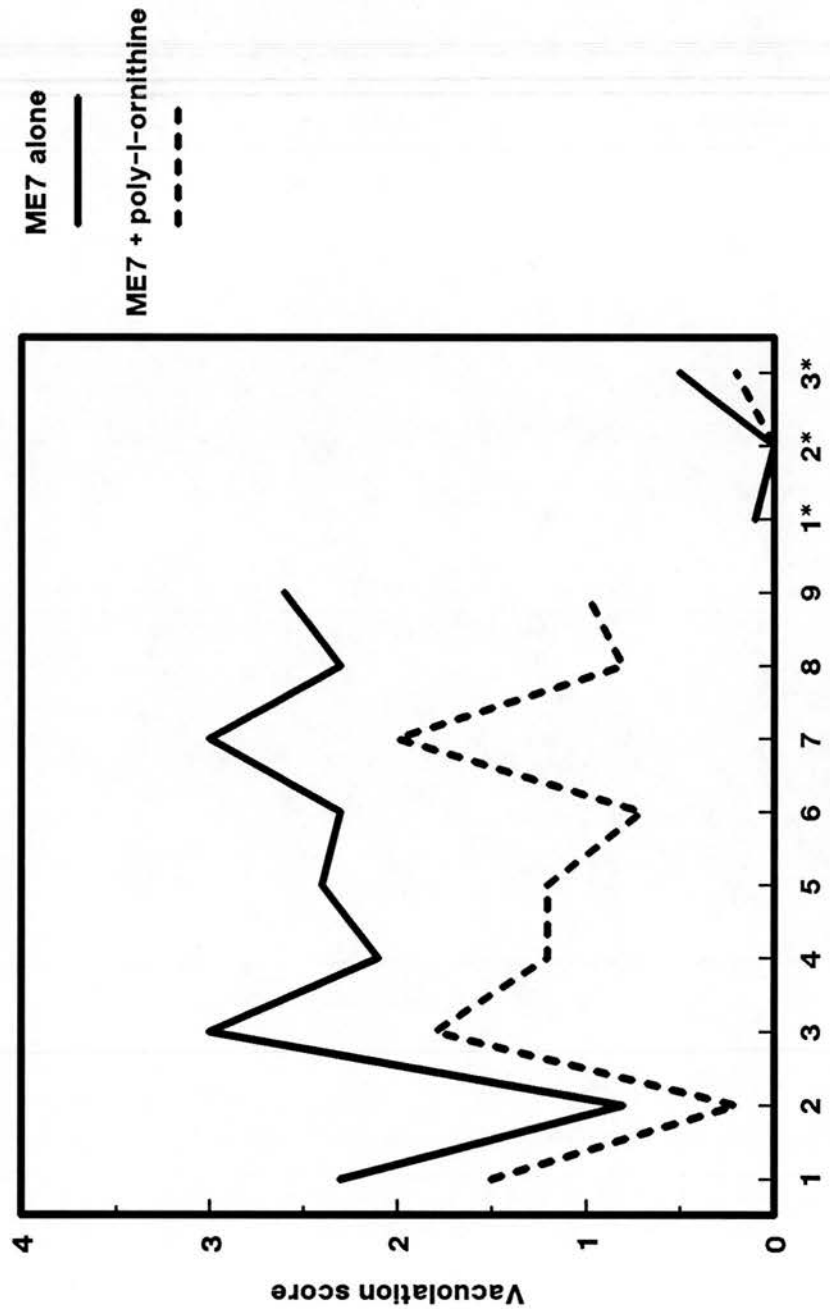

Figure 51. Lesion profiles from experiment 34.

5.2 Non-neural spread of infectivity after i.o. infection.

The enucleation experiments, and others in the previous section, have shown that additional pathways other than those via the optic nerve are available following intraocular injection. In this section, two experiments are described which were designed to investigate these alternative pathways of i.o. pathogenesis. Firstly, since the level of infection in the spleen gives a reasonably good reflection of replication in the lymphoreticular system as a whole (Fraser and Dickinson, 1978), the effect on incubation period of splenectomy before and after i.o. infecion was tested. Secondly, inoculum was instilled into the conjunctival sac to simulate leakage of inoculum from the injection site after i.o. infection, and to investigate such a route of infection.

5.2(a) Does splenectomy affect the i.o. incubation period?

Groups of 20 SM mice were splenectomised (see 2.6) either 7 days before, or 7 days after i.o. infection with a 10% homogenate of ME7 (experiment 35). A third group received the i.o. infection alone. Spleens from the group splenectomised post-infection were frozen for subsequent assay. The incubation period results are shown in Table 36. Splenectomy either before or after infection had no effect on the i.o. incubation period. Lesion profiles from the three groups were not significantly different. This result suggests that other sites in the lymphoreticular system may be more important for replication following i.o. infection than the spleen. The results of experiment 21 (4(e)) in which infectivity was measured in a variety

Table 36. Experiment 35: the effect on incubation period of splenectomy before or after i.o. infection of SM mice with ME7 scrapie.

incubation periods (n)		
splenectomy 7 days before infection	splenectomy 7 days after infection	infection alone
236 ±7 (16)	232 ±4 (20)	242 ±6 (18)

of extra-neural tissues will suggest alternative sites.

5.2(b) Can conjunctival instillation of infection initiate pathogenesis from non-neural sites of replication?

In experiment 36, SM and VL mice were infected by dropping 1ul of a 10% ME7 homogenate into the conjunctival sac (see 2.5). Control groups were i.o. infected as usual. Additional groups of VL mice were enucleated at 6 and 12 hours, and 8 and 35 days following conjunctival instillation; enucleation should have no effect on a non-neural route of infection. Groups of SV mice were also infected with 79A by conjunctival instillation and by the usual i.o. route. Table 37 shows that conjunctival instillation did produce disease in both ME7 and 79A infected mice, but only in a small proportion of the animals infected, indicating a reduced efficiency of infection. However, the ME7 incubation periods for the SM and VL mice are remarkably similar. Although only a few of the enucleated VL mice developed clinical disease (Table 37), the incubation periods lie within the range of the unenucleated SM and VL mouse groups. The lesion profile derived from mice infected by conjunctival instillation is significantly lower than the i.o. profile in scoring areas 3,5,6,7,8, and 9 (Fig. 52), but not significantly different from the 12 hour enucleation group from experiment 28(a) (Fig. 50).

Conclusions

The experiments in Chapter 5 were designed to investigate axonal transport of infectivity, and also the non-neural spread of

TABLE 37. Experiment 36: i.o. incubation periods compared with conjunctival instillation of ME7 scrapie in SM and VL mice, and 79A scrapie in SV mice. Groups of VL mice receiving conjunctival instillation were enucleated at 6 and 12 hours, and 8 and 35 days.

		incubation periods*	
		i.o.	conjunctival instillation
ME7 scrapie			
mouse strain	enucleation		
SM	-	242 ±5.9 (18)	322 ±7.4 (6/18)
VL	-	235 ±5.5 (12)	322 ±11.6 (4/9)
VL	6 hours	-	320 ±3.3 (8/10)
VL	12 hours	-	319 (1/6)
VL	8 days	-	319 (1/6)
VL	35 days	-	340 ±4.0 (3/6)
79A scrapie			
SV	-	201 ±5.7 (14)	232 ±35 (3/12)

* n in incubation period / total including survivors and intercurrent deaths.

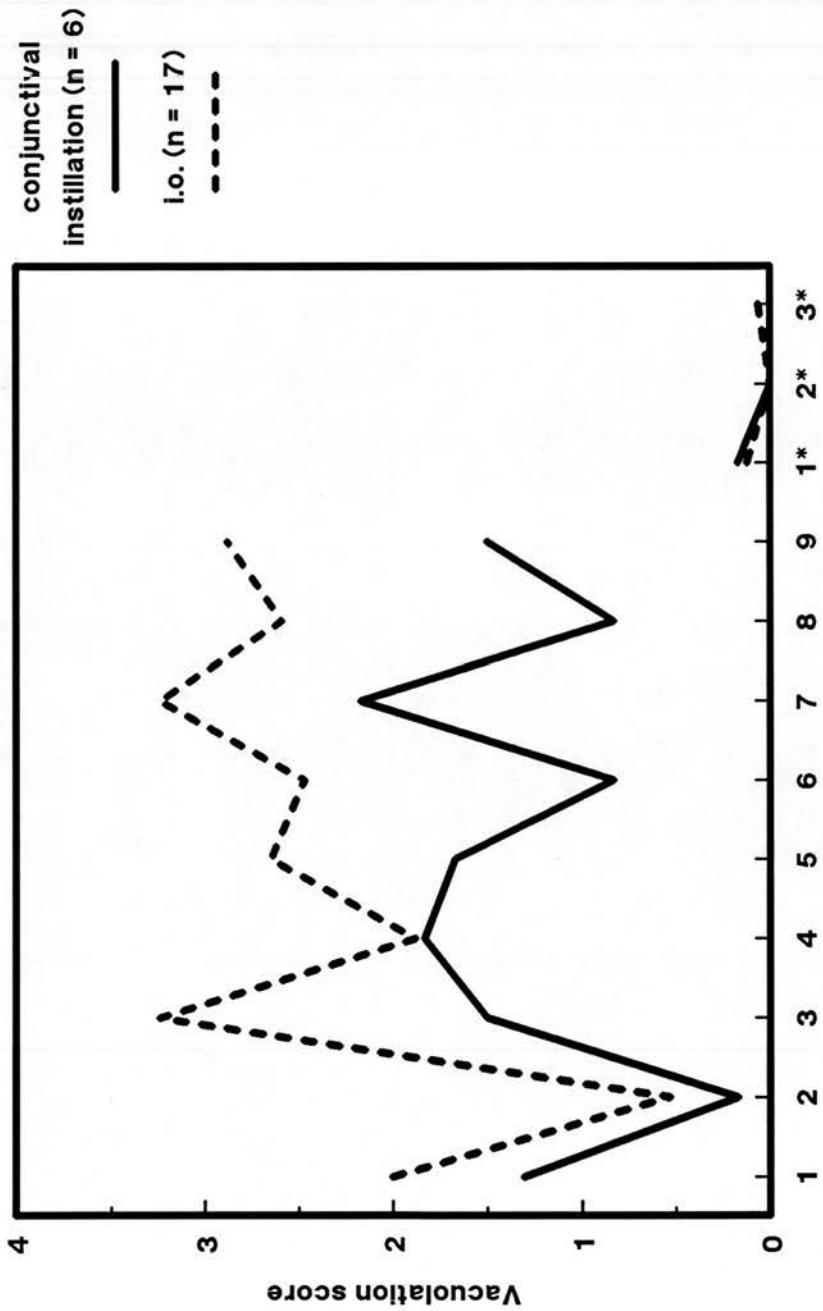

Figure 52. Lesion profiles from SM mice in experiment 36.

infection. It has been shown that scrapie spreads slowly from the retina to the brain at a rate consistent with slow axonal transport. This rate appears to be common to at least 3 strains of scrapie, despite their quite different incubation periods, suggesting that infectivity utilises this normal cellular transport system. The implications of these findings are discussed in Chapter 6.2. It has also been shown that following i.o. infection, inoculum from the eye initiates lymphoreticular infection. Since splenectomy has no effect, it is probable that the initial site(s) of replication are the cervical lymph nodes. It has also been shown that disease can develop following conjunctival instillation. This could be a route for iatrogenic and natural infection.

Chapter 6. Discussion

Scrapie research has always been constrained by problems due to the long asymptomatic time course of the disease, the failure to identify the nature of the infecting pathogen, and the absence of an *in vitro* test, making bioassay the only index of infection. Consequently, much scrapie research has been the province of only a few dedicated workers (Mims, 1977). The subject of scrapie has become widely debated by both scientists and the public at large, because of the implications of the epidemic of BSE in the U.K. (see 1.1). Much present research is directed towards determining genetic susceptibility to these diseases, to finding a diagnostic test for scrapie and BSE infection in the preclinical stages and to identifying the nature of the causal organism. The work in this thesis does not contribute directly to these goals, but was prompted by different objectives. The investigation of the intraocular route of infection is a step towards identifying the cellular mechanisms involved in the infectious process; knowledge without which there can be no hope of developing treatments for the already infected animal.

This investigation of the intraocular route falls into three main areas: firstly, the differences in timing and site of pathological changes dependent on the strain of scrapie and mouse genotype; secondly, the patterns of replication in the retina and its projections, and thirdly, the evidence from enucleation and other studies for the axonal transport of infectivity. The relationship between these is discussed in the following three

sections.

6.1 The relationship between infectivity and pathology.

Although the pathogenesis of scrapie has been investigated following various routes of infection (reviewed in Kimberlin and Walker, 1988b), the only attempt to systematically correlate the progress of the infection with the associated degenerative changes was by Cole and Kimberlin (1985), who examined the dynamics of vacuolation in the brain and spinal cord following i.p. infection. However, with i.c. and peripheral routes of infection, the routes of spread within the CNS, and access to clinical target areas (Fraser and Dickinson, 1973; Kimberlin and Walker, 1983) are not known, and it would be impracticable to assay all the relevant neuroanatomical targets. Neural spread of scrapie following both peripheral infection, and direct injection of the sciatic nerve has been demonstrated (Kimberlin and Walker, 1989a; Kimberlin et al, 1983), but no study of the co-localisation with pathology has been made. Cole (1981) did relate i.o. 263K infection in hamsters to degenerative changes in the CNS, but as a minor part of a major study of degenerative changes in hamster scrapie models.

The i.o. route of infection provides the simplest model to study the correlation of infectivity and vacuolar degeneration within the CNS. This neuroanatomical system is one of the most studied and understood in the CNS (see 1.3). The targeting of scrapie pathology to the murine retinal projections was first described by Fraser (1982), who later showed a correlation with infectivity levels in optic nerve and superior colliculus in assays

from about 65 days post-infection of C3H mice with ME7 scrapie (Fraser and Dickinson, 1985). Pathogenesis following i.o. infection has also been studied using the hamster 263K model by Buyukmihci et al (1983) and Kimberlin and Walker (1986a), although neither looked at sequential pathological changes in the CNS. One aim of the experiments in this thesis was to extend the previous work in this area by comparing the timing and site of the initial lesions in the retinal projections with the first detectable infectivity in these sites.

The type of degeneration produced by scrapie infection is remarkably consistent throughout all sheep, goat and rodent scrapie models. The lesions vary in severity and distribution, but vacuolar morphology in the neuropil of the grey matter, occasionally within neurons, and in some models in white matter tracts, remains consistent in all situations (Fraser, 1979). The distribution of lesions with natural or experimental routes of infection is strictly symmetrical, except for the special case where foci of ME7 infection are induced as a result of mutation of the 87A strain of scrapie (Bruce, 1985). The amyloid plaques produced by some strains of scrapie have no obvious topographical relationship with vacuolar degeneration, although it has been suggested that they occur as a result of the loss of the innervation to plaque affected areas from degenerating subcortical neurons. This would permit the accumulation of an amyloid precursor which was normally removed by the projections into the area (Fraser et al, 1986). Plaques contain a high proportion of PrP, the major protein constituent of SAF. The implications of the copurification of SAF and infectivity (which was exploited in experiments 25 and 26) are discussed in section 6.3.

Experiments 1, 2, 3 and 15 followed the sequential appearance of lesions in various mouse strains following i.o. infection with ME7 scrapie, and showed that the sequence of development of lesions at successive sites was consistent. The first lesions developed on the contralateral side to the injection site, initially in the SC, at between 140 and 188 dpi in Sinc s7 mice. Secondary lesions occurred shortly afterwards in the dLGN, then in the visual cortex, and in some strains of mouse, in the suprachiasmatic nucleus. Subsequent lesions occurred on both sides of the brain, and the terminal lesion profile was indistinguishable from that of i.c. infected mice. From experiment 17, it can be seen that infectivity is detected in almost the same sequence; retina (between 14 and 21 days), SC (56 days), dLGN (77 days) and finally optic nerve, visual cortex and cerebellum (98 days). The difficulties of obtaining an accurate dissection of visual cortex (discussed in 4(a)) make it likely that the level of infectivity found here is an underestimate, or artificially late in the incubation period. This correlation between the spread of vacuolar lesions and infectivity also follows the neuroanatomical progression. These observations suggest that sites of vacuolation, especially in the early lesions, develop subsequently to produce high levels of infectivity as a direct consequence of replication. Low infectivity levels in the optic nerve suggest that infectivity is being transported through, but not replicating, in this tissue (Kimberlin and Walker, 1986a). Accumulation of infectivity, as opposed to replication, could be difficult to distinguish at later stages in the incubation period.

A direct relationship between replication of infectivity and

vacuolation has rarely been considered (apart from Cole and Kimberlin, 1985), whereas several workers have stressed the apparent importance of amyloid in the pathogenesis of the disease (Diringer et al, 1983; Merz et al, 1983; Prusiner, 1985). This may be because of the difference in timing between the detection of infectivity and the much later appearance of vacuolation, and the absence of pathological changes in the lymphoreticular system and PNS, even in the presence of high levels of infectivity. Recent ultrastructural evidence of prevacuolar changes occurring in neurons much earlier than can be seen with the light microscope (Jeffrey et al, in prep) suggests that the interval between replication and neuronal damage is less than can be calculated from optical microscopy. Immunocytochemical localisation of SAF protein to areas of vacuolation in models which do not produce amyloid plaques (Bruce et al, 1989) indicates that PrP pathology could play a primary part in the pathogenesis of the disease, and that amyloid deposition is secondary. Scott et al (1989) have produced firm evidence that the PrP gene is the homologue of the Sinc gene, by transferring the hamster PrP gene to mice, and producing an extremely dramatic shortening of incubation period. This may provide a means of finding the basis of the molecular pathology and its relationship with scrapie replication at the cellular level. How replication can programme neuronal dysfunction which results in vacuolation is not known. Evidence from scrapie models which develop severe vacuolation in the hippocampus suggests that the loss of pyramidal neurons which occurs in these models is a result of long-term pathological damage to the dendrites of these cells (Scott and Fraser, 1984).

Although there are no obvious incubation period differences

between i.o. infected rd mutants and normal mice, there is some evidence of a difference in the timing of first lesions. In 3(c), following 79A infection, the first lesions occurred in (normal) MM and SV mice at 58% and 60% of the incubation period respectively, but not until 69% of the incubation period in (rd) C3H mice. Fig. 13 shows a similar result with ME7; in experiment 2, all SM mice were positive by 176 dpi, whereas there was no positive C3H group until 218 dpi. These results appear to reflect the differences in uptake and slow transport found in rd mutants by Grafstein et al (1972), described in 1.3. This is further evidence for the slow axonal transport of infectivity.

One inconsistency in associating infectivity to degenerative pathology is posed in the retina. Ontogenetically, the retina arises as a local outgrowth from the lateral walls of the rostral part of the brain, and is considered in the adult to be part of the CNS. Nevertheless, high levels of infectivity in the retina of Sinc s7 mice infected with ME7 are not associated with retinal pathology. Experiment 18 indicates that photoreceptor cells in the retina support replication, and experiment 19 demonstrates that the eventual loss of photoreceptor cells seen with 79A infection (and shown to be a primary scrapie lesion by Foster et al, 1986b) occurs after even higher retinal infectivity titres than those found with ME7 infection have been demonstrated. Therefore in the retina, it appears that extremely high levels of infectivity are needed for photoreceptor cell damage to occur. The specialised neurons of the retina may react to infection in a way that does not give rise to vacuolation, but results eventually in cell death (as in the hippocampal pyramidal cells) after prolonged replication of

infectivity. Curtis et al (1989), using electroretinography (ERG) and EM to study retinopathy in mice infected with 79A, showed that the primary lesion affected the integrity of the photoreceptor cells, and coincided with the loss of B wave amplitude in the ERG. These results suggest a loss of the most specialised feature of these cells, that of disc membranogenesis.

Some of the most interesting results in this thesis concern the differences in pathology and infectivity levels in the two Sinc genotypes of mice. Experiments 2, 15 and 16 demonstrate that the dramatic prolongation of incubation period in Sinc p7 mice infected with ME7 (and comparable shortening with 22A infection) also correlate with proportional changes in the timescale of the appearance of vacuolation. For example, although the incubation period in experiment 2 is 237 days in s7 mice, and 539 days in p7 mice, the initial lesions in the contralateral SC appear at 59% and 53% of the incubation period respectively. This indicates that the action of the Sinc gene can be identified at a single neuronal relay. This result is borne out in experiment 20, where infectivity is detected at 76 dpi in the SV (s7) SC, but not until 132 dpi in the VM (p7) SC, and this 50 - 60 day difference is maintained as infectivity levels rise (Fig. 49). Since this assay compares infectivity levels in a single neuronal relay from the retina to the SC, it would appear that the action of the Sinc gene is responsible for a delay of 50 - 60 days in the transport or replication of infectivity within this relay (although the evidence from the enucleation experiments suggests that this delay is in replication, not in transport; see 6.3). The difference in i.o. incubation period between SV and VM mice is about 250 days, therefore an equivalent

delay at a subsequent 4 neuronal relays between SC and clinical target areas could in theory account for the Sinc gene mediated prolongation in incubation period. This may seen a simplistic interpretation of this result, but it has been shown that following infection of the spinal cord (Kimberlin et al, 1987b), the incubation period is even shorter than after i.c. infection, because infection is being introduced neuroanatomically closer to the clinical target areas.

Experiment 16 was also designed to investigate the apparent allelic overdominance seen with 22A infection. Previous studies (Dickinson and Meikle, 1971) have shown that the incubation period of the F_1 cross between the two Sinc homozygotes is longer than in either of the parent mouse strains. This result is substantiated in experiment 16, with an incubation period in the Sinc s7 mice of 615 days (with survivors), compared to the F_1 of 700 days. The timing of the initial lesions was also in proportion to the incubation period length, at 51% and 47% in the C57BL and F_1 strains respectively. Whether this is a true effect of overdominance is not known; current thinking has pointed out that the major effect of the Sinc gene when all scrapie models are considered is that the F_1 incubation period is always longer than the s7; the incubation period with the p7 homozygote apparently occurs independently, suggesting that the s7 allele is dominant in all situations (G. W. Outram, pers. comm.; Bruce, in prep.).

One other result which is particularly well-illustrated by experiment 16 is the initial targeting of lesions to either the SC or dLGN. In the majority of scrapie models studied in Chapter 3, the first vacuolar lesions appeared in the SC. However, in some models

(VM and MB mice infected with 87V, SM mice infected with 22C, and VM and C57BL X VM mice infected with 22A) the initial targeting is to the dLGN. In experiment 16, following 22A infection, the first lesions were seen in the left SC in C57BL mice, but in the left dLGN in VM and the F_1 cross. The major murine retinal projection is to the SC (see 1.3), but the dLGN receives a collateral projection from the majority of retinal ganglion cell axons. The reasons for this 'switch' in targeting are unknown, but it suggests that the specificity is dictated by the 'targets' in the SC and dLGN and is not a property of the optic nerve axons. Strikingly similar targeting differences are seen with reovirus variants (Spriggs et al, 1983) and rabies mutants (Kucera et al, 1985). Further investigation of this alternative targeting may elucidate the basis of the different lesion distributions found in different scrapie models.

Variation in both susceptibility to infection, and support for replication of different populations of neurons must account for the different patterns of lesion targeting in the models described in Chapter 3. If vacuolation is a direct consequence of replication, as it appears to be with ME7 scrapie, then models with widespread lesions might be expected to have shorter incubation periods, and vice versa. Although the spectrum of lesion development and terminal lesion profiles is broad and complex, there is some evidence to support this hypothesis. If the effect of the Sinc gene is ignored (since Sinc appears to control replication rate, but not the eventual distribution of lesions) then long incubation period models such as 22A (Fig. 23) have lower lesion profiles than 22L (Fig. 31), 22C (Fig. 28(a)), or ME7 (Figs. 12 and 33). A similar difference

between 'wild type' and 'mutant' (or experimental) strains of scrapie was pointed out by Fraser et al (1986). The scrapie model with the shortest i.c. incubation period is 263K in golden hamsters. This model has high titres and relatively severe lesions in the terminal brain (Cole, 1981), suggesting that the majority of the neuronal population is susceptible to replication. At the other extreme lie models such as 87V, which has a long incubation period and restricted lesions, indicating that the pathway from the site of infection to the clinical target areas is limited to a few susceptible groups of neurons (see Kimberlin and Walker, 1988b). Since the delay between replication and lesion development is also longer in these models, it is possible that infection of the clinical target areas will result in neuronal dysfunction and clinical disease before microscopic lesions appear (Cole and Kimberlin, 1985). This could explain the few, long incubation period models in which little vacuolation occurs (Fraser, 1976).

The discrete targeting of lesions to projections of the visual system described in Chapter 3 provides substantial evidence to support the concept of neural spread of infection within the CNS. With some strains of scrapie, lesions developed in several specific areas outwith the SC and geniculocortical pathways, for example the suprachiasmatic nucleus with ME7 (Fig. 9) and 22C (Fig. 26(a)), the dorsal raphe with 87V (Fig. 14), the parabigeminal nucleus with 22C (Fig. 26(b)) and the cochlear nucleus with 22L (Fig. 30(a)). These differences in targeting indicate a strain-specific affinity for neuronal subsets and pathways relatively early in the incubation period which has not been revealed by other routes of infection. Future experiments have been planned to assay infectivity in some of

these areas using stereotaxic injection and micro-punch sampling techniques, and to investigate the relationship between these lesions and the early immunocytochemical localisation of altered PrP. There is no evidence from early lesion development for contiguous spread of infection in the absence of a synaptic projection, as might be expected if non-neuronal pathways, such as extracellular or glial spread were involved. Although low levels of infectivity can be recovered from the brain up to 40 days after i.v. infection (Diringer, 1984), it has been suggested by Kimberlin and Walker (1986a) that this is due to the uptake of infection by capillary endothelial cells, in which replication fails to occur, so that this is not a route of access of infection to the neuroectoderm. The evidence from the i.o. route of infection is that spread within the CNS is limited to neuronal pathways.

6.2 The spread of scrapie after intraocular infection, and the factors affecting incubation period length.

The visual projections have been the system of choice for investigation of several viral infections, including herpes simplex (Kristensson et al, 1974), Borna disease and rabies (reviewed by Tyler, 1987). Although herpes spreads through both neurones and glia, both Borna disease (Carbone et al, 1987) and rabies (Kucera et al, 1985) appear to spread through neural pathways. It is interesting that following i.o. infection with rabies, virus is found in the motor neurons innervating the muscles of the eye, and other ocular afferents, suggesting retrograde transport; with scrapie, no primary targeted vacuolar lesions were seen outwith the

retinal projections.

The sequence of spread of infectivity from the retina with ME7 infection has been determined (4(a)), but, since other viral infections spread through additional pathways, can the i.o. incubation period length be determined solely by infection via the optic nerve? The high levels of infection found in spleen 20 days after i.o. infection with 79A (and lower levels with ME7) in experiment 19, and the development of disease in mice enucleated between 24 hours and 7 days after a prolonged incubation period indicate an alternative pathway for the spread of infection from the eye. However, Kimberlin and Walker (1988a) showed that in six i.p. infected scrapie models, there was a strict correlation between the onset of replication in brain and incubation period. They conclude that the incubation period is determined from the time neuroinvasion occurs, within a few days to a few weeks of infection. This result indicates that replication in the lymphoreticular system subsequent to neuroinvasion does not affect incubation period length (although it could well be important in the transmission of natural disease). Since i.o. injection directly initiates infection of the CNS, the non-neural component of pathogenesis is unlikely to affect incubation period length, except where the source of CNS infection is removed, as in the early enucleation groups in experiments 28, 29 and 30. Because 79A and to a lesser extent ME7 (in s7 mice) are known to be neuroinvasive strains, 87V scrapie, which is much less neuroinvasive (Bruce, 1985) was used for the third enucleation experiment (30), in an attempt to increase the incubation period difference between early and late enucleation groups. Although the incubation period results were inconclusive, due to the low titre of

the infecting inoculum, the incidence of early lesions following 87V infection effectively divided the enucleation groups between 14 and 21 days (Table 30). Further evidence that the i.o. incubation period is unaffected by peripheral pathogenesis comes from experiment 35, where splenectomy either before or after infection was shown to have no effect on incubation period. The possibility remains to be tested, however, that in an intensely neuroinvasive model, lesions developing later in the incubation period, outwith the visual projections, could arise from peripheral replication.

The early ME7 and 79A enucleation groups demonstrate that a route of infection initiated by non-neural spread can produce disease after a relatively short prolongation of incubation period. When the leakage from a 1ul i.o. injection of ^{35}S methionine was assessed by scintillation counting (2.10, Table 6) it was found that up to 100% of the amino-acid could be recovered by wiping the cornea with a filter paper pledget immediately after injection (average recovery was just over 24%). Although a 10% brain homogenate is more viscous than a methionine solution, it must be assumed that, like the solution, some inoculum leaks from the injection site, most probably immediately after infection. The sub-arachnoid space is known to extend down the optic nerve head to the back of the globe (Brown et al, 1979); however i.c. infusion of trypan blue (2.10, Fig. 4) demonstrates that in the mouse, the injection site is well removed from the limits of the sub-arachnoid space, precluding direct infection of the CSF. Non-neural spread of infection then, must be initiated either through the lymphoid drainage of the conjunctiva (Forrester, 1988) or drainage through the lacrimal sac and nasal duct to the back of the throat and hence to the gut, or

again to the gut by grooming and licking. The results of experiment 21, in which lacrimal gland, cervical lymph node, popliteal lymph node and Peyer's patches assays were set up, and are still in progress, will help to clarify the precise pathway. The infectivity levels in Peyer's patches will provide a good indication of pathogenesis involving gut; Kimberlin and Walker (1989b) showed that following intragastric infection with 139A scrapie in CW mice, replication was initiated almost immediately in Peyer's patches. It is possible that after i.o. infection, as opposed to i.p., the spleen plays a less important role than the more accessible cervical lymph nodes or even lacrimal glands. Following subcutaneous infection of mink with TME, Hadlow et al (1987) found that the initial replication was confined to lymph nodes draining the site of inoculation.

Infection by conjunctival instillation with ME7 scrapie (experiment 36) produced a narrow incubation period range, from 319 to 335 days (Table 37), although 61% of the infected mice survived. This close spread of incubation periods suggests a simple and consistent infectious pathway, but a low efficiency of infection. The dose of leaked inoculum from an i.o. infection would be much more variable, producing differences in extraneural pathogenesis and hence in incubation period even within the same model. As expected from the absence of asymmetrical lesions, enucleation following infection by conjunctival instillation had no effect (Table 37). The relative success of this route indicates that it may be a possible natural route of infection; corneal transplants from CJD infected donors are a known source of iatrogenic transmission (Duffy et al, 1974), and Davanipour (1984) suggested that CJD may have been

transferred by the use of a tonometer which measures ocular pressure. However, infection by conjunctival instillation does not completely replicate the non-neural route which occurs after i.o. infection. Not only are there survivors, but the incubation periods are slightly longer (compared with 302 - 313 days in ME7 infected mice enucleated between 12 hours and 7 days post-injection), and the lesion profile is much lower than that of the enucleated mice (Fig. 50). Additional infectious pathways must contribute to the pathogenesis of these 12 hour to 7 day enucleation groups. It is possible that some infectivity becomes blood-borne at the time of enucleation; an i.v. infection would give immediate access to many lymphoreticular replication sites. There is no perfect control experiment to cover this aspect of i.o. pathogenesis.

6.3 The implications of axonal transport of scrapie.

Several previous studies (Kimberlin et al, 1987b; Kimberlin and Walker, 1988b and 1989a and b) have demonstrated the importance of neuronal spread of scrapie infection, and others, using the visual system model, have shown evidence for axonal transport of scrapie (Fraser, 1982; Buyukmihci et al, 1983; Fraser and Dickinson, 1985; Kimberlin and Walker, 1986a; Scott and Fraser, 1989). The observations made in Chapter 3 both substantiate and extend these studies.

Three approaches were made to the investigation of axonal transport. In the first, enucleation up to 7 days after i.o.

infection with ME7 scrapie prevented the targeting of lesions to the contralateral SC, and prolonged the incubation period. Enucleation on or later than 14 days post-infection produced lesion targeting and incubation periods similar to those in unenucleated mice. Infectivity appeared to take a minimum of 14 days to establish infection in the contralateral SC (Scott and Fraser, 1989; Appendix C). When this experiment was repeated with closer enucleation dates (28(b)), this time was shown more accurately to be about 10 days. This corresponds with the infectivity assays of retina and SC in s7 mice infected with ME7 (experiments 17, 18, 19 and 20), in which replication was first detected in the retina between 14 and 21 days, and in the SC at 56 days. Enucleation experiments were also carried out with 79A and 87V scrapie, to see if the time taken for infection to reach the SC varied with different scrapie strains. However, neither of these experiments produced complete results. In experiment 29, with 79A, the incubation period was significantly prolonged in the 12 and 24 hour enucleation groups. The 7 day group incubation period was also prolonged, but not significantly. This is more difficult to interpret in the absence of data on the early lesion targeting, but resembles the findings with ME7. In experiment 29, using 87V scrapie, the timing of early lesions, examined at 4 intervals between 280 and 340 days post-infection (Table 30), were very similar to those seen with ME7. However, the incubation period results were uninformative, as relatively few mice were killed with clinical scrapie (Table 31). None of these mice were in the 24 hour, 7 or 14 day enucleation groups, suggesting that the intended prologation of incubation period had been acheived. Both the 79A and 87V enucleation experiments need to be repeated; however, it can be

concluded from the present findings that there is a similar rate of spread of infection in optic nerve axons in all three strains. This important result suggests a constant rate of passive transport of infectivity in the optic nerve, which may also apply to the rest of the CNS.

In the second approach to axonal transport, the incubation periods of mice which had been treated with MSG to deplete the retinal ganglion cell population were compared with those of untreated mice. The i.o. incubation period of MSG-treated mice was significantly prolonged (Table 32) whereas no difference was found in i.c. or i.p. infected groups. Foster et al (in press) have also compared the retinopathy scores of MSG-treated and untreated mice following i.c. infection with 79A scrapie, and have shown that the scores are significantly lower in the MSG-treated group. Depletion of retinal ganglion cell axons appears to inhibit both the anterograde and retrograde spread of infectivity.

The third approach involved several pilot studies (experiments 32, 33 and 34) which attempted to interfere with either uptake of infectivity, or blockade either the fast or slow axonal transport mechanisms. The results were inconclusive, apart from an interesting prolongation of both i.o. and i.c. incubation periods with poly-l-ornithine (Table 35). This polycation is known to enhance the uptake of HRP (Mesulam, 1982). However, its effect on incubation period appears to resemble that of polyanions (Kimberlin and Walker, 1986b; Farquhar and Dickinson, 1986) which are known to suppress peripheral pathogenesis. Poly-l-ornithine, however, also appeared to prolong the i.c. incubation period; the only other compound known to produce this effect is amphotericin B (Pocchiari

et al, 1987). This unexpected result will be clarified by further i.o. and i.c. titrations of ME7 with poly-l-ornithine.

The enucleation experiments indicate that a period of around 10 days is required for infectivity to become established in the SC following i.o. infection. Since the optic nerve and tract can be regarded as a homogeneous projection of retinal ganglion cell axons, measuring between 16 and 20 mm in the mouse, the rate of spread could be estimated at slightly under 2mm per day. This is compatible with the slow axonal transport rate in the normal murine optic nerve, which is between 0.5. and 2mm per day (Grafstein and Forman, 1980; Tytell et al, 1981; Weiss, 1982a), and is concerned with the translocation of cytoskeletal elements such as tubulin and the microtubule-associated proteins (MAPs). The velocity of scrapie infectivity could only be faster if a preceding stage such as packaging or replication in the retina was necessary prior to transport. However, replication in retina was first detected between 14 and 21 days (experiment 17), by which time infection is already established in the SC. Similar slow rates of spread have been shown in the CNS following peripheral infection by sequential detection of replication in discrete sections of spinal cord (Kimberlin and Walker, 1982) and sciatic nerve (Kimberlin et al, 1983). Dysfunction of normal slow axoplasmic flow has been implicated in the pathogenesis of unconventional virus infections; firstly by the immunolabelling of the periphery of amyloid plaques with antibodies to tau protein, one of the MAPs (Brion et al, 1987), and secondly by the immunolabelling of dystrophic neurites with monoclonal antibodies to neurofilament protein in cases of natural and experimental CJD (Liberski et al, 1987). The absence of a fast

component in the axonal spread of scrapie implies a surprisingly specific interaction with the neuron, which may be related to the role of PrP.

The overall rate of spread of infectivity in the CNS as a whole must depend on both transport velocity and replication. The evidence suggests that the axonal transport of scrapie is associated with slow axoplasmic transport, and is similar in models with quite disparate incubation perods. This means that the major constraint on spread is replication. This interpretation is compatible with the delayed targeting of lesions seen in long incubation period models (3(a), (d) and (h)).

Understanding the detailed mechanism of scrapie replication must await the identification either of the causal organism, or of specifically altered biosynthetic pathways. The 'virino' hypothesis (Dickinson and Outram, 1973 and 1983) proposed that the infectious agent is composed of a small informational molecule, possibly a nucleic acid, which specifies the properties of the different scrapie strains, co-existing with a protective host-coded protein coat). Although no scrapie-specific nucleic acid has yet been demonstrated, there is a considerable body of evidence for the existence of a scrapie genome (Bruce and Dickinson, 1987; Kimberlin et al, 1989). It has been suggested, more controversially, that the infectious agent could be a replicating protein (the 'prion' hypothesis (McKinley et al, 1983); however this concept cannot easily account for the many different scrapie strains. Recent evidence that the Sinc and PrP genes are one and the same (Scott et al, 1989), and therefore that PrP is probably the Sinc gene product, together with the immunolabelling of abnormal PrP early in the

incubation period (Bruce at al, 1989), suggest that PrP is the most likely candidate for the host-coded protein component of the virino. The function of PrP in the normal animal is not known, however, its putative structure suggests that it is a membrane bound receptor (Oesch et al, 1985). No major differences in size or charge distribution have been shown by 2-D gel analysis which could account for the strain differences or the differences in lesion targeting (Somerville and Ritchie, 1986). The sequence of the PrP gene and protein have recently been shown to have 32% and 46% homology respectively with ARIA - acetylcholine receptor inducing activity (Fischbach, unpublished). Although the targeting of scrapie strains to different neuronal subsets is too complex to correlate with neurotransmitter differences, it is possible that transneuronal spread of infectivity takes place at the synapse. However, it is perhaps more likely that spread occurs through receptor mediated endocytosis, using the same mechanism as lectins and other large molecules (Fabian and Coulter, 1985) and conventional viruses (Kuypers and Ugolini, 1990). Scrapie too, acts as a transneuronal tracer, but with an impracticable time-scale.

In conclusion, the work described in this thesis both substantiates and advances several areas of scrapie research. A direct relationship between replication and subsequent vacuolation has been demonstrated by the targeting of infectivity and pathology in the retinal projections. The targeting of pathology to specific visual system areas, and axoplasmic transport of infectivity shown by the enucleation experiments provide evidence for the neural spread of infectivity within the CNS. The Sinc gene appears to act

by limiting replication rates, rather than transport of infectivity. These results increase our knowledge of scrapie pathogenesis in the CNS, and will help to identify the basis for strain differences at a cellular level.

References.

Bamberg J R, Bray D and Chapman (1986) Assembly of microtubules at the tip of growing axons. Nature 321: 788-790.

Berk M L and Finkelstein J A (1981) An autoradiographic determination of the efferent projections of the suprachiasmatic nucleus of the hypothalamus. Br Res 226: 1-13.

Black M M and Lasek R J (1980) Slow components of axonal transport: two cytoskeletal networks. J Cell Biol 86: 616-623.

Black M M, Keyser P and Sobel E (1986) Interval between the synthesis and assembly of cytoskeletal proteins in cultured neurons. J Neurosci 6: 1004-1012.

Bowsher D (1979) Introduction to the Anatomy and Physiology of the Nervous System. 4th edition. Blackwell, Oxford.

Brion J P, Fraser H, Flament-Durant J and Dickinson A G. (1987) Amyloid scrapie plaques share common antigens with tau, a microtubule-associated protein. Neurosci Lett 78: 113-118.

Brown P (1980) An epidemiological critique of Creutzfeldt-Jakob disease, Epid Rev 2: 113-135.

Brown P, Cathala F, Raubertas R F (et al) (1987) The epidemiology of Creutzfeldt-Jakob disease: conclusion of a 15 year investigation in France and review of the world literature. Neurology 37: 895-904.

Brown G C, Shields J A, Patty B E and Goldburg R E (1979) Congenital pits of the optic nerve head. Arch Optical Mol 97: 1341-1344.

Bruce M E (1985) Agent replication dynamics in a long incubation period model of mouse scrapie. J Gen Virol 66: 2517-2522.

Bruce M E (in prep) The disease characteristics of different strains of scrapie in Sinc congenic mouse lines: implications for the nature of the agent and host control of pathogenesis.

Bruce M E and Dickinson A G (1985) genetic control of amyloid plaque production and incubation period in scrapie-infected mice. Neuropath and Exp Neurol 44: 285-294.

Bruce M E and Dickinson A G (1987) Biological evidence that scrapie has an independent genome. J Gen Virol 68: 79-89.

Bruce M E and Fraser H (1981) Effect of the route of infection on the frequency and distribution of cerebral amyloid plaques in scrapie mice. Neuropath and Appl Neurobiol 7: 289-298.

Bruce M E, Dickinson A G and Fraser H (1976) Cerebral amyloidosis in

the mouse: effect of agent strain and mouse genotype. Neuropath and Appl Neurobiol 2: 471-478.

Bruce M E, McBride P A and Farquhar C F (1989) Precise targeting of the pathology of the sialoglycoprotein, PrP, and vacuolar degeneration in mouse scrapie. Neurosci Lett 102: 1-6.

Burger D, Hartsough G R (1965) Encephalopathy of mink. II Experimental and natural transmission. J Infect Dis 115: 393-399.

Buyukmihci N, Goering-Harmon F and Marsh R F (1982) Retinal degeneration during clinical scrapie encephalopathy in hamsters. J Comp Neurol 205: 153-160.

Buyukmihci N, Goering-Harmon F and Marsh R F (1983) Neural pathogenesis of experimental scrapie after intraocular inoculation of hamsters. Exp Neurol 81: 396-406.

Carbone KM, Duchala C S, Griffin J W, Kincaid A L and Narayan O (1987) Pathogenesis of Borna disease in rats: evidence that intra-axonal spread is the major route for virus dissemination and the determinant for disease incubation. J Virol 61: 3431-3440.

Carp, R I, Kascsak R J, Wiesniewski H M, Merz P A, Rubenstein R, Bendheim P, Bolton D (1989) The nature of the unconventional slow infection agent remains a puzzle. Alz Dis and Assoc Dis 3: 79-99.

Chandler R L (1961) Encephalopathy in mice produced by inoculation with scrapie brain material. Lancet 1: 1378–1379.

Chelle P L (1942) Un cas de tremblante chez la chevre. Bull Acad Vet Fr, 15: 294–295.

Chihara E, Sakugawa M and Entani S (1982) Recovery of fast axonal transport and retinal protein synthesis in the rabbits after intraocular administration of vinblastine. Br Res 241: 179–181.

Cole S (1981) Quantitative histopathological studies of experimental scrapie. PhD thesis, University of Reading, pp. 117–120.

Cole S and Kimberlin R H (1985) Pathogenesis of mouse scrapie: dynamics of vacuolation in brain and spinal cord after intraperitoneal infection. Neuropath and Appl Neurobiol 11: 213–227.

Collinge J, Owen F, Lofthouse R, Shah T, Harding A E, Poulter M, Boughey A M and Crow T J (1989) Diagnosis of Gerstmann–Straussler Syndrome in familial dementia with prion protein gene analysis. Lancet, 8653: 15–17.

Cuille J and Chelle P L (1936) La maladie dite tremblante du mouton est-elle inoculable? Compte Rendu de L'Academie des Sciences, Paris, 203: 1552–1554.

Curtis R, Fraser H, Foster J D and Scott J R (1989) The correlation of electroretinographic and histopathological findings in the eyes of mice infected with the 79A strain of scrapie. Neuropath and Appl Neurobiol 15: 75-89.

Davies D C and Kimberlin R H (1985) Selections of Swaledale sheep of reduced susceptibility to experimental scrapie. Vet Rec, 116: 211-214.

Davinipour Z, Goodman L, Alter M, Sobel E, Asher D and Gajdusek D C (1984) Possible modes of transmission of Creutzfeldt-Jakob disease. New Engl J Med 311: 1582-3.

Dickinson A G (1976) Scrapie in sheep and goats. In: Slow Virus Diseases of Animals and Man. Ed. R H Kimberlin, North-Holland, Amsterdam, pp 209-214.

Dickinson A G and Meikle V M H (1971) Host-genotype and agent effects in scrapie incubation: change in allelic interaction with different strains of agent. Mol Gen Genet 112: 73-79.

Dickinson A G and Outram G W (1973) The scrapie replication-site hypothesis and its implications for pathogenesis. In: Slow Transmissible Diseases of the Nervous System. Vol. 2 Eds Prusiner S B and Hadlow W, Academic Press, New York, pp 13-31

Dickinson A G and Outram G W (1983) Operational limitations in the characterisation of the infective virus of scrapie. In: Virus Non-conventionnels et Affections du System Nerveaux Central Ed. L. Court Masson, Paris, pp 3-16.

Dickinson A G and Outram G W (1988) Genetic aspects of unconventional virus infections: the basis of the virino hypothesis. In: Novel Infectious Agents and the Central Nervous System. Ed. G Bock and J Marsh, Wiley, Chichester, pp 63-83.

Dickinson A G, Meikle V M H and Fraser H (1968b) Identification of a gene which controls the incubation period of some strains of scrapie in mice. J Comp Pathol 78: 293-299.

Dickinson A G, Meikle V M H and Fraser H (1969) Genetical control of the concentration of ME7 scrapie agent in the brain of mice. J Comp Pathol 79: 15-22.

Dickinson A G, Stamp J T, Renwick C C and Rennie J C (1968a) Some factors controlling the incidence of scrapie in Cheviot sheep injected with a Cheviot passaged scrapie agent. J Comp Pathol, 78: 313-321.

Diringer H, Gelderblom H, Hilmert H, Ozel M, Edenbluth C and Kimberlin RH (1983) Scrapie infectivity, fibrils and low molecular weight protein. Nature 306: 476-478.

Diringer H (1984) Sustained viraemia in experimental hamster scrapie. Arch Virol 82: 105-109.

Dowling J E (1987) The retina: an approachable part of the brain. Harvard University Press, Cambridge, MA.

Drager U C (1974) Autoradiography of tritiated proline and fucose transported transneuronally from the eye to the visual cortex in pigmented and albino mice. Br Res 82: 284-292.

Drager U C and Olsen J F (1980) Origins of crossed and uncrossed retinal projections in pigmented and albino mice. J Comp Neurol 191: 383-412.

Duffy P, West J, Collins G, Devoe A G, Streeton B and Conner D (1974) Possible person-to-person transmission of Creutzfeldt-Jakob disease. N Engl J Med 290: 692-693.

Eklund C M, Kennedy R C and Hadlow W J (1967) Pathogenesis of scrapie virus infection in the mouse. J Infect Dis 117: 15-22.

Fabian R H and Coulter J D (1985) Transneuronal transport of lectins. Br Res 82: 284-292.

Farquhar C F and Dickinson A G (1986) Prolongation of scrapie incubation period by an injection of dextran sulphate 500 within the month before or after infection. J Gen Virol 67: 463-473.

Forrester J V (1987) Immunological findings in diseases of the eye. In: Clinical Neuroimmunology. Eds. J A Aarli, W M H Behan and P O Behan, Blackwell, Oxford, pp 291-309.

Foster J D, Davies D and Fraser H (1986a) Primary retinopathy in scrapie in mice deprived of light. Neuroci Lett 72: 111-114.

Foster J D, Fraser H and Bruce M E (1986b) Retinopathy in mice with experimental scrapie. Neuropath and Appl Neurobiol 12: 185-196.

Foster J A, Scott J R and Fraser H (in press) The use of monosodium glutamate in identifying neuronal populations in mice infected with scrapie. Neuropath and Appl Neurobiol.

Fraser H (1976) The pathology of natural and experimental scrapie. In: Slow Virus Diseases of Animals and Man. Ed. R H Kimberlin, Elsevier, North-Holland, Amsterdam, pp. 267-305.

Fraser H (1979) Neuropathology of scrapie: the precision of the lesions and their diversity. In: Slow Transmissible Diseases of the Nervous System, Vol 1. Eds. S B Prusiner and W J Hadlow, Academic Press, New York, pp 387-405.

Fraser H (1982) Neuronal spread of scrapie agent and targeting of lesions within the retinotectal pathway. Nature 295: 149-150.

Fraser H and Dickinson A G (1967) Distribution of experimentally induced scrapie lesions in the brain. Nature 216: 1310-1311.

Fraser H and Dickinson A G (1968) The sequential development of the brain lesions of scrapie in 3 strains of mice. J Comp Path 78: 301-310.

Fraser H and Dickinson A G (1973) Scrapie in mice: agent-strain differences in the distribution and intensity of grey matter vacuolation. J Comp Pathol 83: 29-40.

Fraser H and Dickinson A G (1978) Studies of the lymphoreticular system in the pathogenesis of scrapie: the role of spleen and thymus. J Comp Pathol 88: 563-573.

Fraser H and Dickinson A G (1985) Targeting of scrapie lesions and spread of agent within the retino-tectal projection. Br Res 346: 32-41.

Fraser H and Farquhar C F (1987) Ionising radiation has no influence on scrapie incubation period in mice. Vet Microbiol 13: 211-223.

Fraser H and McBride P A (1985) Parallels and contrasts between scrapie and dementia of the Alzheimer type and ageing: strategies and problems for experiments involving life-span studies. In: Senile Dementia of the Alzheimer Type. Eds. J Traber and W J Gispen, Springer, Heidelberg, pp 250-268.

Fraser H, McBride P A, Scott J R and Bruce M E (1986) Infectious degeneration of the nervous system. In: Advanced Medicine 22, Ed. D R Triger, Balliere Tindall, London, pp. 371-384.

Gajdusek D C (1977) Unconventional viruses and the origin and disappearance of kuru. Science 197: 943-960.

Gardiner A C (1965) Gel diffusion reactions of tissues and sera from scrapie-affected animals. Res Vet Sci 7: 190.

Gilmour J S, Bruce M E and MacKellar A (1986) Cerebrovascular amyloidosis in scrapie affected sheep. Neuropath and Appl Neurobiol, 12: 173-183.

Grafstein B and Forman D S (1980) Intracellular transport in neurons. Physiol Rev 60: 1167-1283.

Grafstein B and Laureno R (1973) Transport of radioactivity from eye to visual cortex in the mouse. Exp Neurol 39: 44-57.

Grafstein B, Murray M and Ingoglia N A (1972) Protein synthesis and axonal transport in retinal ganglion cells of mice lacking visual receptors. Br Res 44: 37-48.

Graybiel A M (1978) A satellite system of the superior colliculus: the parabigeminal nucleus and its projections to the superficial collicular layers. Br Res 145: 365-374.

Hadlow W J (1961) The pathology of experimental scrapie in the dairy goat. Res Vet Sci 2: 289-314.

Hadlow W J, Race R E and Kennedy R C (1987) Temporal distribution of transmissible mink encephalopathy virus in mink inoculated subcutaneously. J Virol 61: 3235-3240.

Hogan R N, Kingsbury D T, Baringer J R and Prusiner S B (1983) Progressive retinal degeneration in scrapie-infected hamsters: a light and electron microscopic analysis. Lab Invest 44: 34-42.

Hope J, Morton L J D, Farquhar C F, Multhaup G, Beyreuther K and Kimberlin R H (1986) The major polypeptide of scrapie-associated fibrils (SAF) has the same size, charge distribution and N-terminal protein sequence as predicted for the normal brain protein (PrP). EMBO Journal 5: 2591-2597.

Hunter N, Hope J, McConnell I and Dickinson A G (1987) Linkage of the scrapie- associated fibril protein (PrP) gene and Sinc using congenic mice and RFLP analysis. J Gen Virol 68: 2711-2716.

Hunter N, Foster J D, Dickinson A G and Hope J (1989) Linkage of the SAF protein (PrP) to Sip in Cheviot sheep. Vet Rec 124: 364-366.

Itaya S K (1980) Retinal efferents from the pretectal area in the rat. Br Res 201: 436-441.

Jeffrey M, Scott J R and Fraser H (in prep) Intraocular scrapie inoculation of mice: light and electron microscopy of the superior colliculus.

Karber G (1931) Beitrag zur Kollectiven Behandlung Pharmkologische Reihenversuche. Arch Exp Path and Pharm 162: 480-483.

Kim Y S, Carp R I, Callahan S M and Wisniewski H M (1987) Incubation periods and survival times for mice injected stereotaxically with three scrapie strains in different brain regions. J Gen Virol 68: 695-702.

Kimberlin R H and Walker C A (1977) Characteristics of a short incubation period model of scrapie in the golden hamster. J Gen Virol 34: 295-304.

Kimberlin R H and Walker C A (1978) Evidence that the transmission of one source of scrapie agent to hamsters involves separation of agent strains from a mixture. J Gen Virol 89: 487-496.

Kimberlin R H and Walker C A (1982) Pathogenesis of mouse scrapie: patterns of agent replication in different parts of the CNS following intraperitoneal infection. J R Soc Med 75: 618-624.

Kimberlin R H and Walker C A (1983) Invasion of the CNS by scrapie agent and its spread to different parts of the brain. In: Virus Non-Conventionnels et Affections du Systeme Nerveaux Central. Eds. L.A. Court and F. Cathala, Masson, Paris, pp 17-33.

Kimberlin R H and Walker C A (1986a) Pathogenesis of scrapie (strain 263K) in hamsters infected intracerebrally, intraperitoneally or intraocularly. J Gen Virol 67: 255-263.

Kimberlin R H and Walker C A (1986b) Suppression of scrapie infection in mice by HPA-23, dextran sulphate, and some other polyanions. Antimicrobiol Agents and Chemotherapy. 30: 409-413.

Kimberlin R H and Walker C A (1988a) Incubation periods in six models of intraperitoneally infected scrapie depend mainly on the dynamics of replication within the nervous system and not the lymphoreticular system. J Gen Virol 69: 2953-2960.

Kimberlin R H and Walker C A (1988b) Pathogenesis of experimental scrapie. In: Novel Infectious Agents and the Central Nervous System. Ed. G Bock, J Marsh. Ciba Foundation Symposium No. 135. Wiley, Chichester, pp. 37-62.

Kimberlin R H and Walker C A (1989a) The role of the spleen in neuroinvasion of scrapie in mice. Vir Res 12: 201-212.

Kimberlin R H and Walker C A (1989b) Pathogenesis of scrapie in mice after intragastric infection. Vir Res 12: 213-220.

Kimberlin R H, Cole S and Walker C A (1987a) Temporary and permanent modifications to a single strain of mouse scrapie on transmission to rats and hamsters. J Gen Virol 68: 1875-1881.

Kimberlin R H, Cole S and Walker C A (1987b) Pathogenesis of scrapie is faster when infection is intraspinal instead of intracerebral. Microb Pathogen 2: 405-415.

Kimberlin R H, Hall S M, Walker C A (1983) Pathogenesis of mouse scrapie: evidence for direct neural spread of infection to the CNS after infection of the sciatic nerve. J Neurol Sci 61: 315-325.

Kimberlin R H, Walker C A and Fraser H (1989) The genomic identity of different strains of mouse scrapie is expressed in hamsters and preserved on reisolation in mice. J Gen Virol 70: 2017-2025.

Kozlowski P B, Moretz R C, Carp R I and Wisniewski H M (1982) Retinal damage in scrapie mice. Acta Neuropath 56: 9-12.

Kristensson K, Ghetti B and Wisniewski H M (1974) Study of the propagation of herpes simplex (type 2) into the brain after intraocular infection. Br Res 69: 189-201.

Kucera P, Dolivo M, Doulon P and Flammand A (1985) Pathways of the early propagation of virulent and avirulent rabies strains from the eye to the brain. J Virol 55: 158-162.

Kuypers H G J M and Ugolini G (1990) Viruses as transneuronal tracers. TINS: 13, 71-75.

Lasek R J (1980) Axonal transport: a dynamic view of neuronal structures. TINS 3: 87-91.

Lasek R J, Garner J A and Brady S T (1984) Axonal transport of the cytoplasmic matrix. J Cell Biol 99: 212s-221s.

LaVail J H, Nixon R A and Sidman P L. (1978) Genetic control of retinal ganglion cell projections. J Comp Neurol 182: 399-422.

Liberski P P, Shankar S K, Gibbs C J and Gajdusek D C (1987) Electron microscopic and immunohistochemical evidence for impairment of axonal transport in Creutzfeldt-Jakob disease. Ann Neurol 22: 157.

Linden R and Perry V H (1983) Massive retinotectal projection in rats. Br Res 272: 145-149.

Lowry O H, Rosebrough N, Farr A L and Rendall R J (1951) Protein measurement with the Folin phenol reagent. J Biol Chem 193: 265-275.

Marsh R F and Hanson R P (1979) On the origin of transmissible mink encephalopathy. In: Slow Transmissible Diseases of the Nervous System. Eds. S B Prusiner and W J Hadlow. Academic Press, New York, pp 451-460.

Matus A (1987) Putting together the neuronal cytoskeleton. TINS 10: 186-188.

Merz P A, Somerville R A and Wisniewski H M (1983) Abnormal fibrils in scrapie and senile dementia of the Alzheimer type. In: Virus non conventionnels et affections du systeme nerveux central. Ed. L A Court, Masson, Paris, pp 259-281.

Merz P A, Somerville R A, Wisniewski H M and Iqbal K (1981) Abnormal fibrils in scrapie infected brain. Acta Neuropath 65: 63-74.

Mesulam M M (1982) Principles of horseradish peroxidase neurohistochemistry and their applications for tracing neural pathways - axonal transport, enzyme histochemistry and light microscopic analysis. In: Tracing Neuronal Connections with Horseradish Peroxidase. Ed. M M Mesulam IBRO handbook series, Wiley, Bath, pp 1-152.

Millson G C, Hunter G D and Kimberlin R H (1976) The physicochemical nature of the scrapie agent. In: Slow Virus Diseases of Animals and Man. Ed. R H Kimberlin, Frontiers in Biology Series, North Holland, Amsterdam, 44: 244-261.

Mims C A (1977) A personal view of scrapie research. Lancet 1144-45.

McKinley M P, Bolton D C and Prusiner S B (1983) A protease-resistant protein as a structural component of the scrapie prion. Cell 35: 57-62.

Noell W K (1958) Differentiation, metabolic organisation and viability of the visual cell. A M A Opthalmol 60: 724-729.

Nussbaum R E, Henderson W M, Pattison I H, Elcock N V and Davies D C (1975) The establishment of sheep flocks of predictable susceptibility to experimental scrapie. Res Vet Sci 18: 49-58.

Oesch B, Westaway D and Walchi M (1985) A cellular gene encodes scrapie PrP 27-30 protein. Cell 40: 735-746.

Outram G W (1980) Mouse scrapie: black box models and the slow encephalopathies. In: Animal Models of Neurological Disease. Ed. F Clifford Rose and P O Behan, Pitman Medical, Tunbridge Wells.

Palmer A C (1957) Vacuolated neurones in sheep affected with scrapie. Nature, 179: 480-482.

Parhad I M, Griffin J W, Hoffman P N,and Kores J F (1986) Selective interuption of axonal transport of neurofilament proteins in the visual system by B-B'-iminodipropionitrile (IDPN) intoxication. Br Res 363: 315-324.

Pattison I H, Millson G C and Smith K (1964) Res Vet Sci 5: 116-22.

Paxinos G and Watson C (1986) The Rat Brain in Stereotaxic Coordinates. 2nd. edition. Academic Press, Australia.

Pocchiari M, Schmittinger S and Masullo C (1987) Amphoteracin B delays the incubation period of scrapie in intracerebrally inoculated hamsters. J Gen Virol 68: 219-223.

Porter D D Porter H G and Cox N A (1973) Failure to demonstrate a humoral immune response to scrapie infection in mice. J Immunol 111: 1407-1413.

Potts A M, Modrell M S and Kingsbury B S (1960) Permanent fractionation of the electroretinogram by sodium glutamate. Am J Opthalmol 50: 900-907.

Prusiner S B (1982) Novel proteinaceous particles cause scrapie. Science 216: 135-144.

Prusiner S B (1985) Scrapie prions, brain amyloid and senile dementia. Cur Top Cell Reg 26: 79-95.

Rogers (1979) Techniques of Autoradiography. 3rd edition, Elsevier/North Holland, Amsterdam.

Scott M, Foster D, Mirenda C, Serban D, Coufal F, Walchli M, Torchia M, Groth D, Carlson G, DeArmond S J, Westaway D and Prusiner S B (1989) Transgenic mice expressing hamster prion protein produce species-specific scrapie infectivity and amyloid plaques. Cell 59: 847-857.

Scott J R and Fraser H (1984) Degenerative hippocampal pathology in mice infected with scrapie. Acta Neuropath 65: 62-68.

Scott J R and Fraser H (1989) Enucleation after intraocular scrapie injection delays the spread of infection. Br Res 504: 301-305.

Sefton A J and Dreher B (1985) Visual System. In: The Rat Nervous System: I Forebrain and Midbrain. Ed. G Paxinos, Academic Press, Australia.

Sidman R L, Angevine J B, Pierce E T (1971) Atlas of the Mouse Brain and Spinal Cord, Harvard University Press, Cambridge M.A.

Sigurdsson B (1954) Rida, a chronic encephalopathy of sheep. Br Vet J 110: 341-354.

Somerville R A and Carp R I (1983) Altered scrapie infectivity estimates by titration and incubation period in the presence of detergents. J Gen Virol 64: 2045-2050.

Somerville R A and Ritchie L A (1986) Are scrapie associated fibrils a pathological product of infection? In: Unconventional Virus Diseases of the Central Nervous System. Eds. L A Court, D Dormont, P Brown and D T Kingsbury, Paris, pp 521-535.

Somerville R A, Merz P A & Carp R I (1986) Partial copurification of scrapie-associated fibrils and scrapie infectivity. Inter Virol 25: 48-55.

Southwood R (1989) Report of the working party on bovine spongiform encephalopathy. Department of Health and Ministry of Agriculture, Fisheries and Food.

Sprecht S and Grafstein B (1973) Accumulation of radioactive protein in mouse cerebral cortex after injection of 3H-fucose into the eye. Exp Neurol 41: 705-722.

Sprecht S and Grafstein B (1977) Axonal transport and transneuronal transfer in mouse visual system following injection of [3H] fucose into the eye. Exp Neurol 54 352-368.

Spriggs D R, Bronson R T and Fields B N (1983) Haemagglutin variants of reovirus type 3 have altered central nervous system tropism. Science 220: 505-507.

Tyler K L (1987) Host and viral factors the influence viral neotropism. II Viral genes, host genes, site of entry and route of spread of virus. TINS 10, 12: 492-497.

Tyrell D A J (1989) Interim report of the consultative committee on research into Spongiform Encephalopathies. Ministry of Agriculture and Fisheries and Food. Department of Health.

Tytell M, Black M M, Garner J A and Lasek R J (1981) Axonal transport: each major rate component reflects the movement of distinct macromolecular complexes. Science 214: 179-181.

Vancouver C (1794) General view of agriculture in the County of Cambridge (Board of Agriculture), pp. 12-13.

Weiss D G (1982a) General properties of axoplasmic transport. In: D G Weiss and A Gorio (Eds) Axoplasmic Transport in Physiology and Pathology. Springer, Berlin pp 1-14.

Weiss D G (Ed) (1982b) Axoplasmic Transport. Springer-Verlag, Berlin.

Wells G A H, Scott A C, Johnson C T Gunning R F, Hancock R D, Jeffrey M, Dawson M and Bradley P (1987) A novel progressive encephalopathy in cattle. Vet Rec 121: 419-420.

Wyatt J M, Pearson G R, Smerdon T, Gruffydd-Jones T J and Wells G A H (1990) Spongiform encephalopathy in a cat. Vet Rec (letter) 216: 513.

Zlotnik I (1958) The histopathology of the brainstem of sheep affected with natural scrapie. J Comp Pathol, 68: 148-156.

Zlotnik I and Rennie J C (1962) The pathology of the brain of mice inoculated with tissues from scrapie sheep. J Comp Pathol 72: 360-365.

ACKNOWLEDGEMENTS

I would like to thank my internal supervisor, Hugh Fraser, for his unfailing advice and encouragement, my collegue Moira Bruce for helpful discussions, and Richard Kimberlin for his constructive comments on the first draft. I must also thank my supervisors Dr. Neil Watt and Professor Ian McConnell for their interest and advice.

I am also indebted to Val Thomson, who prepared many high quality histological sections, Davie Davies, who supervised the mouse experiments, Laurence Doughty, for his photographic skills, and Paula Dickson for clerical assistance.

APPENDIX A. Abbreviations.

ARIA	acetylcholine receptor inducing activity
BSE	bovine spongiform encephalopathy
dLGN	dorsal lateral geniculate nucleus
dpi	days post-injection
DPM	disintegrations per minute
GSS	Gerstmann Straussler Scheinker disease
HRP	horseradish peroxidase
EM	electron microscopy
i.c.	intracerebral
i.o.	intraocular
i.p.	intraperitoneal
i.v.	intravenous
OCM	oculomotor nucleus
ONL	outer nuclear layer
PAGE	polyacrylamide gel electrophoresis
PrP	prion protein
psig	pounds per square inch gauge
RFLP	restriction fragment length polymorphism
RGC	retinal ganglion cell
SAF	scrapie-associated fibrils
SC	superior colliculus
TME	transmissible mink encephalopathy
VC	visual cortex

APPENDIX B. Dose-response curves.

1. **C57BL i.c. unspun titration of ME7.**
2. **C57BL i.c. unspun titration of 79A.**

C57BL i.c. unspun titration of ME7 (0.02ml)

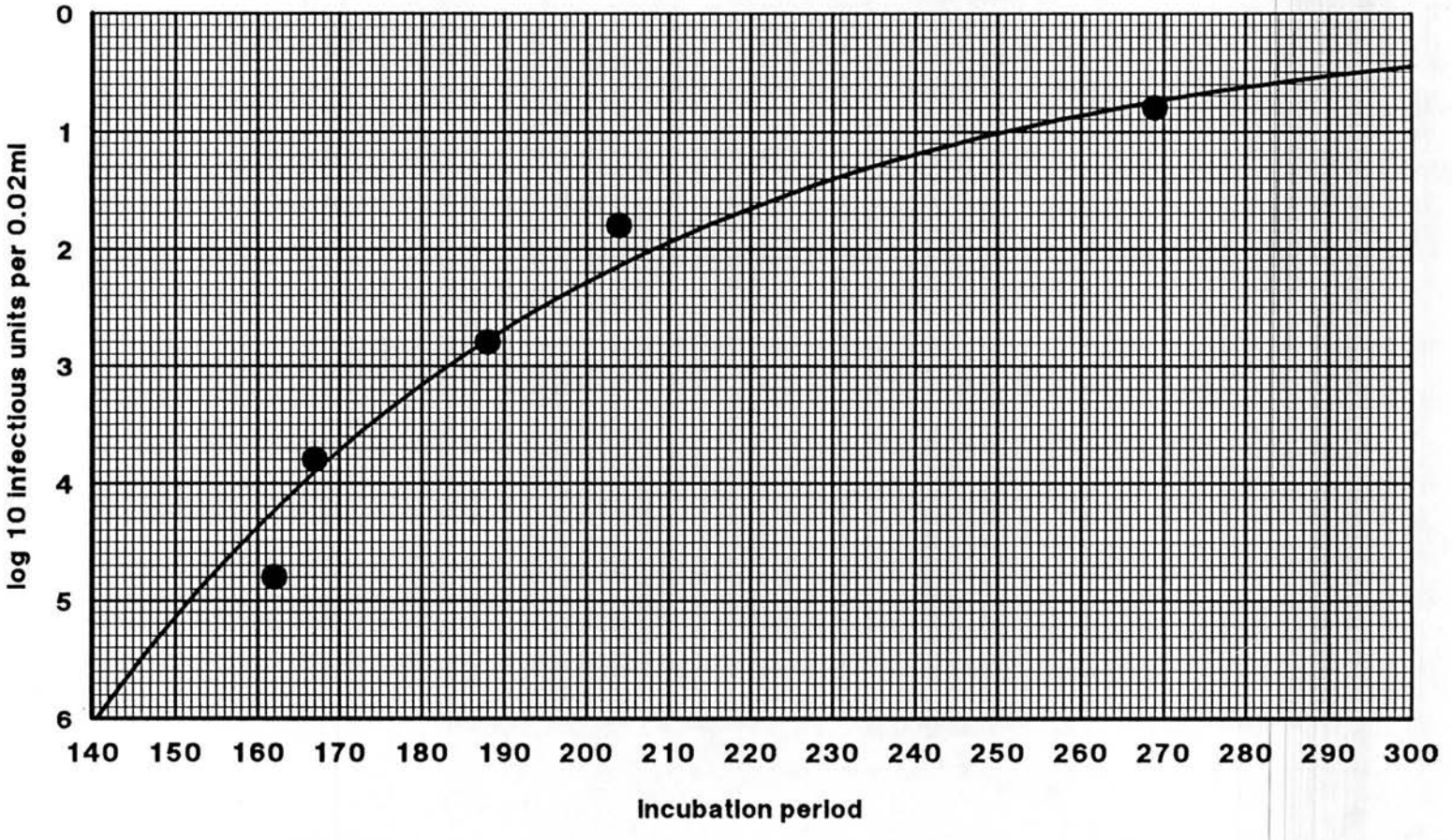

from 135A-7T, Karber 10 -7.0

r2 = 0.89; exponential regression curve.

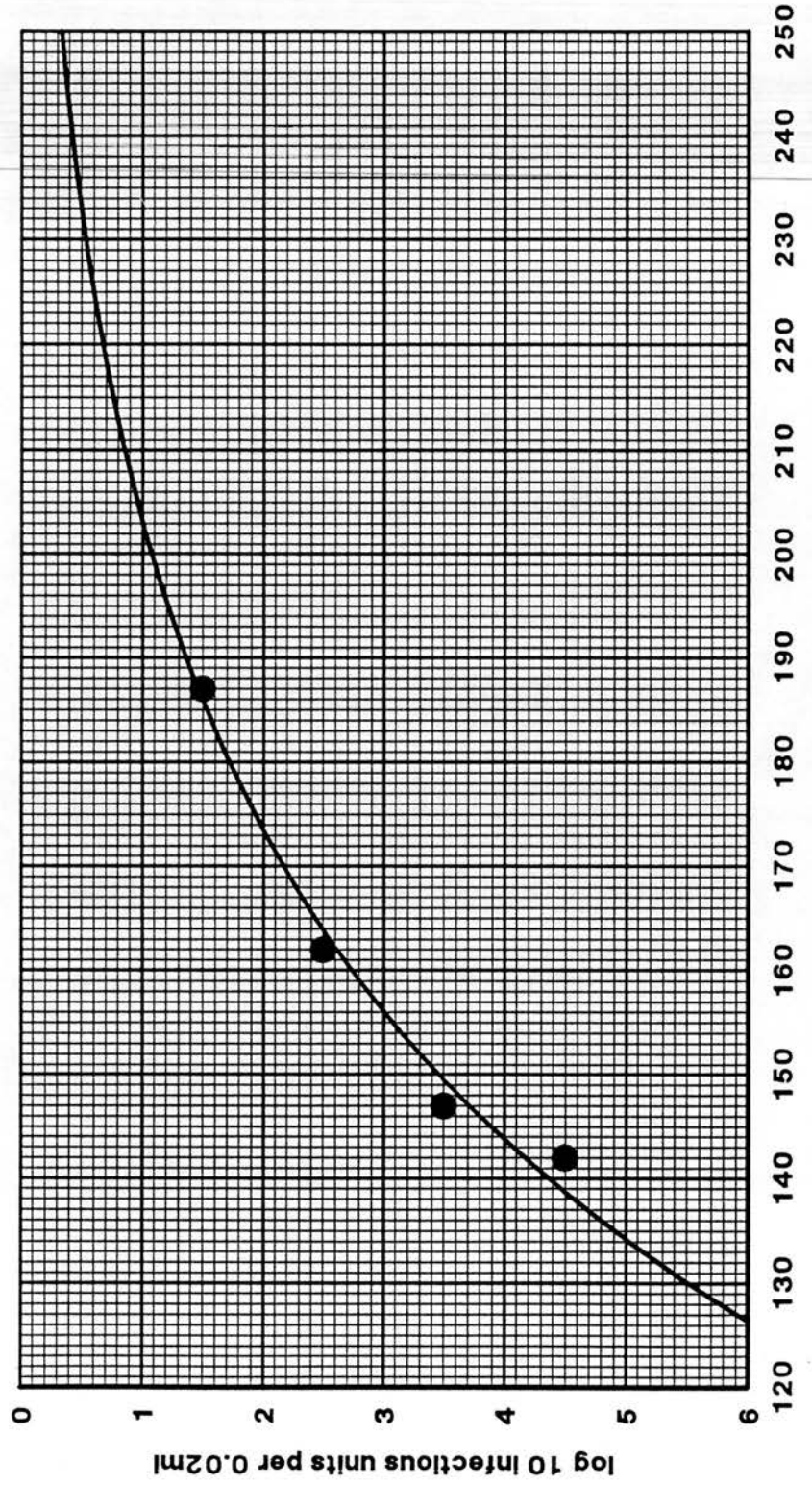

from 79A-4J, Karber 10 -6.5

APPENDIX C. Re-estimation of i.o. sampling times from experiment 7.

Table I. Recalculation of serial killing dates based on i.c. incubation periods of groups of SV mice.

Experiment number	injection group	injection date (day:year)	i.c. incubation period	i.c. incubation period as % of shortest group	number of i.c. infectious units injected
7.	a	340:84	174 ±7.4	125	$10^{2.6}$
	b	355:84	147 ±2.6	106	$10^{3.6}$
	c	14:85	153*	110	-
	d	31:85	153*	110	-
	e	45:85	151$	109	$10^{3.4}$
	f	59:85	153*	110	-
	g	73:85	163 ±9.1	117	$10^{3.0}$
	h	94:85	153*	110	-
	i	101:85	158 ±1.7	114	$10^{3.2}$
	j	115:85	142 ±0.5	102	$10^{3.8}$
	k	130:85	139 ±0	100	$10^{4.0}$

* no i.c. incubation period available, so group given nominal value from mean of other groups.

$ only one mouse was given an incubation period in this group (other incubation periods are calculated from at least 4 mice.)

TABLE II. Recalculated serial killing dates for groups of SV mice i.o. infected with 79A scrapie.

mouse strain	injection group	date group killed (dpi)	% difference between i.c. IP* and IP of shortest group	calculated date of killing
SV	f	125	10	113
	e	139	9	127
	d	153	10	138
	k	164	0	164
	c	170	10	153
	j	179	2	176
	i	193	14	166
	b	195	6	183
	h	200	10	180
	a	210	25	158

* incubation period

TABLE III. Recalculated serial killing dates for groups of C3H mice i.o. infected with 79A scrapie.

mouse strain	injection group	date group killed (dpi)	% difference between i.c. IP and IP of shortest group	calculated date of killing
C3H	g	111	17	92
	f	125	10	113
	e	139	9	127
	d	153	10	138
	k	167	0	167
	c	170	10	153
	j	182	2	178
	b	195	6	183
	i	196	14	169
	h	209	10	188
	a	210	25	158

* incubation period

TABLE IV. Recalculated serial killing dates for groups of MM mice i.o. infected with 79A scrapie.

mouse strain	injection group	date group killed (dpi)	% difference between i.c. IP* and IP of shortest group	calculated date of killing
MM	f	125	10	113
	e	139	9	127
	d	153	10	138
	c	170	10	153
	k	180	0	180
	b	195	6	183
	i	196	14	169
	a	210	25	158
	i	209	14	178
	h	245	10	221

* incubation period

APPENDIX D. PUBLICATIONS

Scott J R and Fraser H (1986) The IInd nerve and its central projections as a simple scrapie model. In: Unconventional Virus Diseases of the Central Nervous System. Eds. L A Court, D Dormont, P Brown and D T Kingsbury, Commissariat a l'Energie Atomique, Fontenay-aux-Roses, pp 575-586.

Permission has been given by the editor (L A Court) to include a photocopy of the above chapter.

Scott J R and Fraser H (1989) Transport and targeting of scrapie infectivity and pathology in the optic nerve projections folowing intraocular infection. In: Alzheimer's Disease and Related Disorders. Eds. K Iqbal, H M Wisniewski and B Winblad, Progress in Clinical and Biological Research vol 317, Liss, New York, pp 645-652.

Scott J R and Fraser H (1989) Enucleation after intraocular scrapie infection delays the spread of infection. Br Res 504: 301-305.

Permission to include the above publications has been given by my co-author.

19.
THE 2ND, NERVE AND ITS CENTRAL PROJECTIONS AS A SIMPLE SCRAPIE MODEL

J.R. Scott and H. Fraser**

SUMMARY

By injecting scrapie into the vitreous of one eye (i.o. injection) in mice, infectivity and then vacuolation are targeted into the contralateral optic tectum and lateral geniculate nucleus, via axons of the retinal ganglion cells. Secondary trans-neuronal spread of lesions has also been demonstrated to the ventral thalamic nucleus when 87V strain of scrapie is used (in Sinc^{p7} *mice), and approximately to layer IV of the visual cortex when the ME7 strain is used (in* Sinc^{s7} *mice). The occurrence of the first targeted lesions is much later with 87V than with ME7, and these differences closely parallel the incubation period differences between these models of scrapie, for both the i.c. and i.o. injection routes. When ME7 is introduced i.o. into mice of the* Sinc^{p7} *genotype, the interval before the first tectal lesions occurs is considerably longer than with* Sinc^{s7} *mice; this is the first evidence for an action of* Sinc *operating at the level of a simple neuron-neuron system. Monocular enucleation at intervals following i.o. injection of* Sinc^{s7} *mice with ME7 scrapie strain shows that the agent reaches the CNS from the retina after an interval of between 7 and 21 days, showing that, unlike many viruses, the slowest rate of axoplasmic transport may be utilised at least in the optic nerve. Monocular enucleation of mice with either near-terminal scrapie lesions, or prior to their development, does not affect the occurrence or intensity of vacuolar degeneration in the deafferented central targets; this is* de facto *evidence that the primary lesion is not a pre-synaptic one.*

Although this work proves that scrapie infectivity and vacuolar degeneration can be co-targeted anterogradely via the retino-central pathways, cerebral amyloid plaques cannot be targeted in this manner, but appear disassociated from vacuolation, both in time and space.

The investigation of scrapie pathogenesis is hampered by the lack of a useful *in vitro* system in which to identify the cellular changes provoked by infection. The majority of scrapie experiments rely on parenteral or intracerebral (i.c.) infection techniques which, although useful for studying many facets of the disease, provide no opportunity to resolve events at the level of simple cell to cell interactions. In studies based on such routes of infection, the precise molecular changes involved in replication, and its progression to cell degeneration can only be indirectly inferred

* AFRC and MRC Neuropathogenesis Unit, West Mains Rd., Edinburgh, UK.

from sequential biochemical or infectivity assays of whole tissues or organs, and from analysis of neuropathology.

In 1982, it was shown that both scrapie infectivity and spongy pathology could be targeted to the central projections of the retina (figure 1), via the the optic nerve, following intraocular infection (4). This route of infection provides a simple "neuron to neuron" model which can be used to study, for example, the targeting of scrapie infectivity, the action of the gene *Sinc*, and the intracellular transport of scrapie agent.

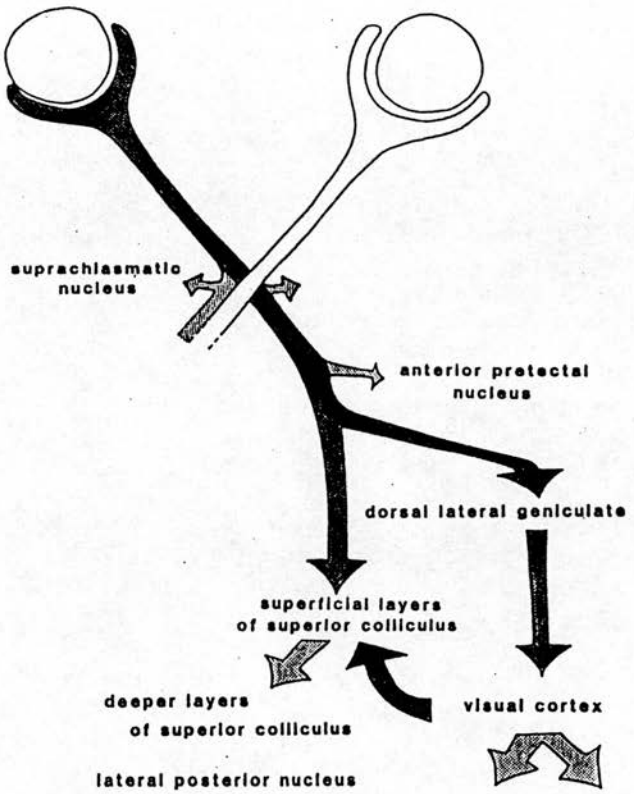

FIGURE 1 – Diagram of the major primary and secondary retinal projections.

Although the retina is recognised as being part of the CNS, the incubation period following intraocular (i.o.) infection with scrapie is considerably longer than with an equivalent i.c. infection (7, Table I); the spread of infection appears to be hindered by the restricted access to the rest of the CNS available through the optic nerve. Peripheral routes of infection also produce longer incubation periods

Scrapie strain	*Mouse strain*	*First positive i.o. lesions (days)*	*Mean incubation period ± SE (days)*	
			i.c.	*i.o.*
ME 7	SM	140	170 ± 1	237 ± 4
87 V	VM	260	312 ± 10[1]	437 ± 16[2]

TABLE I – Relative timings of appearance of first positive lesions, and i.o. and i.c. incubation periods with ME 7 and 87 V strains of scrapie.
[1] n = 6, including 4 survivors.
[2] n = 5, including 1 survivor.

than i.c., because a lymphoreticular replication phase must precede and initiate CNS infection. Incubation period length is determined by the time taken for agent to spread and gain access to replication sites in the small number of highly localised centres in the CNS necessary for the animal's survival, and produce the functional neuronal damage that results from replication (6, 11, and Kimberlin and Walker, this volume). Direct infection of the sciatic nerve (13) or the spinal cord (12) can produce even shorter incubation periods than following i.c. infection, presumably by providing the agent with more direct access to these centres, in contrast to the prolongation of incubation period after i.o. infection. Routing infection through the known pathways of the retinal ganglion cell projections provides a unique opportunity to identify and examine the factors involved in scrapie pathogenesis.

Experimental techniques

Inbred mouse strains of both *Sinc* genotypes were used, including the $Sinc^{s7}$ strains C57BL, C3H and SM, and the $Sincp^{7}$ strains VM and IM. C3H mice have retinas lacking the visual receptor layer (9). The decussation at the optic chiasm is greater in albino mice (VM) although even in pigmented mice it exceeds 95 %. Scrapie strains used were ME7, 87V and 79A (see 7).

Adult mice were injected into the vitreous of the right eye with lul of 10^{-1} or higher dilutions of 500 g supernates of brain homogenates prepared from terminal scrapie affected mice, using a 10 µl Hamilton syringe with a 26 g needle. This dose is approximately 10^4 i.c. ID_{50} units.

Monocular enucleations were performed by clamping the optic nerve and artery behind the orbit with small artery forceps. Intraocular and intracerebral injections, and enucleations were performed under pentobarbitone anaesthesia.

Sequential studies were carried out at intervals of between 10 days and three weeks, starting well before any pathological changes were seen (120 days post-injection for ME7 in s7s7 mice, and 200 days in p7p7 mice) and continuing until the terminal stages of the disease. Coronal semi-serial sections of brain were prepared from each animal to include all the major visual projection areas in the diencephalon, mesencephalon and occipital cortex, which were examined for degenerative spongy pathology.

The incubation period in mice reaching terminal stages of infection was determined by the clinical scoring system devised by Dickinson *et al.* (1). A standard index of the pattern and severity of vacuolation in the brains of terminally affected mice ("lesion profile") was calculated from the mean vacuolation scores in each of nine standard grey matter areas of brains, as described by Fraser and Dickinson (5).

Infectivity and pathology in IInd. nerve pathways

The sequence of the appearance of spongy pathology in the visual projection areas varies with the strain of scrapie agent (Table I). With a standard i.o. ME7 infection in s7s7 mice, the first positive scrapie lesions are seen in the contralateral superior colliculus (SC) (figure 2) from around 140 days post-infection. However,

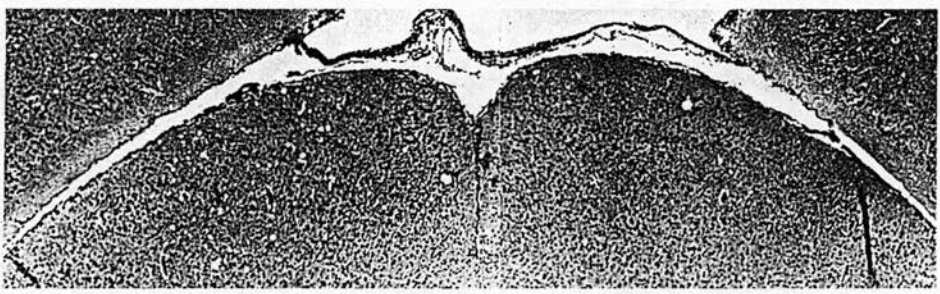

FIGURE 2 – Early positive spongiosis in the contralateral SC of an SM mouse, 162 days after i.o. infection with ME7.

there is wide variation in the timing of early lesions, probably due to differences between individual mice in the efficiency of i.o. infection resulting from leakage of inoculum at the time of injection. Nevertheless, the sequence of progressive spongy degeneration is always the same : firstly, after the initial lesions in the contralateral SC, vacuolation appears in the contralateral dorsal lateral geniculate nucleus (DLG) after a delay of about 10-15 days, and then in the contralateral visual cortex (7). These are all areas where vacuolation occurs in terminal animals following i.c. infection with ME7 agent. Secondly, more advanced cases have symmetrical lesions in many non-visual areas including the telencephalon, main areas of thalamus and tegmentum, cerebellum and brain stem. Finally, terminal mice have a pattern of spongy pathology indistinguishable from that seen following an i.c. infection (figure 4), except, in some cases, for a residual asymmetry in the severity of vacuolation between the two sides of the SC.

Other strains of scrapie produce quite different patterns of vacuolation after i.o. infection. With 87V agent, which has a very much longer incubation period with all routes of injection (Table I), the very earliest vacuolation following i.o. infection of p7p7 mice can be seen in the contralateral DLG at 260 days, in the absence of

lesions in the SC at this time. The spongy pathology progresses to include both of the DLG and the contralateral SC, followed by the contralateral ventral thalamic nucleus (figure 3), before spreading to resemble the pattern of spongiosis seen in terminal mice following i.c. infection. Close comparison of the lesion profiles of terminal mice, however, shows that spongy pathology in the SC (position 3) of i.c. infected mice does not become as severe as that seen in those infected by the i.o. route (figure 5). The 87V agent, unlike ME7, produces very little vacuolation in the cortex, with either the i.o. or i.c. route, and in particular, there is no vacuolation in the visual cortex. 87V also produces many amyloid plaques, and although these plaques can be seen in the brains of terminal mice after i.o. infection, their number and distribution resembles that seen following intraperitoneal infection; there is no direct targeting of plaques within the retino-tectal projection (8).

The relationship between the occurrence of spongy pathology and infectivity in specific areas of tissue can also be resolved with the intraocular route of infection. Scrapie infectivity can only be estimated using long-term *in vivo* assays, either by titration using serial dilutions of tissue homogenates in groups of recipient mice, or by comparing the incubation periods of mice receiving a single dilution of the tissue to be assayed with an established dose-response curve for that exact model (10, 2). Sequential incubation period assays of the left and right optic

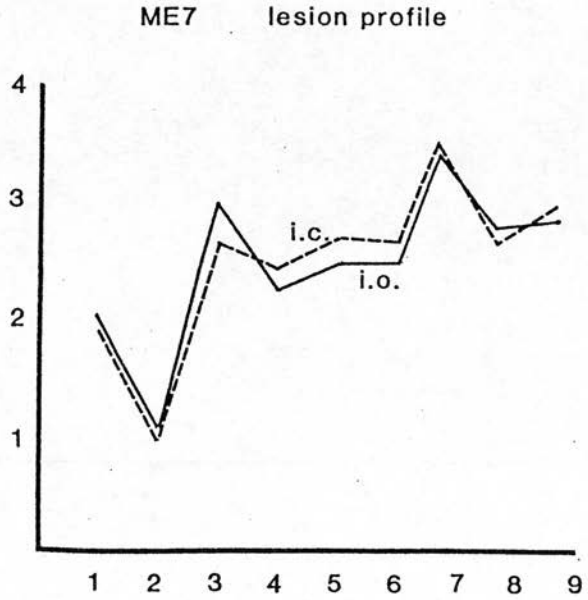

FIGURE 3 – Lesion profiles in terminal mice which received the same dose of ME7 by an i.c. (broken line) and i.o. route (solid line). The SC is scored at position 3 in the profile, but the other major retinal projections do not lie within scoring areas.

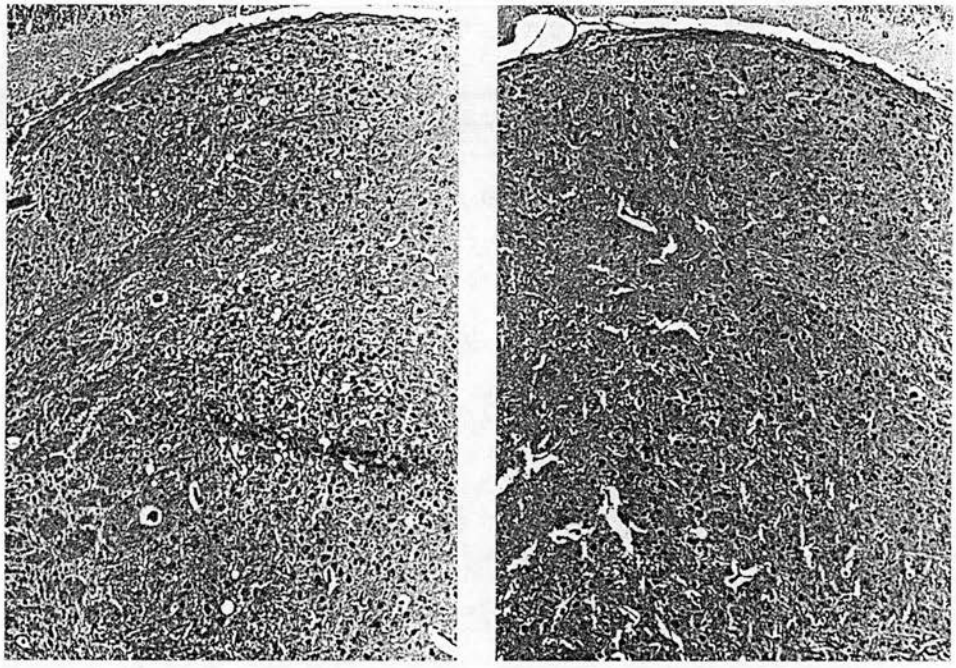

FIGURE 4 – Vacuolation in the contralateral DLG and ventral thalamic nuclei in a VM mouse 373 days after i.o. infection with 87V agent.

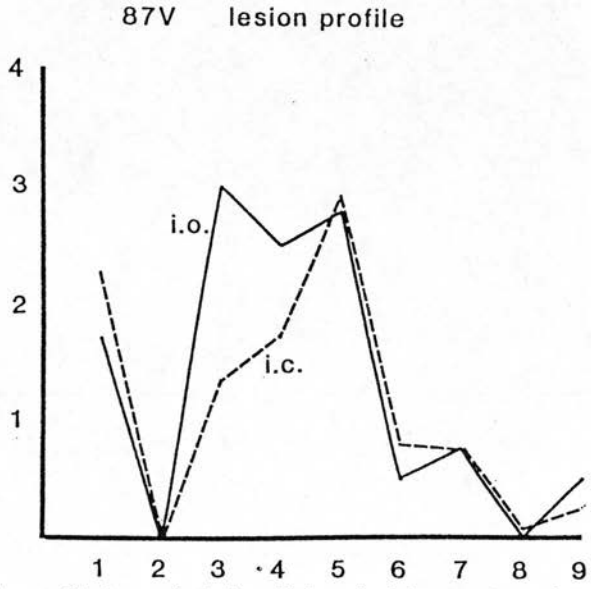

FIGURE 5 – Lesion profiles in terminal mice which received the same dose of 87V by an i.c. (broken line) an i.o. route (solid line).

nerve and SC after right i.o. infection with ME7 (7) have shown that infectivity can be detected in the left (contralateral) SC at 63 days post-infection; this is about 80 days before the first pathological changes are seen. Infectivity in the ipsilateral SC and in both optic nerves cannot be detected until between 100 and 120 days post-injection. This much later involvement of the optic nerves suggests that ME7 agent does not replicate within the axons, but is transported by them; both towards the SC to initiate infection, and probably back to the retina when high titres become established in the CNS as a whole. To resolve these unknowns, further assays of visual projection areas following i.o. infection are in progress, and include retina, DLG and visual cortex as well as optic nerves and SC, and non-visually associated control regions.

The scrapie strains ME7 and 87V, although very different in incubation period and pattern of terminal pathology, are both strains which produce spongiosis in grey matter rather than white. Other strains, such as 79A and 139A produce severe vacuolation of white matter tracts, including the optic nerve and tract after i.o. infection, with relative sparing of the SC and DLG. Unlike ME7 and 87V, which produce no morphological changes in the retina even in terminal mice, infection with 79A or 139A results in a primary degeneration of the photoreceptor layer (3). These differences in the pathogenesis of 79A and 139A can be sought by using an intraocular route of infection.

The Sinc gene

The scrapie incubation period is highly characteristic for each combination of scrapie strain and mouse genotype. This genotype depends on which alleles of the gene *Sinc* are present; most inbred strains are homozygous for the s7 allele which gives rise to relatively short incubation periods of about 170 days when infected i.c. with a high dose of ME7 or other strains of the ME7 group; mice homozygous for the p7 allele have prolonged incubation periods (about 330 days) with the equivalent ME7 infection. Scrapie strains in the 22A group, however, will reverse the ranking, so that p7p7 mice have the shorter incubation periods (about 200 days) and s7s7 mice are much longer (about 425 days). When mice of either genotype are infected i.o. with ME7 (Table II), the mean incubation periods are proportionally longer than the equivalent i.c. incubation period : about 240 days in s7 mice, and 530 days in p7. The first appearance of positive spongy pathology in the left SC, however, is also delayed in the p7 mice (263 days post-infection)

Sinc *genotypes*	*First positive lesions*[1]	*100 % positive lesions*[2]	*Mean i.o. incubation period ± SE*
s7s7	141	176	237 ± 4
p7p7	263	284	532 ± 12

TABLE II – Relative timings of the appearance of positive lesions, and the i.o. incubation period in mice of two *Sinc* homozygous genotypes, after infection of R eyes with ME 7 agent.

[1] In left superior colliculus only

[2] In left superior colliculus, dorsal lateral geniculate and visual cortex.

compared to the s7 recipients (141 days). These timings are in the same proportions as those seen following i.c. infection, showing that *Sinc* is exerting its effect on the infection and pathogenesis within the first neuronal relay in which replication occurs.

Evidence for postsynaptic localisation of pathology

The differences in the pattern and distribution of spongy pathology produced by different scrapie models have been recognised for many years (5, 6). However, the i.o. model provides the first opportunity to target the initial positive pathological changes to specified areas at predetermined times. This means that this route can be exploited to investigate the cellular localisation of these vacuolar changes, since very little evidence exists concerning their subcellular site of origin. One way of identifying the site of vacuoles within the neuropil is by removing a major part of the innervation of the SC and DLG by monocular enucleation, which results in the destruction of the ganglion cell terminals within days, and subsequent degeneration of the axons and myelin. If the presynaptic retinal projection to the SC and DLG is removed by enucleation at various times during either an i.c. or an i.o. incubation period (table III), the expected pattern of

Route	*Mean incubation period (days ± SE)*	*Time of enucleation (days post-infection)*	*Time of killing after enucleation*
i.o.	260 ± 4	21	232[1]
		86	75
		100	61
		114	47
i.c.	170 ± 1	114	56[1]
		160-170	1-7[1]

TABLE III – Times at which i.o. or i.c. infected mice have been enucleated without affecting either the development of early positive vacuolation, or the retention of existing spongiosis in the SC. All brains were examined as 6 u coronal paraffin sections stained with haematoxylin and eosin.
[1] Mice were killed with terminal scrapie.

vacuolation still occurs. If the enucleation is performed near the end of an i.c. incubation period, when there is already severe vacuolation in the SC and LGN, the established vacuolation is retained (figure 6), despite the degeneration of the presynaptic terminals. Retinal ganglion cells innervate the superficial layers of the SC, entering through the optic layer, and terminating in the superficial grey layer. The cells lying within these layers project to deeper layers and have other, more complex, interactions (17). Early positive spongy changes seen in these

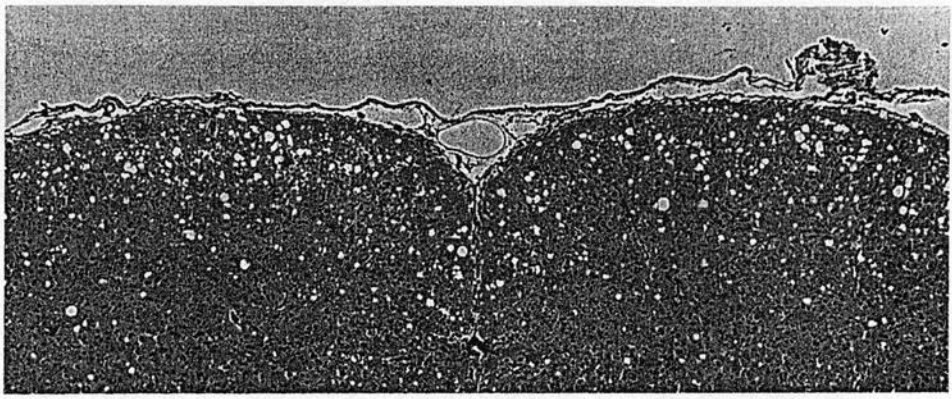

FIGURE 6 – Superior colliculus from MB × C3H mouse which had R enucleation 3 days prior to killing with terminal ME7 scrapie. Vacuolation is unaffected despite the deafferentation of the outer layers.

superficial layers must lie either within the ganglion cell terminals, the neurons of the SC, or the glia. Depriving the superficial layers of their massive retinal input without affecting the vacuolation points to a localisation either in the post-synaptic terminals of SC neurons, or the glia. Although degenerating neurites can be seen ultrastructurally within the SC contralateral to enucleation, the devastation of the tissue structure associated with vacuolation makes it very difficult to identify the vacuoles with either neuronal or glial processes, although Lampert *et al.* (14), found membrane-bound vacuoles within both pre- *and* post-synaptic neuronal terminals in the cortex of terminal scrapie infected mice. The IInd nerve model shows that the progression of vacuolation during the incubation period reflects the increasing infectivity titres in retinal projection areas, providing strong evidence for the axonal transport of scrapie. It seems unlikely that an agent transported within and between connecting neurons would produce a primary lesion in adjacent glia. Although alternative mechanisms, such as transport within glia, could be proposed for the retino-tectal projection, they do not explain the precise geniculo-cortical transport of ME7 agent. These findings provide substantial evidence that the primary vacuolar lesion is a neuronal one, and is post-synaptic at least in these retinal targets. Further EM studies on i.o. infected and enucleated animals should help to relate vacuolation to the well studied morphology of the SC.

Axonal transport of scrapie agent

It should be possible to identify the interval between infection and the establishment of infection in the retinal projection areas by serial enucleation after i.o. infection. Groups of mice infected i.o. with ME7 were enucleated between 1 hour and 28 days after infection (Table IV), and semi-serial sections of SC were examined for positive spongiosis 160 and 185 days post-injection. No positive lesions were seen in any of the mice enucleated up to 7 days post-injection. Agent appears to take between 14 and 28 days to establish infection in the SC after which time the source of infection in the eye can be removed without compromising the

Time of enucleation	*% positive spongiosis in retino-central targets (days post-injection)*	
	160	*185*
1 hour	0	0
12 hours	0	0
18 hours	0	0
24 hours	0	0
7 days	0	0
14 days	–	20
21 days	30	56
28 days	–	80
Unenucleated	50	100

TABLE IV – Effect of enucleation at different times after infection on the number of mice showing positive spongiosis at 160 and 185 days.
SV mice infected in R eye with ME 7 agent.

pathogenesis. This rate of spread of infection, about 1 mm per day, was also found in the CNS following both intraperitoneal infection (11) and infection of sciatic nerve (13); this suggests that agent is carried within axons at the slowest rate of axonal transport. Five different velocities of axonal transport in optic nerve have been described by Lasek (15), and the materials carried at the slowest rate (0.5 to 2 mm per day in the optic nerve) have been identified as cytoskeletal elements such as tubulin, fodrin and the 3 neurofilament proteins. However, the measurement of rate of transport of scrapie is not the simple timing of arrival in the ganglion cell terminals in the SC of labelled proteins or amino-acids, but the time taken to initiate infection in the next "relay", where vacuolation occurs. This additional factor must contribute to the measured transport rate. The rate of turnover of slowly transported structural proteins in the terminal is between 1 and 4 weeks, and Sandberg *et al.* (16) have suggested that the degradation in the terminals of both fast and slowly transported proteins to acid-soluble components could potentially provide a source of substances important in neurotransmission. If agent is transported at the slow rate, then this could be one way for transneuronal spread to occur.

CONCLUSIONS

The evidence from the infectivity and enucleation studies supports the conclusion that both ME7 and 87V scrapie strains, injected into the vitreous chamber of

the eye, are taken up by retinal ganglion cells and transported to replication sites in the primary visual projection areas in the CNS. There is a suggestion that different agents may replicate preferentially in either SC or DLG, if it is assumed that vacuolation, at least in these areas, is a direct sequel to previous replication of infection. Both areas become vacuolated at an early stage following infection, but the two agents seem to have an initial predilection for either SC or DLG.

Despite the evidence for axonal transport of ME7 by retinal ganglion cells, these neurons appear, at a morphological level, to be unaffected at any stage of the incubation period (3, and pers comm). No pathological changes can be detected in the retina, the optic nerves, and the vacuolation in the projection fields has been shown to be unaffected by the removal of the RGC terminals; mice in the terminal stages of the disease still show fast and slow transport of ^{3}H proline from retina to SC within the range for control mice (Scott, unpublished results). On the basis of these observations, retinal ganglion cells appear to transport agent without themselves becoming affected. Fraser *et al.* (8) suggested that the diversity of pathology seen in scrapie models could be influenced by whether neurons passively transport a particular strain of scrapie and remain unaffected (non-permissive neurons), or whether transport of that agent leads to replication and eventual dysfunction and cell death (permissive neurons); retinal ganglion cells can therefore be categorised as non-permissive. Differences in the capabilities of different neuronal sub-sets to pinocytose and transport specific agents would also impose restrictions on their ability to spread agent, and on the distribution of lesions. However, the eventual appearance of spongy pathology must be determined by the *Sinc* control of the dynamics of agent replication within groups of "permissive" neurons (see Kimberlin, and Walker, this volume). The contribution to scrapie pathogenesis of these different factors can now be examined within the framework of the IInd nerve model.

REFERENCES

1 A.G. DICKINSON, V.M.H. MEIKLE and H. FRASER, Identification of a gene which controls the incubation period of some strains of scrapie in mice. J. Comp. Path., 1968, 78, 293-299.

2 A.G. DICKINSON, V.M.H. MEIKLE and H. FRASER, Genetical control of the concentration of ME7 agent in the brain of mice. J. Comp. Path., 1969, 79, 15-22.

3 J.D. FOSTER, H. FRASER and M.E. BRUCE, Retinopathy in mice with experimental scrapie. Neuropath. Appl. Neurobiol., 1986, 12, 185-196.

4 H. FRASER, Neuronal spread of scrapie agent and targeting of lesions within the retino-tectal pathway. Nature, London, 1982, 295, 149-150.

5 H. FRASER and A.G. DICKINSON, The sequential development of the brain lesions of scrapie in three strains of mice. J. Comp. Path., 1968, 78, 301-311.

6 H. FRASER and A.G. DICKINSON, Scrapie in mice. Agent strain differences in the distribution and intensity of grey matter vacuolation. J. Comp. Path., 1973, 83, 29-39.

7 H. FRASER and A.G. DICKINSON, Targeting of scrapie lesions and spread of agent via the retino-tectal projection. Br. Res., 1985, 346, 32-41.

8 H. FRASER, P.A. McBRIDE, J.R. SCOTT and M.E. BRUCE, Infectious degeneration of the nervous system. D.R. Triger, ed., Advanced Medicine, Balliere Tindall, 1986, 22, 371-384.

9 J.L. FULLER and R.E. WIMER, Neural, sensory and motor functions. E.L. Green Hill ed., Biology of the Laboratory Mouse, McGraw Hill (publisher) 2nd edition, New York, 1986, 609-628.

10 G.D. HUNTER, G.C. MILLSON and R.L. CHANDLER, Observations on the comparative infectivity of cellular fractions derived from homogenates of mouse-scrapie brain. Res. Vet. Sci., 1963, 4, 543-549.

11 R.H. KIMBERLIN and C.A. WALKER,
Pathogenesis of mouse scrapie : patterns of agent replication in different parts of the CNS following intraperitoneal infection.
J. Roy. Soc. Med., 1982, 75, 618-624.

12 R.H. KIMBERLIN,
S. COLE and C.A. WALKER,
Pathogenesis of scrapie is faster when infection is intraspinal instead of intracerebral.
Microbial Pathogenesis, 1987, 2, 405-415.

13 R.H. KIMBERLIN,
S.M. HALL and C.A. WALKER,
Pathogenesis of mouse scrapie. Evidence of direct neural spread of infection to the CNS after injection of sciatic nerve.
J. Neurol. Sci., 1983, 61, 315-325.

14 P. LAMPERT, J. HOOKS,
C.J. GIBBS and D.C. GAJDUSEK,
Altered plasma membranes in experimental scrapie.
Acta Neuropath., Berlin, 1971, 19, 81-93.

15 R.J. LASEK,
The dynamic ordering of neuronal cytoskeletons.
Neurosci Res. Prog. Bull., 1981, 19, 7-32.

16 M. SANDBERG, A. HAMBERGER,
I. JACOBSSEN and J.O KARLSSON,
Fate of axonally transported proteins in the nerve terminal.
D.G. Weiss and A. Gorio, eds., Axoplasmic Transport in Physiology and Pathology, Springer-Verlag, Berlin Heidelberg, 1982, 27-31.

17 A.J. SEFTON and B. DREHER,
Visual system.
G. Paxinos, ed., The rat nervous system : I Forebrain and midbrain, Academic Press, Australia, 1985, 169-221.

Alzheimer's Disease and Related Disorders, pages 645–652

TRANSPORT AND TARGETING OF SCRAPIE INFECTIVITY AND PATHOLOGY IN THE OPTIC NERVE PROJECTIONS FOLLOWING INTRAOCULAR INFECTION.

J R Scott and H Fraser

AFRC and MRC Neuropathogenesis Unit, Institute for Animal Health, West Mains Rd., Edinburgh, U.K.

SUMMARY

The initial development of scrapie lesions can be seen following intraocular infection to be directly related to sequential infection of connecting neuronal relays within the projections of the optic nerve. For example, intraocular infection of VM mice with 22A virus produces lesions in the contralateral dorsal lateral geniculate nucleus (dLGN) and superior colliculus around halfway through the incubation period of about 360 days; the next lesions appear in the visual cortex, presumably as a result of the transport of infection through the geniculo-cortical tract. Infection of the same strain of mouse with 87V virus produces similar lesions in the dLGN slightly later in the incubation period of about 440 days, although cortical lesions are never seen with this agent. Subsequent lesions with both strains of the virus occur symmetrically in sites which are recognised targets with other routes of infection. Differences of this type provide the opportunity to relate levels of infectivity in sets of neurons directly to subsequent pathological changes. If the two murine Sinc genotypes (Sinc controls incubation period length) are compared after intraocular infection with ME7 virus, the timing of the appearance of the first lesions is in proportion to the length of the incubation period; this may provide a means of identifying the action of Sinc at a cellular level. Serial enucleation following infection of the right eye with ME7 virus has shown that infection takes between 7 and 14 days to reach the superior colliculus and initiate infection via this

pathway. This slow rate of spread of infectivity suggests that ME7 is carried in an anterograde direction by the slow rate of axonal transport.

INTRODUCTION

In 1982, it was shown that both scrapie infectivity and spongy pathology could be targeted to the central projections of the retina via the optic nerve, following intraocular infection (Fraser, 1982). This route of infection provides a simple 'neuron to neuron' model which can be used to study, for example, the targeting of scrapie infectivity, the action of the gene Sinc, and the intracellular transport of scrapie agent.

Although the retina is recognised as being part of the CNS, the incubation period following intraocular (i.o.) infection with scrapie is considerably longer than with an equivalent i.c. infection (Fraser and Dickinson, 1985); the spread of infection appears to be hindered by the restricted access to the rest of the CNS available through the optic nerve. Peripheral routes of infection also produce longer incubation periods than i.c., because a lymphoreticular replication phase must precede and initiate CNS infection. Incubation period length is determined by the time taken for agent to spread and gain access to replication sites in the small number of highly localised centres in the CNS necessary for the animal's survival, and produce the functional neuronal damage that results from replication (Fraser and Dickinson, 1973; Kimberlin and Walker, 1982). Direct infection of the sciatic nerve (Kimberlin et al, 1983) or the spinal cord (Kimberlin et al 1987) can produce even shorter incubation periods than following i.c. infection, presumably by providing the agent with more direct access to these centres, in contrast to the prolongation of incubation period after i.o. infection. Routeing infection through the known pathways of the retinal ganglion cell projections provides a unique opportunity to identify and examine the factors involved in scrapie pathogenesis.

INFECTIVITY AND PATHOLOGY IN OPTIC NERVE PATHWAYS

The sequence of the appearance of spongy pathology in the visual projection areas varies with the strain of

scrapie agent. With a standard i.o. ME7 infection in s7s7 mice, the first scrapie lesions are seen in the contralateral superior colliculus (SC) from around 140 days post-infection. However, there is wide variation in the timing of early lesions, probably due to differences between individual mice in the efficiency of i.o. infection resulting from leakage of inoculum at injection. Nevertheless, the sequence of progressive spongy degeneration is always the same: firstly, after the initial lesions in the contralateral SC, vacuolation appears in the contralateral dorsal lateral geniculate nucleus (DLG) after a delay of about 10 - 15 days, and then in the contralateral visual cortex (Fraser and Dickinson, 1985). These are all areas where vacuolation occurs in terminal animals following i.c. infection with ME7 agent. Secondly, more advanced cases have symmetrical lesions in many non-visual areas including the telencephalon, thalamus, tegmentum, cerebellum and brain stem. Finally, terminal mice have a pattern of spongy pathology indistinguishable from that seen following an i.c. infection (Figure 1), except, in some cases, for a residual asymmetry in the severity of vacuolation between the two sides of the SC.

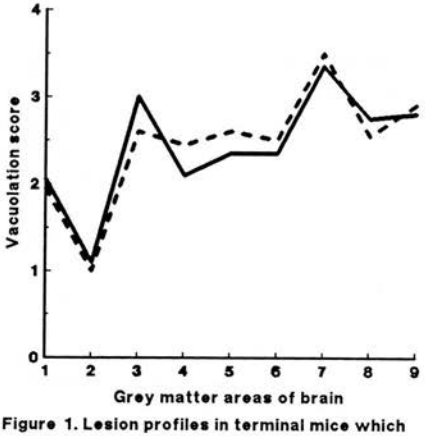

Figure 1. Lesion profiles in terminal mice which received the same dose of ME7 by an i.c.(broken line) and an i.o. route (solid line).

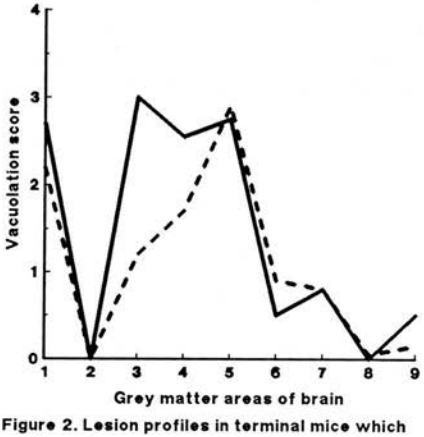

Figure 2. Lesion profiles in terminal mice which received the same dose of 87V by an i.c.(broken line) and an i.o. route (solid line).

Other strains of scrapie produce different patterns of vacuolation after i.o. infection. With 87V agent, which has a very much longer incubation period with all routes, the earliest vacuolation following i.o. infection of p7p7 mice occurs in the contralateral DLG at 260 days, in the absence of lesions in the SC. The pathology progresses to include both of the DLG and the contralateral SC, followed by the contralateral ventral thalamic nucleus, before spreading to resemble the pattern of spongiosis seen in terminal mice following i.c. infection. Close comparison of the lesion profiles of terminal mice, however, shows that spongy pathology in the SC (position 3) of i.c. infected mice does not become as severe as that seen in those infected by the i.o. route (Figure 2). The 87V agent, unlike ME7, produces very little vacuolation in the cortex, with either the i.o. or i.c. route, and in particular, there is no vacuolation in the visual cortex. 87V also produces many amyloid plaques, and although these plaques can be seen in the brains of terminal mice after i.o. infection, their number and distribution resembles that seen following intraperitoneal infection; there is no direct targeting of plaques within the retino-tectal projection (Fraser et al, 1986).

The relationship between the occurrence of spongy pathology and infectivity in specific areas of tissue can also be resolved with the intraocular route. Scrapie infectivity can only be estimated using long-term *in vivo* assays, either by titration using serial dilutions in groups of recipient mice, or by comparing the incubation periods of mice receiving a single dilution of the tissue to be assayed with an established dose-response curve (Hunter et al, 1963; Dickinson et al, 1969). Sequential incubation period assays of the left and right optic nerve and SC after right i.o. infection with ME7 (Fraser and Dickinson, 1985) have shown that infectivity can be detected in the left (contralateral) SC at 63 days post-infection; this is about 80 days before the first pathological changes are seen. Infectivity in the ipsilateral SC and in both optic nerves cannot be detected until between 100 and 120 days post-injection. This much later involvement of the optic nerves suggests that ME7 agent does not replicate within the axons, but is transported by them; both towards the SC to initiate infection, and probably back to the retina when high titres become established in the CNS as a whole. To

resolve these unknowns, further assays of visual projection areas following i.o. infection are in progress, and include retina, DLG and visual cortex as well as optic nerves and SC, and non-visually associated control regions.

The scrapie strains ME7 and 87V, although very different in incubation period and pattern of terminal pathology, are both strains which produce spongiosis in grey matter rather than white. Other strains, such as 79A and 139A produce severe vacuolation of white matter tracts, including the optic nerve and tract after i.o. infection, with relative sparing of the SC and DLG. Unlike ME7 and 87V, which produce no morphological changes in the retina even in terminal mice, infection with 79A or 139A results in a primary degeneration of the photoreceptor layer (Foster et al, 1986). These differences in the pathogenesis of 79A and 139A can be sought by using an intraocular route of infection.

THE *Sinc* GENE

The scrapie incubation period is highly characteristic for each combination of scrapie strain and mouse genotype. This genotype depends on which allele of the *Sinc* gene is present; most inbred strains are homozygous for the s7 allele which gives rise to relatively short incubation periods when infected i.c. with a high dose of ME7 mice homozygous for the p7 allele have prolonged incubation periods with the same infection. When mice of either genotype are infected i.o. with ME7, the mean incubation periods are proportionally longer than the equivalent i.c. incubation period: about 240 days in s7 mice, and 530 days in p7. The first appearance of spongy pathology in the left SC, however, is also delayed in the p7 mice (263 days post-infection) compared to the s7 recipients (141 days). These timings are in the same proportions as those seen following i.c. infection, showing that *Sinc* is exerting its effect on the infection and pathogenesis within the first neuronal relay in which replication occurs.

AXONAL TRANSPORT OF SCRAPIE AGENT

Using the intraocular route, it should be possible to identify the interval between exposure of the retina to

inoculum, and the establishment of infection in the retinal projection areas by serial enucleation. Groups of mice infected i.o. with ME7 were enucleated between 1 hour and 28 days later, and semi-serial sections of SC were examined for positive spongiosis 160 and 185 days post-injection. No positive lesions were seen in any of the mice enucleated up to 7 days post-injection. Agent appears to take between 14 and 28 days to establish infection in the SC after which time the source of infection in the eye can be removed without compromising the development of disease. This rate of spread of infection, about 1mm per day, was also found in the CNS following both intraperitoneal infection (Kimberlin and Walker, 1982) and infection of sciatic nerve (Kimberlin et al, 1983); this suggests that agent is carried within axons at the slowest rate of axonal transport. Five different velocities of axonal transport in optic nerve have been described by Lasek (1981), and the materials carried at the slowest rate (0.5 to 2mm per day in the optic nerve) have been identified as cytoskeletal elements such as tubulin, fodrin and the 3 neurofilament proteins. However, the measurement of rate of transport of scrapie is not the simple timing of arrival in the ganglion cell terminals in the SC of labelled proteins or amino-acids, but the time taken to initiate infection in the next 'relay', where vacuolation occurs. This additional factor must contribute to the measured transport rate.

CONCLUSIONS

The evidence from the infectivity and enucleation studies supports the conclusion that both ME7 and 87V scrapie strains, injected into the vitreous chamber of the eye, are taken up by retinal ganglion cells and transported to replication sites in the primary visual projection areas in the CNS. There is a suggestion that different agents may replicate preferentially in either SC or DLG, if it is assumed that vacuolation, at least in these areas, is a direct sequel to previous replication of infection. Both areas become vacuolated at an early stage following infection, but the two agents seem to have an initial predilection for either SC or DLG.

Despite the evidence for axonal transport of ME7 by retinal ganglion cells, these neurons appear, at a morphological level, to be unaffected at any stage of the incubation period (Foster et al, 1986). No pathological changes can be detected in the retina or the optic nerves, and the vacuolation in the projection fields has been shown to be unaffected by the removal of the RGC terminals; mice in the terminal stages of the disease still show fast and slow transport of ^{3}H proline from retina to SC within the range for control mice (Scott, unpublished results). On the basis of these observations, retinal ganglion cells appear to transport agent without themselves becoming affected. Fraser et al (1986) suggested that the diversity of pathology seen in scrapie models could be influenced by whether neurons passively transport a particular strain of scrapie and remain unaffected (non-permissive neurons), or whether transport of that agent leads to replication and eventual dysfunction and cell death (permissive neurons); retinal ganglion cells can therefore be categorised as non-permissive. Differences in the capabilities of different neuronal sub-sets to pinocytose and transport specific agents would also impose restrictions on their ability to spread agent, and on the distribution of lesions. However, the eventual appearance of spongy pathology must be determined by the *Sinc* control of the dynamics of agent replication within groups of 'permissive' neurons. The contribution to scrapie pathogenesis of these different factors can now be examined within the framework of the visual system model of infection.

REFERENCES

Dickinson A G, Meikle V M H, Fraser H (1969). Genetical control of the concentration of ME7 agent in the brain of mice. J Comp Path 79: 15-22.

Fraser H (1982). Neuronal spread of scrapie agent and targeting of lesions within the retino-tectal pathway. Nature 295: 149-150.

Fraser H and Dickinson A G (1973). Scrapie in mice. Agent strain differences in the distribution and intensity of grey matter vacuolation. J Comp Path 83: 29-39.

Fraser H and Dickinson A G (1985). Targeting of scrapie lesions and spread of agent via the retino-tectal projection. Br Res 346: 32-41.

Fraser H, McBride P A, Scott J R and Bruce M E (1986). Infectious degeneration of the nervous system. In Triger D R (ed): "Advanced Medicine 22," London: Balliere Tindall, pp 371–384.

Foster J D, Fraser H, Bruce M E (1986). Retinopathy in mice with experimental scrapie. Neuropath Appl Neurobiol 12: 185–196.

Hunter G D, Millson G C and Chandler R L (1963). Observations on the comparative infectivity of cellular fractions derived from homogenates of mouse-scrapie brain. Res Vet Sci 4: 543–549.

Kimberlin R H and Walker C A (1982). Pathogenesis of mouse scrapie: patterns of agent replication in different parts of the CNS following intraperitoneal infection. J Roy Soc Med 75: 618–624.

Kimberlin R H, Cole S and Walker C A (1987). Pathogenesis of scrapie is faster when infection is intraspinal instead of intracerebral. Microb Pathogen 2: 405–415.

Kimberlin R H, Hall S M and Walker C A (1983). Pathogenesis of mouse scrapie. Evidence of direct neural spread of infection to the CNS after injection of sciatic nerve. J Neurol Sci 61: 315–325.

Lasek R J (1981). The dynamic ordering of neuronal cytoskeletons. Neurosci Res Prog Bull 19: 7–32.

Brain Research, 504 (1989) 301–305
Elsevier

BRES 23837

Enucleation after intraocular scrapie injection delays the spread of infection

J.R. Scott and H. Fraser

AFRC and MRC Neuropathogenesis Unit, Institute for Animal Health, Edinburgh (U.K.)

(Accepted 15 August 1989)

Key words: Scrapie; Intraocular infection; Spongiosis; Enucleation; Mouse

After right intraocular infection, mice develop lesions in the contralateral retinal projections long before clinical disease occurs. Enucleation up to 7 days post-infection prevented targeting of lesions to visual projections, and prolonged the incubation period. When enucleation was delayed until at least 14 days post-infection, lesion targeting and incubation periods were similar to unenucleated mice. It was concluded that infectivity took a minimum of 14 days to reach the brain via the optic nerve.

Recent studies of the pathogenesis of scrapie infection have shown that the key events in determining incubation period are the time (and site) at which infection enters the nervous system[17], and the dynamics of replication within the CNS[18]. With the non-neural, parenteral routes of infection, there is an obligatory phase of scrapie replication in the lymphoreticular system, and infection then spreads from spleen and visceral lymph nodes to mid-thoracic cord via sympathetic nerves[19]. Similar pathways are involved after intragastric infection except that replication in Peyer's patches is probably more important in initiating neuroinvasion than replication in spleen and lymph nodes[20]. Injection of the spinal cord[21] and sciatic nerve[22] show that once neuroinvasion has been initiated, scrapie spreads within the PNS and the CNS[15] at a similar slow rate (about 1 mm day). These studies demonstrate the importance of neuronal networks in the transport of scrapie infection. However, they all involve complex neuroanatomical pathways in which the spread of infectivity can only be estimated by sequential bioassay of small pieces of nervous tissue. Infection via the retina provides a much simpler route, because the murine optic nerve is essentially a single neuron relay; the ganglion cells in the retina project to the outer layers of the contralateral superior colliculus (SC) on the surface of the mid-brain. Murine retinal ganglion cell projections have been used extensively to investigate axonal physiology in both normal and diseased neurons[7,14,25,28]. The intraocular route provides an opportunity to study initiation of infection within the retina and also the dynamics of scrapie replication and transport within a well-defined sequence of neuronal connections. After unilateral intraocular (i.o.) infection with ME7 scrapie, sequential assays of the contralateral SC have shown that an increase in infectivity can be detected by 68 days post-injection[12]. Similar timings have been shown in other scrapie models[4,16], although all these studies lack the early assay times which could help to estimate the time of arrival of infectivity in the SC. Only an estimation of infectivity is possible, due to the inherent inefficiencies of the bioassay system. The spongy lesions characteristic of scrapie start to develop in the contralateral SC about 60 days after infectivity, around 130 days post-injection, and then progress to other central retinal targets, such as the dorsal lateral geniculate nucleus[10,13,29]. This evidence suggests that spongy lesions develop as an eventual consequence of accumulation or replication of infectivity in specific sets of neurons. The possibility that infection could spread from the retina to visual projections in the CNS via non-neuronal pathways is extremely unlikely in view of the precise targeting of lesions seen in this model, especially the secondary targeting in the visual cortex resulting from transport of infectivity through the geniculocortical tract[13].

The present study used sequential enucleation following i.o. infection to take the infectivity studies a stage further, by using both incubation period and targeting of spongy lesions to define the time necessary for infection to spread via the optic nerve to the SC.

VM/Dk-*Sinc*^{s7} mice were used for all experiments, except for those involving conjunctival instillation for which SM/Rr//Dk mice were used. Both of these strains

Correspondence: J.R. Scott, AFRC and MRC Neuropathogenesis Unit, West Mains Rd., Edinburgh EH9 3JF, U.K.

carry the s7 allele of the gene *Sinc*, the major gene controlling incubation period[6]; from previous studies, no difference between their incubation periods or lesion profiles was expected. Since SM mice are pigmented, the decussation at the optic chiasma is slightly less (95%) than in the albino VM strain (99%)[7].

The ME7 strain of scrapie was used for all experiments. It was originally isolated from a natural case of scrapie in a Suffolk sheep[3], and had been passaged 10 times, including 3 high dilution cloning passes. Inoculum was prepared from the frozen brain of a C57BL/6Jbgbg mouse terminally affected with cloned ME7. The tissue was homogenised in physiological saline at a dilution of 10%, and 500 g supernatants used as inocula.

Infection was by one of four routes: intracerebral, i.o. (into the vitreous chamber of the right eye), intravenous (into the tail vein), and by conjunctival instillation (dropping the inoculum into the conjunctival sac of the right eye, with no penetration of the tissues). All injections were made with a 10 μl Hamilton syringe fitted with a 27-gauge needle, which was blunted before the conjunctival instillations were made. The volume for all routes was 1 μl, which gave a dose of approximately 10^4 i.c. ID_{50} units. Inoculations and enucleations were carried out under pentobarbitone anaesthesia, supplemented with ether if necessary. Mice were allocated to coded groups at the time of infection and appropriate groups were enucleated at 12 and 24 h, and 7, 14, 21 and 28 days post-infection. The right eye was removed after clamping behind the orbit with small artery forceps. Age-matched uninfected controls killed 30–86 days post-enucleation showed evidence of Wallerian degeneration in the optic tract and in the white matter of the SC contralateral to the enucleation[8]. However, infected enucleated mice were not examined until at least 157 days post-enucleation (185 days post-injection minus 28 days post-injection), by which time the degeneration had resolved to a withering and gliosis of the optic tract and a condensation of the neuronal perikarya in the SC.

One half of each group of mice enucleated between 12 h and 28 days was killed at 185 days post-injection, and the other half was retained until they developed advanced clinical signs of scrapie; the earliest clinical signs were seen about 230 days. Incubation periods were measured from time of injection to the terminal stages of the disease, when clinically affected animals were scored using a standard method[6]. All brains were formol-fixed, paraffin-embedded and stained with haematoxylin and eosin. Brains from the majority of terminal mice were cut to give 4 coronal levels as described by Fraser and Dickinson[11]. The distribution and intensity of spongy lesions is usually estimated by scoring 9 standard grey matter areas of brain on a scale from 0 to 5 to give a 'lesion profile'[11], a score of 1 being 'few vacuoles, widely and unevenly scattered', and 5 being 'dense vacuolation with most of the field confluent'. The 9 areas are: 1 medulla, 2 cerebellum, 3 superior colliculus, 4 hypothalamus, 5 thalamus, 6 hippocampus, 7 paraterminal body, 8 cerebral cortex (posterior midline) and 9 cerebral cortex (anterior midline). This assessment of the pathological changes in the mouse brain has been widely used in scrapie studies, especially in distinguishing different scrapie strains[2,12,21]. Lesion profiles also vary with different routes of infection; intracerebral (and i.o.) profiles are higher than those resulting from a peripheral route, e.g. intraperitoneal[9]. Brains from mice killed at 185 days post-infection, and representatives from clinical groups were cut to give coronal semi-serial sections (1 every 20 μm) from the level of the paraterminal body to the inferior colliculus (levels 209 to 413)[30], which allowed more extensive examination of the SC (and other visual areas), and separate scoring of lesions on left and right sides.

TABLE I

Effect of enucleation on the occurrence of lesions in the superior colliculus (SC) 185 days after i.o. infection of the right eye; n = 5–9

Time of enucleation	*Mice with spongy changes in left SC (%) at 185 days*		*Mean SC lesion score at 185 days*	
	No.	*%*	*Left*	*Right*
12 h	0	0	–	–
24 h	0	0	–	–
7 days	0	0	–	–
14 days	1	20	3.0	1.0
21 days	5	56	2.4	1.2
28 days	4	80	2.5	0.3
Unenucleated	7	88	2.1	0.4

Of the unenucleated i.o. mice killed at 185 days post-infection, 88% had lesions in the left SC (Table I), and many of them had more widespread lesions. In contrast, at this time, there were no lesions in the SC, or in any other area of the brain in mice enucleated at 7 days or earlier. Only 20% of mice enucleated at 14 days (one mouse out of 5) had lesions in the contralateral SC. This proportion rose to 80% for mice enucleated at 28 days, which was almost as high as in the unenucleated group. Lesions in the contralateral (left) SC were invariably more severe than those on the right (Table I); typical lesions are shown in Fig. 1 in a mouse enucleated at 21 days post-infection.

The effect of enucleation on the groups killed at 185 days was reflected in the groups which developed clinical disease. Enucleation up to 7 days post-infection significantly prolonged incubation periods compared to both the later enucleation groups and the unenucleated group (Table II). Mice in these early enucleation groups also

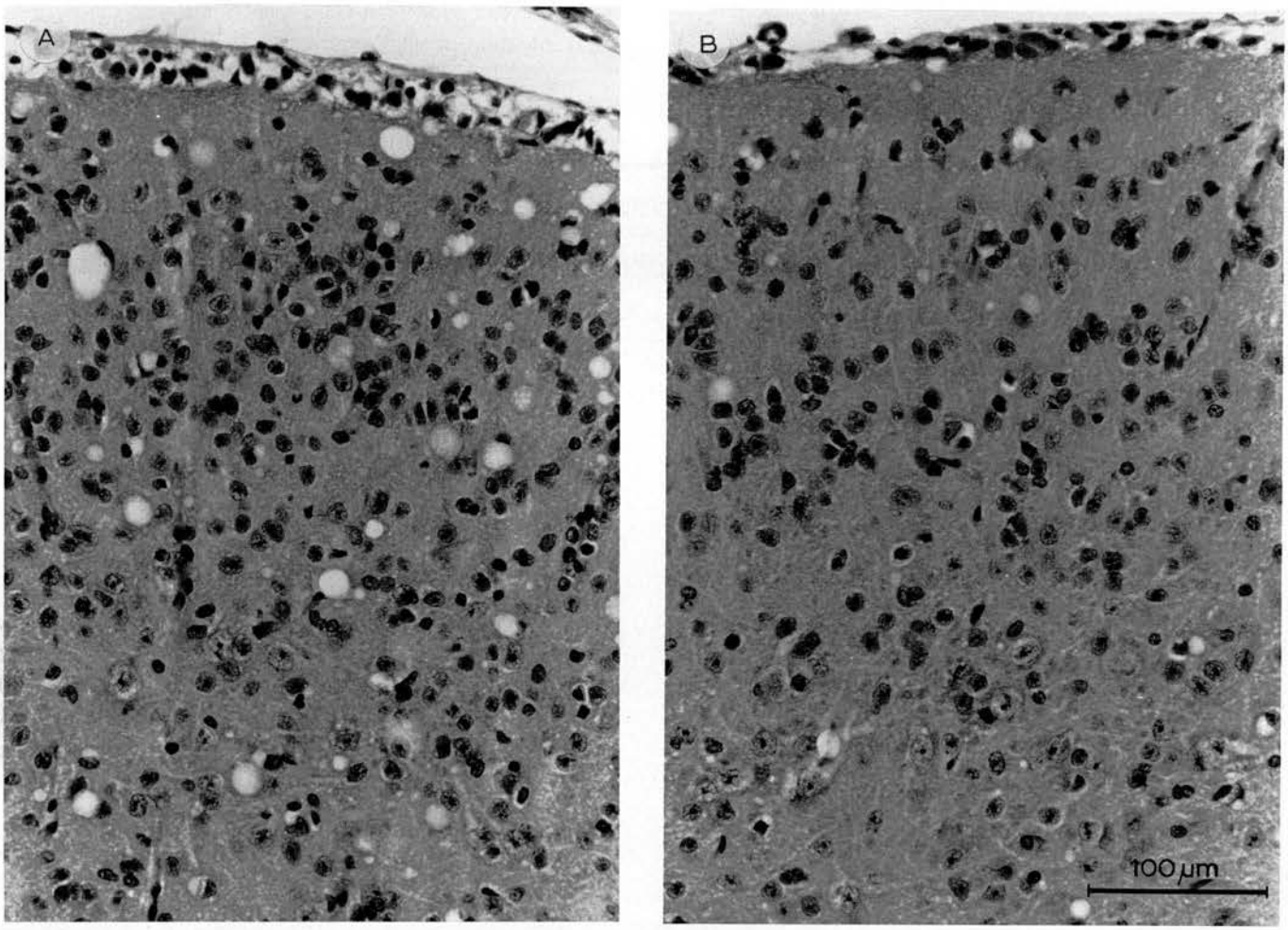

Fig. 1. Left (A) and right (B) sides of the superior colliculus from a mouse enucleated 21 days after right intraocular infection, and killed 157 days later. The lesions are targeted to the left side, contralateral to the injected eye.

had less severe terminal lesions, particularly in the SC, with no evidence of asymmetry (Table II). The lesion profiles of unenucleated mice, and of mice enucleated on or after 14 days were indistinguishable, and resembled the profile of mice infected by the intracerebral route (Fig. 2). The possibility that enucleation per se induced the development of asymmetrical pathology in the SC, perhaps by triggering the release of circulating infectivity, was tested by enucleating 18 hours post-intravenous infection. This had no effect on either the incubation period (Table II) or the terminal lesion profile.

In summary, enucleation on or before 7 days after i.o. infection prevented the early development of spongy degeneration in the contralateral SC and prolonged the incubation period. Enucleation at 14 days or later had no effect on the incubation period, although the percentage of mice per group with lesions at 185 days only reached that of controls in mice enucleated after 28 days. Therefore, the earliest enucleation time which permits infection via the optic nerve in individual animals is 14 days.

TABLE II

Differences in incubation period and terminal lesion severity in the superior colliculus (SC) in mice enucleated up to 28 days after intraocular infection, and after infection intravenously, and by conjunctival instillation

Time of enucleation	*Incubation period [mean ± S.E.M. of (n) mice]*	*Mean terminal SC lesion score*	
		Left	*Right*
Intraocular infection			
12 h	302 ± 12* (7)	1.8	1.8
24 h	313 ± 7*** (7)	1.9	1.7
7 days	304 ± 12** (6)	1.6	1.6
14 days	285 ± 14 (6)	2.2	1.8
21 days	283 ± 16 (6)	2.6	2.5
28 days	267 ± 11 (6)	3.0	2.5
Unenucleated	260 ± 4 (14)	3.2	3.2
Intravenous infection			
18 h	278 ± 7 (3)	3.0	3.0
Unenucleated	283 ± 9 (4)	2.5	2.5
Conjunctival instillation			
Unenucleated	322 ± 7 (6)[§]	1.0	1.0

Statistical analysis by Student's *t*-test; compared to unenucleated control, $***P < 0.001$; $**P < 0.01$; $*P < 0.02$.

[§] Only 6 out of 18 mice developed scrapie.

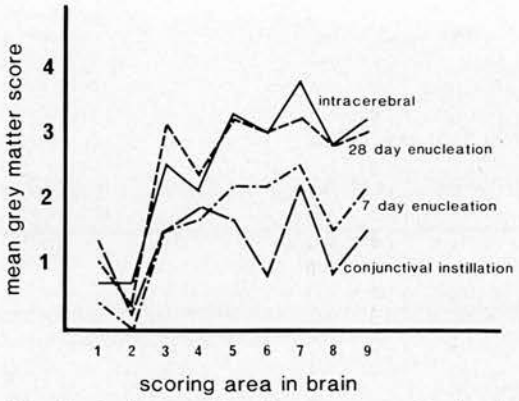

Fig. 2. Lesion profiles from groups of mice infected by an intracerebral route (n = 10), i.o. route followed by enucleation at 28 days (n = 6), i.o. route followed by enucleation at 7 days (n = 6) and by conjunctival instillation (n = 6). Scoring position 3 is the superior colliculus; see text for other scoring areas.

Although enucleation on or before 7 days prevented the infection spreading through the optic nerve, clinical disease still occurred, but after a much longer delay. This demands an explanation because the major source of infection is removed with the eye. However, inoculum which escapes from the globe of the eye at the time of injection is likely to gain access to lymphoreticular replication sites from the lymphatic drainage of the orbit: carbon particles injected into the soft tissues behind the eye were visible in the cervical lymph nodes 24 h later (Scott and Fraser, unpublished observation). In addition, drainage from the conjunctival sac through the tear duct could lead to infection via the respiratory and alimentary systems. This diversity of alternative routes of infection may explain the wide range of incubation periods (229 to 336 days over all groups), which is reflected in the standard errors of the means (Table II). Conjunctival instillation was used to simulate leakage of inoculum from the globe, to test the prediction that the pattern of lesions and incubation periods produced would be similar to those seen in mice from these early enucleation groups (7 days post-infection or before). To some extent this was true. The lesion profile was much lower than with i.o. infection (Fig. 2), and the lesions in the SC were even less severe than those of mice enucleated before 7 days, although the incubation periods were similar (Table II). However, only 6 out of 18 SM mice infected by conjunctival instillation developed clinical scrapie. The remaining 12 mice were killed after 438 days, and were clinically and histologically normal. Therefore, although infection can spread from the conjunctival sac, there is clearly some additional route contributing to the peripheral infection in mice enucleated up to 7 days.

The molecular and cellular mechanisms involved in the uptake and transport of scrapie are unknown, but this work indicates that at least a 14-day period is necessary to establish infection in the SC in this model. Evidence for rates of spread of about 1 mm/day have been found in both CNS and PNS by measuring the interval between the detection of replication in discrete parts of the CNS, or the delay between initial infection and the detectable onset of replication elsewhere, as with the i.o. route[4,15,16,22]. In the present study, infection spread about 16–20 mm from the retina to the SC in the mouse, in not less than 14 days. This represents an approximate overall transport rate of slightly over 1 mm per day. If the optic nerve and tract are regarded as a homogeneous axonal projection, then this velocity suggests an association between the spread of scrapie and slow axonal transport. This is known to be between 0.5 and 2 mm/day in the normal murine optic nerve, where it is concerned with the translocation of cytoskeletal elements such as tubulin and the MAP proteins[14,31,32]. In other words, scrapie infectivity may be passively transported in association with slow axonal transport. Only if another step such as replication or packaging is necessary before transport takes place, could the transport of scrapie be faster. However, other studies (Scott, unpublished observation) suggest that the spread of scrapie infection to SC occurred before any increase in infectivity could be detected in the retina.

The spread of conventional viruses through neuronal pathways has been recognised in experimental herpes simplex[23], rabies[24] and Borna disease[5] infections. Studies with herpes simplex[27] have shown the importance of anterograde axonal transport as a mechanism for the spread of infection. This study indicates that scrapie also uses this route.

Dysfunction of normal slow axoplasmic flow has been implicated in the pathogenesis of scrapie by (a) the immunolabelling of the periphery of amyloid plaques with antibodies to tau protein, one of the MAPs[1] and by (b) the immunolabelling of dystrophic neurites with monoclonal antibodies to neurofilament protein in cases of natural and experimental Creutzfeldt-Jakob disease, the human analogue of scrapie[26]. Preliminary evidence from further enucleation studies using 79A and 87V strains of scrapie suggests that the rate of transport is the same for all scrapie models irrespective of the incubation period.

1 Brion, J.P., Fraser, H., Flament-Durant, J. and Dickinson, A.G., Amyloid scrapie plaques in mice, and Alzheimer senile plaques, share common antigens with tau, a microtubule-associated protein, *Neurosci. Lett.*, 78 (1987) 113–118.
2 Bruce, M.E. and Dickinson, A.G., Biological evidence that scrapie agent has an independent genome, *J. Gen. Virol.*, 68